Prefix

The calibration report of the 2023 European TWSTFT calibration campaign is composed of the following three parts:

Part I: “European TWSTFT Calibration Campaign 2023 Calibration Report” reported by VSL. This part includes the calibration results of TWSTFT links between TIM, PL, PTB, VSL, LTFB, ROA, OP, NPL, SP, IT, and CH.

Part II: “GSOP TWSTFT CALIBRATION REPORT” reported by ROA. This part includes the calibration results of TWSTFT links between SP, PTB, IT, OP, and ROA.

Part III: “Annex: Results Validation”. This part demonstrates the comparison and validation of the calibration results obtained by VSL and ROA.

Part I

European TWSTFT Calibration Campaign 2023 Calibration Report

This part includes the calibration results of TWSTFT links between TIM, PL, PTB, VSL, LTFB, ROA, OP, NPL, SP, IT, and CH.

European TWSTFT Calibration Campaign 2023
Calibration Report

Identification	2023_TW-EU-Calibration
Coordinator	Erik Dierikx, VSL
Calibration Type	Site-mode and baseline-mode calibration using a mobile TWSTFT station
Participating Stations	TIM01 PL01 PTB05 PTB04 VSL01 LTFB01 ROA01 OP01 NPL02 SP01 IT01 CH01
Campaign Period	August 15, 2023 – November 13, 2023

Document Code	2023_TW-EU-CAL_v1.1
Version	Version 1.1
Date	13/08/2024

National Metrology Institute

Document preparation

Prepared by	Yan Xie (VSL)
Approved by	Erik Dierikx (VSL)

Participating partners approval

Approved by	Wolfgang Schaefer (TimeTech)	(signature and date)
Approved by	Czubla Albin (GUM)	(signature and date)
Approved by	Dirk Piester (PTB)	(signature and date)
Approved by	Erik Dierikx (VSL)	(signature and date)
Approved by	Eric Meyer (LNE-LTFB)	(signature and date)
Approved by	Héctor Álvarez (ROA)	(signature and date)
Approved by	Joseph Achkar (LNE-SYRTE)	(signature and date)
Approved by	Conway Langham (NPL)	(signature and date)
Approved by	Carsten Rieck (RISE)	(signature and date)
Approved by	Ilaria Sesia (INRIM)	(signature and date)
Approved by	Christian Schlunegger (METAS)	(signature and date)

Summary

A European-wide TWSTFT calibration campaign was carried out from August 2023 to November 2023. Eleven European UTC laboratories equipped with twelve sets of TWSTFT station facilities participated in this calibration campaign. The participating TWSTFT stations include TIM01, PL01, PTB05, PTB04, VSL01, LTFB01, ROA01, OP01, NPL02, SP01, IT01, and CH01.The purpose of this calibration campaign is to calibrate the TWSTFT links, which are composed of the participating TWSTFT stations, using a TWSTFT mobile station. Since the previous calibration campaign was conducted approximately four years ago and the replacement of the satellite transponder and modifications to the settings of Europe-to-Europe links were experienced afterwards, this calibration campaign is in demand to maintain the time transfer accuracy of Europe-to-Europe TWSTF links. VSL initiated this calibration campaign and was assigned as the coordinator of the campaign by all the participating partners. Timetech was appointed as the mobile station provider to perform on-site measurements.

This document is to record the technical description and report the CALibration Result (CALR) obtained from this calibration campaign. In this calibration campaign, on-site measurement data from multiple Rx channels of the participating stations, including Rx1, Rx2, and SDR, are processed when the corresponding measurement data are available, and therefore CALR values between the participating Rx channels are computed accordingly. Two calibration methods are adopted for the computation of CALR values for the TW links, respectively: site-mode calibration and baseline-mode calibration. Commensurately, the uncertainty budget of CALR values is analyzed and calculated. In addition, comparisons between the calibration results from the two calibration methods, as well as comparisons between the previous and the new calibration results, are made for evaluation and verification.

The structure of this document is organized as follows:

Chapter 1 introduces the scope and prefix information in this document.

Chapter 2 gives an overview of the organization of this calibration campaign.

Chapter 3 presents the operational information of the participating TW links and the planning of this calibration campaign.

Chapter 4 explains the principle of TWSTFT techniques and the calibration methods.

Chapter 5 describes the operation of the TWSTFT mobile station used in this calibration campaign.

Chapter 6 deduces the data processing of the CALR value and analyzes the uncertainty budget of CALR.

Chapter 7 collects and processes the site-mode measurement data at each participating station, as well as the closure measurement results.

Chapter 8 gives the site-mode calibration results for TW links in calibration.

Chapter 9 collects and processes the baseline-mode measurement data at each participating station.

Chapter 10 gives the baseline-mode calibration results for TW links in calibration.

Chapter 11 compares the new CALR values obtained from this calibration campaign with the old CALR values in use.

Chapter 12 compares the CALR values obtained from the site-mode method and the baseline-mode method and then verifies the new CALR values by triangle closures.

Chapter 13 concludes this calibration campaign, and Chapter 14 states the acknowledgement.

Table of contents

List of figures

List of tables

1 Introduction

1.1 Scope of the document

This document represents the description and the calibration results of the 2023 TWSTFT European calibration campaign.

TWSTFT and GNSS techniques are the two primary time transfer approaches applied for UTC generation. With metrological calibration on each TW link, the TWSTFT network operates absolute time transfers independently with typical 1ns uncertainty [RD01]. Therefore, performing TW link calibrations among UTC laboratories which are participating in the TWSTFT network via a calibration campaign is essential to maintain the time transfer facilities contributing to UTC.

In this calibration campaign, a mobile station (MOB) is used as a common reference to be compared with fixed Earth Stations in UTC labs. This calibration approach allows the independent TW link delay measurements and the-state-of-the-art lowest level of measurement uncertainty between each pair of TW stations.

11 European laboratories equipped with 12 sets of TWSTFT facilities participated in this calibration campaign, and the whole duration of this calibration campaign lasted for approximately 4 months, from August 2023 to November 2023.

In this document, all the Earth Stations (ESs) mentioned in the context are in chronological order of this calibration campaign. The chronology is illustrated in Table 3-6 List of planned MOB travel map and travel schedule.

1.2 Acronyms and abbreviations

1.2.1 General abbreviations in the document

Table 1-1 lists the general abbreviations mentioned in this document.

Table 1-1 List of general abbreviations in the document

Abbreviations	Definition
BIPM	Bureau International des Poids et Mesures
BPSK	Binary Phase-Shift Keying
BW	frequency BandWidth
CCTF	Consultative Committee for Time and Frequency
FDIS	Frequency DIStribution amplifier
GEO	GEOstationary orbit
IF	Intermediate Frequency
IGS	International GNSS service
IIOTIC	Intelligent In/Out Time Interval Counter
ISO	International Organization for Standardization
ITRF	International Terrestrial Reference Frame
ITU	International Telecommunication Union
MJD	Modified Julian Date
MOB	MOBile station

PDIS	Pulse DIStribution amplifier
PN	Pseudorandom Noise
PPS	Pulse Per Second
RF	Radio-Frequency
RX	Receiver
SATRE	SAtellite time Transfer and Ranging Equipment
stdev	standard deviation
TCC	Triangle Closure Calibration
TDEV	Time DEViation
TIC	Time Interval Counter
TW	Two-Way (short for TWSTFT)
TWSTFT	Two-Way Satellite Time and Frequency Transfer
TX	Transmitter
UTC	Coordinated Universal Time
VSAT	Very Small Aperture Terminal

1.2.2 TWSTFT specific acronyms

Table 1-2 lists acronyms that are defined in TWSTFT-related formulas and TW data files.

Table 1-2 List of TWSTFT-specific acronyms

TWSTFT acronyms	Definition	Source in the document
CALR(1,2)	CALibration Result between ES1 and ES2	See equation (9)
CCD	Common Clock Difference	See equation (11)
CSD	Combined Standard Deviation	See equation (50)
DLD	Double Delay Difference	See equation (4)
ES	Earth Station	See [RD06]
ESDVAR	Earth Station Delay VARiations	See [RD06]
ESIG	standard measurement uncertainty of ESDVAR	See [RD06]
HT	HeighT in geodetic coordinates	See equation (10)
LA	LAtitude in geodetic coordinates	See equation (10)
LO	LOngitude in geodetic coordinates	See equation (10)
LOC	LOCal earth station	See [RD06]
NTL	Nominal Track Length	See [RD06]
REFDELAY(k)	DELAY between the REFerence point of an ES and UTC(k)	See equation (6)
REM	REMote earth station	See [RD06]
SCD	Sagnac-effect Correction value in the Downlink	See equation (1)

SCU	Sagnac-effect Correction value in the Uplink	See equation (1)
SP	Signal Path delay, summation of SPD, SPT and SPU	See equation (3)
SPD	Signal Path Downlink delay	See equation (1)
SPT	Satellite Path delay through the Transponder	See equation (1)
SPU	Signal Path Uplink delay	See equation (1)
TS(k)	local Time Scale of an ES at Site k	See equation (1)
TW(k)	Result of a quadratic fit over the TIC Two-Way reading data collected during one session of an ES at Site k	See [RD06] and equation (1)

1.3 Reference documents

The following documents listed in Table 1-3 are cited as the references in this calibration report.

Table 1-3 Reference documents

Ref No.	Title	Code	Version	Date
RD01	Calibration of TWSTFT links through the triangle closure condition	40th Annual PTTI Meeting	--	12/2008
RD02	TWSTFT Calibration Guidelines for UTC Time Links	--	3.0	04/2015
RD03	Summary for the GSOP 2019 TWSTFT calibration report	GAL-TN-ROA-GSOP-2019001	3	10/2019
RD04	Results of the 2019 TWSTFT Calibration Campaign involving five European Stations	2nd_2019_TW-EU-Calibration	2	03/2021
RD05	Calibration bridging for the June and July 2021 satellite transponder frequency changes for European and transatlantic TWSTFT links	TM289-D	1	02/2022
RD06	The operational use of two-way satellite time and frequency transfer employing pseudorandom noise codes	Recommendation ITU-R TF.1153-4	--	08/2015
RD07	Site Preparation Document for Two-Way Calibration Campaign	MOB-TIM-Site_Prep_7	7	10/2023
RD08	Mobile Calibration Station Calibration Report	CAL-TIM-RP-0002	1/1	12/2013
RD09	Summary for the 2019 SDR TWSTFT OP-PTB calibration report	0517-2020	5.2	01/2020
RD10	European TWSTFT Calibration Campaign 2016 Calibration Report	--	--	01/2017
RD11	European TWSTFT Calibration Campaign 2014	0380-2014	--	2015
RD12	Calibration of IT01 station – 2022	0584-2022	--	04/2022
RD13	Calibration of IT01 station for non-UTC links – 2022	0585-2022	--	09/2022
RD14	IONEX: The IONosphere Map Exchange Format Version 1	Proceedings of the IGS AC Workshop	--	02/1998
RD15	A. Kleusberg, “Analytical GPS Navigation Solution”	DOI:10.1007/978-3-662-05296-9_7	--	2003

2 Organization of the TWSTFT calibration campaign

The 2023 TWSTFT calibration campaign was initiated and coordinated by VSL, together with 11 TWSTFT station sites which participate in EU-to-EU TWSTFT links, including TIM, PL, PTB, VSL, LTFB, ROA, OP, NPL, SP, IT, and CH. TimeTech GmbH was entrusted to operate on-site measurements with their mobile station as the reference.

2.1 General information on the 2023 TWSTFT calibration campaign

Table 2-1 summarizes the general information on the organization of this calibration campaign.

Table 2-1 General information on the 2023 TWSTFT calibration campaign

Identification	2023_TW-EU-Calibration
Purpose	TWSTFT link calibration for UTC links
Coordinator	Erik Dierikx, VSL
Calibration Type	Site-mode and baseline-mode calibration using a mobile TWSTFT station
Mobile Station ID and Provider	MOB02, TimeTech GmbH
Participating Earth Stations	TIM01, PL01, PTB05, PTB04, VSL01, LTFB01, ROA01, OP01, NPL02, SP01, IT01, CH01
Pivot Earth Station	PTB05
Station for Closure Measurements	PTB05
Calibration Campaign Period	Aug 15, 2023 – Nov 13, 2023
Effective Measurement Duration	See Table 3-7 List of the effective measurement duration at the sites

2.2 Motivation of the calibration campaign

TWSTFT network is the independent network performing time transfer and comparison via a geostationary communication satellite. The TW Earth Station (ES), normally affiliated with a local UTC realisation, contributes to UTC computation and local UTC timekeeping by comparing the local ES timescale to the remote ES timescale via the TW link. Therefore, the regular calibration of the absolute delays of TW links is crucial to the accuracy of TW time transfer and further influences UTC calculations and local UTC maintenance.

A TWSTFT link calibration campaign can be carried out using a TWSTFT mobile station (MOB) and/or a GNSS travelling system which is circulated among participating TW Earth Stations (ES). Among these two calibration techniques, using a TWSTFT mobile station is recommended as the primary technique used for a UTC TWSTFT time link calibration, and calibration via GNSS can be used as a supplement or an alternative when the TWSTFT mobile calibration is not applicable [RD02].

The latest TWSTFT calibration campaigns with a mobile station were implemented in 2019, containing two calibration campaigns: the first campaign was performed from Feb to May 2019, covering 8 stations (TIM, RISE, PTB, PTF2, INRIM, PTF1, ROA, OP) [RD03], and the second campaign was conducted from August to October 2019, covering 6 stations (TIM, NPL, VSL, PTB, AOS, CH) [RD04].

The replacement of the satellite transponder and expansion of the bandwidth of the Europe-to-Europe (EU-to-EU) links, which occurred on MJD 59361(UTC: 2021-05-27) and MJD 59397 (UTC: 2021-07-02), resulted in the changes of TW link delays accordingly. After these changes, BIPM applied the bridging calibration to UTC links, that is to compare the TW links to GPS IPPP links which maintain continuity during the whole procedure of TW link changes, and then using Triangle Closure Calibration (TCC) to non-UTC links to calculate the new CALR values and obtain new Calibration IDs (CI) accordingly [RD05]. The CIs and CALR values presently in use are mainly from the calculation of [RD05].

Since the present CALR values are not directly obtained from the primary TW calibration technique and the previous calibration campaign using a mobile station was 4 years ago, a new calibration campaign with the MOB technique is in demand to enhance the time transfer accuracy of EU-to-EU TW links.

2.3 Coordinator, provider, participants and contacts

Being a member of the CCTF and operating a TWSTFT station, VSL was appointed as the coordinator of this calibration campaign. It was agreed by all the participants in this calibration campaign to follow the guidelines of [RD02]. TimeTech was appointed as the mobile TWSTFT station provider to perform on-site measurements. Eleven participants with twelve TW stations in total joined this calibration campaign. Table 2-2 lists all the participants and contacts in this calibration campaign.

Table 2-2 Participants and contacts

ES Site ID	Affiliated organization	1st contact person	Address
TIM	**TimeTech** TimeTech GmbH	Wolfgang Schaefer Wolfgang.schaefer@timetech.de	Curiestrasse 2 D-70563 Stuttgart, Germany
PL	**GUM** Central Office of Measures	Czubla Albin albin.czubla@gum.gov.pl	ul. Elektoralna 2 00-139 Warszawa, Poland
PTB	**PTB** Physikalisch-Technische Bundesanstalt	Dirk Piester Dirk.Piester@ptb.de	Bundesallee 100 38116 Braunschweig, Germany
VSL	**VSL** National Metrology Institute of the Netherlands	Erik Dierikx edierikx@vsl.nl	Thijsseweg 11 2629 JA, Delft, The Netherlands
LTFB	**LNE-LTFB** OSU-Theta, Université de Franche-Comté, CNRS, Université de Bourgogne, SUPMICROTECH, UBFC	Eric Meyer eric.m.meyer@cnrs.fr	41 bis avenue de l'Observatoire 25010 Besançon, France
ROA	**ROA** Real Instituto y Observatorio de la Armada	Héctor Álvarez halvarez@roa.es	Plaza de las Tres Marinas s/n 11100 San Fernando (Cádiz), Spain
OP	**LNE-SYRTE**	Joseph Achkar joseph.achkar@obspm.fr	61 avenue de l'Observatoire 75014 Paris, France

	Observatoire de Paris - Université PSL, CNRS, Sorbonne Université		
NPL	**NPL** National Physical Laboratory	Conway Langham conway.langham@npl.co.uk	Hampton Road, Teddington Middlesex TW11 0LW, United Kingdom
SP	**RISE** Research Institutes of Sweden Measurement Technology	Carsten Rieck carsten.rieck@ri.se	Brinellgatan 4 504 62 Borås, Sweden
IT	**INRIM** Istituto Nazionale di Ricerca Metrologica	Ilaria Sesia i.sesia@inrim.it	Strada delle Cacce, 91 10135 TORINO, Italy
CH	**METAS** Federal Institute of Metrology	Christian Schlunegger Christian.Schlunegger@metas.ch	Lindenweg 50 CH-3003 Bern-Wabern, Switzerland

3 TWSTFT calibration campaign operational information

With the agreement on the planning by all participants, operational information on the TW link settings during this calibration campaign was confirmed in the preparation stage. The details of the operational information during the calibration campaign are described in this chapter, which includes the following five aspects:

- GEO Satellite and TW link information;
- Participating TW stations' geodetic information and signal information;
- Mobile station (MOB) signal information;
- On-site measurement schedule:
  - Planning travel route and on-site measurement dates for each participating ES;
  - Effective on-site measurement duration for each participating ES;
  - Time slots of each ES's TX&RX during this calibration campaign;
- ES channel code designation during this calibration campaign.

3.1 GEO satellite information

Table 3-1 gives the satellite identification, satellite operator, satellite geodetic coordinates and beacon frequency information of the GEO satellite which serves as the transponder for TW links during this calibration campaign.

Table 3-1 GEO satellite information

Satellite ID	Service Provider	LO* (Unit: degree)	Beacon Frequency
Telstar-11N	RiteNet Corp.	E 322° 27' 00.000"	11699.50 MHz, Vertical 11198.25 MHz, Horizontal

*The latitude coordinate of a GEO satellite is normally 0° (LA=N 0°).

3.2 TWSTFT link information

The satellite Telstar-11N operates the TWSTFT network with three transponders. For the Europe-to-Europe (EU-to-EU) links, signals are exchanged through the same transponder K02, while the transatlantic links use separate transponders for each direction: Europe-to-North America (EU-to-NA) and North America-to-Europe (NA-to-EU). In this calibration campaign, the EU-to-EU transponder is the TW signal propagation path in use. Table 3-2 lists the parameters of the TWSTFT transponders running via Telstar-11N.

Table 3-2 TWSTFT link information

Link Category	Link ID	Carrier ID	Trans-ponder ID	Allocated BW	Uplink	Downlink
					Frequency, Polarization	Frequency, Polarization
EU-to-EU	23	112677.03	K02	4.1 MHz	14253.9500 MHz, Horizontal	10953.9500 MHz, Vertical

Transatlantic	21	EU-to-NA	112673.02	K30	3.9 MHz	14047.7400 MHz, Horizontal	11747.7400 MHz, Vertical
		NA-to-EU	112701.02	K10	3.9 MHz	14297.0600 MHz, Horizontal	11497.0600 MHz, Vertical

3.3 Participating TWSTFT Earth Stations information

3.3.1 Geographical information

Table 3-3 lists the geodetic coordinates of all the participating ESs in this calibration campaign. The coordinates of the ES antennas are obtained from the header of ITU files generated on the first day of the on-site measurements with the MOB and have been confirmed by the participants. The ITU file names of the ESs are listed in Table 3-8, and the first days of measurements for the participating stations are listed in Table 3-7.

Table 3-3 List of geographical information of participating Earth Stations

ES Site ID	ES Location	Designated ES Code	ITRF Coordinates of the ES Antenna		
			LA (Unit: degree)	LO (Unit: degree)	HT (Unit: meter)
TIM	Stuttgart, DE	TIM01	N 48° 44' 16.272"	E 09° 06' 45.106"	529.00
PL	Warsaw, PL	PL01	N 52° 10' 22.08"	E 21° 11' 43.80"	137.5
PTB	Braunschweig, DE	PTB05	N 52° 17' 47.246"	E 10° 27' 50.072"	146.32
		PTB04	N 52° 17' 47.246"	E 10° 27' 50.072"	146.32
VSL	Delft, NL	VSL01	N 51° 59' 07.820"	E 04° 23' 16.950"	76.80
LTFB	Besancon, FR	LTFB01	N 47° 15' 04.652"	E 05° 59' 36.420"	358.793
ROA	San Fernando, ES	ROA01	N 36° 27' 51.530"	W 06° 12' 22.333"	74.67
OP	Paris, FR	OP01	N 48° 50' 09.236"	E 02° 20' 05.873"	78.00
NPL	Teddington, UK	NPL02	N 51° 25' 32.800"	E 359° 39' 23.300"	68.00
SP	Borås, SE	SP01	N 57° 42' 55.000"	E 012° 53' 27.000"	225.00
IT	Torino, IT	IT01	N 45° 00' 53.987"	E 7° 38' 20.686"	306.64
CH	Bern, CH	CH01	N 46° 55' 25.386"	E 7° 27' 51.002"	612.82

3.3.2 Earth Station signal information

Table 3-4 lists the TX&RX signal information of all the participating ESs during this calibration campaign.

Table 3-4 List of signal information of participating Earth Stations

ES Site ID		TX Signal Information	RX Signal Information

	Designated ES Code	TX PN Code	TX Offset Frequency (Unit: kHz)	RX Frequency from Satellite (Unit: kHz)	Downlink Frequency (Unit: kHz)	Carrier Frequency (Unit: Hz)
TIM	TIM01	14	-13.416	10954123.584	10953937	69937770
PL	PL01	10	-4.472	10954122.528	10953946	69946704
PTB	PTB05	4	17.889	10954152.889	10953968	69969073
	PTB04	24	44.721	10953995.721	10953995	69995721
VSL	VSL01	2	8.944	10954144.944	10953959	69960129
LTFB	LTFB01	15	31.305	10953982.305	10953982	69982305
ROA	ROA01	7	-44.721	10953906.279	10953906	69906279
OP	OP01	0	-8.944	10954112.328	10953941	69942226
NPL	NPL02	1	0	10954123.000	10953950	69951172
SP	SP01	3	-17.889	10954117.111	10953932	69933295
IT	IT01	6	-26.833	10954110.167	10953923	69924353
CH	CH01	9	4.472	10954137.472	10953955	69955654

3.4 Mobile Station information

Table 3-5 lists the TX&RX signal information of the mobile station MOB02. In the whole duration of this calibration campaign, the signal settings listed in Table 3-5 were kept constant.

Table 3-5 Signal information of the Mobile Station (MOB)

MOB site ID	Designated MOB Code	TX Signal Info		RX Signal Info		
		TX PN Code	TX Offset Frequency (Unit: kHz)	RX Frequency from Satellite (Unit: kHz)	Downlink Frequency (Unit: kHz)	Carrier Frequency (Unit: Hz)
MOB@<Site k>	MOB02	31	-31.305	10954105.695	10953919	69919881

Here <Site k> refers to the ES site ID at which the MOB is located during the on-site measurements.

3.5 Travel schedule and measurement plans

3.5.1 Mobile station travel map and schedule

Figure 3-1 shows a travel map of the mobile station for the calibration campaign. The pins in the map marked the visiting sites where the ESs are located. Table 3-6 lists the visiting ES sites ID, the traveling distance, and the planned measurement duration at the sites, respectively. Note that, this is the initial traveling plan which was pre-set before the calibration campaign, the actual measurement duration in the calibration campaign is listed in Table 3-7.

Figure 3-1 Mobile station travel map

Table 3-6 List of planned MOB travel map and travel schedule

Pin in the map	ES Site ID	MOB Travel Distance	Planning Measurement Duration			
			Date in ISO 8601 Format		Date in MJD Format	
			From	To	From	To
A	TIM	--	2023-08-14	2023-08-18	60170	60174
B	PL	1135 km	2023-08-25	2023-08-28	60181	60184
C	PTB	487 km	2023-09-04	2023-09-08	60191	60195
D	VSL	476 km	2023-09-11	2023-09-15	60198	60202
E	LTFB	687 km	2023-09-18	2023-09-22	60205	60209
F	ROA	1997 km	2023-09-25	2023-09-29	60212	60216
G	OP	1850 km	2023-10-02	2023-10-06	60219	60223
H	NPL	482 km	2023-10-09	2023-10-13	60226	60230
I	SP	1610 km	2023-10-16	2023-10-20	60233	60237

J	IT	1894 km	2023-10-23	2023-10-27	60240	60244
K	CH	338 km	2023-10-30	2023-11-03	60247	60251
L	TIM	301 km	--	--	--	--

Total distance: 11571 km.

3.5.2 Calibration measurement time slot plans

In addition to routine TWSTFT operations where the TW measurements only occur during even hours, measurements were also performed during odd hours in this calibration campaign. Figure 3-2 lists the measurement time slots for each ES during even-hour sessions, including the participants of this calibration campaign and other ESs joining in routine TW operations. Figure 3-3 lists the measurement time slots during odd-hour sessions which were specially arranged for this calibration campaign. In odd-hour time slots, only ESs enrolling in this campaign were included.

Accordingly, the measurement results are divided into data obtained from even hours and odd hours, and these measurement data are evaluated separately in the post-data processing procedure.

Since the measurement time interval for each TW link is set to 2 minutes, the nominal track length (NTL) of all participating Rx channels set to 119 samples, including both Rx channels of the SATRE modem and SDR channels.

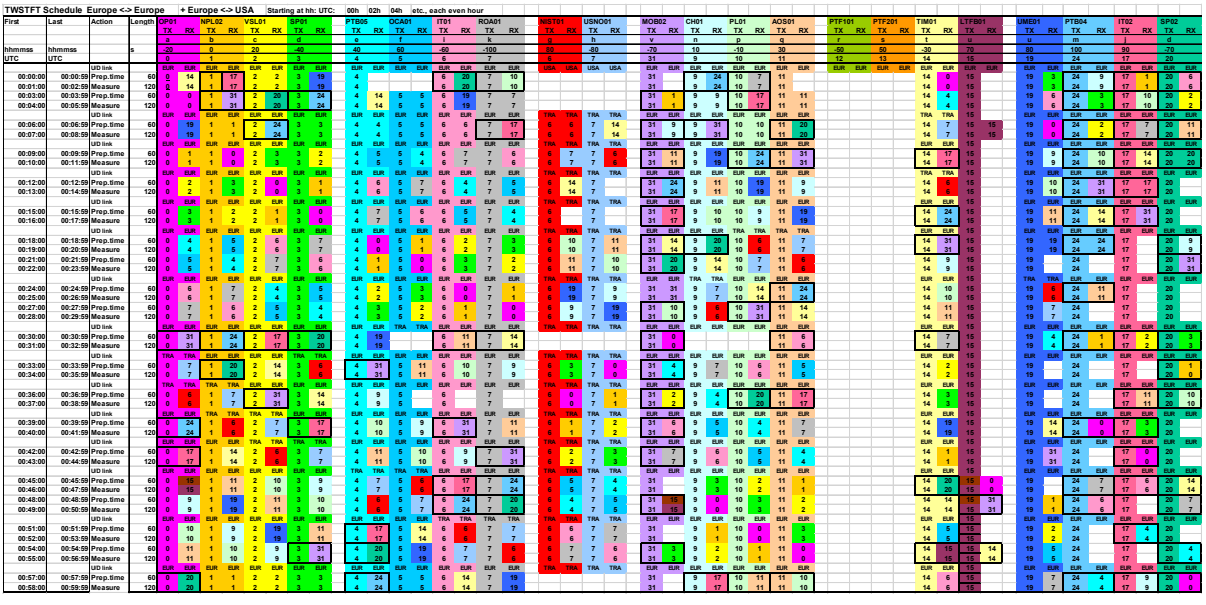

Figure 3-2 Measurement time slots in even hours session

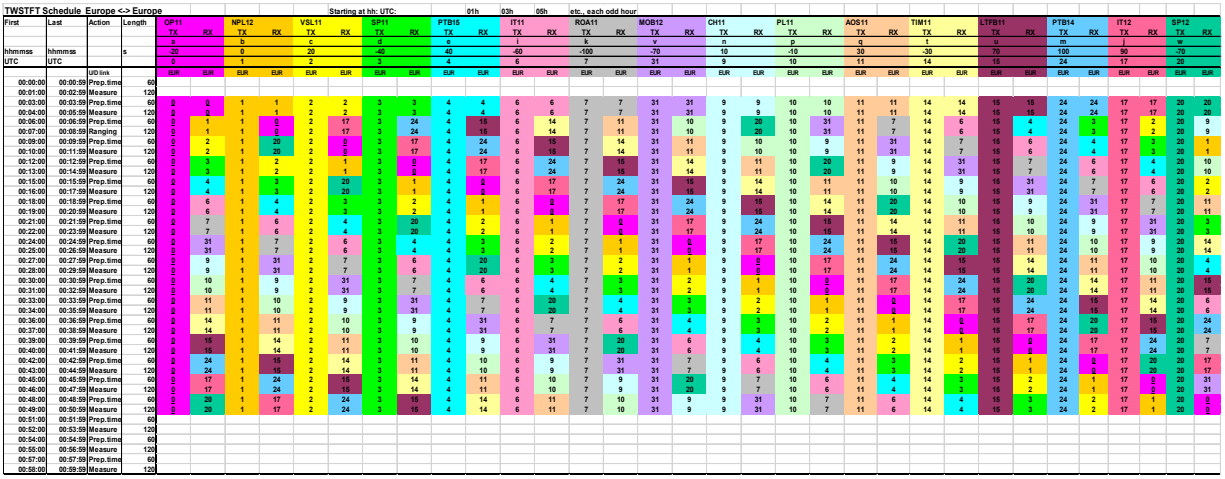

Figure 3-3 Measurement time slots in odd hours session

3.5.3 Effective measurement duration

Combining the MOB travel schedule planned in Table 3-6 and the actual on-site implementation, the effective measurement durations of the participating ESs are listed in Table 3-7. The effective measurement duration ensures the reliable status of the whole measurement set-up, including the MOB system and the ES. Table 3-7 indicates the effective measurement duration for which the on-site measurement data taken into calculation. The last column, 'Total Number of Scheduled Samples', counts the total number of measurement data that each Rx channel was scheduled to collect for the site-mode measurement during the effective intervals, according to the measurement time slots in Figure 3-2 and Figure 3-3. All the data in post-data processing listed in Chapter 7 and Chapter 9 are taken within these effective time durations.

Table 3-7 List of the effective measurement duration at the sites

ES Site ID	Effective Measurement Duration				Total Number of Scheduled Samples
	UTC Time in ISO 8601 Format		UTC Time in MJD Format		
	From	To	From	To	
TIM	2023-08-15 14:00:00	2023-08-18 15:00:00	60171.58333	60174.62500	73
PL	2023-08-25 06:00:00	2023-08-28 05:00:00	60181.25000	60184.20833	70
PTB	2023-09-04 14:00:00	2023-09-08 05:00:00	60191.58333	60195.20833	87
VSL	2023-09-11 15:00:00	2023-09-15 06:00:00	60198.62500	60202.25000	87
LTFB	2023-09-18 16:00:00	2023-09-22 06:00:00	60205.66667	60209.25000	86
ROA	2023-09-23 20:00:00	2023-09-28 06:00:00	60210.83333	60215.25000	105

OP	2023-10-03 20:00:00	2023-10-07 05:00:00	60220.83333	60224.20833	81
NPL	2023-10-09 19:00:00	2023-10-13 07:00:00	60226.79167	60230.29167	84
SP	2023-10-16 14:00:00	2023-10-19 14:00:00	60233.58333	60236.58333	72
IT	2023-10-31 20:00:00	2023-11-04 06:00:00	60248.83333	60252.25000	82
CH	2023-10-27 18:00:00	2023-10-31 04:00:00	60244.75000	60248.16667	82
PTB (closure measurements)	2023-11-09 09:30:00	2023-11-13 06:00:00	60257.39583	60261.25000	93

3.5.4 ES channel code assignments

During the routine TWSTFT operations, the designated ES code is composed of two parts: the ES Site ID and the Modem Code. The ES Site IDs normally consist of 2~4 bit letters which specify the location of the ES, and the 2-bit numeric Modem Code is to specify the TW Modem at the Site.

$$< ES\ Code > = \frac{< ES\ Site\ ID >}{2\sim4 \text{ bits letters}} \frac{< Modem\ Code >}{2 \text{ bits numerics}}$$

Since extra odd-hour measurement sessions and more Rx channels were added during this calibration campaign, small modifications were made to the designated ES code to identify the measurement sessions and Rx channels. ES codes were temporarily extended to ES channel codes with the second-to-last bit numeric number to specify hour sessions and Rx channels:

In general, the ES channel code designation follows the following format:

$$< ES\ Channel\ Code > = \frac{< ES\ Site\ ID >}{2\sim4 \text{ bits letters}} \frac{< Hour\ Session\ \&\ Rx\ Channel >}{1 \text{ bit numeric}} \frac{< 1bit\ Modem\ Code >}{1 \text{ bit numeric}}$$

In the $< Hour\ Session\ \&\ Rx\ Channel >$ bit, “0” indicates Rx1 channel measurements of the TW modem in even hours, “1” indicates Rx1 channel measurements in odd hours, “2” means Rx2 channel measurements in even hours, “3” means Rx2 channel measurements in odd hours measurements, and “5” means the SDR Rx channel measurements in both even hours and odd hours. However, exceptions occurred in some stations. The actual denotations of the ES channel code in each TW station’s ITU files are listed in Table 3-8.

Table 3-8 List of ES channel code assignments in the calibration campaign

Designated ES Code (Modem Manufacturer ID)	**Rx Channel**	**Hour Session**	**ES’s ITU File Denotation**			**MOB@<ES Site> ITU File Denotation**	
			ES Channel Code (LOC)	**MOB Channel Code (REM)**	**ITU file name**	**MOB Channel Code (LOC)**	**ES Channel Code (REM)**
TIM01 (SATRE 500)	Rx1	Even Hours	TIM01	MOB02	twtim<mj.ddd>	MOB02	TIM01
		Odd Hours	TIM11	MOB12	twtim<mj.ddd>	MOB12	TIM11
	Rx2	Even Hours	TIM01	MOB22	twtim<mj.ddd>	MOB02	TIM01

		Odd Hours	TIM11	MOB32	twtim<mj.ddd>	MOB12	TIM11
PL01 (SATRE 733)	Rx1	Even Hours	PL01	MOB02	twPL<mj.ddd>	MOB02	PL01
		Odd Hours	PL11	MOB12	twPL<mj.ddd>	MOB12	PL11
	SDR	Even Hours	PL51	MOB52	TWPL<mj.ddd>	MOB02	PL01
		Odd Hours	PL51	MOB52	TWPL<mj.ddd>	MOB12	PL11
PTB05 (SATRE 076)	Rx1	Even Hours	PTB05	MOB02	twptb<mj.ddd>	MOB02	PTB05
		Odd Hours	PTB15	MOB12	twptb<mj.ddd>	MOB12	PTB15
	Rx2	Even Hours	PTB05	MOB22	twptb<mj.ddd>	MOB02	PTB05
		Odd Hours	PTB15	MOB32	twptb<mj.ddd>	MOB12	PTB15
	SDR	Even Hours	PTB55	MOB52	sdrptb<mj.ddd>	MOB02	PTB05
		Odd Hours	PTB55	MOB52	sdrptb<mj.ddd>	MOB12	PTB15
PTB04 (SATRE 280)	Rx1	Even Hours	PTB04	MOB02	twptb4<mj.ddd>	MOB02	PTB04
		Odd Hours	PTB14	MOB12	twptb4<mj.ddd>	MOB12	PTB14
VSL01 (SATRE 716)	Rx1	Even Hours	VSL01	MOB02	TWVSL<mj.ddd>	MOB02	VSL01
		Odd Hours	VSL11	MOB12	TWVSL<mj.ddd>	MOB12	VSL11
	Rx2	Even Hours	VSL01	MOB22	TWVSL<mj.ddd>	MOB02	VSL01
		Odd Hours	VSL11	MOB32	TWVSL<mj.ddd>	MOB12	VSL11
	SDR	Even Hours	VSL51	MOB52	SDRVSL<mj.ddd>	MOB02	VSL01
		Odd Hours	VSL51	MOB52	SDRVSL<mj.ddd>	MOB12	VSL11
LTFB01 (SATRE 727)	Rx1	Even Hours	LTFB01	MOB02	TWLTFB<mj.ddd>	MOB02	LTFB01
		Odd Hours	LTFB11	MOB12	TWLTFB11<mj.ddd>	MOB12	LTFB11
	Rx2	Even Hours	LTFB21	MOB02	TWLTFB<mj.ddd>	MOB02	LTFB01
		Odd Hours	LTFB31	MOB12	TWLTFB11<mj.ddd>	MOB12	LTFB11
ROA01 (SATRE 448)	Rx1	Even Hours	ROA01	MOB02	TWROA<mj.ddd>	MOB02	ROA01
		Odd Hours	ROA11	MOB12	TWROA<mj.ddd>	MOB12	ROA11
	Rx2	Even Hours	ROA21	MOB22	TWROA<mj.ddd>	MOB02	ROA01
		Odd Hours	ROA31	MOB32	TWROA<mj.ddd>	MOB12	ROA11
	SDR	Even Hours	ROA51	MOB52	sdrroa<mj.ddd>	MOB02	ROA01
		Odd Hours	ROA51	MOB52	sdrroa<mj.ddd>	MOB12	ROA11
OP01	Rx1	Even Hours	OP01	MOB02	twop<mj.ddd>	MOB02	OP01

(SATRE 077)		Odd Hours	OP11	MOB12	twop11<mj.ddd>	MOB02	OP11
	SDR	Even Hours	OP51	MOB52	sdrop<mj.ddd>	MOB02	OP01
		Odd Hours	OP51	MOB52	sdrop<mj.ddd>	MOB02	OP11
NPL02 (SATRE 074)	Rx1	Even Hours	NPL02	MOB02	TWNPL<mj.ddd>	MOB02	NPL02
		Odd Hours	NPL12	MOB12	TWNPL<mj.ddd>	MOB12	NPL12
SP01 (SATRE 262)	Rx1	Even Hours	SP01	MOB02	twsp<mj.ddd>	MOB02	SP01
		Odd Hours	SP11	MOB12	twsp<mj.ddd>	MOB12	SP11
	Rx2	Even Hours	SP21	MOB22	twsp<mj.ddd>	MOB02	SP01
		Odd Hours	SP31	MOB32	twsp<mj.ddd>	MOB12	SP11
	SDR	Even Hours	SP51	MOB52	sdrsp<mj.ddd>	MOB02	SP01
		Odd Hours	SP51	MOB52	sdrsp<mj.ddd>	MOB12	SP11
IT01 (SATRE 416)	Rx1	Even Hours	IT01	MOB02	TWIT<mj.ddd>	MOB02	IT01
		Odd Hours	IT11	MOB12	TWIT<mj.ddd>	MOB12	IT11
	Rx2	Even Hours	IT21	MOB22	TWIT<mj.ddd>	MOB02	IT01
		Odd Hours	IT31	MOB32	TWIT<mj.ddd>	MOB12	IT11
	SDR	Even Hours	IT51	MOB51	SDRIT<mj.ddd>	MOB02	IT01
		Odd Hours	IT51	MOB51	SDRIT<mj.ddd>	MOB12	IT11
CH01 (SATRE 281)	Rx1	Even Hours	CH01	MOB02	TWCH<mj.ddd>	MOB02	CH01
		Odd Hours	CH11	MOB12	TWCH<mj.ddd>	MOB12	CH11
	Rx2	Even Hours	CH01	MOB22	TWCH<mj.ddd>	MOB02	CH01
		Odd Hours	CH11	MOB32	TWCH<mj.ddd>	MOB12	CH11
	SDR	Even Hours	CH01	MOB52	TWCH<mj.ddd>	MOB02	CH01
		Odd Hours	CH11	MOB62	TWCH<mj.ddd>	MOB12	CH11

<mj.ddd> denotes the 5-digit numeric of the MJD date on which measurement data are recorded, with a ‘dot’ splitting between the higher two digits and lower three digits.

4 Background information on TWSTFT techniques and TWSTFT calibration

4.1 Principle of TWSTFT

TWSTFT is a technology which exchanges timing signals through a GEO satellite for high-precision and high-accuracy remote clock comparisons. It is done by transmission and reception of radiofrequency (RF) signals with pseudorandom noise (PN) codes binary phase-shift keying (BPSK) modulated on the intermediate frequency (IF). The modulation signal which is generated by the local modem is synchronized with the local clock and is then sent to the remote modem. In the meantime, the signal which is received from the remote modem is compared with the local clock. By this two-way timing message exchange between two remote modems, the two local clock signals are compared via signal propagation path through GEO satellite transponders. The modem involved in time signal modulation and demodulation is called the TWSTFT modem (or TW modem for short), and the time message exchange link between two remote TW modems is called a TWSTFT link (or TW link for short).

In this section, the introduction to the principle of TWSTFT technology takes Recommendation ITU-R TF.1153-4 [RD06] as the reference. All the denotations are aligned with this ITU-R Recommendation.

4.1.1 TWSTFT set-up

The setup for the implementation of the TWSTFT system is shown in Figure 4-1. As described by Figure 4-1, time messages are exchanged between Site 1 and Site 2 remotely via a GEO satellite. At each site, the local set-up to implement TWSTFT is called an Earth Station (ES) or a TWSTFT station, which mainly includes:

- A local physical clock, which is connected or is traceable to the local time scale such as local UTC realization.
- A local TW modem, which is connected to the local time-scale and performs IF signal modulation and de-modulation.
- A transmitter and a receiver, which are the general names for the front-end RF stage. A transmitter includes the up-converter, the front-end power amplifier, the very small aperture terminal (VSAT) antenna, etc. A receiver includes the VSAT antenna, the front-end low-noise amplifier, the down-converter, etc.
- A time interval counter (TIC), which compares the local time with the demodulated time signals sent from the remote station via a TW link.

In addition, a GEO satellite, which contains one or more transponders, receives and then forwards time signals from one ES to another via transponders to implement a time message propagation path between two ESs.

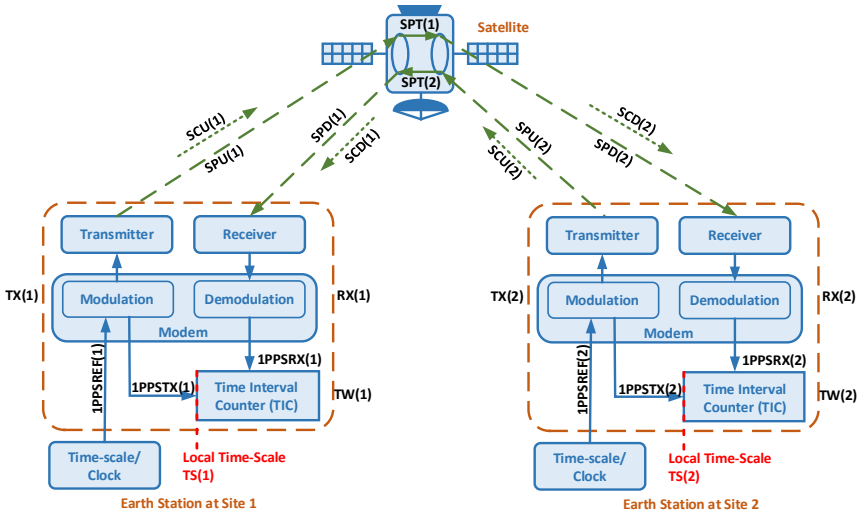

Figure 4-1 TWSTFT principle

4.1.2 TWSTFT mathematical model

Based on the TW system architecture illustrated by Figure 4-1, signals and latencies in the TW set-up can be defined and subtracted from hardware set-ups, resulting in a mathematical model.

In a TWSTFT station, the timescale (TS) of the local TW system is defined as the 1PPSTX signal generated by the TW modem. Take Figure 4-1 for instance, the 1PPSTX output signal from the TW modem at Site k can be defined as $\mathrm{TS(k)} \stackrel{\text{def}}{=} \mathrm{1PPSTX(k)}$, where k=1 or 2. In the receiver path, the output signal from the demodulation unit of the TW modem at Site k, which is a demodulated signal received from the remote station and reconstituted to a 1PPS signal, is named 1PPSRX(k). The phase of 1PPSTX(k) and 1PPSRX(k) is compared by a TIC, and the TIC reading at Site k is denoted as TW(k).

In the propagation path of a TW station, the transmitter delay of an ES at Site k is defined as the latency of the transmission path in an ES and is named TX(k). The receiver delay of an ES at Site k is defined as the latency of the reception path in an ES and is named RX(k).

In the free-space propagation path of the TW messages, SPU(k) is defined as the signal path uplink delay from Site k to the satellite transponder, SPD(k) is defined as the signal path downlink delay from Site k to the satellite transponder, SCU(k) and SCD(k) are the Sagnac corrections in the uplink and downlink from Site k to the satellite, respectively.

In the satellite transponders, SPT(k) is the satellite path delay of the TW message sent from Site k through the transponder.

Then, the TIC reading of the Earth Station at Site 1(ES1) can be concluded as:

$$\mathrm{TW(1)} = \mathrm{TS(1)} - \mathrm{TS(2)} + \mathrm{TX(2)} + \mathrm{SPU(2)} + \mathrm{SCU(2)} + \mathrm{SPT(2)} + \mathrm{SPD(1)} + \mathrm{SCD(1)} + \mathrm{RX(1)} \quad (1)$$

Accordingly, the TIC reading at ES2 is:

$$\mathrm{TW(2)} = \mathrm{TS(2)} - \mathrm{TS(1)} + \mathrm{TX(1)} + \mathrm{SPU(1)} + \mathrm{SCU(1)} + \mathrm{SPT(1)} + \mathrm{SPD(2)} + \mathrm{SCD(2)} + \mathrm{RX(2)} \quad (2)$$

Therefore, the time-scale difference between the two remote TW stations can be calculated by subtracting the TIC readings of these two stations. Then the following relation can be obtained which is called *two-way equation*:

$$\begin{aligned}\mathrm{TS(1)} - \mathrm{TS(2)} = \ & 0.5[\mathrm{TW(1)} - \mathrm{TW(2)}] \\ & +0.5[\mathrm{SPT(1)} - \mathrm{SPT(2)}] \\ & -0.5[\mathrm{SCD(1)} - \mathrm{SCU(1)}]\end{aligned}$$

$$
\begin{aligned}
&+0.5[\mathrm{SCD}(2)-\mathrm{SCU}(2)]\\
&+0.5[\mathrm{SPU}(1)-\mathrm{SPD}(1)]\\
&-0.5[\mathrm{SPU}(2)-\mathrm{SPD}(2)]\\
&+0.5[\mathrm{TX}(1)-\mathrm{RX}(1)]\\
&-0.5[\mathrm{TX}(2)-\mathrm{RX}(2)]
\end{aligned}
\qquad (3)
$$

Since SPU(k), SPD(k), SCU(k) and SCD(k) are computed from the geographical location of the ESs and the GEO satellite, the following relations can be determined: $\mathrm{SCU(k)}=-\mathrm{SCD(k)}$ and $\mathrm{SPU(k)}=\mathrm{SPD(k)}$, where k=1 or 2. The sign of the Sagnac correction for the downlink SCD(k) is opposite to the sign of the Sagnac correction for the uplink SCU(k) due to the opposite propagation directions of the signals.

When the on-satellite TX&RX antenna and the on-satellite transponder channel are the same for bi-directional signals in a TW link, the signal delays through the satellite can be considered as the same in both directions, where $\mathrm{SPT}(1)=\mathrm{SPT}(2)$. Defining the bi-directional signal total propagation delays outside the ESs as $\mathrm{SP}(1)=\mathrm{SPU}(1)+\mathrm{SPT}(1)+\mathrm{SPD}(2)$ and $\mathrm{SP}(2)=\mathrm{SPU}(2)+\mathrm{SPT}(2)+\mathrm{SPD}(1)$ respectively, $\mathrm{SP}(1)=\mathrm{SP}(2)$ can be deduced in the scenario of reciprocity. In the TW EU-to-EU link with the link ID of 23, all the participating TW links share the same transponder K02 and the same uplink & downlink frequencies, as indicated in Table 3-2, therefore, all the TW links in this calibration campaign fit the scenario of reciprocity.

In summary, the *two-way equation* (3) can be simplified as the following expression when satisfying the relations of $\mathrm{SCU}(1)=-\mathrm{SCD}(1),\mathrm{SCU}(2)=-\mathrm{SCD}(2)$ and $\mathrm{SP}(1)=\mathrm{SP}(2)$:

$$
\begin{aligned}
\mathrm{TS}(1)-\mathrm{TS}(2)=\ & 0.5[\mathrm{TW}(1)-\mathrm{TW}(2)]\\
&\underbrace{-[\mathrm{SCD}(1)-\mathrm{SCD}(2)]+0.5[\mathrm{DLD}(1)-\mathrm{DLD}(2)]}_{\mathrm{CALR}(1,2)}\\
=\ & 0.5[\mathrm{TW}(1)-\mathrm{TW}(2)]+\mathrm{CALR}(1,2)
\end{aligned}
\qquad (4)
$$

where $\mathrm{DLD(k)}$ is defined as the signal-delay difference between the transmitter and the receiver path of TW station k and denoted as $\mathrm{DLD(k)}=\mathrm{TX(k)}-\mathrm{RX(k)},\mathrm{k}=1\ \mathrm{or}\ 2$. $\mathrm{CALR}(1,2)$ is defined as $\mathrm{CALR}(1,2)\triangleq-[\mathrm{SCD}(1)-\mathrm{SCD}(2)]+0.5[\mathrm{DLD}(1)-\mathrm{DLD}(2)]$.

CALR(1,2) covers the factors of the ES delay asymmetries and the Sagnac correction delays. The CALR(1,2) value should be constant when the variations related to temperature are ignored.

4.1.3 Time dissemination from UTC(k) to TWSTFT ES local timescale

In order to remotely compare two UTC realizations via the TW system, the local timescale of the TW station TS(k) (or named 1PPSTX(k)) needs to be traceable to the local UTC realization UTC(k).

UTC(k) could be either a physical timescale or a mathematical timescale, and it can be represented by a physical clock CLOCK(k). Each UTC laboratory determines the relation between [UTC(k)-CLOCK(k)]. In the meantime, as illustrated in Figure 4-1, the ES at Site k takes the external signal 1PPSREF(k) as the reference clock, and the local ES timescale 1PPSTX(k) is tracking to 1PPSREF(k) with fixed delay [1PPSREF(k)-1PPSTX(k)]. When connecting the signal from CLOCK(k) to the reference clock input of the ES, with the delay of [CLOCK(k)-1PPSREF(k)], the local UTC time is disseminated to the local ES time scale. This time dissemination chain is demonstrated in Figure 4-2, and the relation between UTC(k) and 1PPSTX(k) is expressed by the following equation:

$$
\begin{aligned}
\mathrm{UTC(k)}&=\overbrace{\mathrm{1PPSTX(k)}}^{\mathrm{TS(k)}}+\underbrace{[\mathrm{UTC(k)}-\mathrm{CLOCK(k)}]+[\mathrm{CLOCK(k)}-\mathrm{1PPSREF(k)}]+[\mathrm{1PPSREF(k)}-\mathrm{1PPSTX(k)}]}_{\mathrm{REFDELAY(k)}}\\
&=\mathrm{TS(k)}+\mathrm{REFDELAY(k)}
\end{aligned}
\qquad (5)
$$

where $\mathrm{REFDELAY(k)}$ indicates the time dissemination from the local UTC to the timescale of the local ES, and is defined as:

$$\mathrm{REFDELAY(k)}\triangleq[\mathrm{UTC(k)}-\mathrm{CLOCK(k)}]+[\mathrm{CLOCK(k)}-\mathrm{1PPSREF(k)}]+[\mathrm{1PPSREF(k)}-\mathrm{1PPSTX(k)}]$$

$$= \mathrm{UTC(k)} - \mathrm{1PPSTX(k)} \qquad (6)$$

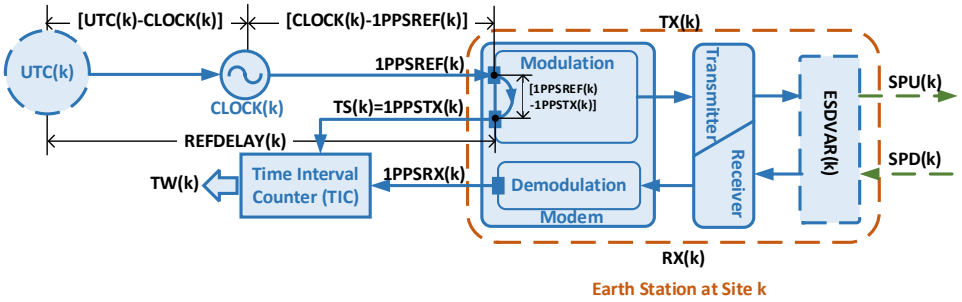

Figure 4-2 Time dissemination from UTC(k) to ES timescale TS(k)

Furthermore, an additional correction item can be supplemented to the original structure of an ES (see Figure 4-1) to improve the flexibility of the ES model. When there is an extra delay variation on an ES with respect to the ES delay present at the time of calibration, a delay variation item, named ESDVAR(k), can be added to correct the delay changes of the ES at Site k. Figure 4-2 shows the correction added to the original ES structure.

The delay variation of an ES leads to the change in TIC reading accordingly. After the delay changes of the ES, the total transmission/reception propagation delay of the time message is represented by $[\mathrm{TW(k)} + \mathrm{ESDVAR(k)}]$ instead of $\mathrm{TW(k)}$. In the case of the additional ES internal delay modification, equation (1) and equation (2) are revised as:

$$[\mathrm{TW}(1) + \mathrm{ESDVAR}(1)] = \mathrm{TS}(1) - \mathrm{TS}(2) + \mathrm{TX}(2) + \mathrm{SPU}(2) + \mathrm{SCU}(2) + \mathrm{SPT}(2) + \mathrm{SPD}(1) + \mathrm{SCD}(1) + \mathrm{RX}(1) \qquad (7)$$

$$[\mathrm{TW}(2) + \mathrm{ESDVAR}(2)] = \mathrm{TS}(2) - \mathrm{TS}(1) + \mathrm{TX}(1) + \mathrm{SPU}(1) + \mathrm{SCU}(1) + \mathrm{SPT}(1) + \mathrm{SPD}(2) + \mathrm{SCD}(2) + \mathrm{RX}(2) \qquad (8)$$

In the scenario of reciprocity where $\mathrm{SCU}(1) = -\mathrm{SCD}(1), \mathrm{SCU}(2) = -\mathrm{SCD}(2)$ and $\mathrm{SP}(1) = \mathrm{SP}(2)$, the relation between local UTC realization and TW station measurement parameters is obtained by combining equation (7), equation (8) with equation (5), as:

$$\begin{aligned} \mathrm{UTC}(1) - \mathrm{UTC}(2) = \; & 0.5\,[\mathrm{TW}(1) + \mathrm{ESDVAR}(1)] + \mathrm{REFDELAY}(1) \\ & -0.5\,[\mathrm{TW}(2) + \mathrm{ESDVAR}(2)] - \mathrm{REFDELAY}(2) \\ & \underbrace{-[\mathrm{SCD}(1) - \mathrm{SCD}(2)] + 0.5[\mathrm{DLD}(1) - \mathrm{DLD}(2)]}_{\mathrm{CALR}(1,2)} \end{aligned} \qquad (9)$$

where $\mathrm{CALR}(1,2) \triangleq -[\mathrm{SCD}(1) - \mathrm{SCD}(2)] + 0.5[\mathrm{DLD}(1) - \mathrm{DLD}(2)]$.

Here equation (9) can be considered as an extension to the simplified two-way equation (4), where the traceability to UTC(k) and the extra delay variation of the ESs are taken into consideration. Based on equation (9), the absolute time difference of two remote UTC realizations is obtained by reading TIC outputs and pre-processing REFDELAYs, ESDVARs and CALR(1,2). REFDELAYs and ESDVARs are determined by each ES. CALR(1,2) for all the TW link combinations of the participating ESs will be determined by this calibration campaign.

4.1.4 Sagnac-effect correction

For a geostationary (GEO) satellite where the latitude of the satellite is 0° in geodetic coordinates, the Sagnac correction for the downlink path from the GEO satellite to the Earth Station at Site k is calculated by the following equation with sufficient accuracy [RD06]:

$$\mathrm{SCD(k)} = \frac{\Omega}{c^2}\mathrm{R}(\mathrm{a}\cos[\tan^{-1}\{(1-\mathrm{f})\tan[\mathrm{LA(k)}]\}] + \mathrm{H(k)}\cos[\mathrm{LA(k)}])\sin[\mathrm{LO(k)} - \mathrm{LO(s)}] \quad (10)$$

where the Earth is considered an ellipsoid at first approximation, and

$\mathrm{SCD(k)}$ is the Sagnac correction value in the downlink at Site k,

Ω is the Earth rotation rate, and $\Omega = 7.2921 \times 10^{-5}\ \mathrm{rad/s}$,

c is the speed of light, and $c = 299\,792\,458\ \mathrm{m/s}$,

R is the satellite orbit radius, and $\mathrm{R} = 42\,164\,000\ \mathrm{m}$,

a is the Earth equarorial radius, and $\mathrm{a} = 6\,378\,137\ \mathrm{m}$,

f is the Flattening of the Earth ellipsoid, and $\mathrm{f} = 1/298.257222$,

$\mathrm{LA(k)}$ is the latitude of the ES at Site k in geodetic coordinates and is in unit of rad,

$\mathrm{H(k)}$ is the height of the ES at Site k in the unit of meter,

$\mathrm{LO(k)}$ is the longitude of the ES at Site k in geodetic coordinates and is in unit of rad,

$\mathrm{LO(s)}$ is the longitude of the GEO satellite in geodetic coordinates and is in unit of rad.

4.2 TWSTFT calibration methods

The purpose of the TWSTFT calibration is to determine CALR(1,2) in TW links, as a consequence, the local timescale differences between two remote TW stations is calculated following equation (9). In general, two calibration methods can be adopted for CALR(1,2) determination: site-mode calibration and baseline-mode calibration. Both methods require a mobile TWSTFT station (MOB) to be involved in the measurements, where the MOB is taken as the common reference to be compared with the delay asymmetry of the ESs under test.

4.2.1 Site-mode calibration scheme

The working principle of the site-mode calibration method is demonstrated in Figure 4-3, where ES1 denotes the ES located at Site 1 and ES2 denotes the ES located at Site 2, MOB@1 and MOB@2 indicates the same MOB placed at Site 1 and Site 2, respectively. To calibrate a pair of stations ES1 and ES2 in a TW link using site-mode calibration, two separate measurements are included:

- Measurement S1 located at Site 1
- Measurement S2 located at Site 2

At each site, the MOB and the local ES need to be traceable to the same timescale, for instance, local UTC realization. This setup can normally be implemented by connecting the MOB and the local ES to the same clock. After the on-site set-up, TW link of [ES1-MOB@1] is operated in Measurement S1. And similarly, TW link of [ES2-MOB@2] is operated in Measurement S2. The measurement scheme and the post-data processing are described in detail as follows:

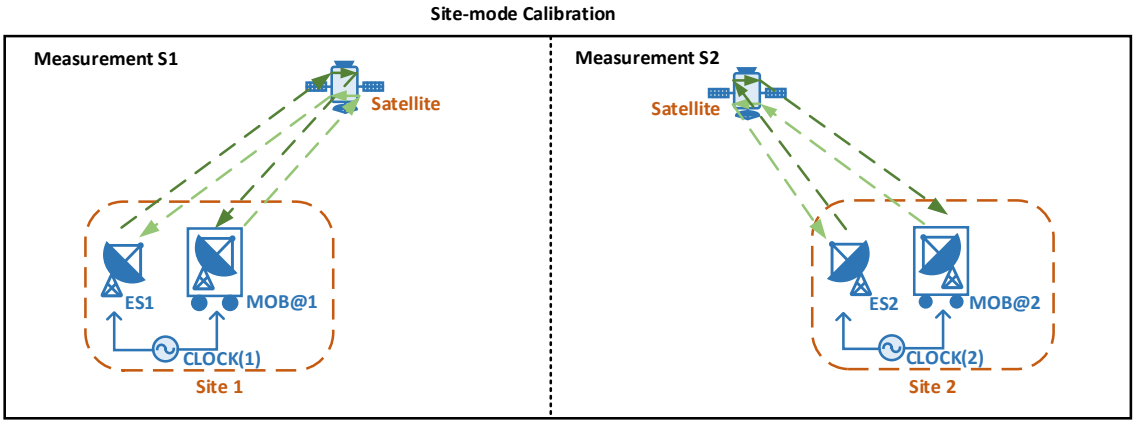

Figure 4-3 Principle of site-mode calibration

Measurement S1: TWSTFT link measurement between ES1 and MOB@1 at Site 1

At site 1, use the simplified two-way equation to describe the TW link between ES1 and MOB@1. In this scenario, equation (4) is re-written as:

$$\underbrace{[\mathrm{TS}(1)-\mathrm{TS}(\mathrm{MOB@1})]}_{\text{TW Link [ES1−MOB@1]}} = 0.5[\mathrm{TW}(1)-\mathrm{TW}(\mathrm{MOB@1})] + \underbrace{\left\{-[\mathrm{SCD}(1)-\mathrm{SCD}(\mathrm{MOB@1})] + \underbrace{0.5[\mathrm{DLD}(1)-\mathrm{DLD}(\mathrm{MOB@1})]}_{\mathrm{CCD}(1,\mathrm{MOB@1})}\right\}}_{\mathrm{CALR}(1,\mathrm{MOB@1})}$$
$$= 0.5[\mathrm{TW}(1)-\mathrm{TW}(\mathrm{MOB@1})] + \mathrm{CALR}(1,\mathrm{MOB@1})$$

(11)

where Common Clock Difference (CCD) between ES1 and MOB at Site 1 is defined as $\mathrm{CCD}(1,\mathrm{MOB@1}) \triangleq 0.5[\mathrm{DLD}(1)-\mathrm{DLD}(\mathrm{MOB@1})]$, and accordingly $\mathrm{CALR}(1,\mathrm{MOB@1}) \triangleq -[\mathrm{SCD}(1)-\mathrm{SCD}(\mathrm{MOB@1})] + \mathrm{CCD}(1,\mathrm{MOB@1})$.

Since ES1 and MOB@1 are in the same location during Measurement S1, the equation $\mathrm{SCD}(1) = \mathrm{SCD}(\mathrm{MOB@1})$ holds in this case. Then $\mathrm{CALR}(1,\mathrm{MOB@1})$ is obtained from the relation described by equation (11) as:

$$\mathrm{CALR}(1,\mathrm{MOB@1}) = \mathrm{CCD}(1,\mathrm{MOB@1}) = \underbrace{[\mathrm{TS}(1)-\mathrm{TS}(\mathrm{MOB@1})]}_{\text{TW Link [ES1−MOB@1]}} - 0.5[\mathrm{TW}(1)-\mathrm{TW}(\mathrm{MOB@1})]$$

(12)

Meanwhile, considering the time dissemination at Site 1, the timescale (TS) of ES1 and MOB@1 are both connected to the same local timescale at Site 1(e.g. UTC(Site 1)) in the set-up. According to the time dissemination relation explained in equation (5), the relation between TS of ES1 and MOB@1 reads:

$$\mathrm{UTC(Site\ 1)} = \mathrm{TS}(1) + \mathrm{REFDELAY}(1)$$
$$= \mathrm{TS}(\mathrm{MOB@1}) + \mathrm{REFDELAY}(\mathrm{MOB@1})$$

(13)

Hence the TS difference between ES1 and MOB@1 is obtained from the perspective of local time dissemination as:

$$\underbrace{[\mathrm{TS}(1)-\mathrm{TS}(\mathrm{MOB@1})]}_{\text{Local time dissemination [ES1− MOB@1]}} = -[\mathrm{REFDELAY}(1)-\mathrm{REFDELAY}(\mathrm{MOB@1})]$$

(14)

Combing equation (12) and equation (14), the CALR of the TW link [ES1-MOB@1] is derived as:

$$\mathrm{CALR}(1,\mathrm{MOB@1}) = \mathrm{CCD}(1,\mathrm{MOB@1}) = -[\mathrm{REFDELAY}(1) - \mathrm{REFDELAY}(\mathrm{MOB@1})] - 0.5[\mathrm{TW}(1) - \mathrm{TW}(\mathrm{MOB@1})] \quad (15)$$

Measurement S2: TWSTFT link measurement between ES2 and MOB at Site 2

Similar to Measurement S1, Measurement S2 builds up the TW link between ES2 and MOB at Site 2 as:

$$\underbrace{[\mathrm{TS}(2) - \mathrm{TS}(\mathrm{MOB@2})]}_{\text{TW Link [ES2−MOB@2]}} = 0.5[\mathrm{TW}(2) - \mathrm{TW}(\mathrm{MOB@2})] \underbrace{-[\mathrm{SCD}(2) - \mathrm{SCD}(\mathrm{MOB@2})] + \underbrace{0.5[\mathrm{DLD}(2) - \mathrm{DLD}(\mathrm{MOB@2})]}_{\mathrm{CCD}(2,\mathrm{MOB@2})}}_{\mathrm{CALR}(2,\mathrm{MOB@2})} \quad (16)$$

where $\mathrm{CCD}(2,\mathrm{MOB@2}) \triangleq 0.5[\mathrm{DLD}(2) - \mathrm{DLD}(\mathrm{MOB@2})]$, $\mathrm{CALR}(2,\mathrm{MOB@2}) \triangleq -[\mathrm{SCD}(2) - \mathrm{SCD}(\mathrm{MOB@2})] + \mathrm{CCD}(2,\mathrm{MOB@2})$, and the relation of $\mathrm{SCD}(2) = \mathrm{SCD}(\mathrm{MOB@2})$ is also valid since ES2 and MOB@2 are in the same location. Then CALR(2, MOB@2) is deduced from equation (16) as:

$$\mathrm{CALR}(2,\mathrm{MOB@2}) = \mathrm{CCD}(2,\mathrm{MOB@2}) = \underbrace{[\mathrm{TS}(2) - \mathrm{TS}(\mathrm{MOB@2})]}_{\text{TW Link [ES2−MOB@2]}} - 0.5[\mathrm{TW}(2) - \mathrm{TW}(\mathrm{MOB@2})] \quad (17)$$

Since both ES2 and MOB@2 are connected to the same local time scale e.g. UTC(Site 2) at Site 2, then the TS difference between ES2 and MOB@2 reads:

$$\begin{aligned} \mathrm{UTC}(\text{Site 2}) &= \mathrm{TS}(2) + \mathrm{REFDELAY}(2) \\ &= \mathrm{TS}(\mathrm{MOB@2}) + \mathrm{REFDELAY}(\mathrm{MOB@2}) \end{aligned} \quad (18)$$

$$\underbrace{[\mathrm{TS}(2) - \mathrm{TS}(\mathrm{MOB@2})]}_{\text{Local time dissemination [ES2− MOB@2]}} = -[\mathrm{REFDELAY}(2) - \mathrm{REFDELAY}(\mathrm{MOB@2})] \quad (19)$$

By combining equation (17) and equation (19), the CALR of [ES2-MOB@2] link can be deduced as:

$$\mathrm{CALR}(2,\mathrm{MOB@2}) = \mathrm{CCD}(2,\mathrm{MOB@2}) = -[\mathrm{REFDELAY}(2) - \mathrm{REFDELAY}(\mathrm{MOB@2})] - 0.5[\mathrm{TW}(2) - \mathrm{TW}(\mathrm{MOB@2})] \quad (20)$$

Post-data processing: Calculate CALR of TW link between ES1 and ES2 based on site-mode calibration

Recapping the definition of $\mathrm{CALR}(1,2)$ firstly appeared in equation (4), the CALR of [ES1-ES2] link is expressed as:

$$\mathrm{CALR}(1,2) \triangleq -[\mathrm{SCD}(1) - \mathrm{SCD}(2)] + 0.5[\mathrm{DLD}(1) - \mathrm{DLD}(2)]$$

In Measurement S1 and Measurement S2, the DLD of ES1 and ES2 are compared with the DLD of the MOB, respectively. When transported from one site to another, the internal delay of the MOB is supposed to be constant, and therefore $\mathrm{DLD}(\mathrm{MOB@1}) = \mathrm{DLD}(\mathrm{MOB@2})$ can be assumed. Note that, the consistency of the DLD(MOB) is a nominal assumption. In fact, subtle variations on the DLD(MOB) exist and this term contributes to the uncertainty of the measurement. The variations on DLD(MOB) are evaluated by closure measurements, and the inconsistency of the MOB is added as a Type B uncertainty ub,3. The details on the inconsistency of MOB are analysed in Section 6.3.

Hence the $\mathrm{CALR}(1,2)$ definition equation is re-written by combining the CCD definitions and the relation deduced in equation (15) and (20) as:

$$\begin{aligned}\mathrm{CALR}(1,2) &= -[\mathrm{SCD}(1)-\mathrm{SCD}(2)] + \underbrace{0.5[\mathrm{DLD}(1)-\mathrm{DLD}(\mathrm{MOB@1})]}_{\mathrm{CCD}(1,\mathrm{MOB@1})} - \underbrace{0.5[\mathrm{DLD}(2)-\mathrm{DLD}(\mathrm{MOB@2})]}_{\mathrm{CCD}(2,\mathrm{MOB@2})} \\ &= -[\mathrm{SCD}(1)-\mathrm{SCD}(2)] + [\mathrm{CCD}(1,\mathrm{MOB@1}) - \mathrm{CCD}(2,\mathrm{MOB@2})]\end{aligned} \quad (21)$$

where $\mathrm{SCD}(1)$ and $\mathrm{SCD}(2)$ can be calculated by the Sagnac-effect correction equation (10), $\mathrm{CCD}(1,\mathrm{MOB@1})$ and $\mathrm{CCD}(2,\mathrm{MOB@2})$ is obtained by equation (15) and (20) in Measurement S1 and Measurement S2, respectively. Equation (21) is the final $\mathrm{CALR}(1,2)$ computation equation for TW link [ES1-ES2] in site-mode calibration.

4.2.2 Baseline-mode calibration scheme

The working principle of the baseline-mode calibration method is demonstrated in Figure 4-4, where ES1 denotes the ES located at Site 1 and ES2 denotes the ES located at Site 2, MOB@1 and MOB@2 indicate the same MOB placed at Site 1 and Site 2, respectively. To calibrate a pair of stations ES1 and ES2 in a TW link, at least two separate measurements are included:

- Measurement B1 located at Site 1: which operates the TW link of [ES1-MOB@1]
- Measurement B2 located at Site 2: which operates the TW links of [ES1-ES2] and [ES1-MOB@2]

If applicable, another two measurements can be added for redundancy measurements:

- Measurement B3 located at Site 2: which operates the TW link of [ES2-MOB@2]
- Measurement B4 located at Site 1: which operates the TW links of [ES2-ES1] and [ES2-MOB@1]

When being placed at the site, the MOB needs to be connected to the same clock as the local ES, or the MOB is connected to the clock which is traceable to the same local timescale as the local ES, for instance, the local UTC realization.

The measurement scheme and the post-data processing are described in detail as follows:

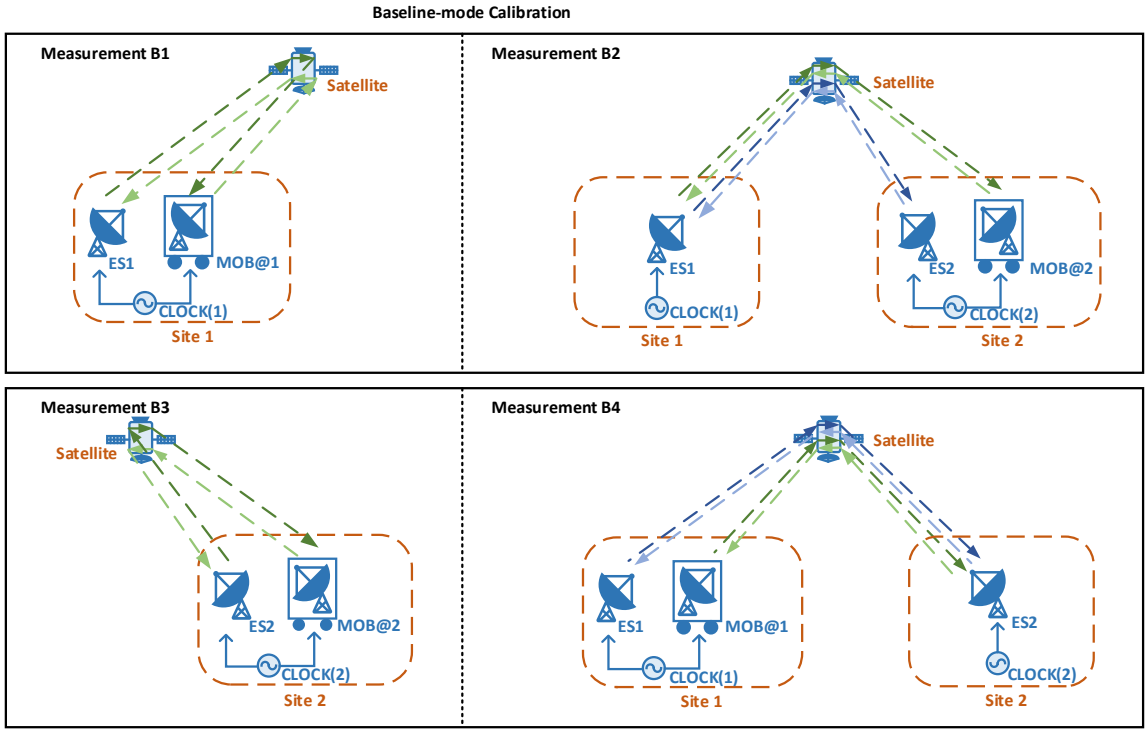

Figure 4-4 Principle of baseline-mode calibration

Measurement B1: TWSTFT link measurement between ES1 and MOB@1 at Site 1

The operation of Measurement B1 is the same as Measurement S1 in site-mode calibration as described in Section 4.2.1, and it can derive the same relation as:

$$\mathrm{CALR}(1,\mathrm{MOB@1}) = \mathrm{CCD}(1,\mathrm{MOB@1}) = -[\mathrm{REFDELAY}(1) - \mathrm{REFDELAY}(\mathrm{MOB@1})] - 0.5[\mathrm{TW}(1) - \mathrm{TW}(\mathrm{MOB@1})] \quad (22)$$

Measurement B2: TWSTFT link measurements between ES1 at Site 1 and ES2&MOB at Site 2

Measurement B2 contains two TW link measurements: The TW link between ES1 at Site 1 and MOB at Site 2 [ES1-MOB@2], and the TW link between ES1 at Site 1 and ES2 at Site 2 [ES1-ES2].

For the scenario of [ES1-MOB@2] link, equation (4) can be re-written to describe the relation in this TW link as:

$$\underbrace{[\mathrm{TS}(1) - \mathrm{TS}(\mathrm{MOB@2})]}_{\text{TW link }[ES1-\mathrm{MOB@2}]} = 0.5[\mathrm{TW}(1) - \mathrm{TW}(\mathrm{MOB@2})] - [\mathrm{SCD}(1) - \mathrm{SCD}(2)] + \underbrace{0.5[\mathrm{DLD}(1) - \mathrm{DLD}(\mathrm{MOB@2})]}_{\mathrm{CCD}(1,\mathrm{MOB@2})} \quad (23)$$

For the TW link of [ES1-ES2], the same relation is deduced according to equation (4):

$$\underbrace{[\mathrm{TS}(1) - \mathrm{TS}(2)]}_{\text{TW link }[ES1-ES2]} = 0.5[\mathrm{TW}(1) - \mathrm{TW}(2)] \underbrace{-[\mathrm{SCD}(1) - \mathrm{SCD}(2)] + 0.5[\mathrm{DLD}(1) - \mathrm{DLD}(2)]}_{\mathrm{CALR}(1,2)} \quad (24)$$

In the meantime, the local time dissemination at Site 2 follows the relation described in equation (5) as:

$$\begin{aligned}\mathrm{UTC(Site\ 2)} &= \mathrm{TS(2)} + \mathrm{REFDELAY(2)} \\ &= \mathrm{TS(MOB@2)} + \mathrm{REFDELAY(MOB@2)}\end{aligned}$$

(25)

Thus, the local time dissemination at Site 2 is linked to the REFELAY relations as:

$$\underbrace{[\mathrm{TS(2)} - \mathrm{TS(MOB@2)}]}_{\text{Local time dissemination [ES2− MOB@2]}} = -[\mathrm{REFDELAY(2)} - \mathrm{REFDELAY(MOB@2)}]$$

(26)

By making the same assumption for Measurement S1, that the DLD of the MOB kept constant during the calibration campaign, the relation $\mathrm{CCD}(1,\mathrm{MOB@2}) = \mathrm{CCD}(1,\mathrm{MOB@1})$ is deduced accordingly. Then the following equation is obtained by combining equation (23), equation (24) and equation (26):

$$\begin{aligned}\mathrm{CALR_{MeasB2}}(1,2) = &-\underbrace{\{-0.5[\mathrm{TW(1)} - \mathrm{TW(MOB@2)}] + 0.5[\mathrm{TW(1)} - \mathrm{TW(2)}] - [\mathrm{REFDELAY(2)} - \mathrm{REFDELAY(MOB@2)}]\}}_{\text{Bridged CCD(2,MOB@2)}} \\ &- [\mathrm{SCD(1)} - \mathrm{SCD(2)}] + \mathrm{CCD}(1,\mathrm{MOB@1}) \\ = &-[\mathrm{SCD(1)} - \mathrm{SCD(2)}] + [\mathrm{CCD}(1,\mathrm{MOB@1}) - \text{Bridged CCD}(2,\mathrm{MOB@2})]\end{aligned}$$

(27)

where the bridged CCD(2,MOB@2) is defined as:

$$\begin{aligned}\text{Bridged CCD}(2,\mathrm{MOB@2}) \overset{\text{def}}{\equiv} &-0.5\underbrace{[\mathrm{TW(1)} - \mathrm{TW(MOB@2)}]}_{\text{from TW link [ES1−MOB@2]}} + 0.5\ \underbrace{[\mathrm{TW(1)} - \mathrm{TW(2)}]}_{\text{from TW link [ES1−ES2]}} \\ &-[\mathrm{REFDELAY(2)} - \mathrm{REFDELAY(MOB@2)}]\end{aligned}$$

(28)

Measurement B3: TWSTFT link measurement between ES2 and MOB@2 at Site 2

The operation of Measurement B3 is the same as Measurement S2 in site-mode calibration described in Section 4.2.1, and the CALR of the [ES2-MOB@2] is obtained accordingly:

$$\mathrm{CALR}(2,\mathrm{MOB@2}) = \mathrm{CCD}(2,\mathrm{MOB@2}) = -[\mathrm{REFDELAY(2)} - \mathrm{REFDELAY(MOB@2)}] - 0.5[\mathrm{TW(2)} - \mathrm{TW(MOB@2)}]$$

(29)

Measurement B4: TWSTFT link measurements between ES2 at Site 2 and ES1&MOB at Site 1

The operation in Measurement B4 is similar to Measurement B2, where the settings in Site 1 and Site 2 are swapped. Similarly, the bridged CCD of the TW link [ES1-MOB@1] and the CALR of [ES2-ES1] link are obtained as follows:

$$\begin{aligned}\text{Bridged CCD}(1,\mathrm{MOB@1}) = &-0.5\underbrace{[\mathrm{TW(2)} - \mathrm{TW(MOB@1)}]}_{\text{from TW link [ES2−MOB@1]}} + 0.5\ \underbrace{[\mathrm{TW(2)} - \mathrm{TW(1)}]}_{\text{from TW link [ES2−ES1]}} \\ &-[\mathrm{REFDELAY(1)} - \mathrm{REFDELAY(MOB@1)}]\end{aligned}$$

(30)

$$\mathrm{CALR_{MeasB4}}(2,1) = -[\mathrm{SCD(2)} - \mathrm{SCD(1)}] + [\mathrm{CCD}(2,\mathrm{MOB@2}) - \text{Bridged CCD}(1,\mathrm{MOB@1})]$$

(31)

Post-data processing: Calculate CALR of TW link between ES1 and ES2 based on baseline-mode calibration

Different from the site-mode calibration in which a direct TW link is set up between the local ES and the MOB at the same site, the bridged CCD measurements do not need a direct TW link between the ES and the MOB. As an alternative, the link between the local ES and the MOB is set up via a remote ES acting as the 'bridge'.

Either Measurement B1 plus Measurement B2 or Measurement B3 plus Measurement B4 can be used to get the calibration result of $\mathrm{CALR}(1,2)$ or $\mathrm{CALR}(2,1)$ respectively. For a pair of ESs in calibration, the CALR values of an ES pair are symmetrical with opposite signs, that is $\mathrm{CALR}(1,2) = \text{-}\mathrm{CALR}(2,1)$.

With Measurement B1 plus Measurement B2, the CALR between a pair of ES1 and ES2 reads:

$$\mathrm{CALR}(1,2) = -\mathrm{CALR}(2,1) = \mathrm{CALR}_{\mathrm{MeasB2}}(1,2) \quad (32)$$

With Measurement B3 and Measurement B4, the CALR between [ES1-ES2] is:

$$\mathrm{CALR}(2,1) = -\mathrm{CALR}(1,2) = \mathrm{CALR}_{\mathrm{MeasB4}}(2,1) \quad (33)$$

With all the four Measurements of Measurements B1, Measurements B2, Measurements B3, and Measurements B4, the averaged CALR of [ES1-ES2] is obtained accordingly:

$$\mathrm{CALR}(1,2) = -\mathrm{CALR}(2,1) = \frac{\mathrm{CALR}_{\mathrm{MeasB2}}(1,2) - \mathrm{CALR}_{\mathrm{MeasB4}}(2,1)}{2} \quad (34)$$

5 Operation of Mobile TWSTFT Station (MOB)

In this chapter, introductions on MOB architecture, signal interface, and working principle in calibration are explained. The full description of the MOB refers to [RD07].

5.1 MOB architecture

5.1.1 Schematics of MOB

A mobile TWSTFT station (MOB) is a fully operational ES which independently implements TW message modulation and de-modulation and set up TW links with other ESs for TW timing message exchange. Meanwhile, when travelling to different sites, the MOB operates with the local ESs under the same local timescale. By taking the DLD of the MOB as the common reference, the DLD difference between ESs is calibrated.

Figure 5-1 describes the simplified block diagram of the MOB, where the following four parts are included:

- An indoor rack (Blue Box), which consists of time and frequency distribution equipment and MOB internal timing delay measurement equipment, provides the interfaces to the site's reference signals as well as the time & frequency source to the TWSTFT equipment in the trailer.
- An outdoor trailer with the full set of TWSTFT equipment, including the motorised antenna and Tx/Rx front-end, the SATRE-mobile for timing message modulation and demodulation, the synchronized reference signal connected to the SATRE-mobile, etc.
- The interface between the local site and the Blue Box: 3 coaxial cables connecting the site's reference clock signals with the Blue Box for the dissemination of the site's clock signals to the MOB.
- The interface between the Blue Box and the trailer: 2 optical cables connecting the Blue Box with the trailer for timing signal delivery and data exchange, respectively.

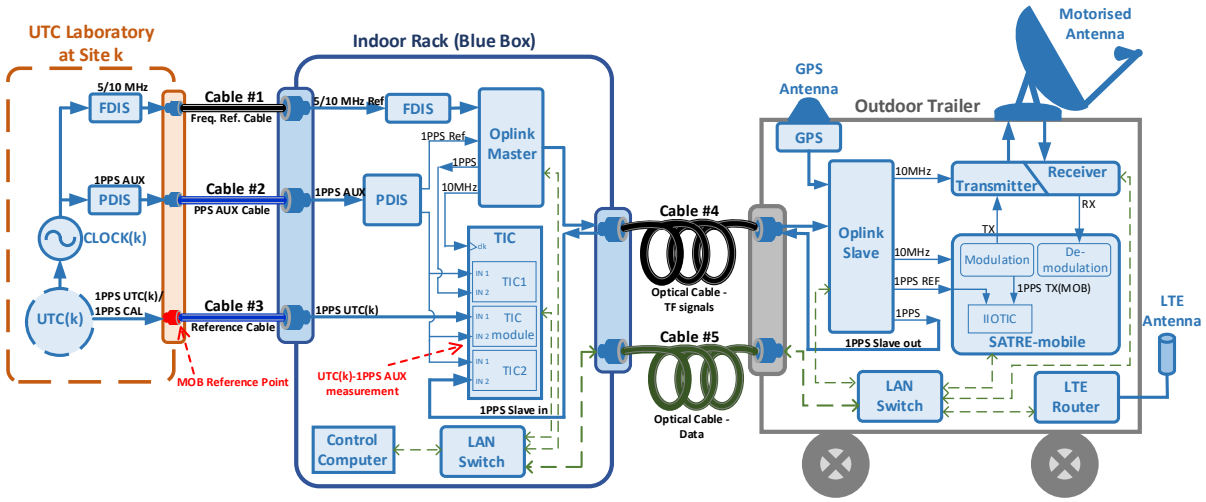

Figure 5-1 Simplified block diagram of the MOB and the MOB interfaces to the site's reference signal

5.1.2 Reference signals from the site

Reference timing signals are provided by the UTC lab at the site, including 5/10MHz reference frequency signal (5/10MHz Ref), 1PPS reference time signal (1PPS AUX), and 1PPS local UTC time-scale (1 PPS UTC(k)/1 PPS CAL).

Among the three reference timing signals, the 5/10MHz frequency signal and 1PPS time signal (1PPS AUX) provide the external reference frequency and phase to the MOB, respectively. And they need to be present for the whole duration of the on-site measurement because the MOB is running driven by the timescale provided by these two reference signals. In contrast, 1PPS UTC(k)/1PPS CAL is used to provide traceability from the MOB's local reference phase 1PPS AUX to the local UTC timescale at Site k UTC(k). As a result, it is sufficient to measure the delay between UTC(k) and 1PPS AUX at the beginning of the on-site measurement and then at the end of the measurement for traceability verification.

Three routes of reference signals are connected to the Blue Box via coaxial cables. The information of the signal format, cables and connectors is listed in Table 5-1.

Table 5-1 Interface between UTC(k) and MOB

Signal Name		5/10MHz Ref*	1 PPS AUX*	1 PPS UTC(k)/ 1 PPS CAL*
Signal Format		Sine-wave	1 PPS pulse	1 PPS pulse
Input Impedance		50 Ω	50 Ω	50 Ω
Signal Power		Working level: +6 to +16 dBm Nominal level: +13 dBm	Logic '0': nominal 0V Logic '1': 1V ~ 5V	Logic '0': nominal 0V Logic '1': 1V ~ 5V
Trigger Level		--	+slope @ 1.0 V	To be provided by the site
Connection Cables	**Cable ID**	Cable #1	Cable #2	Cable #3
	Length/Diameter	7.5 meter/5.40 mm	7.5 meter/5.40 mm	7.5 meter/4.60 mm
	Type	RG223	RG223	Sucotest 18
	Connectors	N(M) – N(M)	N(M) – N(M)	N(M) – BNC(M) with adapter

*All these three routes of signals (5/10MHz Ref, 1 PPS AUX, 1 PPS UTC(k)/1 PPS CAL) shall be coherent to local UTC realization UTC(k).

5.1.3 The reference point of MOB

During the on-site measurements, the MOB needs to operate using the same local clock as the local ES at Site k, as shown in Figure 4-3 and Figure 4-4, where the reference time of the local ES is the local timescale UTC(k). Accordingly, the MOB needs to be traceable to UTC(k) when performing on-site measurements at Site k.

The reference point of the MOB is defined at the end of the BNC connector of Cable #3, which is connected to the local time-scale of the lab at Site k UTC(k), as shown in Figure 5-1. As a consequence, the traceability delay measurement between UTC(k) and 1PPS AUX, which is performed by a built-in TIC in the Blue Box, is actually measuring the delay between the reference point of the MOB and 1PPS AUX. When there is an extra delay between the reference point of the MOB and UTC(k), it needs to be added to the [UTC(k)-1PPS AUX] traceability measurement. The determination of this extra delay and its uncertainty is the responsibility of the visited site.

5.1.4 Time dissemination between Blue Box and trailer

The reference frequency and phase signals (5/10MHz and 1PPS AUX) are delivered from the indoor Blue Box to the outdoor trailer via a pair of optical link devices, OPlink Master and OPlink Slave, which are connected via optical fibres Cable #4. 5/10MHz and 1PPS AUX are the inputs of the OPlink Master in the Blue Box, and then they are delivered

via Cable #4 to the trailer. Inside the trailer, 5/10MHz and 1PPS AUX are recovered on the OPlink Slave side. The recovered 5/10MHz and 1PPS Slave are taken as the reference signals of SATRE-mobile in the trailer. To verify the synchronization of the recovered 1PPS Slave signal, it is transmitted back to the Blue Box via Cable #4 and compared with 1PPS AUX for delay verification.

As shown in Figure 5-1, the interface between the indoor Blue Box and the outdoor trailer consists of two optical cables placed on the drum, named Cable #4 and Cable #5. Cable #4 delivers bi-directional TF signals, and Cable #5 is used to exchange both the communication data and the measurement data between the Blue Box and the trailer. The information on the two rolls of optical cables is listed in Table 5-2.

Table 5-2 Interface between the indoor blue box and outdoor trailer

Signal Name		Optical Cable - TF signals	Optical Cable - Data
Signal Format		Optical signals	Optical signals
Connection Cables	**Cable ID**	Cable #4	Cable #5
	Length/Diameter	200 meter/6.00 mm	200 meter/6.00 mm
	Type	LWL-4HMC	LWL-4LC
	Connectors	HMC-HMC (Connector diameter: 23mm)	LC-LC (The connectors are protected by a pulling aid with a length of 1 m and diameter of 40 mm)

5.2 REFDELAY of MOB at Site k

Similar to the time dissemination from UTC(k) to the ES local timescale at Site k, the reference delay of the MOB at Site k, REFDELAY(MOB@k), is defined as the delay from UTC(k) to the local timescale of the SATRE-mobile modem which is 1PPS TX(MOB). Combining with the architecture of the MOB as shown in Figure 5-1, the time dissemination from UTC(k) to the MOB at Site k is given by:

$$\begin{aligned}&\mathrm{REFDELAY(MOB@k)}\\&= \underbrace{[1\mathrm{PPS\ UTC(k)} - 1\mathrm{PPS\ AUX}]}_{\text{measured by Site k and TIC in Blue Box}} + \underbrace{[1\mathrm{PPS\ AUX} - 1\mathrm{PPS\ Slave}]}_{\text{measured by TIC in Blue Box}} + \underbrace{[1\mathrm{PPS\ Slave} - 1\mathrm{PPS\ TX(MOB)}]}_{\text{measured by built-in IIOTIC}} + \underbrace{\mathrm{AddDLY(MOB@k)}}_{\text{measured by Site k}}\\&= 1\mathrm{PPS\ UTC(k)} - 1\mathrm{PPS\ TX(MOB)} + \mathrm{AddDLY(MOB@k)}\end{aligned}$$

(35)

The first item, $[1\mathrm{PPS\ UTC(k)} - 1\mathrm{PPS\ AUX}]$, indicates the delay between UTC(k) and the reference phase of the MOB 1PPS AUX. It is obtained by measuring the delay between the reference point of the MOB and the 1PPS AUX (measured by a TIC inside the Blue Box). The second item, $[1\mathrm{PPS\ AUX} - 1\mathrm{PPS\ Slave}]$, is the phase difference between 1PPS AUX and the recovered 1PPS AUX in the trailer, denoted as 1PPS Slave. It is measured by a built-in TIC inside the Blue Box. The third item, $[1\mathrm{PPS\ Slave} - 1\mathrm{PPS\ TX(MOB)}]$, is the delay between the input reference signal of SATRE-mobile (1PPS Slave) and the local time-scale of SATRE-mobile (1PPS TX(MOB)), and is measured by a built-in IIOTIC in SATRE-mobile. The IIOTIC measurement values of the third item are listed in column 'REFDELAY' in the ITU file of the MOB. The fourth item, $\mathrm{AddDLY(MOB@k)}$, is the possible additional delay from 1PPS UTC(k) reference point to MOB reference point, and is measured by Site k.

Table 5-3 lists the reference delay and its uncertainty of the MOB from the local UTC reference point to the input of SATRE-mobile when visiting each site during this calibration campaign.

Table 5-3 List of REFDELAY(MOB@k) items in the calibration campaign

ES Site ID	$[1PPS\ UTC(k) - 1PPS\ AUX]$			$[1PPS\ AUX - 1PPS\ Slave]$		$AddDLY(k)$		$REFDELAY(MOB@k)$①	
<Site k>	mean	uncertainty②	Trigger Level	mean	uncertainty②	mean	uncertainty	mean	uncertainty
	Unit: ns	Unit: ns	Unit: V	Unit: ns	Unit: ns	Unit: ns	Unit: ns	Unit: ns	Unit: ns
TIM	30.140	0.009	1.0	-10,307	0.044	81.230	0.030	101.063	0.054
PL	28.050	0.010	0.5	-10,234	0.014	0.100	0.030	17.916	0.035
PTB	27.664	0.010	1.0	-10,286	0.014	2.850	0.005	20.228	0.020
VSL	26.383	0.015	0.5	-10,289	0.015	0.106	0.010	16.254	0.023
LTFB	27.555	0.010	1.2	-10,260	0.015	0.000	0.000	17.295	0.018
ROA	27.769	0.009	1.0	-10,260	0.029	277.500	0.100	295.009	0.105
OP	89.491	0.012	1.0	-10,038	0.016	0.000	0.000	79.453	0.020
NPL	-13.758	0.009	1.0	-10,239	0.060	67.540	0.200	43.543	0.209
SP	27.601	0.010	1.25	-10,338	0.054	21.300	0.100	38.563	0.114
IT	179.059	0.009	1.0	-10,241	0.010	0.000	0.000	168.818	0.013
CH	20.369	0.011	0.5	-10,182	0.110	0.106	0.005	10.293	0.111
PTB_{end}③	60.399	0.009	1.0	-10,214	0.010	2.850	0.005	53.035	0.014

①: The REFDELAY(MOB@k) values listed in this column do not contain the SATRE-mobile built-in IIOTIC measurement values of the third item $[1PPS\ Slave - 1PPS\ TX(MOB)]$ in equation (35).

②: The uncertainties are determined from the maximum TDEV value during the measurement periods.

③: The subscript “end” indicates the TWSTFT closure measurements at the end of the calibration campaign.

6 TWSTFT calibration data processing

6.1 Denotation clarification

In this calibration campaign, multiple TW links are processed, and is more than one TW station and multiple Rx channels located at one site. Hence the calibration set-ups, mathematical equations and denotations need to be extended to identify multiple TW modems and Rx channels. To unify the denotations of the ES Sites, ESs, and ES channels, clarifications on denotations are introduced here. The subsequent data processing follows these denotation rules.

To describe the measurements at one Site, denote the name of the Site as Site k, where <k> represents <ES Site ID> which is composed of 2~4 letters. An ES channel code is denoted as <ki>, where <i> indicates the two-digit <modem code> assigned to a TW modem. Assignments on ES code and ES channel code are explained in Section 3.5.4.

When a pair of ESs at Site 1 and Site 2 in a TW link are mentioned, such as the denotations used in Figure 4-1, use Site k_1 and Site k_2 instead of Site 1 and Site 2 to unify the site denotations. And use <k_1i> and <k_2j> to represent the ES channels located at Site k_1 and Site k_2, respectively.

6.2 CALR data processing

6.2.1 CCD data processing

6.2.1.1 CCD data processing in site-mode measurement

When the MOB is operated at Site k for site-mode calibration measurements, as described by Figure 4-3, equation (15) and equation (20), the CCD measurement results between the local ES channel ki and the MOB at Site k can be computed as:

$$\mathrm{CCD}(\mathrm{ki},\mathrm{MOB@k}) = -[\mathrm{REFDELAY}(\mathrm{ki}) - \mathrm{REFDELAY}(\mathrm{MOB@k})] - 0.5[\mathrm{TW}(\mathrm{ki}) - \mathrm{TW}(\mathrm{MOB@k})] \quad (36)$$

6.2.1.2 Bridged CCD data processing in baseline-mode measurement

Compared to the direct CCD measurements on the TW link [ki-MOB@k], the bridged CCD measurements involve two ESs located at two sites, Site k_1 and Site k_2, respectively, and the CCD between the local ES and the MOB are measured via a bridging ES at a remote location.

The working principle of the bridged CCD measurements is explained in Figure 4-4. As described by Measurement B2 in Figure 4-4, the bridged CCD measurements between an ES channel k_2j and the MOB at Site k_2 are calculated via a bridging ES channel k_1i located at Site k_1. Then the following relation could be obtained as:

$$\mathrm{Bridged\ CCD}(\mathrm{k_2j},\mathrm{MOB@k_2}) = -0.5\underbrace{[\mathrm{TW}(\mathrm{k_1i}) - \mathrm{TW}(\mathrm{MOB@k_2})]}_{\text{from TW link }[\mathrm{k_1i-MOB@k_2}]} + 0.5\underbrace{[\mathrm{TW}(\mathrm{k_1i}) - \mathrm{TW}(\mathrm{k_2j})]}_{\text{from TW link }[\mathrm{k_1i-k_2j}]} - [\mathrm{REFDELAY}(\mathrm{k_2j}) - \mathrm{REFDELAY}(\mathrm{MOB@k_2})] \quad (37)$$

Similarly, as shown in Measurement B4 in Figure 4-4, the bridged CCD measurements between an ES channel k_1i and the MOB at Site k_1 via a bridging ES channel k_2j located at Site k2 is obtained from the following equation:

$$\mathrm{Bridged\ CCD}(\mathrm{k_1i},\mathrm{MOB@k_1}) = -0.5\underbrace{[\mathrm{TW}(\mathrm{k_2j}) - \mathrm{TW}(\mathrm{MOB@k_1})]}_{\text{from TW link }[\mathrm{k_2j-MOB@k_1}]} + 0.5\underbrace{[\mathrm{TW}(\mathrm{k_2j}) - \mathrm{TW}(\mathrm{k_1i})]}_{\text{from TW link }[\mathrm{k_2j-k_1i}]}$$

$$-[\mathrm{REFDELAY}(\mathrm{k_1 i}) - \mathrm{REFDELAY}(\mathrm{MOB@k_1})]$$

(38)

6.2.1.3 CCD in even and odd hour sessions data processing

According to the schedule of this calibration campaign listed in Figure 3-2 and Figure 3-3, the on-site CCD measurements are divided into even-hour and odd-hour sessions. This arrangement is to observe the CCD deviation between even hours and odd hours, so as to investigate possible interference effects between the transmitted PN codes. Therefore, the CCD measurement data from different sessions would be processed separately.

Denote $\mathrm{CCD_{even}(ki, MOB@k)}$ and $\mathrm{CCD_{odd}(ki, MOB@k)}$ as the CCD measurement data (or bridged CCD measurement data) taken during even hours and odd hours, respectively. When computing the CCD measurement results, first take the average of all the CCD measurement data during even hours and odd hours respectively, and then take the average of CCD computation results of even hours and odd hours to get the final CCD measurement results. The computation is expressed in equation (39) below:

$$\mathrm{CCD_{avg}(ki, MOB@k)} = \frac{[\mathrm{CCD_{even}(ki, MOB@k)}]_{\mathrm{avg}} + [\mathrm{CCD_{odd}(ki, MOB@k)}]_{\mathrm{avg}}}{2}$$

(39)

where $\mathrm{CCD_{avg}(ki,MOB@k)}$ is the final CCD computation result between the ES channel ki and the MOB at Site k, and $[\cdot]_{\mathrm{avg}}$ denotes taking the average of the data set $[\cdot]$.

In the case of even hours measurement data $\mathrm{CCD_{even}(ki, MOB@k)}$ presented only or odd hours measurement data $\mathrm{CCD_{odd}(ki, MOB@k)}$ presented only, $[\mathrm{CCD_{even}(ki, MOB@k)}]_{\mathrm{avg}}$ or $[\mathrm{CCD_{odd}(ki, MOB@k)}]_{\mathrm{avg}}$ will be taken as $\mathrm{CCD_{avg}(ki, MOB@k)}$, accordingly.

The difference between even hours and odd hours CCD measurements is calculated as:

$$\mathrm{CCD_{diff}(ki, MOB@k)} = [\mathrm{CCD_{even}(ki, MOB@k)}]_{\mathrm{avg}} - [\mathrm{CCD_{odd}(ki, MOB@k)}]_{\mathrm{avg}}$$

(40)

6.2.1.4 CCD uncertainty evaluation

The uncertainty of CCD (or bridged CCD) is evaluated by means of Time DEViation (TDEV), which reflects the phase fluctuation of the CCD measurements with observation time interval. Among all the observation intervals, daily stability of the CCD measurements is of most interests. Moreover, the phenomenon of diurnals in TW links is also one of the main uncertainty factors according to the previous measurement experiences on TW link performance. Therefore, the measurement interval of 12 hours is taken as the observation interval in CCD (or bridged CCD) uncertainty evaluation.

In detail, the TDEV results of CCD (or bridged CCD) measurements at the time interval of 12 hours during even hours and odd hours are firstly calculated, and then the maximum of the TDEV from both the even and odd hour measurement sessions is taken as the uncertainty value of the total CCD (or bridged CCD) measurements. The CCD uncertainty calculation procedure is described by the following equations:

$$\mathrm{TDEV_{max}[CCD(ki, MOB@k)]} = \max\{\mathrm{TDEV[CCD_{even}(ki, MOB@k)@\tau = 12hr]}, \mathrm{TDEV[CCD_{odd}(ki, MOB@k)@\tau = 12hr]}\}$$

(41)

$$u\mathrm{CCD(ki, MOB@k)} = \mathrm{TDEV_{max}[CCD(ki, MOB@k)]}$$

(42)

where $\mathrm{TDEV_{max}}[\cdot] = \max\{\mathrm{TDEV}[\cdot]@\tau\}$, and $[\cdot]$ represents the data set used in TDEV calculation, and $\mathrm{TDEV}[\cdot]@\tau$ indicates the time deviation value of the data set at the measurement interval of τ. $u\mathrm{CCD(ki, MOB@k)}$ is the final calculated uncertainty value of CCD (or bridged CCD) measurements between the ES channel <ki> and MOB@k.

From equation (36), it can be seen that $u\mathrm{CCD}$ contains the variations from

- TW measurements of the ES channel <ki>;
- TW measurements of the MOB at Site k;

- The third item in $\mathrm{REFDELAY(k)}$ which is $[\mathrm{1PPSREF(k)} - \mathrm{1PPSTX(k)}]$ as shown in equation (6), if this item is obtained by a built-in IIOTIC of the SATRE modem;
- The third item $[\mathrm{1PPS\ Slave} - \mathrm{1PPS\ TX(MOB)}]$ in $\mathrm{REFDELAY(MOB@k)}$ as shown in equation (35), which is measured by a built-in IIOTIC of the SATRE-mobile.

Meanwhile, the other uncertainty factors in $\mathrm{REFDELAY(k)}$ and $\mathrm{REFDELAY(MOB@k)}$, which contain

- The first two items of $\mathrm{REFDELAY(k)}$, which are $[\mathrm{UTC(k)} - \mathrm{CLOCK(k)}] + [\mathrm{CLOCK(k)} - \mathrm{1PPSREF(k)}]$ as shown in equation (6), if the third item of $\mathrm{REFDELAY(k)}$ is obtained by a built-in IIOTIC of the SATRE modem;
- Or all the three items of $\mathrm{REFDELAY(k)}$, if the third item of $\mathrm{REFDELAY(k)}$ is a pre-calibrated fixed value;
- The first two items and the fourth item of $\mathrm{REFDELAY(MOB@k)}$, which are $[\mathrm{1PPS\ UTC(k)} - \mathrm{1PPS\ AUX}] + [\mathrm{1PPS\ AUX} - \mathrm{1PPS\ Slave}] + \mathrm{AddDLY(MOB@k)}$ as shown in equation (35).

are categorized into Type B uncertainties as $u\mathrm{b,6(k_1i,k_2j)}$ which is explained in Section 6.3.2.

6.2.2 CALR data processing in site-mode calibration

Taking equation (21) as the reference, the site-mode calibration results $\mathrm{CALR(k_1i,k_2j)}$ for a pair of ES channels <k_1i> and <k_2j> in a TW link is calculated by:

$$\mathrm{CALR(k_1i,\ k_2j)} = -[\mathrm{SCD(k_1)} - \mathrm{SCD(k_2)}] + \left[\mathrm{CCD_{avg}(k_1i, MOB@k_1)} - \mathrm{CCD_{avg}(k_2j, MOB@k_2)}\right]$$

(43)

where $\mathrm{SCD(k)}$ values are calculated by equation (10), and $\mathrm{CCD_{avg}(ki,MOB@k)}$ values are calculated by equation (36) and equation (39).

When computing the calibration results between Rx channels in the same ES, the calibration results simplify to:

$$\mathrm{CALR(ki_{Rx1}, ki_{Rx2})} = [\underbrace{\mathrm{CCD(ki_{Rx1}, MOB@k)} - \mathrm{CCD(ki_{Rx2}, MOB@k)}}_{\mathrm{CCD(ki_{Rx1}, ki_{Rx2})}}]_{\mathrm{avg}}$$
$$\mathrm{CALR(ki_{Rx1}, ki_{SDR})} = [\underbrace{\mathrm{CCD(ki_{Rx1}, MOB@k)} - \mathrm{CCD(ki_{SDR}, MOB@k)}}_{\mathrm{CCD(ki_{Rx1}, ki_{SDR})}}]_{\mathrm{avg}}$$

(44)

where $\mathrm{ki_{Rx1}}$ and $\mathrm{ki_{Rx2}}$ represent the Rx1 channel and Rx2 channel of the ES <ki>, respectively. $\mathrm{ki_{SDR}}$ represents the Rx channel from SDR which connects to the IF signal of the SATRE modem. Denoting $\mathrm{CCD(ki_{Rx1}, ki_{Rx2})} \stackrel{\mathrm{def}}{\cong} \mathrm{CCD(ki_{Rx1}, MOB@k)} - \mathrm{CCD(ki_{Rx2}, MOB@k)}$ and $\mathrm{CCD(ki_{Rx1}, ki_{SDR})} \stackrel{\mathrm{def}}{\cong} \mathrm{CCD(ki_{Rx1}, MOB@k)} - \mathrm{CCD(ki_{SDR}, MOB@k)}$, the CCD uncertainty of two local Rx channels is calculated as: $u\mathrm{CCD(ki_{Rx1}, ki_{Rx2})} = \mathrm{TDEV_{max}[CCD(ki_{Rx1}, ki_{Rx2})]}$and $u\mathrm{CCD(ki_{Rx1}, ki_{SDR})} = \mathrm{TDEV_{max}[CCD(ki_{Rx1}, ki_{SDR})]}$, respectively.

A step further, the calibration results between the Rx2/SDR channel of the ES <k_1i> and a remote TW station <k_2j> can be transferred via Rx1 channel of the ES <k_1i> as:

$$\mathrm{CALR(k_1i_{Rx2},\ k_2j)} = \mathrm{CALR(k_1i_{Rx1},\ k_2j)} - \mathrm{CALR(ki_{Rx1}, ki_{Rx2})}$$
$$\mathrm{CALR(k_1i_{SDR},\ k_2j)} = \mathrm{CALR(k_1i_{Rx1},\ k_2j)} - \mathrm{CALR(ki_{Rx1}, ki_{SDR})}$$

(45)

6.2.3 CALR data processing in baseline-mode calibration

By taking equation (27) as the reference, the baseline-mode calibration results based on Measurement B1 and Measurement B2 are obtained as:

$$\mathrm{CALR}_{\mathrm{MeasB2}}(\mathrm{k_1i},\ \mathrm{k_2j}) = -[\mathrm{SCD}(\mathrm{k_1}) - \mathrm{SCD}(\mathrm{k_2})] + \left[\mathrm{CCD_{avg}}(\mathrm{k_1i}, \mathrm{MOB@k_1}) - \text{Bridged } \mathrm{CCD_{avg}}(\mathrm{k_2j}, \mathrm{MOB@k_2})\right] \quad (46)$$

Accordingly, when Measurement B3 and Measurement B4 are presented, the CALR is:

$$\mathrm{CALR}_{\mathrm{MeasB4}}(\mathrm{k_2j}, \mathrm{k_1i}) = -[\mathrm{SCD}(\mathrm{k_2}) - \mathrm{SCD}(\mathrm{k_1})] + \left[\mathrm{CCD_{avg}}(\mathrm{k_2j}, \mathrm{MOB@k_2}) - \text{Bridged } \mathrm{CCD_{avg}}(\mathrm{k_1i}, \mathrm{MOB@k_1})\right] \quad (47)$$

The final CALR in baseline-mode calibration can be computed as the average of equation (46) and equation (47) when all the four sets of measurements are presented, and is expressed as:

$$\mathrm{CALR}(\mathrm{k_1i},\ \mathrm{k_2j}) = -\mathrm{CALR}(\mathrm{k_2j}, \mathrm{k_1i}) = \frac{\mathrm{CALR}_{\mathrm{MeasB2}}(\mathrm{k_1i},\ \mathrm{k_2j}) - \mathrm{CALR}_{\mathrm{MeasB4}}(\mathrm{k_2j}, \mathrm{k_1i})}{2} \quad (48)$$

6.3 Uncertainty budget of CALR

Uncertainty contributions to the calibration results of $\mathrm{CALR}(\mathrm{k_1i},\mathrm{k_2j})$ are categorized into Type A and Type B uncertainties. In general, Type A uncertainties are statistical variations of the measurements, and Type B uncertainty is the standard uncertainty evaluated by the sum of the available information regarding the variability of the calibration results.

6.3.1 Type A uncertainties of CALR

For a pair of ESs in a TW link denoted as <k_1i> and <k_2j>, type A uncertainties of $\mathrm{CALR}(\mathrm{k_1i},\mathrm{k_2j})$ are calculated as the geometric sum of the measurement uncertainties of CCD (or bridged CCD) at Site k_1 and Site k_2.

The measurement uncertainties coming from Site k_1 and Site k_2 are denoted as follows, respectively:

$$u\mathrm{a},1(\mathrm{k_1i}) = u\mathrm{CCD}(\mathrm{k_1i}, \mathrm{MOB@k_1})$$

$$u\mathrm{a},2(\mathrm{k_2j}) = u\mathrm{CCD}(\mathrm{k_2j}, \mathrm{MOB@k_2})$$

Then the total CCD measurement uncertainties are expressed as

$$\begin{aligned} u\mathrm{a} &= \sqrt{u\mathrm{a},1(\mathrm{k_1i})^2 + u\mathrm{a},2(\mathrm{k_2j})^2} \\ &= \sqrt{u\mathrm{CCD}(\mathrm{k_1i}, \mathrm{MOB@k_1})^2 + u\mathrm{CCD}(\mathrm{k_2j}, \mathrm{MOB@k_2})^2} \end{aligned} \quad (49)$$

where $u\mathrm{CCD}$ is computed by equation (42).

6.3.2 Type B uncertainties of CALR

Type B uncertainties have been defined and described in Section 6.2.2 of “Summary of the GSOP 2019 TWSTFT calibration report” [RD03] and Section 8 of “Summary for the 2021 TWSTFT AOS, CH, MPL, PTB, VSL calibration report” [RD04]. In this report, the Type B uncertainty budget is revised based on the results and performance analysis made in the framework of this calibration campaign.

- $u\mathrm{b},1$: Impact of MOB temperature variations

  The MOB temperature-induced error is estimated using the following steps: First, determine temperature coefficients for the equipment indoors and outdoors, respectively. Then, calculate the operational equipment temperatures as averages from the equipment temperature sensors for each visited site. And finally, use the difference between maximum and minimum operational temperatures as the temperature variation during the campaign and multiply with the temperature coefficients. The analysis results for MOB indoor and outdoor temperature variations are listed in Table 6-1.

Table 6-1 List of $u_{b,1}$ uncertainty contribution

$u_{b,1}$ Uncertainty	Uncertainty Source	Temperature Coefficient Unit: ps/K	Operational Temperature Range Unit: K	Contribution Unit: ns	Total Contribution Unit: ns
Impact of trailer temperature variations	Outdoor OPlink	25	4.37	0.109	0.125
	SATRE-mobile	10	4.24	0.042	
Impact of Blue Box temperature variations	TIC and Blue Box signal distribution	6	7.06	0.042	
	Residual temperature difference between master source and indoor OPlink	25	0.56	0.014	

- $u_{b,2}$: Carrier frequency and PRN code related impact to SATRE-mobile

  The internal delay of the SATRE-mobile changes with different PN codes and carrier frequencies. Figure 6-1 and Figure 6-2 demonstrate the test results on the relation between the normalized delay and PN code/carrier frequency. Since the PN code and carrier frequency are not independent from each other, these two uncertainty effects need to be added. With additional jitter in each data point, the total impact covering all the effects is listed in Table 6-2.

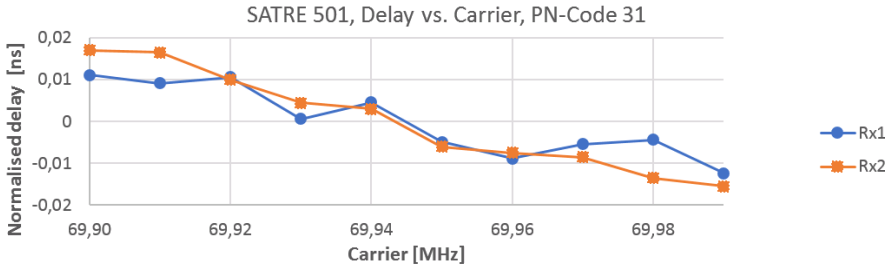

Figure 6-1 Normalized delay of SATRE-mobile related to carrier frequency

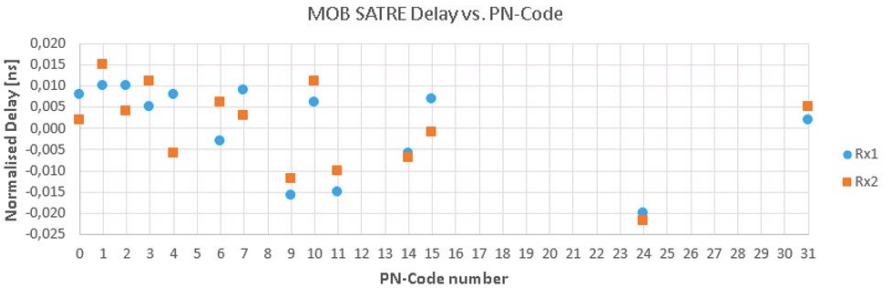

Figure 6-2 Normalized delay of SATRE-mobile related to PRN code

Table 6-2 List of ub,2 uncertainty contribution

ub,2 Uncertainty	Uncertainty Source	Each Site Contribution Unit: ns	TW Link Contribution Unit: ns	Total Contribution Unit: ns
Carrier frequency and PN code related impact to SATRE-mobile	Carrier frequency impact	0.034	0.048	≈0.080
	PN code impact	0.037	0.052	
	Jitter	0.015	0.021	

- ub,3: Instability of the MOB

  This item of uncertainty comes from the internal delay variations of the MOB. The delay instability of the MOB is verified by closure measurements, that is, performing two separate site-mode measurements between MOB02 and $\mathrm{ki}_{\mathrm{closure}}$ at the start and end of the calibration campaign, respectively. $\mathrm{ki}_{\mathrm{closure}}$ denotes the ES channels that are involved in closure measurements, and it includes PTB05, PTB15, PTB25, and PTB35 in this calibration campaign. The difference between the two CCD measurements at different dates indicates the internal delay instability of the MOB.

  The combined uncertainty of two measurements and the absolute difference of the two measurements is calculated as:

$$\mathrm{CSD}(\mathrm{ki}_{\mathrm{closure}},\mathrm{MOB@k}) = \sqrt{u\mathrm{CCD}(\mathrm{ki}_{\mathrm{closure}},\mathrm{MOB@k})_{\mathrm{start}}{}^2 + u\mathrm{CCD}(\mathrm{ki}_{\mathrm{closure}},\mathrm{MOB@k})_{\mathrm{end}}{}^2} \quad (50)$$

$$\Delta\mathrm{CCD}(\mathrm{ki}_{\mathrm{closure}},\mathrm{MOB@k}) = \left|\mathrm{CCD}_{\mathrm{even/odd}}(\mathrm{ki}_{\mathrm{closure}},\mathrm{MOB@k})_{\mathrm{start}} - \mathrm{CCD}_{\mathrm{even/odd}}(\mathrm{ki}_{\mathrm{closure}},\mathrm{MOB@k})_{\mathrm{end}}\right| \quad (51)$$

  To a conservative estimation, the instability of the MOB can be considered as the maximum of CSD and $\Delta\mathrm{CCD}$:

$$u\mathrm{b},3 = \max\{\mathrm{CSD}(\mathrm{ki}_{\mathrm{closure}},\mathrm{MOB@k}), \Delta\mathrm{CCD}(\mathrm{ki}_{\mathrm{closure}},\mathrm{MOB@k})\} \quad (52)$$

  The CSD and $\Delta\mathrm{CCD}$ values calculated in this calibration campaign are listed in Table 7-52 in Section 7.4. An uncertainty ub,3= 0.122 ns is obtained. Explanations about ub,3 refer to [RD03, RD04, RD11].

- ub,4: Impact of SATRE modem temperature variations

  At each site, the temperature variation of the environment results in uncertainty related to the local SATRE modem. By taking the maximal operational temperature range between the two sites and then multiplying with the temperature coefficient of the SATRE modem, the uncertainty contribution from SATRE modem temperature variations is estimated, as listed in .

  Table 6-3.

Table 6-3 List of ub,4 uncertainty contribution

ub,4 Uncertainty	Uncertainty Source	Temperature Coefficient Unit: ps/K	Operational Temperature Range Unit: K	Total Contribution Unit: ns

Impact of SATRE modem temperature variations	SATRE modem of the ES at the site	10	4	0.040

- $u_{b,5}$: SATRE modem measurement resolution

  The SATRE modem measurement resolution error induced by the built-in IIOTIC is integrated into CCD measurement data, which have been included in Type A uncertainty. Here $u_{b,5}$ is set to be 0 in the Type B category.

- $u_{b,6(k_1i,k_2j)}$: Estimation of REFDELAYdiff uncertainty

  REFDELAYdiff is defined as the reference delay difference between the local ES channel <ki> and the MOB in the on-site CCD (or bridged CCD) measurements at Site k, denoted as:

$$\mathrm{REFDLYdiff(ki)} = \mathrm{REFDELAY(ki)} - \mathrm{REFDELAY(MOB@k)} \quad (53)$$

  Besides the REFDELAY parts, which contribute to CCD measurement variations and are taken into account under Type A uncertainties, the REFDELAY uncertainties coming from the pre-calibration are categorized as follows:

$$u\mathrm{REFDLYdiff(ki)} = \sqrt{u\mathrm{REFDELAY(ki)}^2 + u\mathrm{REFDELAY(MOB@k)}^2} \quad (54)$$

$$u_{b,6(k_1i,k_2j)} = \sqrt{u\mathrm{REFDLYdiff}(k_1i)^2 + u\mathrm{REFDLYdiff}(k_2j)^2} \quad (55)$$

  where $u\mathrm{REFDELAY(ki)}$ and $u\mathrm{REFDELAY(MOB@k)}$ values are read from the column RSIG in ITU files of the ES and Table 5-3, respectively.

- $u_{b,7}$: Laboratory signal distribution equipment

  The uncertainty contribution resulting from the signal distribution equipment of the lab is estimated as $u_{b,7}$=0.200 ns for a TW link [RD03, RD04, RD11].

- $u_{b,8}$: TIC resolution

  The minimum duration for the [1PPS UTC(k)-1PPS AUX] measurements was 30 minutes, with TDEV@1000s less than 1ps. Thus, this item of uncertainty contribution is negligible.

- $u_{b,9}$: TIC systematic contributions

  A TIC module from TIM was used for measurements. The systematic contributions from the TIC module to a TW link is listed in Table 6-4.

Table 6-4 List of $u_{b,9}$ uncertainty contribution

$u_{b,9}$ Uncertainty	**Uncertainty Source**	**Each Site Contribution** Unit: ns	**Link Contribution** Unit: ns	**Total Contribution** Unit: ns

TIC systematic contributions	Input channel crosstalk	0.040	0.057	0.098
	Channel non-linearity	0.040	0.057	
	Re-trace error on power cycling	0.040	0.057	

- $u_{b,10}$: Satellite communication TX power, C/N0

  During this calibration campaign, the nominal power of all the participating stations was unchanged. Ideally, there is no effect on the power and C/N0 in a well-defined situation; however, take $u_{b,10}$=0.010 ns for any residual effect by considering the fact that the configuration is not ideal.

- $u_{b,11}$: Atmosphere

  The uncertainty contributions related to the atmosphere consist of four aspects: the ionosphere, troposphere, temperature variations on the ES front-end, and humidity changes.

  The ionosphere error during this calibration campaign is calculated using global ionosphere maps [RD14], which are provided by IGS for each link. It is proposed to use the absolute value of the highest average deviation from zero as the ionosphere uncertainty contribution, where the PL-NPL link contributes the maximum deviation of 48 ps. This stated uncertainty is valid at the time of the on-site calibration, but it will change over time. The ionospheric delay depends on the solar activity, which has a cycle of about 11 years. Note that, diurnal variations are not part of the systematic uncertainty budget, since they can be reduced by averaging.

  Since each site used different equipment in the front-end of the local ES system and they operated under different temperature stabilized environments, it is necessary to assign the temperature variation uncertainty according to the operation environment of each TW station. Here, TW stations are divided into two groups: Temperature Stable ES (TSES) and Temperature Unstable ES (TUES) based on the $u\mathrm{CCD}(\mathrm{ki}, \mathrm{MOB@k})$ values of the on-site CCD measurement results. When $u\mathrm{CCD}(\mathrm{ki}, \mathrm{MOB@k}) < 100$ ps, ES <ki> is categorized as a TSES; otherwise, it is categorized as a TUES when $u\mathrm{CCD}(\mathrm{ki}, \mathrm{MOB@k}) \geq 100$ ps. Table 6-5 lists the estimation of the temperature variation contribution for two groups of ESs, respectively. For a TW link, the temperature variation contribution to the link is the sum of the contributions of the two ESs accordingly.

  According to [RD06], a value of 10 ps shall be added to the troposphere uncertainty contribution. Besides, the contribution of 10 ps from humidity changes is added. Table 6-6 summarizes all the uncertainty contributions from the impact of the atmosphere.

Table 6-5 Temperature variation contribution estimation

Site Category	Temperature Coefficient Unit: ps/K	Operational Temperature Range Unit: K	Temperature Variation Contribution Unit: ns
Temperature Stable ES (TSES)	12	6	0.072
Temperature Unstable ES (TUES)	12	12	0.144

Table 6-6 List of $u_{b,11}$ uncertainty contribution

$u_{b,11}$ Uncertainty	Uncertainty Source	Contribution	Total Contribution

			Unit: ns	Unit: ns
Impact of the atmosphere	Ionosphere		0.048	0.152/0.222/0.292
	Troposphere		0.010	
	Temperature variations on ES front-end	Scenario 1: TSES-TSES	0.144	
		or Scenario 2: TSES-TUES	0.216	
		or Scenario 3: TUES-TUES	0.288	
	Humidity changes		0.010	

- $u_{b,12}$: Satellite motion

  The Sagnac error has two sources: the incorrect ES site position and the deviations of the satellite position from nominal. By conservatively assuming a site position error of 100 m, it gives an error of the Sagnac effect of 3 ps for one site and 4 ps for a link. To estimate the error due to the deviation of the satellite position from nominal, the satellite orbit is calculated using a modified algorithm according to [RD15]. The error of the Sagnac effect on a link increases with the longitude difference between the two sites, since the Sagnac effect is proportional to the projection of the area spanned by the position vectors of the satellite and the ES to the Earth's rotational plane. In this calibration campaign, the maximum longitude difference between two sites occurred in the [PL01-ROA01] link, where the difference between the nominal Sagnac effect and the mean value of the Sagnac effect calculated from the satellite orbit is 22 ps. Taking this value as the estimation basis, an uncertainty contribution of 30 ps is deemed appropriate here.

  The path delay difference error depends on the link geometry and the range rates measured at both sites. Besides, the latitude difference also has a significant impact on this error. With the maximum path difference possible in the EU TWSTFT network, an average deviation of -0.5 ps was calculated during the period of the calibration campaign. The calculation was done using the ranging measurements from the ITU files. And therefore, the path delay uncertainty of 2 ps is estimated for this item.

  Table 6-7 lists all the uncertainty contributions related to the satellite motion.

  Table 6-7 List of $u_{b,12}$ uncertainty contribution

$u_{b,12}$ Uncertainty	Uncertainty Source		Contribution Unit: ns	Total Contribution Unit: ns
Satellite motion	Sagnac error	Incorrect ES positions	0.004	0.030
		Satellite position deviation	0.030	
	Path delay difference between two sites		0.002	

- $u_{b,13}$: Even and odd hours measurements as possible interferences between PN codes

  Previous calibration experiences revealed that there were differences between even and odd hour CCD values for one station, and the differences varied among stations. This phenomenon was caused by possible interference effects among the transmitted PN codes. In order to take this effect into consideration, a supplementary uncertainty contribution $u_{b,13}$ was added. $u_{b,13}$ was estimated from the standard deviation of the residuals of the CCD differences of all the Rx channels during this calibration campaign [RD03, RD04]. $u_{b,13}$ can be expressed by the equation as:

$$u\mathrm{b},13 = \mathrm{stdev}\{\mathrm{CCD_{diff}}(\mathrm{ki},\mathrm{MOB@k})\}$$

(56)

where ki includes the set of all the participating ES channels, $\mathrm{CCD_{diff}}(\cdot)$ is defined in equation (40), and stdev{·} denotes the standard deviation of all the data in the set {·}.

By summarizing the measurement data at all sites, as shown in Table 7-47 and Table 7-48, ub,13 is calculated as $\mathrm{stdev}\{\mathrm{CCD_{diff}}(\mathrm{ki},\mathrm{MOB@k})\}$= 0.039 ns (SATRE channels)/0.041 ns (SDR channels) in this calibration campaign. This value is below the $u\mathrm{CCD}$ of each site, which indicates that there are not obvious PN code interference differences between even and odd measurement sessions; therefore, this item is negligible in this calibration campaign.

The overall Type B uncertainty sources and specifications are concluded in Table 6-8.

6.3.3 Summary of total uncertainties of CALR

The combined standard deviation of CALR is the sum of Type A and Type B uncertainties, and the total $u\mathrm{CALR}$ between a pair of ES channels <k1i> and <k2j> in a TW link is expressed as follows:

$$u\mathrm{CALR}(\mathrm{k_1i},\ \mathrm{k_2j}) = \sqrt{u\mathrm{a}^2 + u\mathrm{b}^2}$$

(57)

where

$$u\mathrm{a} = \sqrt{u\mathrm{a},1(\mathrm{k_1i})^2 + u\mathrm{a},2(\mathrm{k_2j})^2}$$

(58)

$$u\mathrm{b} = \sqrt{u\mathrm{b},\mathrm{I}^2 + u\mathrm{b},\mathrm{II}^2 + u\mathrm{b},\mathrm{III}(\mathrm{k_1i},\ \mathrm{k_2j})^2 + u\mathrm{b},\mathrm{IV}^2} = \sqrt{\sum_{\mathrm{x}=1}^{13} u\mathrm{b},\mathrm{x}^2}$$

(59)

Specifically, Type B uncertainties for the CALR between two local Rx channels belonging to the same ES can be considered as 0, since all the Type B uncertainties sources for the two Rx channels are the same. Therefore, the total $u\mathrm{CALR}$ between two local Rx channels is equivalent to the Type A uncertainty of the CALR, and it can be expressed as:

$$u\mathrm{CALR}(\mathrm{ki_{Rx1}},\mathrm{ki_{Rx2}}) = u\mathrm{a} = u\mathrm{CCD}(\mathrm{ki_{Rx1}},\mathrm{ki_{Rx2}})$$
$$u\mathrm{CALR}(\mathrm{ki_{Rx1}},\mathrm{ki_{SDR}}) = u\mathrm{a} = u\mathrm{CCD}(\mathrm{ki_{Rx1}},\mathrm{ki_{SDR}})$$

(60)

Table 6-8 List of CALR uncertainty budget

Uncertainty Type	Uncertainty Denotation		Uncertainty Source	Contribution	Total Contribution
	Group	Sub-group		Unit: ns	Unit: ns
Type A	ua: Measurements	ua,1(k1i)	CCD measurements at Site k1	$u\mathrm{CCD}(\mathrm{k_1i},\mathrm{MOB@k_1})$	
		ua,2(k2j)	CCD measurements at Site k2	$u\mathrm{CCD}(\mathrm{k_2j},\mathrm{MOB@k_2})$	
Type B	ub, I:	ub,1	Impact of MOB temperature variations	0.125	0.192

	MOB system	$u_{b,2}$	Carrier frequency and PN code related impact to SATRE-mobile	0.080	
		$u_{b,3}$	Instability of the MOB	0.122	
	$u_{b,II}$: ES SATRE modem	$u_{b,4}$	Impact of SATRE modem temperature variations	0.040	0.040
		$u_{b,5}$	SATRE modem measurement resolution	0.000	
	$u_{b,III(k_1i,k_2j)}$: Interface between MOB and UTC(k)	$u_{b,6(k_1i,k_2j)}$	Estimation of REFDELAYdiff uncertainty	0.030~0.578	0.225 ~ 0.619
		$u_{b,7}$	Laboratory signal distribution equipment	0.200	
		$u_{b,8}$	TIC resolution	negligible	
		$u_{b,9}$	TIC systematic contributions	0.098	
	$u_{b,IV}$: Satellite link and environment	$u_{b,10}$	Satellite communication TX power, C/NO	0.010	0.156/0.224 /0.294
		$u_{b,11}$	Impact of the atmosphere	0.152/0.222/ 0.292	
		$u_{b,12}$	Satellite motion	0.030	
		$u_{b,13}$	Even and odd hours measurements as possible interferences between PN codes	negligible	

7 ES site-mode measurement data

This chapter collects all the pre-setting parameters and on-site measurement data prepared for CALR and its uncertainty calculation with site-mode calibration method. All the denotations and data processing methods displayed in this chapter follow the description in Chapter 6.

7.1 SCD calculations at the sites

In Table 7-1, coordinates data were taken from Table 3-1 and Table 3-3 with uniform conversion into radian units. SCD(ki) values are calculated according to equation (10). uSCD(ki) values are estimated referring to Table 6-7.

Table 7-1 SCD calculation results at the sites

ES Site ID <k>	Designated ES Code <ki>	LA(ki) Unit: rad	LO(ki) Unit: rad	HT(ki) Unit: meter	LO(s) Unit: rad	SCD(ki) Unit: ns	uSCD(ki) Unit: ns
TIM	TIM01	0.851	0.159	529.00	5.628	104.87	0.030
PL	PL01	0.911	0.370	137.5	5.628	114.64	0.030
PTB	PTB05	0.913	0.183	146.32	5.628	99.40	0.030
	PTB04	0.913	0.183	146.32	5.628	99.40	0.030
VSL	VSL01	0.907	0.077	76.80	5.628	90.00	0.030
LTFB	LTFB01	0.825	0.105	358.793	5.628	102.22	0.030
ROA	ROA01	0.636	6.175	74.67	5.628	91.39	0.030
OP	OP01	0.852	0.041	78.00	5.628	92.27	0.030
NPL	NPL02	0.898	6.277	68.00	5.628	82.44	0.030
SP	SP01	1.007	0.225	225.00	5.628	90.07	0.030
IT	IT01	0.786	0.133	306.64	5.628	109.62	0.030
CH	CH01	0.819	0.130	612.82	5.628	105.60	0.030

7.2 REFDELAY results at the sites

The REFDELAY(ki) and uREFDELAY(ki) values of each ES listed in Table 7-2 are obtained from REFDELAY and ESIG parameters of the ES's ITU files on the first day of the on-site CCD measurement, respectively. The ITU file designations of all the ESs are listed in Table 3-8, and the first days of measurements for the participating stations are listed in Table 3-7. REFDELAY(MOB@k) and uREFDELAY(MOB@k) values are taken from Table 5-3. REFDLYdiff(ki) and uREFDLYdiff(ki) are calculated by equation (53) and equation (54), respectively.

Table 7-2 REFDELAY calculation results at the sites

ES Site ID <k>	Designated ES Code <ki>	REFDELAY(ki) Unit: ns	u REFDELAY(ki) /RSIG(ki) Unit: ns	REFDELAY (MOB@k)* Unit: ns	u REFDELAY (MOB@k) Unit: ns	REFDLYdiff(ki) Unit: ns	u REFDLYdiff (ki) Unit: ns
TIM	TIM01	706.011①	0.010①	101.063	0.054	604.948	0.055
PL	PL01	797.780②	0.200②	17.916	0.035	779.864	0.203
	PL51	787.650②	0.200②	17.916	0.035	769.734	0.203
PTB	PTB05④	736.134②	0.000②	20.228	0.020	715.906	0.020
	PTB04	777.949②	0.041②	20.228	0.020	757.721	0.046
VSL	VSL01④	737.990②	0.100②	16.254	0.023	721.736	0.103
LTFB	LTFB01④	751.798②	0.070②	17.295	0.018	734.503	0.072
ROA	ROA01④	964.858②	0.050②	295.009	0.105	669.849	0.116
OP	OP01④	828.280②	0.010②	79.453	0.020	748.827	0.022
NPL	NPL02	74.300②	0.200②	43.543	0.209	30.757	0.289
SP	SP01④	784.722①	0.050①	38.563	0.114	746.159	0.124
IT	IT01④	834.021①	0.500①	168.818	0.013	665.203	0.500
CH	CH01④	777.521①	0.020①	10.293	0.111	767.228	0.113
PTB_{end}③	PTB05④	736.134②	0.000②	53.035	0.014	683.099	0.014

*: REFDELAY(MOB@k) value listed in this table is the delay from the local timescale UTC(k) to the SATRE-mobile reference input signal 1PPS Slave. The actual REFDELAY(MOB@k) value taken into CCD calculation is the sum of the listed values and the values from the REFDELAY column in the MOB's ITU files. See Section 5.2 for details.

① The REFDELAY and RSIG listed in the related ITU files are generated by the internal IIOTIC of the SATRE modem. The REFDELAY values used in CCD calculations are taken from real-time measurements.

② The REFDELAY and RSIG listed in the related ITU files are constant values obtained from pre-calibration.

③ The subscript "end" indicates the closure measurements at the end of the calibration campaign.

④ The REFDELAY and RSIG of the SDR Rx channel are the same as the Rx1 and/or Rx2 channels in the ES.

7.3 CCD measurement results at the sites

In the following tables, all the samples at the sites are taken within the effective measurement duration as listed in Table 3-7. The statistics and the results of the CCD measurements are recorded and calculated according to equation (36), equation (39), equation (40), equation (42) and equation (44). The stdev of CCD data are obtained from the standard deviation of CCD measurements. A few outliers in the CCD measurement data are removed by applying a 3-σ filter.

In the following figures and tables, the Rx channels are denoted either by identifying <ES channel code> or by specifying <ES code> along with Rx channel names. The definitions of <ES code> and <ES channel code> are mentioned in Section 3.5.4.

7.3.1 CCD measurements at TIM

Figure 7-1 and Figure 7-2 show the site top view of TIM and the view of MOB during the on-site measurements at TIM.

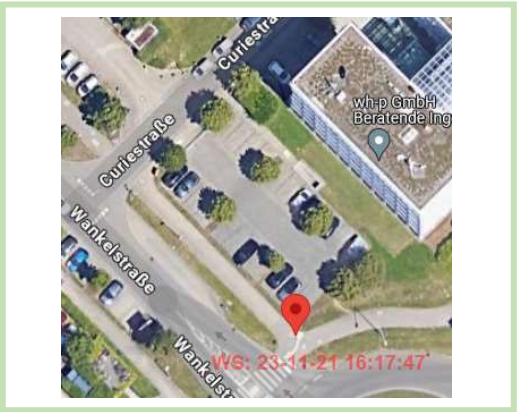

Figure 7-1 Site top view of TIM

Figure 7-2 View of MOB at TIM

Figure 7-3 and Figure 7-4 show the CCD measurement data plot and TDEV of the data plot on the Rx1 channel of ES TIM01.

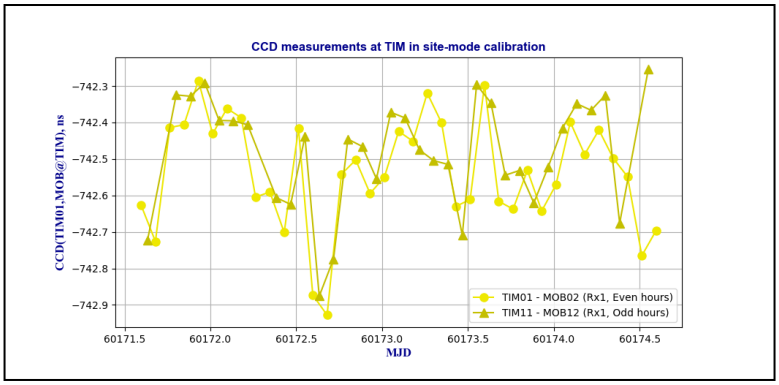

Figure 7-3 CCD measurements at TIM in site-mode calibration (<ki>=TIM01)

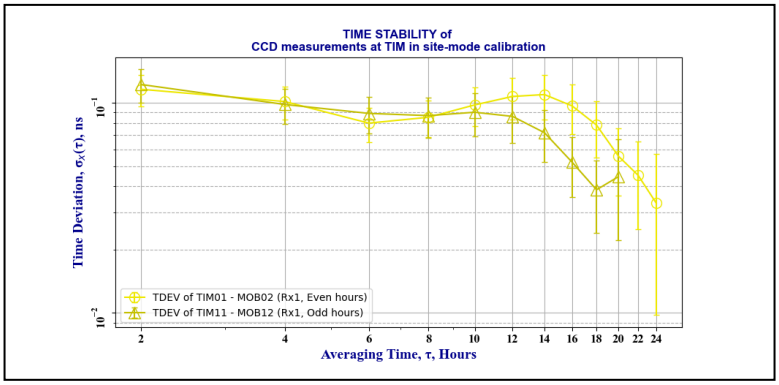

Figure 7-4 Time deviation of CCD measurements at TIM in site-mode calibration (<ki>=TIM01)

Figure 7-5 and Figure 7-6 show the CCD measurement data plot and TDEV of the data plot on the Rx2 channel of ES TIM01.

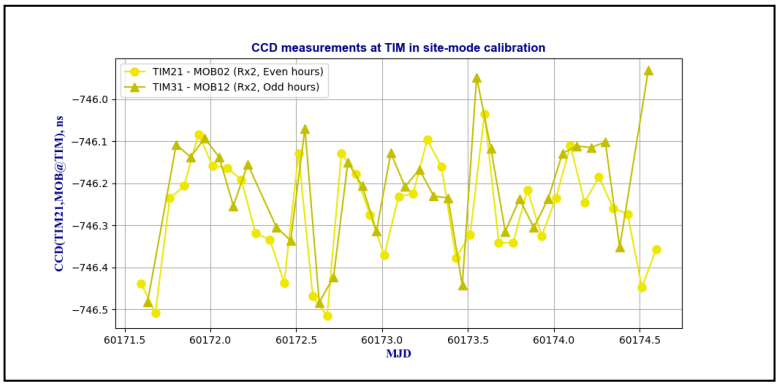

Figure 7-5 CCD measurements at TIM in site-mode calibration (<ki>=TIM21)

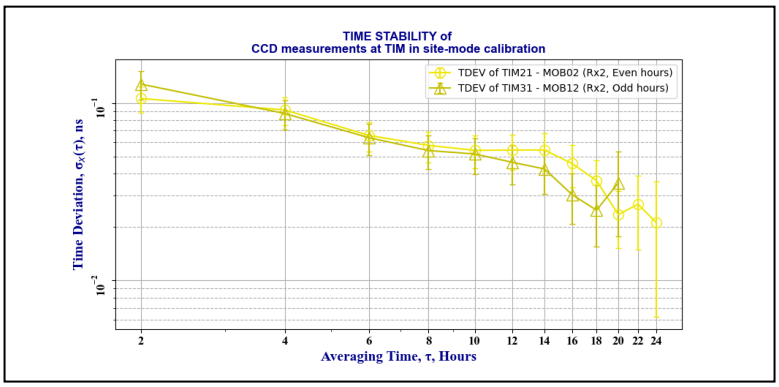

Figure 7-6 Time deviation of CCD closure measurements at TIM in site-mode calibration (<ki>=TIM21)

Table 7-3 lists the statistics of the CCD measurements on ES TIM01, including Rx1 and Rx2 channels. And Table 7-4 gives the results of the CCD measurements calculation on ES TIM01.

Table 7-3 Statistics of [TIM01-MOB02] CCD measurements at TIM

CCD Data Denotation	CCD Data Statistics		TDEV[CCD]		No. of Samples	No. of Gaps
	mean Unit: ns	stdev Unit: ns	TDEV Unit: ns	@ τ Unit: hr		
CCD_{even}(TIM01,MOB@TIM)	-742.537	0.151	0.107	12	37	0
CCD_{odd}(TIM11,MOB@TIM)	-742.481	0.153	0.086	12	33	3
CCD_{even}(TIM21,MOB@TIM)	-746.268	0.124	0.054	12	37	0
CCD_{odd}(TIM31,MOB@TIM)	-746.211	0.136	0.046	12	33	3

Table 7-4 CCD measurement results at TIM

Rx Channel	CCD_{avg}(TIM01,MOB@TIM) Unit: ns	uCCD(TIM01,MOB@TIM) Unit: ns	CCD_{diff}(TIM01,MOB@TIM) Unit: ns	Total No. of Samples
Rx1	-742.509	0.107	-0.057	70
Rx2	-746.240	0.054	-0.057	70

To investigate the relative CCD measurements between two local Rx channels within the same ES, Figure 7-7 and Figure 7-8 show the data plot and TDEV of the CCD between Rx1 and Rx2 of ES TIM01, respectively.

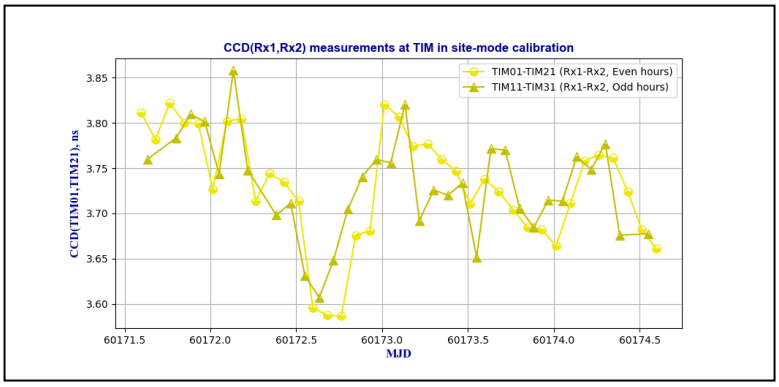

Figure 7-7 CCD(Rx1,Rx2) measurements on TIM01

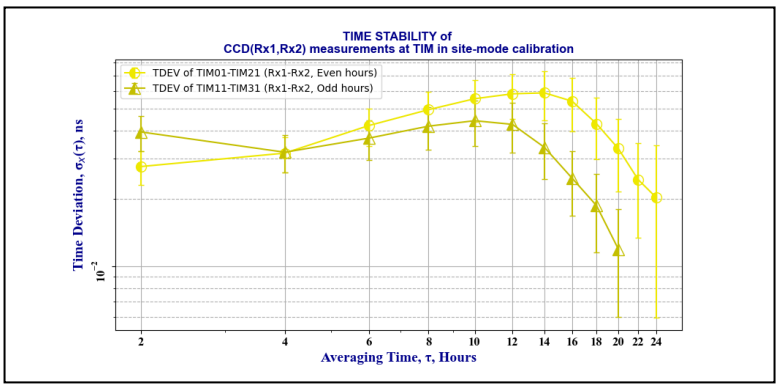

Figure 7-8 Time deviation of CCD(Rx1,Rx2) measurements on TIM01

Table 7-5 and

Table 7-6 summarize the statistics and final calculation results of CCD(Rx1,Rx2), respectively.

Table 7-5 Statistics of [TIM01-TIM21] CCD measurements at TIM

CCD Data Denotation	CCD Data Statistics	TDEV[CCD]		

	mean Unit: ns	stdev Unit: ns	TDEV Unit: ns	@ τ Unit: hr	No. of Samples	No. of Gaps
CCD_{even}(TIM01,TIM21)	3.731	0.063	0.058	12	37	0
CCD_{odd}(TIM11,TIM21)	3.730	0.056	0.043	12	33	3

Table 7-6 [TIM01-TIM21] CCD measurement results at TIM

Rx Channel	CCD_{avg}(TIM01,TIM21) Unit: ns	uCCD(TIM01,TIM21) Unit: ns	CCD_{diff}(TIM01,TIM21) Unit: ns	Total No. of Samples
Rx1-Rx2	3.731	0.058	0.000	70

7.3.2 CCD measurements at PL

Figure 7-9 and Figure 7-10 show the site top view of PL and the view of MOB during the on-site measurements at PL.

Figure 7-9 Site top view of PL

Figure 7-10 View of MOB at PL

Figure 7-11 and Figure 7-12 show the CCD measurement data plot and TDEV of the data plot on the Rx1 channel of ES PL01.

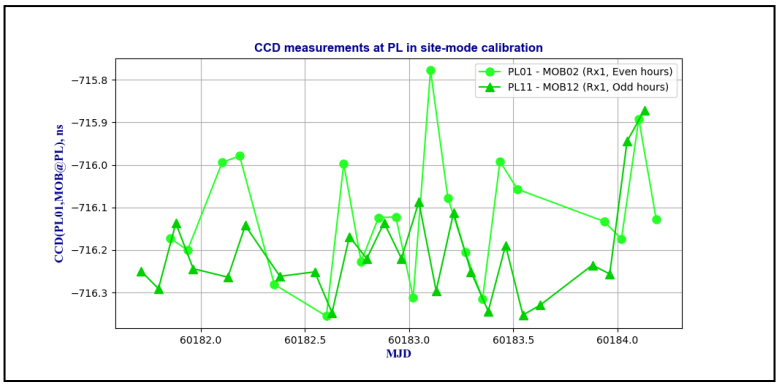

Figure 7-11 CCD measurements at PL in site-mode calibration (<ki>=PL01)

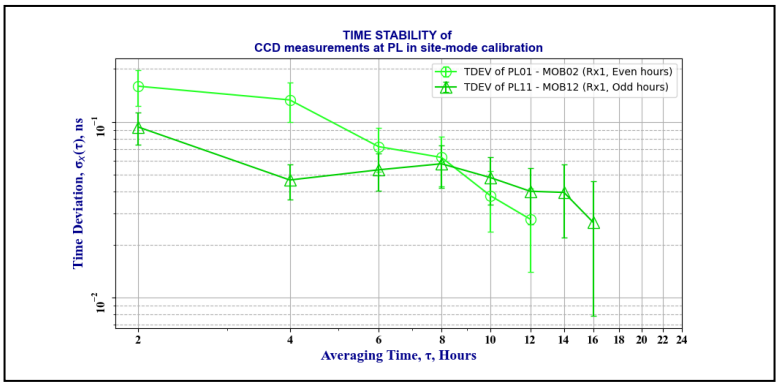

Figure 7-12 Time deviation of CCD measurements at PL in site-mode calibration (<ki>=PL01)

Figure 7-13 and Figure 7-14 show the CCD measurement data plot and TDEV of the data plot on the SDR channel of ES PL01.

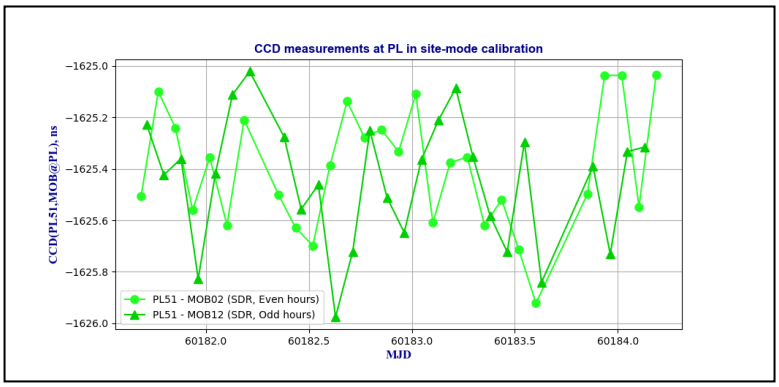

Figure 7-13 CCD measurements at PL in site-mode calibration (<ki>=PL51)

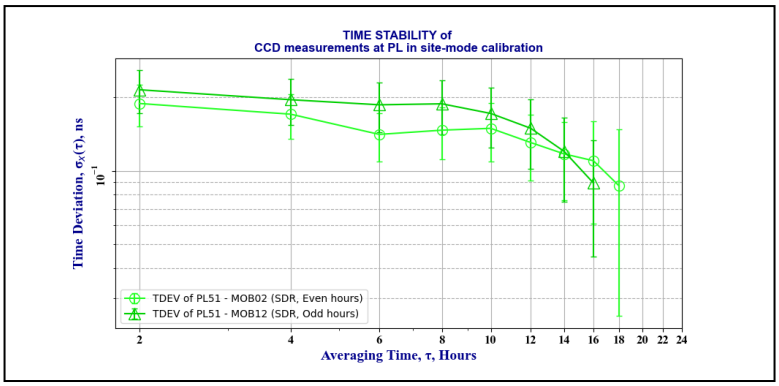

Figure 7-14 Time deviation of CCD measurements at PL in site-mode calibration (<ki>=PL51)

Table 7-7 lists the statistics of the CCD measurements on ES PL01, including Rx1 and SDR channels. And Table 7-8 gives the results of the CCD measurements calculation on ES PL01.

Table 7-7 Statistics of [PL01-MOB02] CCD measurements at PL

CCD Data Denotation	CCD Data Statistics		TDEV[CCD]		No. of Samples	No. of Gaps
	mean Unit: ns	stdev Unit: ns	TDEV Unit: ns	@ τ Unit: hr		
CCD_{even}(PL01,MOB@PL)	-716.120	0.146	0.028	12	21	8
CCD_{odd}(PL11,MOB@PL)	-716.208	0.117	0.040	12	25	5
CCD_{even}(PL51,MOB@PL)	-1625.399	0.235	0.131	12	28	3
CCD_{odd}(PL51,MOB@PL)	-1625.445	0.245	0.150	12	27	3

Table 7-8 [PL01-MOB02] CCD measurement results at PL

Rx Channel	CCD_{avg}(PL01,MOB@PL) Unit: ns	uCCD(PL01,MOB@PL) Unit: ns	CCD_{diff}(PL01,MOB@PL) Unit: ns	Total No. of Samples
Rx1	-716.164	0.040	0.088	46
SDR	-1625.422	0.150	0.046	55

To investigate the relative CCD measurements between two local Rx channels within the same ES, Figure 7-15 and Figure 7-16 show the data plot and TDEV of the CCD between Rx1 and SDR of ES PL01, respectively.

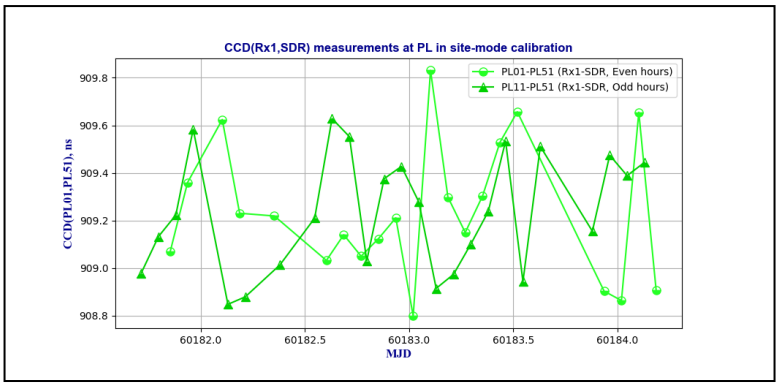

Figure 7-15 CCD(Rx1,SDR) measurements on PL01

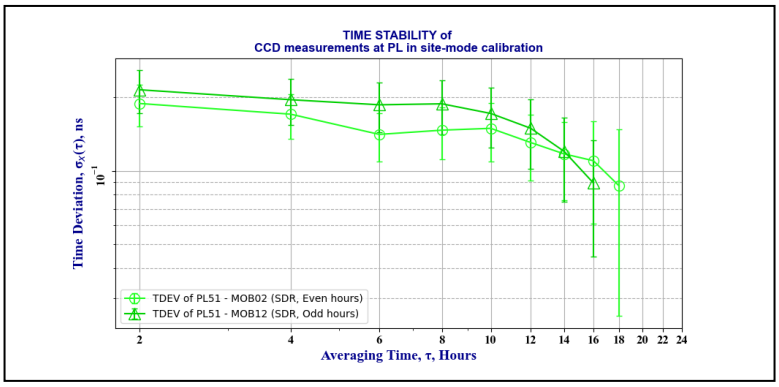

Figure 7-16 Time deviation of CCD(Rx1,SDR) measurements on PL01

Table 7-9 and Table 7-10 summarize the statistics and final calculation results of CCD(Rx1,SDR), respectively.

Table 7-9 Statistics of [PL01-PL51] CCD measurements at PL

CCD Data Denotation	CCD Data Statistics		TDEV[CCD]		No. of Samples	No. of Gaps
	mean Unit: ns	stdev Unit: ns	TDEV Unit: ns	@ τ Unit: hr		
CCD_{even}(PL01,PL51)	909.236	0.287	0.050	12	21	8
CCD_{odd}(PL11,PL51)	909.233	0.246	0.135	12	25	5

Table 7-10 [PL01-PL51] CCD measurement results at PL

Rx Diff	CCD_{avg}(PL01,PL51) Unit: ns	uCCD(PL01,PL51) Unit: ns	CCD_{diff}(PL01,PL51) Unit: ns	Total No. of Samples
Rx1-SDR	909.235	0.135	0.002	46

7.3.3 CCD measurements at PTB

Figure 7-17and Figure 7-18 show the site top view of PTB and the view of MOB during the on-site measurements at PTB.

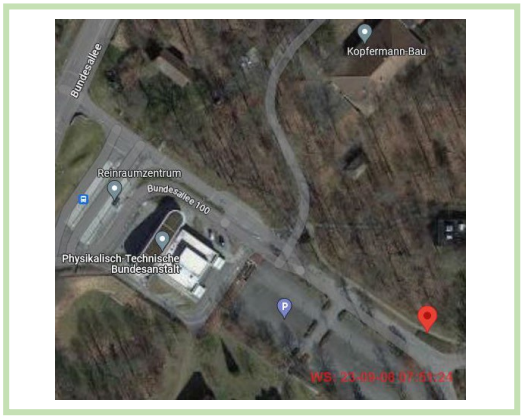

Figure 7-17 Site top view of PTB

Figure 7-18 View of MOB at PTB

7.3.3.1 CCD measurements on PTB05

Figure 7-19 and Figure 7-20 show the CCD measurement data plot and TDEV of the data plot on the Rx1 channel of ES PTB05.

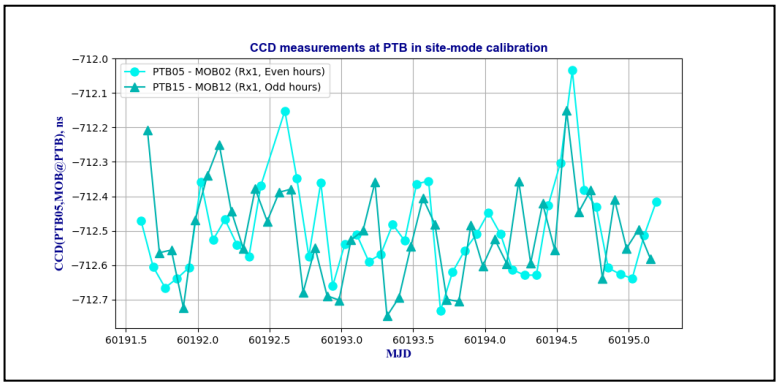

Figure 7-19 CCD measurements at PTB in site-mode calibration (<ki>=PTB05)

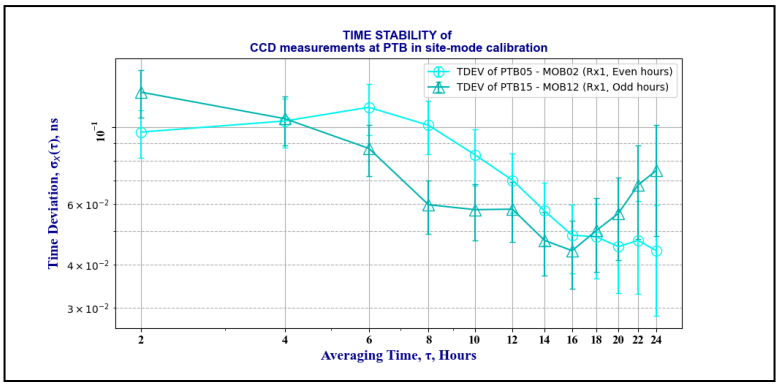

Figure 7-20 Time deviation of CCD measurements at PTB in site-mode calibration (<ki>=PTB05)

Figure 7-21 and Figure 7-22 show the CCD measurement data plot and TDEV of the data plot on the Rx2 channel of ES PTB05.

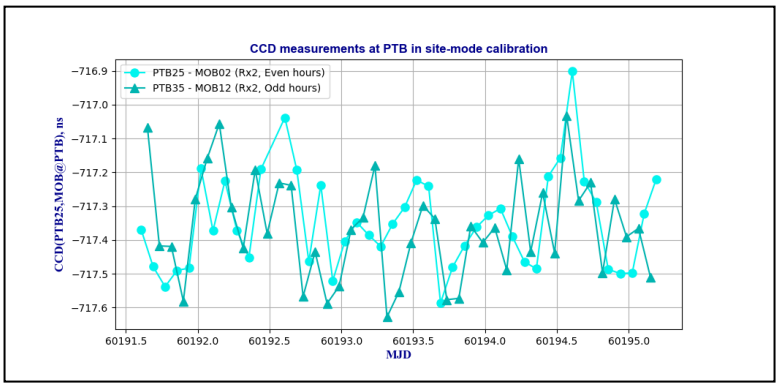

Figure 7-21 CCD measurements at PTB in site-mode calibration (<ki>=PTB25)

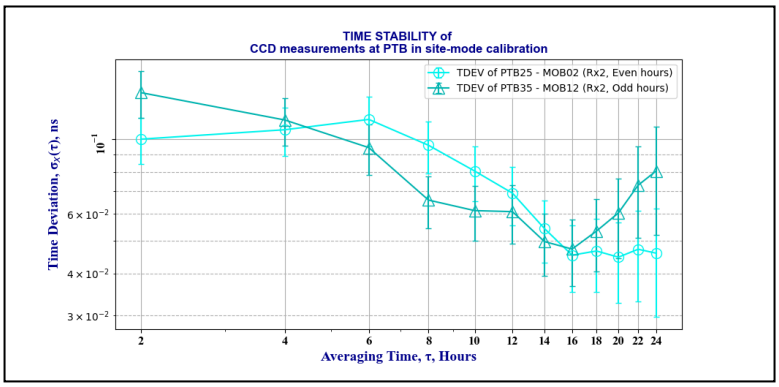

Figure 7-22 Time deviation of CCD measurements at PTB in site-mode calibration (<ki>=PTB25)

Figure 7-23 and Figure 7-24 show the CCD measurement data plot and TDEV of the data plot on the SDR channel of ES PTB05.

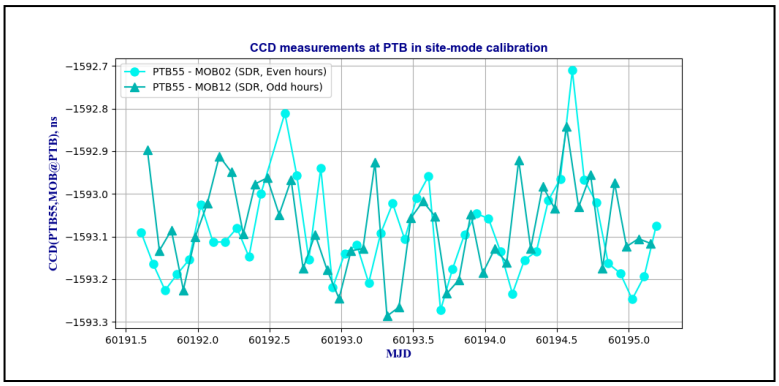

Figure 7-23 CCD measurements at PTB in site-mode calibration (<ki>=PTB55)

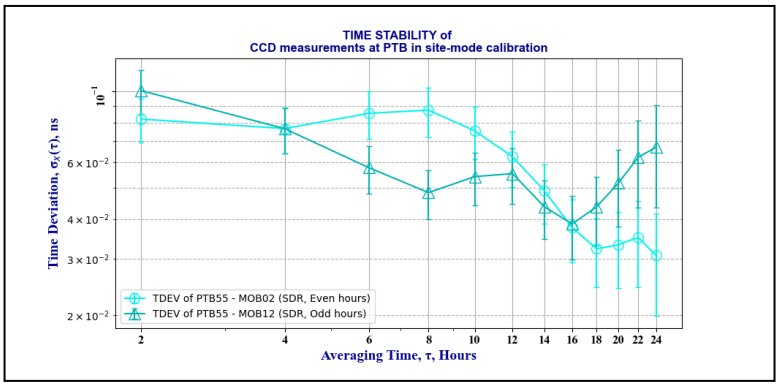

Figure 7-24 Time deviation of CCD measurements at PTB in site-mode calibration (<ki>=PTB55)

Table 7-11 lists the statistics of the CCD measurements on ES PTB05, including Rx1, Rx2 and SDR channels. Table 7-12 gives the results of the CCD measurements calculation on ES PTB05.

Table 7-11 Statistics of [PTB05-MOB02] CCD measurements at PTB

CCD Data Denotation	CCD Data Statistics		TDEV[CCD]		No. of Samples	No. of Gaps
	mean Unit: ns	stdev Unit: ns	TDEV Unit: ns	@ τ Unit: hr		
CCD_{even}(PTB05,MOB@PTB)	-712.500	0.140	0.070	12	43	1
CCD_{odd}(PTB15,MOB@PTB)	-712.507	0.141	0.058	12	43	0
CCD_{even}(PTB25,MOB@PTB)	-717.347	0.142	0.069	12	43	1
CCD_{odd}(PTB35,MOB@PTB)	-717.363	0.153	0.061	12	43	0
CCD_{even}(PTB55,MOB@PTB)	-1593.090	0.114	0.063	12	43	1
CCD_{odd}(PTB55,MOB@PTB)	-1593.076	0.109	0.055	12	43	0

Table 7-12 [PTB05-MOB02] CCD measurement results at PTB

Rx Channel	CCD_{avg}(PTB05,MOB@PTB) Unit: ns	uCCD(PTB05,MOB@PTB) Unit: ns	CCD_{diff}(PTB05,MOB@PTB) Unit: ns	Total No. of Samples
Rx1	-712.503	0.070	0.007	86
Rx2	-717.355	0.069	0.016	86
SDR	-1593.083	0.063	-0.014	86

To investigate the relative CCD measurements between three local Rx channels within the same ES, Figure 7-25 and Figure 7-26 show the data plot and TDEV of the CCD between Rx1 and Rx2 of ES PTB05, respectively. And Figure 7-27 and Figure 7-28 show the data plot and TDEV of the CCD between Rx1 and SDR of ES PTB05, respectively.

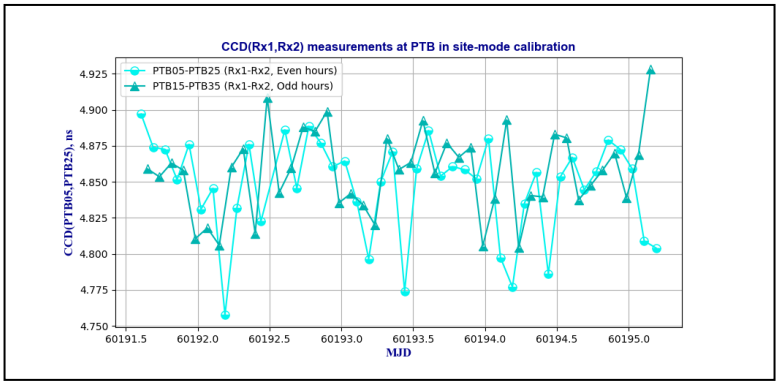

Figure 7-25 CCD(Rx1,Rx2) measurements on PTB05

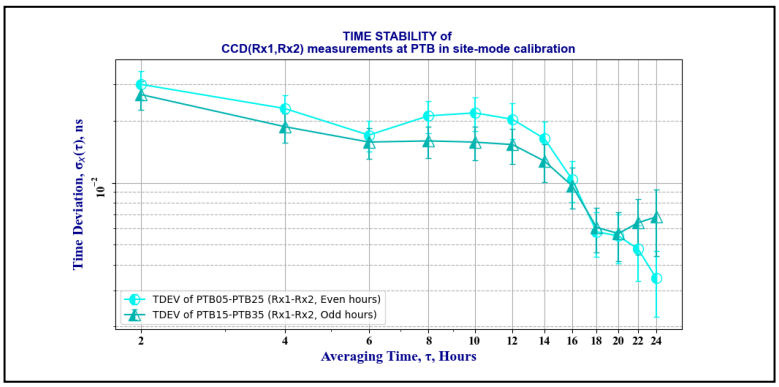

Figure 7-26 Time deviation of CCD(Rx1,Rx2) measurements on PTB05

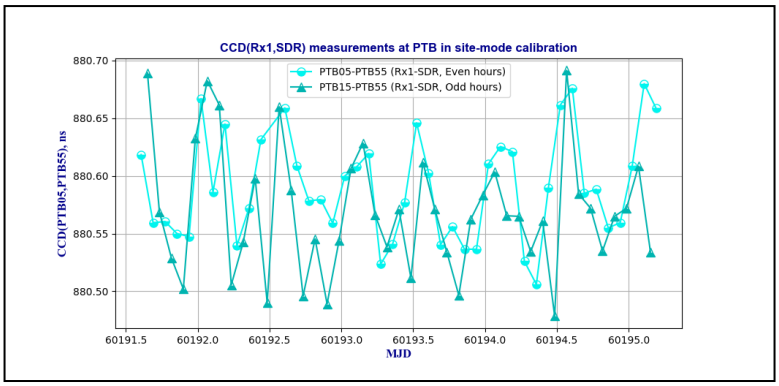

Figure 7-27 CCD(Rx1,SDR) measurements on PTB05

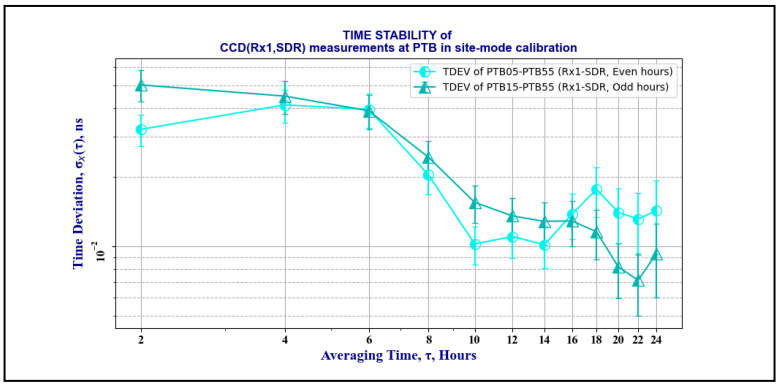

Figure 7-28 Time deviation of CCD(Rx1,SDR) measurements on PTB05

Table 7-13 and Table 7-14 summarize the statistics and final calculation results of CCD(Rx1,Rx2) and CCD(Rx1,SDR), respectively.

Table 7-13 Statistics of [PTB05-PTB25] and [PTB05-PTB25] CCD measurements on PTB05

CCD Data Denotation	CCD Data Statistics		TDEV[CCD]		No. of Samples	No. of Gaps
	mean Unit: ns	stdev Unit: ns	TDEV Unit: ns	@ τ Unit: hr		
CCD_{even}(PTB05,PTB25)	4.847	0.034	0.020	12	43	1
CCD_{odd}(PTB15,PTB25)	4.857	0.029	0.015	12	43	0
CCD_{even}(PTB05,PTB55)	880.591	0.046	0.011	12	43	1
CCD_{odd}(PTB15,PTB55)	880.569	0.055	0.014	12	43	0

Table 7-14 [PTB05-PTB25] and [PTB05-PTB55] CCD measurement results on PTB05

Rx Differ.	CCD_{avg}(PTB05,<i_{Rx}>)	uCCD(PTB05,<i_{Rx}>)	CCD_{diff}(PTB05,<i_{Rx}>)	

Rx1-<i_{Rx}>	Unit: ns	Unit: ns	Unit: ns	Total No. of Samples
Rx1-Rx2	4.852	0.020	-0.009	86
Rx1-SDR	880.580	0.014	0.021	86

7.3.3.2 CCD measurements on PTB04

Figure 7-29 and Figure 7-30 show the CCD measurement data plot and TDEV of the data plot on the Rx1 channel of ES PTB04.

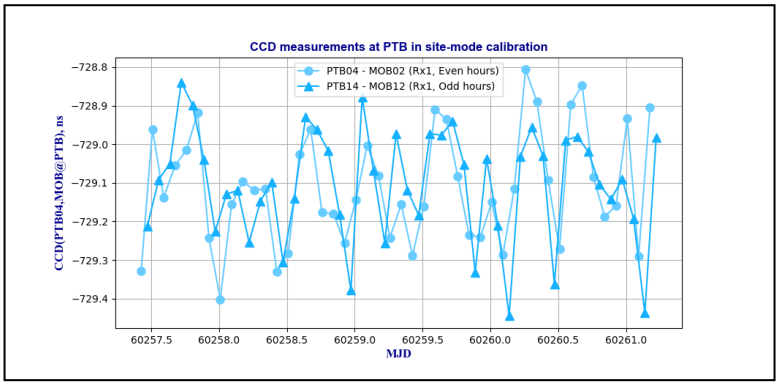

Figure 7-29 CCD measurements at PTB in site-mode calibration (<ki>=PTB04)

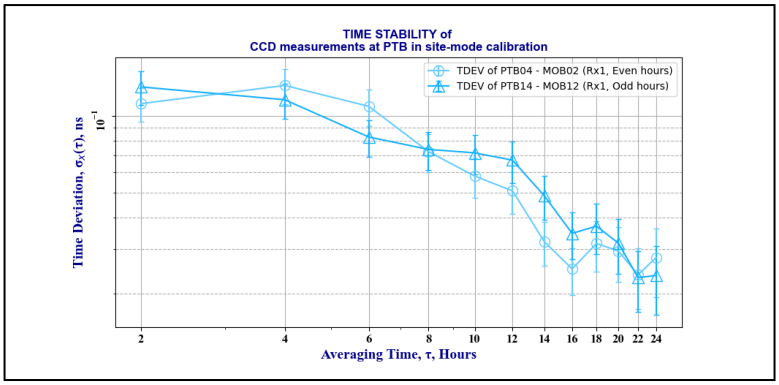

Figure 7-30 Time deviation of CCD measurements at PTB in site-mode calibration (<ki>=PTB04)

Table 7-15 lists the statistics of the CCD measurements on Rx1 channel of ES PTB04. Table 7-16 gives the results of the CCD measurements calculation on ES PTB04.

Table 7-15 Statistics of [PTB04-MOB02] CCD measurements on PTB04

CCD Data Denotation	CCD Data Statistics		TDEV[CCD]		No. of Samples	No. of Gaps
	mean Unit: ns	stdev Unit: ns	TDEV Unit: ns	@ τ Unit: hr		

CCD_{even}(PTB04,MOB@PTB)	-729.112	0.051	0.146	12	46	0
CCD_{odd}(PTB14,MOB@PTB)	-729.104	0.067	0.147	12	46	0

Table 7-16 [PTB04-MOB02] CCD measurement results on PTB04

Rx Channel	CCD_{avg}(PTB04,MOB@PTB) Unit: ns	uCCD(PTB04,MOB@PTB) Unit: ns	CCD_{diff}(PTB04,MOB@PTB) Unit: ns	Total No. of Samples
Rx1	-729.108	0.067	-0.008	92

7.3.4 CCD measurements at VSL

Figure 7-31 and Figure 7-32 show the site top view of VSL and the view of MOB during the on-site measurements at VSL.

Figure 7-31 Site top view of VSL

Figure 7-32 View of MOB at VSL

Figure 7-33 and Figure 7-34 show the CCD measurement data plot and TDEV of the data plot on the Rx1 channel of ES VSL01.

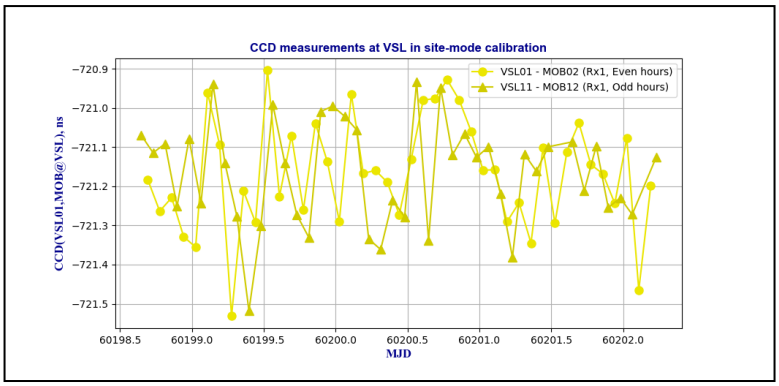

Figure 7-33 CCD measurements at VSL in site-mode calibration (<ki>=VSL01)

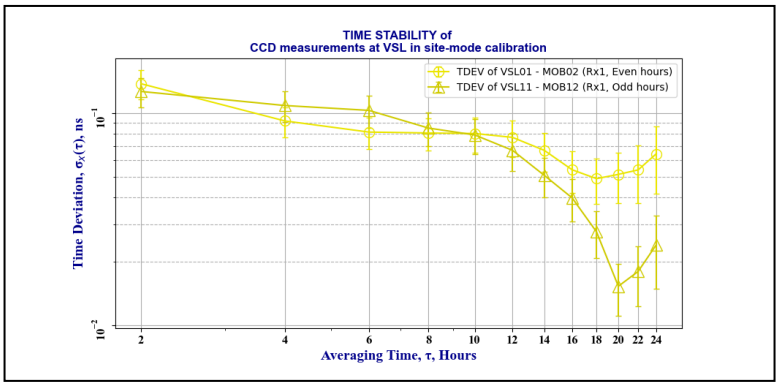

Figure 7-34 Time deviation of CCD measurements at VSL in site-mode calibration (<ki>=VSL01)

Figure 7-35 and Figure 7-36 show the CCD measurement data plot and TDEV of the data plot on the Rx2 channel of ES VSL01.

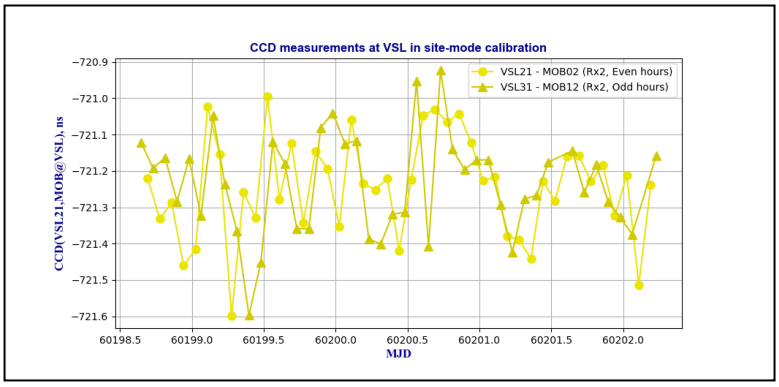

Figure 7-35 CCD measurements at VSL in site-mode calibration (<ki>=VSL21)

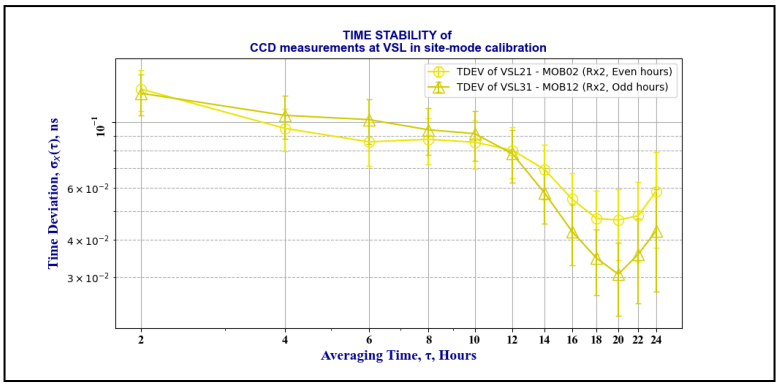

Figure 7-36 Time deviation of CCD measurements at VSL in site-mode calibration (<ki>=VSL21)

Figure 7-37 and Figure 7-38 show the CCD measurement data plot and TDEV of the data plot on the SDR channel of ES VSL01.

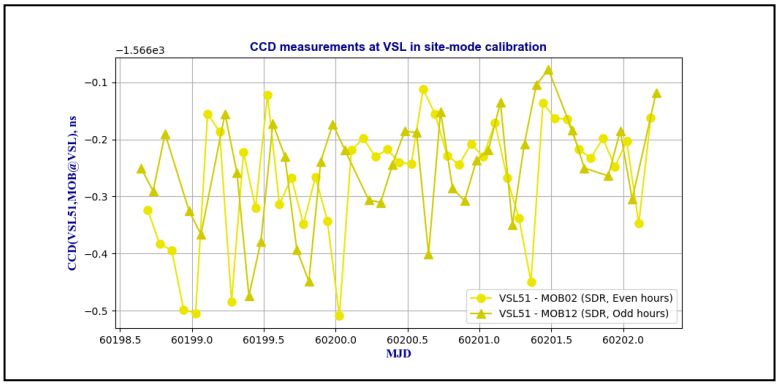

Figure 7-37 CCD measurements at VSL in site-mode calibration (<ki>=VSL51)

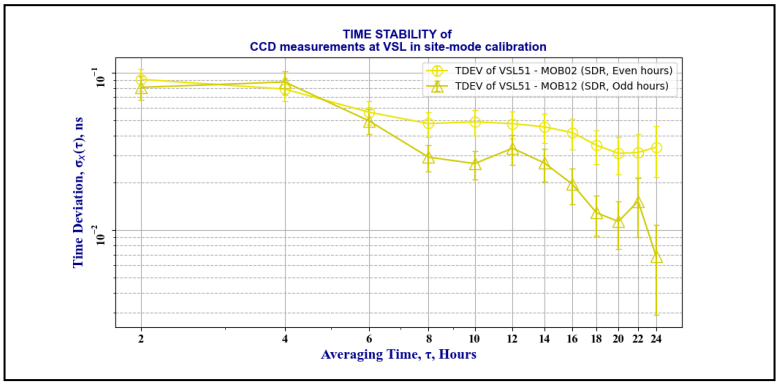

Figure 7-38 Time deviation of CCD measurements at VSL in site-mode calibration (<ki>=VSL51)

Table 7-17 lists the statistics of the CCD measurements on ES VSL01, including Rx1, RX2 and SDR channels. Table 7-18 gives the results of the CCD measurements calculation on ES VSL01.

Table 7-17 Statistics of [VSL01-MOB02] CCD measurements at VSL

CCD Data Denotation	CCD Data Statistics		TDEV[CCD]		No. of Samples	No. of Gaps
	mean Unit: ns	stdev Unit: ns	TDEV Unit: ns	@ τ Unit: hr		
CCD_{even}(VSL01,MOB@VSL)	-721.168	0.140	0.077	12	43	0
CCD_{odd}(VSL11,MOB@VSL)	-721.165	0.133	0.067	12	42	2
CCD_{even}(VSL21,MOB@VSL)	-721.242	0.138	0.080	12	43	0
CCD_{odd}(VSL31,MOB@VSL)	-721.235	0.138	0.078	12	42	2
CCD_{even}(VSL51,MOB@VSL)	-1566.267	0.107	0.047	12	43	0
CCD_{odd}(VSL51,MOB@VSL)	-1566.252	0.095	0.033	12	38	6

Table 7-18 [VSL01-MOB02] CCD measurement results at VSL

Rx Channel	CCD_{avg}(VSL01,MOB@VSL) Unit: ns	uCCD(VSL01,MOB@VSL) Unit: ns	CCD_{diff}(VSL01,MOB@VSL) Unit: ns	Total No. of Samples
Rx1	-721.166	0.077	-0.003	85
Rx2	-721.239	0.080	-0.007	85
SDR	-1566.259	0.047	-0.015	81

To investigate the relative CCD measurements between three local Rx channels within the same ES, Figure 7-39 and Figure 7-40 show the data plot and TDEV of the CCD between Rx1 and Rx2 of ES VSL01, respectively. And Figure 7-41 and Figure 7-42 show the data plot and TDEV of the CCD between Rx1 and SDR of ES VSL01, respectively.

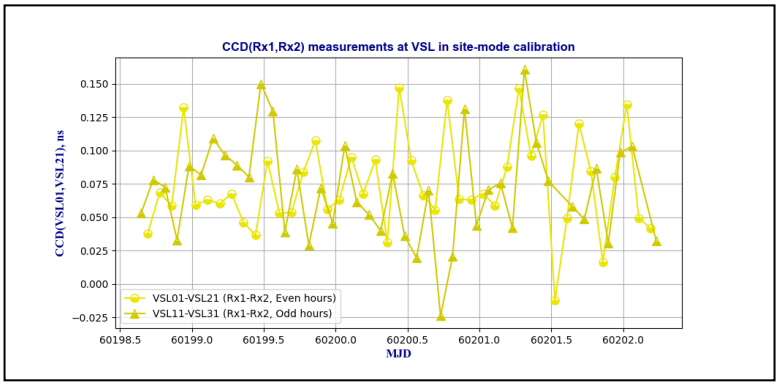

Figure 7-39 CCD(Rx1,Rx2) measurements on VSL01

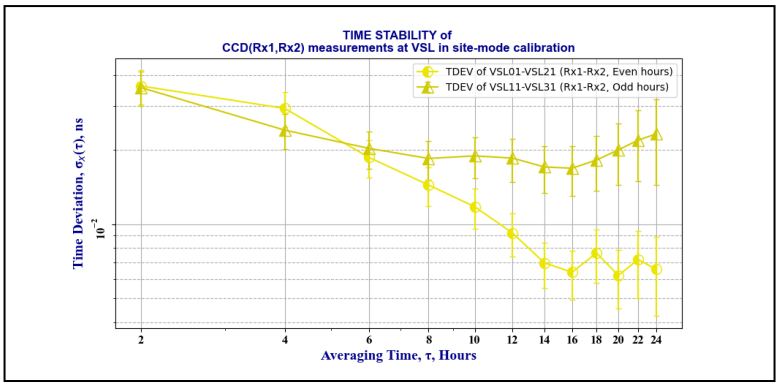

Figure 7-40 Time deviation of CCD(Rx1,Rx2) measurements on VSL01

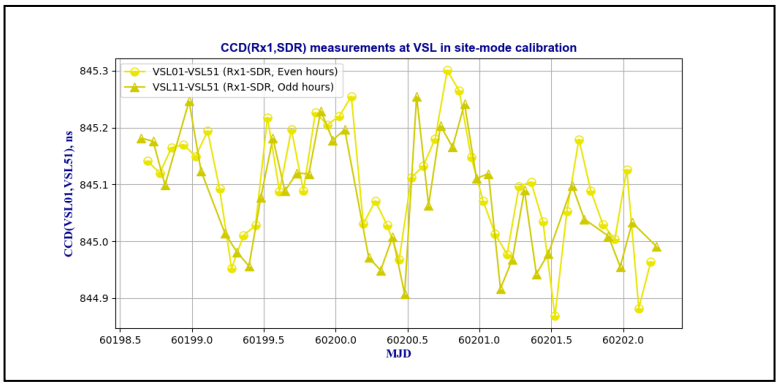

Figure 7-41 CCD(Rx1,SDR) measurements on VSL01

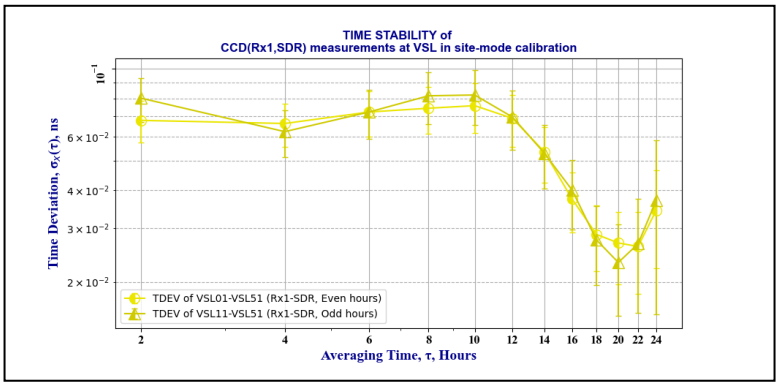

Figure 7-42 Time deviation of CCD(Rx1,SDR) measurements on VSL01

Table 7-19 and Table 7-20 summarize the statistics and final calculation results of CCD(Rx1,Rx2) and CCD(Rx1,SDR), respectively.

Table 7-19 Statistics of [VSL01-VSL21] and [VSL01-VSL51] CCD measurements at VSL

CCD Data Denotation	CCD Data Statistics	TDEV[CCD]		

	mean Unit: ns	stdev Unit: ns	TDEV Unit: ns	@ τ Unit: hr	No. of Samples	No. of Gaps
CCD_{even}(VSL01,VSL21)	0.074	0.035	0.009	12	43	0
CCD_{odd}(VSL11,VSL21)	0.070	0.037	0.018	12	42	2
CCD_{even}(VSL01,VSL51)	845.099	0.100	0.069	12	43	0
CCD_{odd}(VSL11,VSL51)	845.079	0.102	0.070	12	38	6

Table 7-20 [VSL01-VSL21] and [VSL01-VSL51] CCD measurement results at VSL

Rx Differ. Rx1-<i_{Rx}>	CCD_{avg}(VSL01,<i_{Rx}>) Unit: ns	uCCD(VSL01,<i_{Rx}>) Unit: ns	CCD_{diff}(VSL01,<i_{Rx}>) Unit: ns	Total No. of Samples
Rx1-Rx2	0.072	0.018	0.004	85
Rx1-SDR	845.089	0.070	0.020	81

7.3.5 CCD measurements at LTFB

Figure 7-43 and Figure 7-44 show the site top view of LTFB and the view of MOB during the on-site measurements at LTFB.

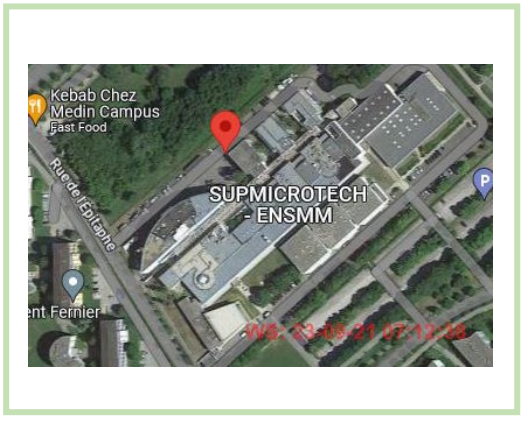

Figure 7-43 Site top view of LTFB

Figure 7-44 View of MOB at LTFB

Figure 7-45 and Figure 7-46 show the CCD measurement data plot and TDEV of the data plot on the Rx1 channel of ES LTFB01.

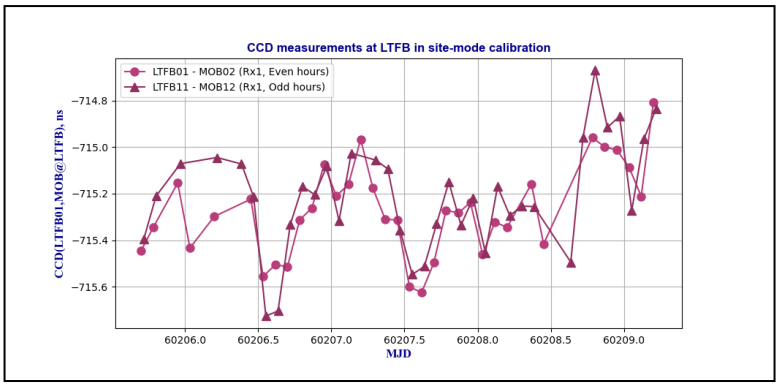

Figure 7-45 CCD measurements at LTFB in site-mode calibration (<ki>=LTFB01)

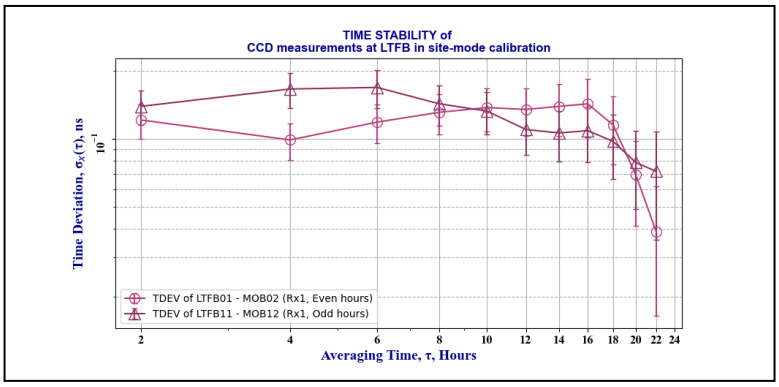

Figure 7-46 Time deviation of CCD measurements at LTFB in site-mode calibration (<ki>=LTFB01)

Figure 7-47 and Figure 7-48 show the CCD measurement data plot and TDEV of the data plot on the Rx2 channel of ES LTFB01.

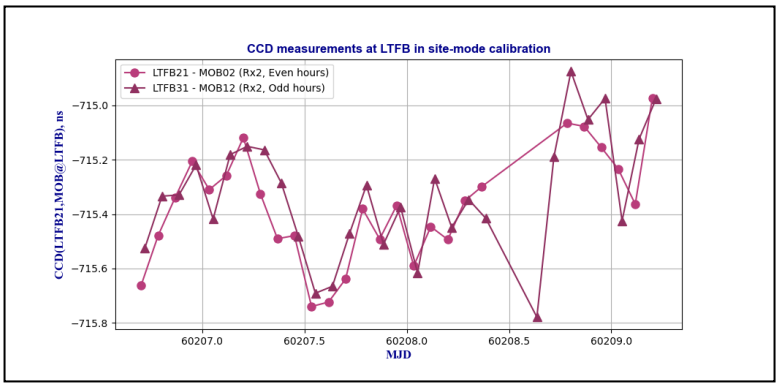

Figure 7-47 CCD measurements at LTFB in site-mode calibration (<ki>=LTFB21)

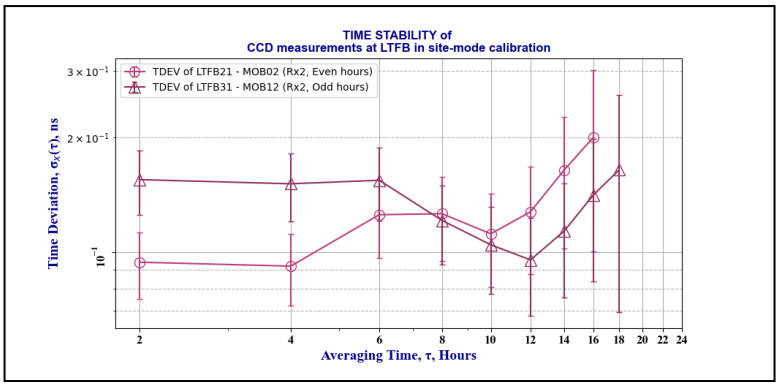

Figure 7-48 Time deviation of CCD measurements at LTFB in site-mode calibration (<ki>=LTFB21)

Table 7-21 lists the statistics of the CCD measurements on ES LTFB01, including Rx1 and Rx2 channels. Table 7-22 gives the results of the CCD measurements calculation on ES LTFB01.

Table 7-21 Statistics of CCD measurements at LTFB

CCD Data Denotation	CCD Data Statistics		TDEV[CCD]		No. of Samples	No. of Gaps
	mean Unit: ns	stdev Unit: ns	TDEV Unit: ns	@ τ Unit: hr		
CCD_{even}(LTFB01,MOB@LTFB)	-715.273	0.195	0.135	12	35	8
CCD_{odd}(LTFB11,MOB@LTFB)	-715.210	0.233	0.110	12	36	7
CCD_{even}(LTFB21,MOB@LTFB)	-715.373	0.202	0.128	12	27	16
CCD_{odd}(LTFB31,MOB@LTFB)	-715.330	0.222	0.095	12	29	14

Table 7-22 CCD measurement results at LTFB

Rx Channel	CCD_{avg}(LTFB01,MOB@LTFB) Unit: ns	*u*CCD(LTFB01,MOB@LTFB) Unit: ns	CCD_{diff}(LTFB01,MOB@LTFB) Unit: ns	Total No. of Samples
Rx1	-715.242	0.135	-0.063	71
Rx2	-715.352	0.128	-0.042	56

To investigate the relative CCD measurements between two local Rx channels within the same ES, Figure 7-49 and Figure 7-50 show the data plot and TDEV of the CCD between Rx1 and Rx2 of ES LTFB01, respectively.

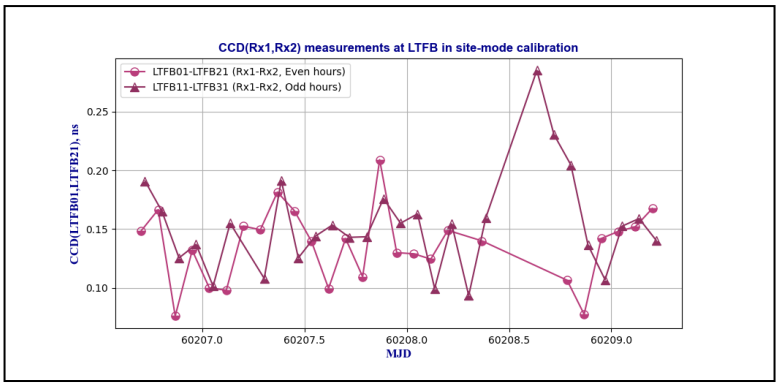

Figure 7-49 CCD(Rx1,Rx2) measurements on LTFB01

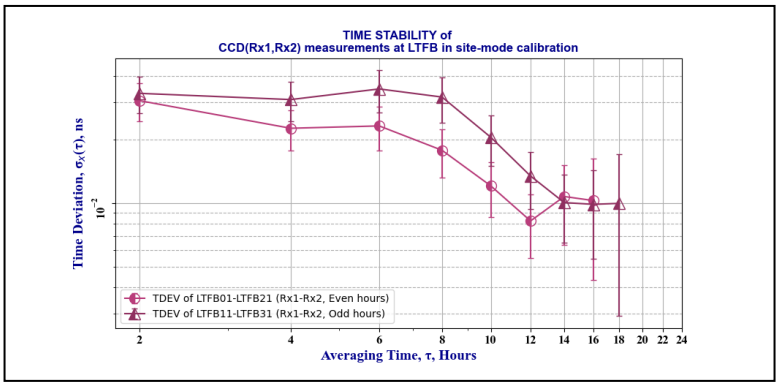

Figure 7-50 Time deviation of CCD(Rx1,Rx2) measurements on LTFB01

Table 7-23 and Table 7-24 summarize the statistics and final calculation results of CCD(Rx1,Rx2), respectively.

Table 7-23 Statistics of [LTFB01-LTFB21] CCD measurements at LTFB

CCD Data Denotation	CCD Data Statistics		TDEV[CCD]		No. of Samples	No. of Gaps
	mean Unit: ns	stdev Unit: ns	TDEV Unit: ns	@ τ Unit: hr		
CCD_{even}(LTFB01,LTFB21)	0.136	0.031	0.008	12	26	17
CCD_{odd}(LTFB11,LTFB21)	0.154	0.041	0.013	12	28	15

Table 7-24 [LTFB01-LTFB21] CCD measurement results at LTFB

Rx Differ.	CCD_{avg}(LTFB01,LTFB21) Unit: ns	uCCD(LTFB01,LTFB21) Unit: ns	CCD_{diff}(LTFB01,LTFB21) Unit: ns	Total No. of Samples
Rx1-Rx2	0.145	0.013	-0.018	54

7.3.6 CCD measurements at ROA

Figure 7-51 and Figure 7-52 show the site top view of ROA and the view of MOB during the on-site measurements at ROA.

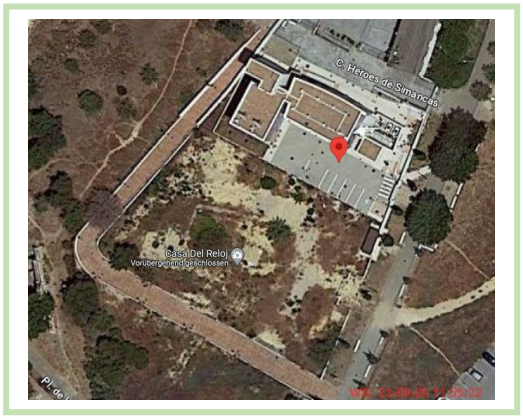

Figure 7-51 Site top view of ROA

Figure 7-52 View of MOB at ROA

Figure 7-53 and Figure 7-54 show the CCD measurement data plot and TDEV of the data plot on the Rx1 channel of ES ROA01.

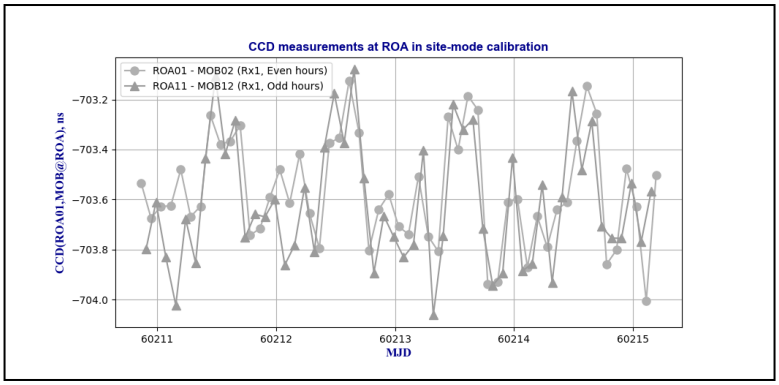

Figure 7-53 CCD measurements at ROA in site-mode calibration (<ki>=ROA01)

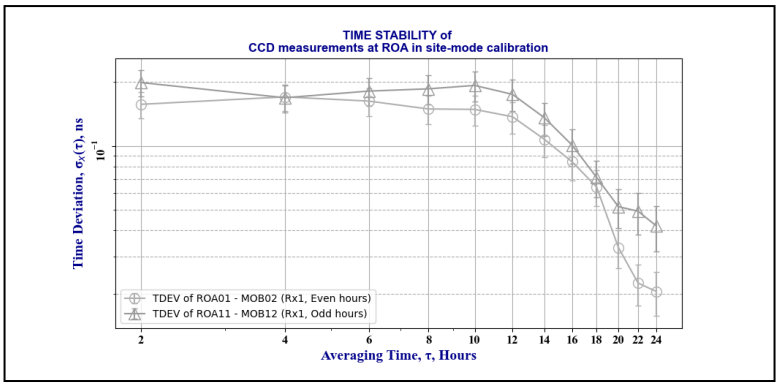

Figure 7-54 Time deviation of CCD measurements at ROA in site-mode calibration (<ki>=ROA01)

Figure 7-55 and Figure 7-56 show the CCD measurement data plot and TDEV of the data plot on the Rx2 channel of ES ROA01.

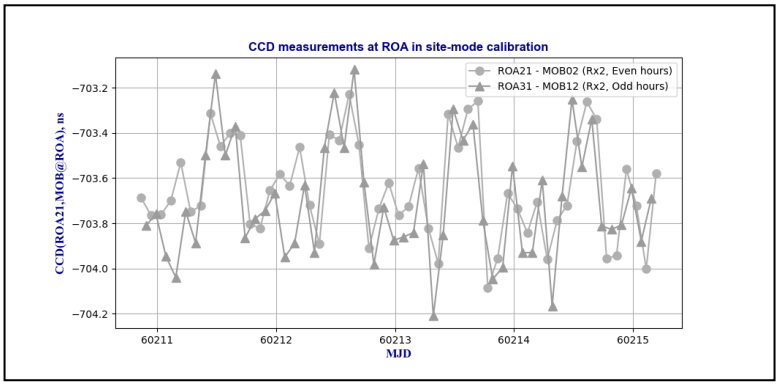

Figure 7-55 CCD measurements at ROA in site-mode calibration (<ki>=ROA21)

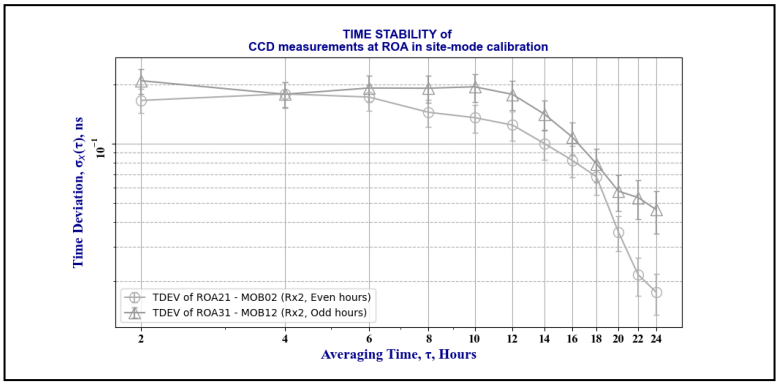

Figure 7-56 Time deviation of CCD measurements at ROA in site-mode calibration (<ki>=ROA21)

Figure 7-57 and Figure 7-58 show the CCD measurement data plot and TDEV of the data plot on the SDR channel of ES ROA01.

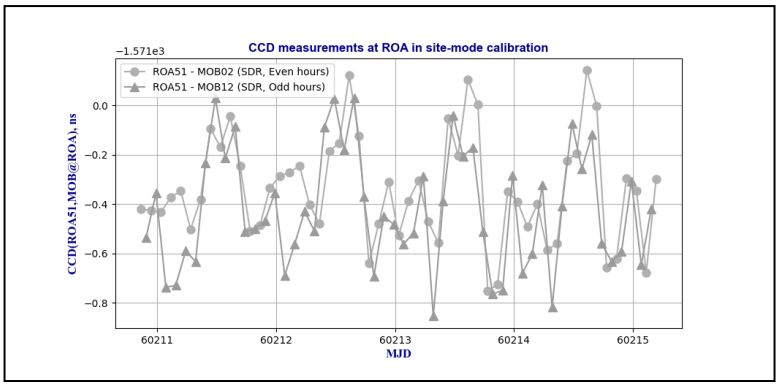

Figure 7-57 CCD measurements at ROA in site-mode calibration (<ki>=ROA51)

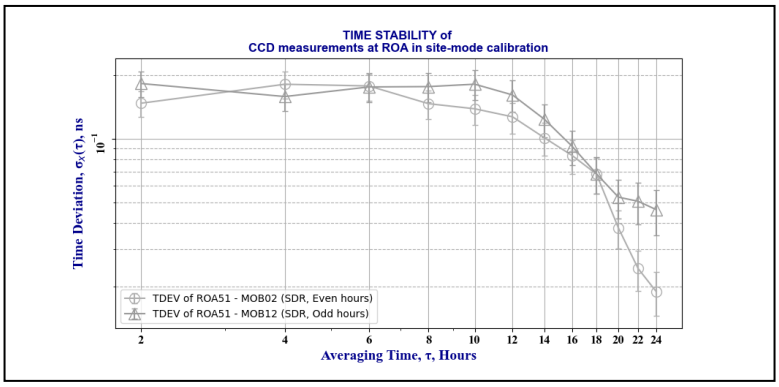

Figure 7-58 Time deviation of CCD measurements at ROA in site-mode calibration (<ki>=ROA51)

Table 7-25 lists the statistics of the CCD measurements on ES ROA01, including Rx1, Rx2 and SDR channels. Table 7-26 gives the results of the CCD measurements calculation on ES ROA01.

Table 7-25 Statistics of [ROA01-MOB02] CCD measurements at ROA

CCD Data Denotation	CCD Data Statistics		TDEV[CCD]		No. of Samples	No. of Gaps
	mean	stdev	TDEV	@ τ		
	Unit: ns	Unit: ns	Unit: ns	Unit: hr		
CCD_{even}(ROA01,MOB@ROA)	-703.567	0.216	0.137	12	53	0
CCD_{odd}(ROA11,MOB@ROA)	-703.616	0.249	0.175	12	52	0
CCD_{even}(ROA21,MOB@ROA)	-703.647	0.221	0.124	12	53	0
CCD_{odd}(ROA31,MOB@ROA)	-703.702	0.259	0.178	12	52	0
CCD_{even}(ROA51,MOB@ROA)	-1571.341	0.215	0.127	12	53	0
CCD_{odd}(ROA51,MOB@ROA)	-1571.425	0.237	0.162	12	52	0

Table 7-26 [ROA01-MOB02] CCD measurement results at ROA

Rx Channel	CCD_{avg}(ROA01,MOB@ROA) Unit: ns	uCCD(ROA01,MOB@ROA) Unit: ns	CCD_{diff}(ROA01,MOB@ROA) Unit: ns	Total No. of Samples
Rx1	-703.592	0.175	0.048	105
Rx2	-703.674	0.178	0.055	105
SDR	-1571.383	0.162	0.084	105

To investigate the relative CCD measurements between two local Rx channels within the same ES, Figure 7-59 and Figure 7-60 show the data plot and TDEV of the CCD between Rx1 and Rx2 of ES ROA01, respectively. And Figure 7-61 and Figure 7-62 show the data plot and TDEV of the CCD between Rx1 and SDR of ES ROA01, respectively.

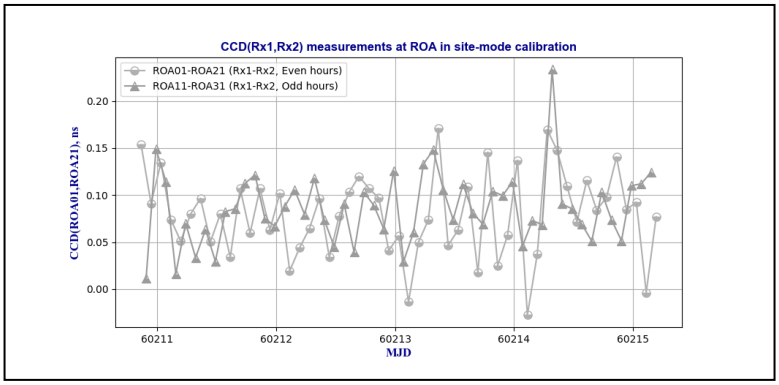

Figure 7-59 CCD(Rx1,Rx2) measurements on ROA01

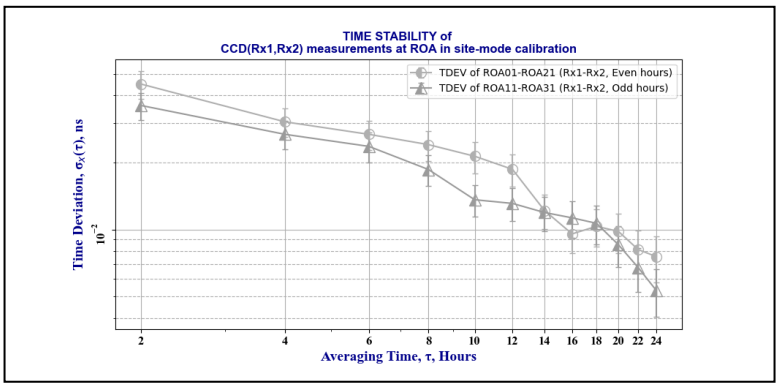

Figure 7-60 Time deviation of CCD(Rx1,Rx2) measurements on ROA01

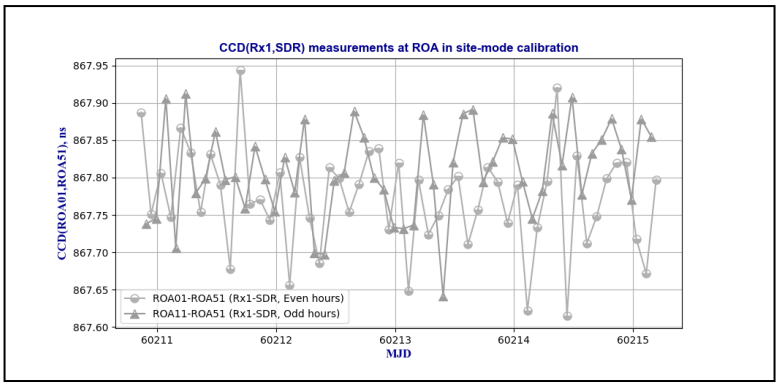

Figure 7-61 CCD(Rx1,SDR) measurements on ROA01

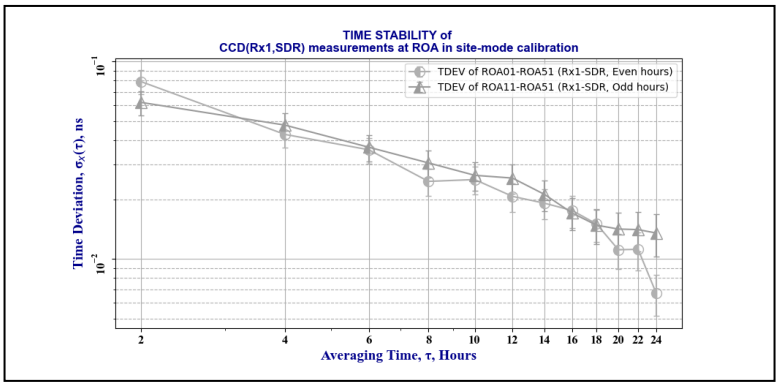

Figure 7-62 Time deviation of CCD(Rx1,SDR) measurements on ROA01

Table 7-27 and Table 7-28 summarize the statistics and final calculation results of CCD(Rx1,Rx2) and CCD(Rx1,SDR), respectively.

Table 7-27 Statistics of [ROA01-ROA21] and [ROA01-ROA51] CCD measurements at ROA

CCD Data Denotation	CCD Data Statistics		TDEV[CCD]		No. of Samples	No. of Gaps
	mean Unit: ns	stdev Unit: ns	TDEV Unit: ns	@ τ Unit: hr		
CCD_{even}(ROA01,ROA21)	0.080	0.044	0.019	12	53	0
CCD_{odd}(ROA11,ROA21)	0.086	0.038	0.013	12	52	0
CCD_{even}(ROA01,ROA51)	867.773	0.068	0.021	12	53	0
CCD_{odd}(ROA11,ROA51)	867.809	0.062	0.026	12	52	0

Table 7-28 [ROA01-ROA21] and [ROA01-ROA51] CCD measurement results at ROA

Rx Differ.	CCD_{avg}(ROA01,<i_{Rx}>)	uCCD(ROA01,<i_{Rx}>)	CCD_{diff}(ROA01,<i_{Rx}>)	

Rx1-<i_{Rx}>	Unit: ns	Unit: ns	Unit: ns	Total No. of Samples
Rx1-Rx2	0.083	0.019	-0.006	105
Rx1-SDR	867.791	0.026	-0.036	105

7.3.7 CCD measurements at OP

Figure 7-63 and Figure 7-64 show the site top view of OP and the view of MOB during the on-site measurements at OP.

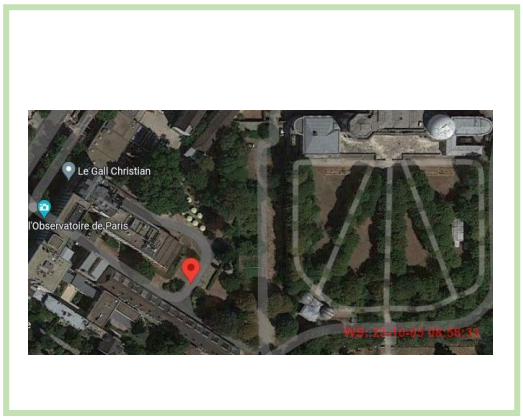

Figure 7-63 Site top view of OP

Figure 7-64 View of MOB at OP

Figure 7-65 and Figure 7-66 show the CCD measurement data plot and TDEV of the data plot on the Rx1 channel of ES OP01.

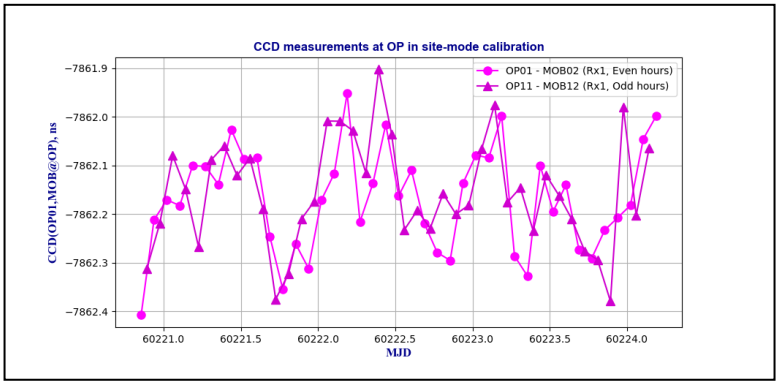

Figure 7-65 CCD measurements at OP in site-mode calibration (<ki>=OP01)

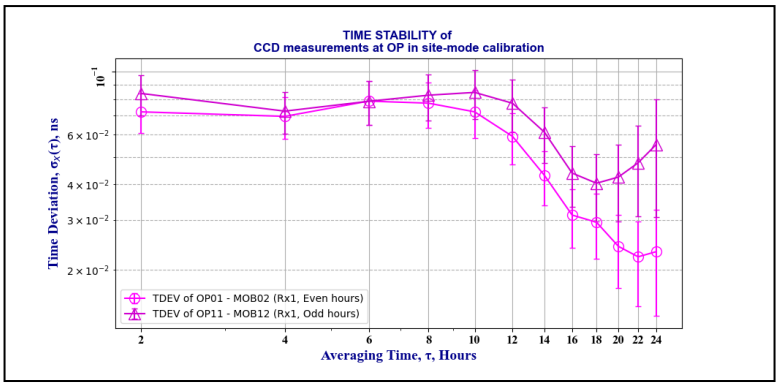

Figure 7-66 Time deviation of CCD measurements at OP in site-mode calibration (<ki>=OP01)

Figure 7-67 and Figure 7-68 show the CCD measurement data plot and TDEV of the data plot on the SDR channel of ES OP01. For the TW link of [OP51-MOB02], there is no even-hour sessions data in CCD measurements.

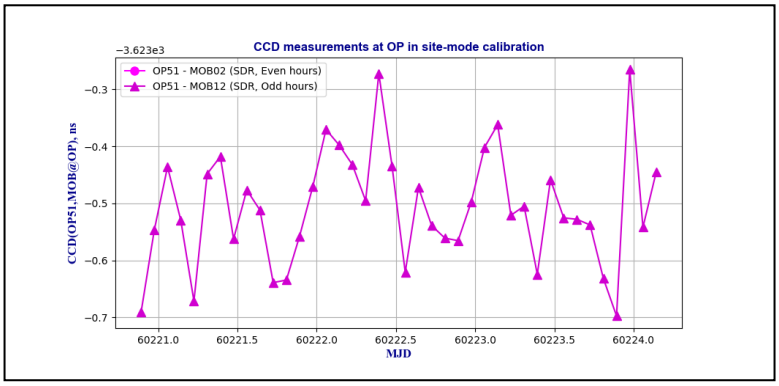

Figure 7-67 CCD measurements at OP in site-mode calibration (<ki>=OP51)

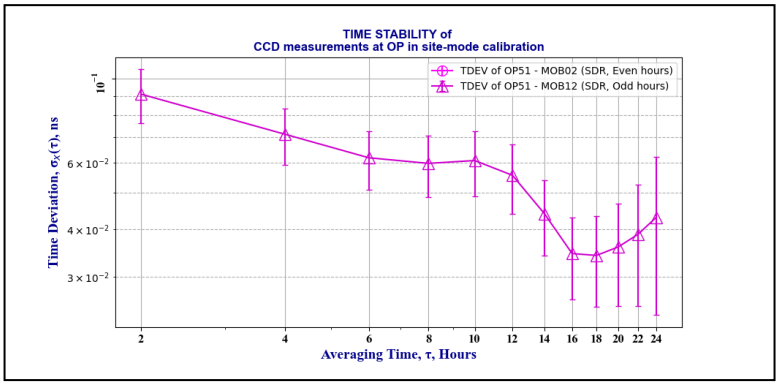

Figure 7-68 Time deviation of CCD measurements at OP in site-mode calibration (<ki>=OP51)

Table 7-29 lists the statistics of the CCD measurements on ES OP01, including Rx1 and SDR channels. Table 7-30 gives the results of the CCD measurements calculation on ES OP01.

Table 7-29 Statistics of [OP01-MOB02] CCD measurements at OP

CCD Data Denotation	CCD Data Statistics		TDEV[CCD]		No. of Samples	No. of Gaps
	mean Unit: ns	stdev Unit: ns	TDEV Unit: ns	@ τ Unit: hr		
CCD_{even}(OP01,MOB@OP)	-7862.169	0.106	0.059	12	41	0
CCD_{odd}(OP11,MOB@OP)	-7862.156	0.111	0.077	12	40	0
CCD_{even}(OP51,MOB@OP)	--	--	--	--	--	--
CCD_{odd}(OP51,MOB@OP)	-3623.507	0.102	0.056	12	40	0

Table 7-30 [OP01-MOB02] CCD measurement results at OP

Rx Channel	CCD_{avg}(OP01,MOB@OP) Unit: ns	uCCD(OP01,MOB@OP) Unit: ns	CCD_{diff}(OP01,MOB@OP) Unit: ns	Total No. of Samples
Rx1	-7862.162	0.077	-0.013	81
SDR	-3623.507	0.056	--	40

To investigate the relative CCD measurements between two local Rx channels within the same ES, Figure 7-69 and Figure 7-70 show the data plot and TDEV of the CCD between Rx1 and SDR of ES OP01, respectively.

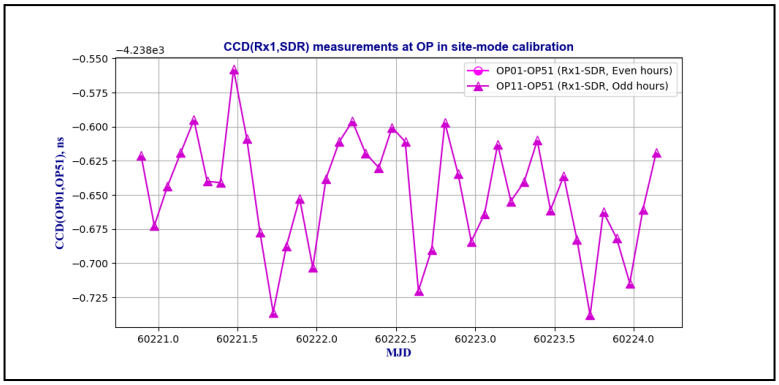

Figure 7-69 CCD(Rx1,SDR) measurements on OP01

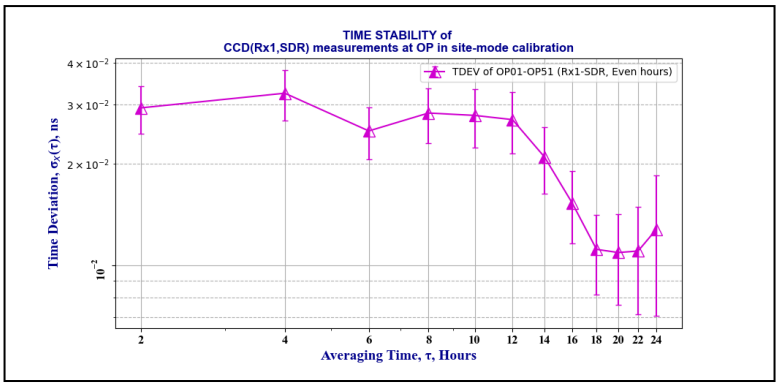

Figure 7-70 Time deviation of CCD(Rx1,SDR) measurements on OP01

Table 7-31 and Table 7-32 summarize the statistics and final calculation results of CCD(Rx1,SDR), respectively.

Table 7-31 Statistics of [OP01-OP51] CCD measurements at OP

CCD Data Denotation	CCD Data Statistics		TDEV[CCD]		No. of Samples	No. of Gaps
	mean Unit: ns	stdev Unit: ns	TDEV Unit: ns	@ τ Unit: hr		
CCD_{even}(OP01,OP51)	--	--	--	--	--	--
CCD_{odd}(OP11,OP51)	-4238.648	0.042	0.027	12	40	40

Table 7-32 [OP01-OP51] CCD measurement results at OP

Rx Differ.	CCD_{avg}(OP01,OP51) Unit: ns	*u*CCD(OP01,OP51) Unit: ns	CCD_{diff}(OP01,OP51) Unit: ns	Total No. of Samples
Rx1-SDR	-4238.648	0.027	--	40

7.3.8 CCD measurements at NPL

Figure 7-71 and Figure 7-72 show the site top view of NPL and the view of MOB during the on-site measurements at NPL.

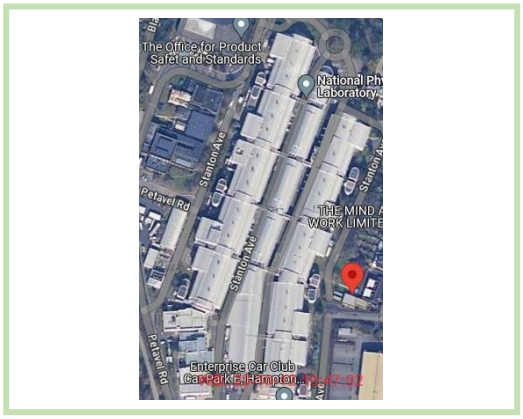

Figure 7-71 Site top view of NPL

Figure 7-72 View of MOB at NPL

Figure 7-73 and Figure 7-74 show the CCD measurement data plot and TDEV of the data plot on the Rx1 channel of ES NPL01.

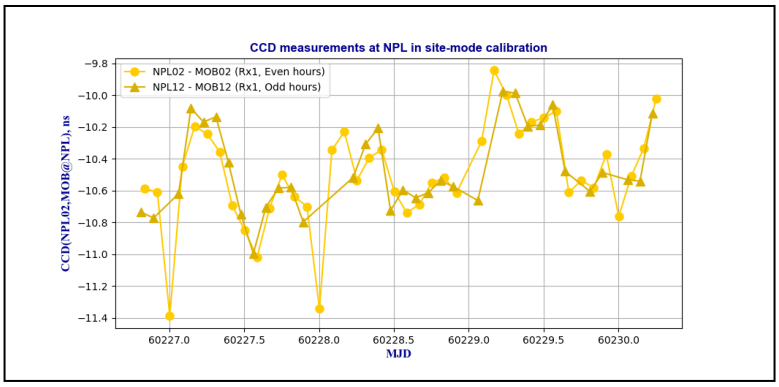

Figure 7-73 CCD measurements at NPL in site-mode calibration (<ki>=NPL02)

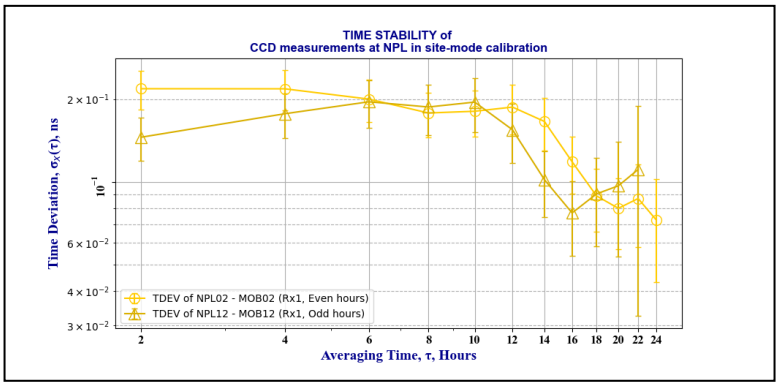

Figure 7-74 Time deviation of CCD measurements at NPL in site-mode calibration (<ki>=NPL02)

Table 7-33 lists the statistics of the CCD measurements on Rx1 channel of ES NPL01. Table 7-34 gives the results of the CCD measurements calculation on ES NPL01.

Table 7-33 Statistics of CCD measurements at NPL

CCD Data Denotation	CCD Data Statistics		TDEV[CCD]		No. of Samples	No. of Gaps
	mean Unit: ns	stdev Unit: ns	TDEV Unit: ns	@ τ Unit: hr		
CCD_{even}(NPL02,MOB@NPL)	-10.497	0.318	0.187	12	41	1
CCD_{odd}(NPL12,MOB@NPL)	-10.468	0.265	0.155	12	34	8

Table 7-34 CCD measurement results at NPL

Rx Channel	CCD_{avg}(NPL02,MOB@NPL) Unit: ns	uCCD(NPL02,MOB@NPL) Unit: ns	CCD_{diff}(NPL02,MOB@NPL) Unit: ns	Total No. of Samples
Rx1	-10.483	0.187	-0.029	75

7.3.9 CCD measurements at SP

Figure 7-75 and Figure 7-76 show the site top view of SP and the view of MOB during the on-site measurements at SP.

Figure 7-75 Site top view of SP

Figure 7-76 View of MOB at SP

Figure 7-77 and Figure 7-78 show the CCD measurement data plot and TDEV of the data plot on the Rx1 channel of ES SP01.

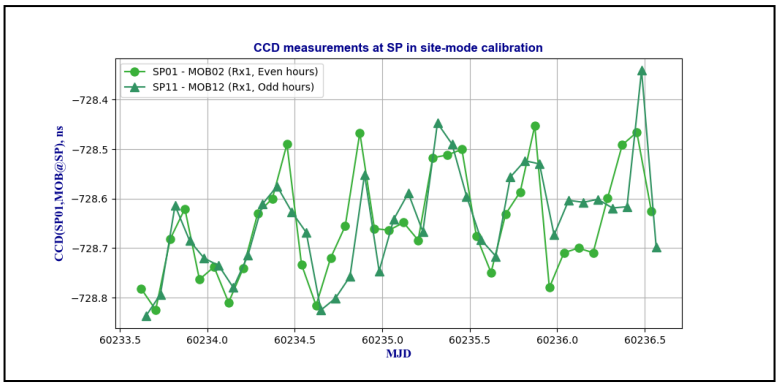

Figure 7-77 CCD measurements at SP in site-mode calibration (<ki>=SP01)

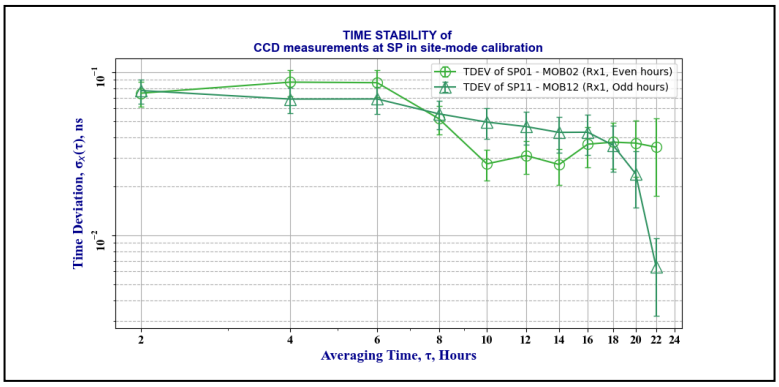

Figure 7-78 Time deviation of CCD measurements at SP in site-mode calibration (<ki>=SP01)

Figure 7-79 and Figure 7-80 show the CCD measurement data plot and TDEV of the data plot on the Rx2 channel of ES SP01.

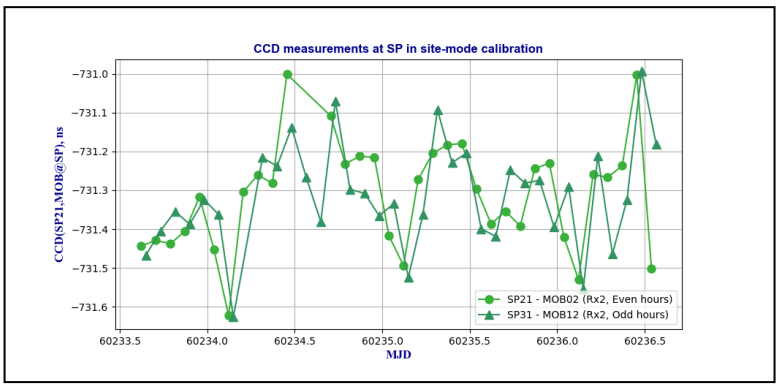

Figure 7-79 CCD measurements at SP in site-mode calibration (<ki>=SP21)

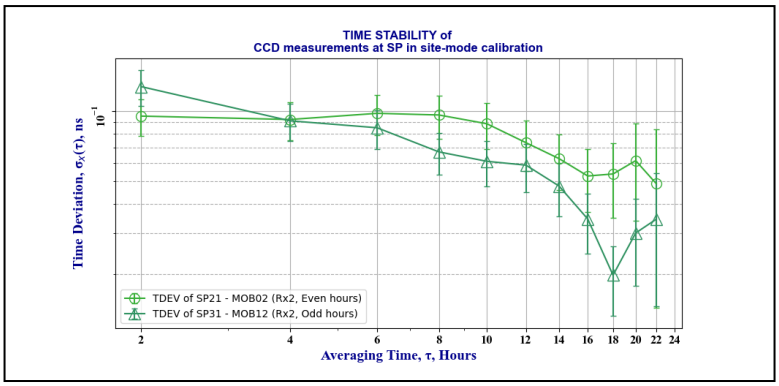

Figure 7-80 Time deviation of CCD measurements at SP in site-mode calibration (<ki>=SP21)

Figure 7-81 and Figure 7-82 show the CCD measurement data plot and TDEV of the data plot on the SDR channel of ES SP01.

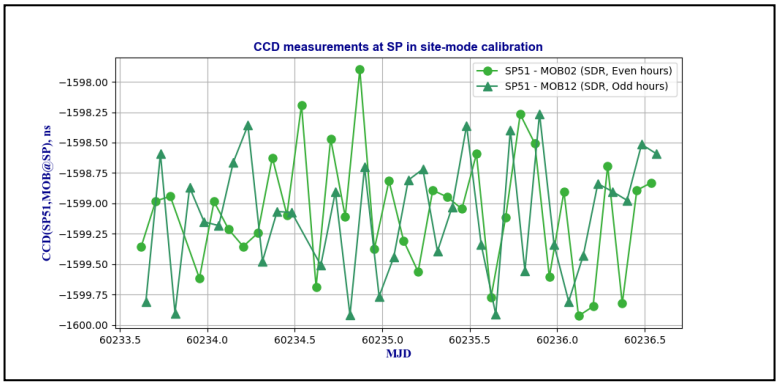

Figure 7-81 CCD measurements at SP in site-mode calibration (<ki>=SP51)

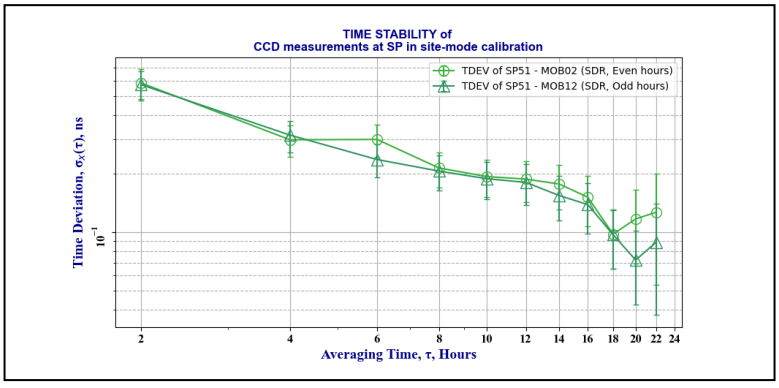

Figure 7-82 Time deviation of CCD measurements at SP in site-mode calibration (<ki>=SP51)

Table 7-35 lists the statistics of the CCD measurements on ES SP01, including Rx1, Rx2 and SDR channels. Table 7-36 gives the results of the CCD measurements calculation on ES SP01.

Table 7-35 Statistics of [SP01-MOB02] CCD measurements at SP

CCD Data Denotation	CCD Data Statistics		TDEV[CCD]		No. of Samples	No. of Gaps
	mean Unit: ns	stdev Unit: ns	TDEV Unit: ns	@ τ Unit: hr		
CCD_{even}(SP01,MOB@SP)	-728.651	0.108	0.031	12	36	0
CCD_{odd}(SP11,MOB@SP)	-728.646	0.108	0.046	12	36	0
CCD_{even}(SP21,MOB@SP)	-731.312	0.141	0.073	12	34	2
CCD_{odd}(SP31,MOB@SP)	-731.314	0.134	0.059	12	35	1
CCD_{even}(SP51,MOB@SP)	-1599.071	0.493	0.188	12	35	1
CCD_{odd}(SP51,MOB@SP)	-1599.102	0.495	0.180	12	35	1

Table 7-36 [SP01-MOB02] CCD measurement results at SP

Rx Channel	CCD_{avg}(SP01,MOB@SP) Unit: ns	uCCD(SP01,MOB@SP) Unit: ns	CCD_{diff}(SP01,MOB@SP) Unit: ns	Total No. of Samples
Rx1	-728.648	0.046	-0.005	72
Rx2	-731.313	0.073	0.002	69
SDR	-1599.086	0.188	0.031	70

To investigate the relative CCD measurements between three local Rx channels within the same ES, Figure 7-83 and Figure 7-84 show the data plot and TDEV of the CCD between Rx1 and Rx2 of ES SP01, respectively. And Figure 7-85 and Figure 7-86 show the data plot and TDEV of the CCD between Rx1 and SDR of ES SP01, respectively.

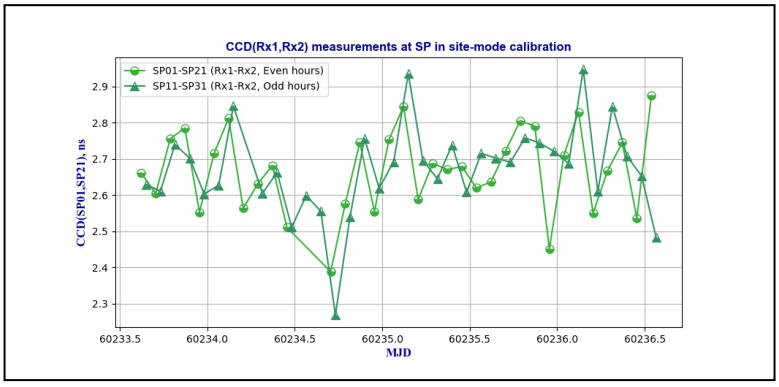

Figure 7-83 CCD(Rx1,Rx2) measurements on SP01

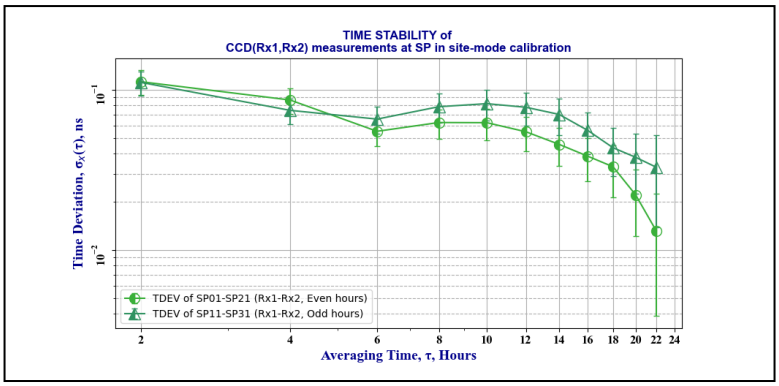

Figure 7-84 Time deviation of CCD(Rx1,Rx2) measurements on SP01

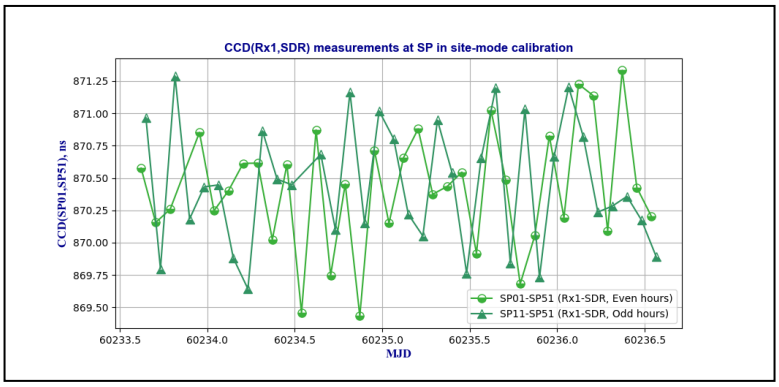

Figure 7-85 CCD(Rx1,SDR) measurements on SP01

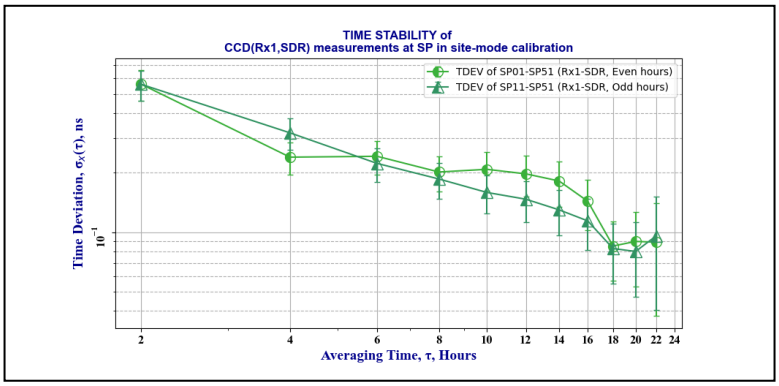

Figure 7-86 Time deviation of CCD(Rx1,SDR) measurements on SP01

Table 7-37 and Table 7-38

Table 7-38 summarize the statistics and final calculation results of CCD(Rx1,Rx2) and CCD(Rx1,SDR), respectively.

Table 7-37 Statistics of [SP01-SP21] and [SP01-SP51] CCD measurements at SP

CCD Data Denotation	CCD Data Statistics	TDEV[CCD]		

	mean Unit: ns	stdev Unit: ns	TDEV Unit: ns	@ τ Unit: hr	No. of Samples	No. of Gaps
CCD_{even}(SP01,SP21)	2.668	0.116	0.055	12	34	2
CCD_{odd}(SP11,SP21)	2.670	0.125	0.078	12	35	1
CCD_{even}(SP01,SP51)	870.419	0.462	0.198	12	35	1
CCD_{odd}(SP11,SP51)	870.456	0.479	0.147	12	35	1

Table 7-38 [SP01-SP21] and [SP01-SP51] CCD measurement results at SP

Rx Differ. Rx1-<i_{Rx}>	CCD_{avg}(SP01,<i_{Rx}>) Unit: ns	uCCD(SP01,<i_{Rx}>) Unit: ns	CCD_{diff}(SP01,<i_{Rx}>) Unit: ns	Total No. of Samples
Rx1-Rx2	2.669	0.078	-0.003	69
Rx1-SDR	870.438	0.198	-0.038	70

7.3.10 CCD measurements at IT

Figure 7-87 and Figure 7-88 show the site top view of IT and the view of MOB during the on-site measurements at IT.

Figure 7-87 Site top view of IT

Figure 7-88 View of MOB at IT

Figure 7-89 and Figure 7-90 show the CCD measurement data plot and TDEV of the data plot on the Rx1 channel of ES IT01.

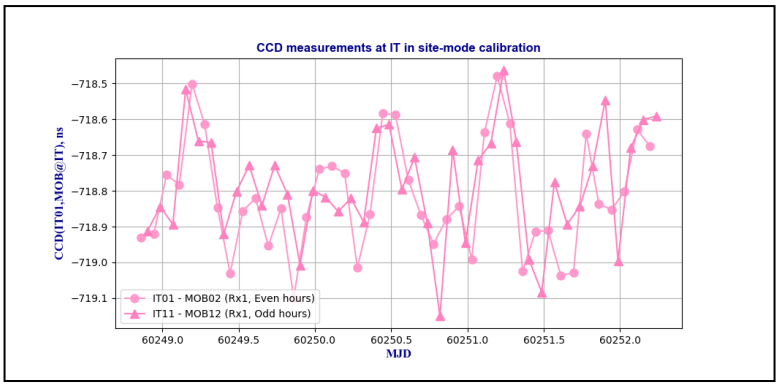

Figure 7-89 CCD measurements at IT in site-mode calibration (<ki>=IT01)

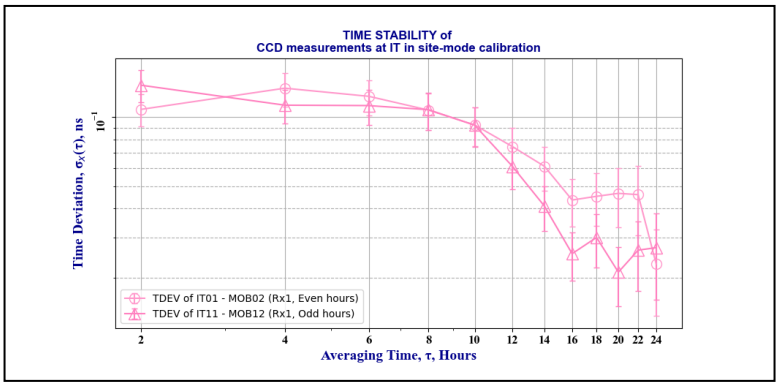

Figure 7-90 Time deviation of CCD measurements at IT in site-mode calibration (<ki>=IT01)

Figure 7-91 and Figure 7-92 show the CCD measurement data plot and TDEV of the data plot on the Rx2 channel of ES IT01.

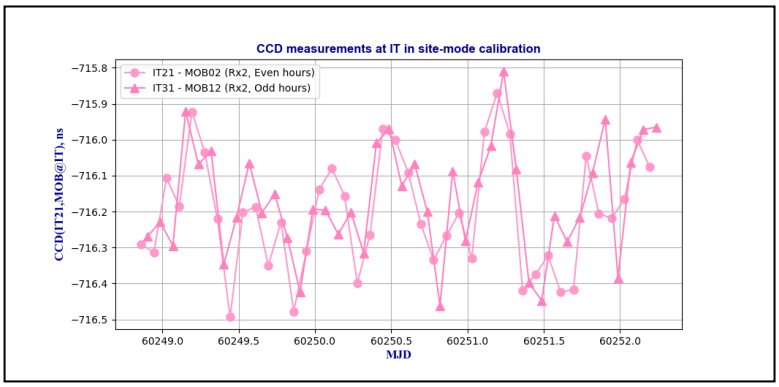

Figure 7-91 CCD measurements at IT in site-mode calibration (<ki>=IT21)

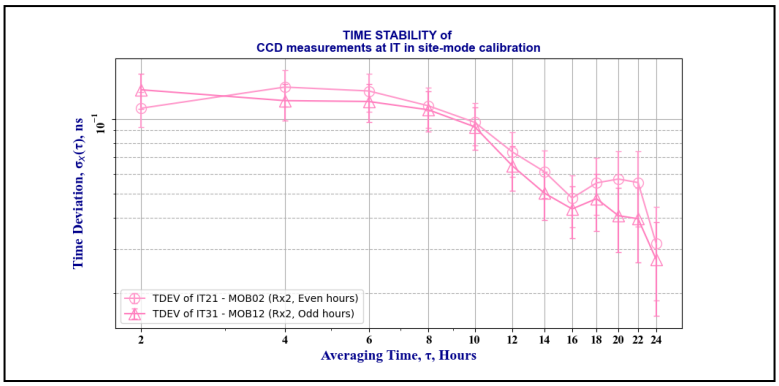

Figure 7-92 Time deviation of CCD measurements at IT in site-mode calibration (<ki>=IT21)

Figure 7-93 and Figure 7-94 show the CCD measurement data plot and TDEV of the data plot on the SDR channel of IT01.

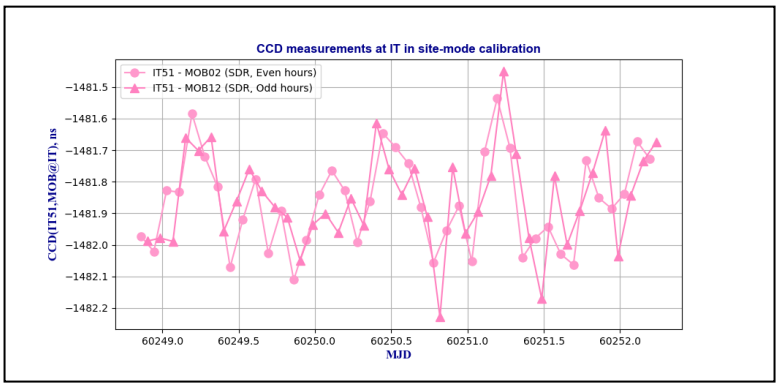

Figure 7-93 CCD measurements at IT in site-mode calibration (<ki>=IT51)

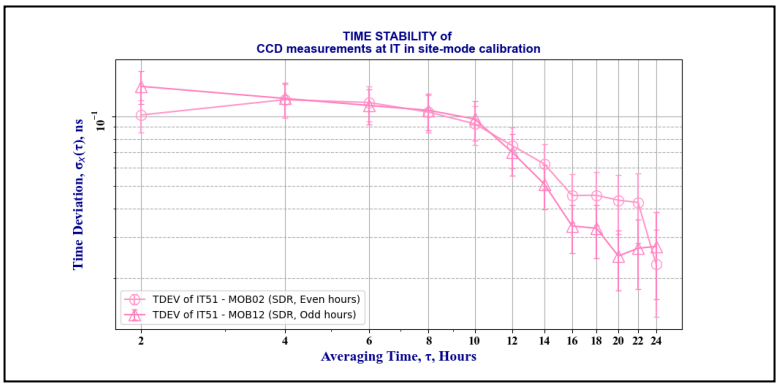

Figure 7-94 Time deviation of CCD measurements at IT in site-mode calibration (<ki>=IT51)

Table 7-39 lists the statistics of the CCD measurements on ES IT01, including Rx1, Rx2 and SDR channels. Table 7-40 gives the results of the CCD measurements calculation on ES IT01.

Table 7-39 Statistics of [IT01-MOB02] CCD measurements at IT

CCD Data Denotation	CCD Data Statistics		TDEV[CCD]		No. of Samples	No. of Gaps
	mean Unit: ns	stdev Unit: ns	TDEV Unit: ns	@ τ Unit: hr		
CCD_{even}(IT01,MOB@IT)	-718.817	0.156	0.074	12	41	0
CCD_{odd}(IT11,MOB@IT)	-718.784	0.153	0.061	12	41	0
CCD_{even}(IT21,MOB@IT)	-716.202	0.160	0.074	12	41	0
CCD_{odd}(IT31,MOB@IT)	-716.167	0.155	0.065	12	41	0
CCD_{even}(IT51,MOB@IT)	-1481.865	0.146	0.075	12	41	0
CCD_{odd}(IT51,MOB@IT)	-1481.854	0.154	0.070	12	41	0

Table 7-40 [IT01-MOB02] CCD measurement results at IT

Rx Channel	CCD_{avg}(IT01,MOB@IT) Unit: ns	uCCD(IT01,MOB@IT) Unit: ns	CCD_{diff}(IT01,MOB@IT) Unit: ns	Total No. of Samples
Rx1	-718.801	0.074	-0.032	82
Rx2	-716.185	0.074	-0.035	82
SDR	-1481.859	0.075	-0.011	82

To investigate the relative CCD measurements between three local Rx channels within the same ES, Figure 7-95 and Figure 7-96 show the data plot and TDEV of the CCD between Rx1 and Rx2 of ES IT01, respectively. And Figure 7-97 and Figure 7-98 show the data plot and TDEV of the CCD between Rx1 and SDR of ES IT01, respectively.

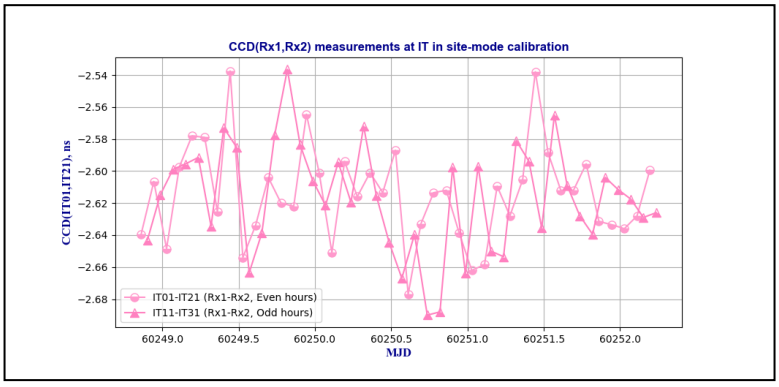

Figure 7-95 CCD(Rx1,Rx2) measurements on IT01

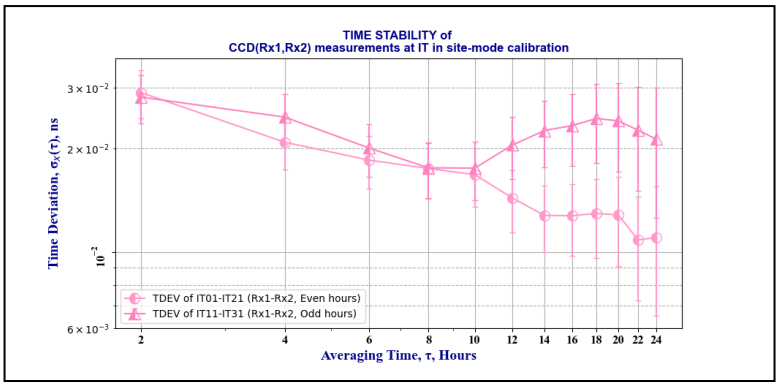

Figure 7-96 Time deviation of CCD(Rx1,Rx2) measurements on IT01

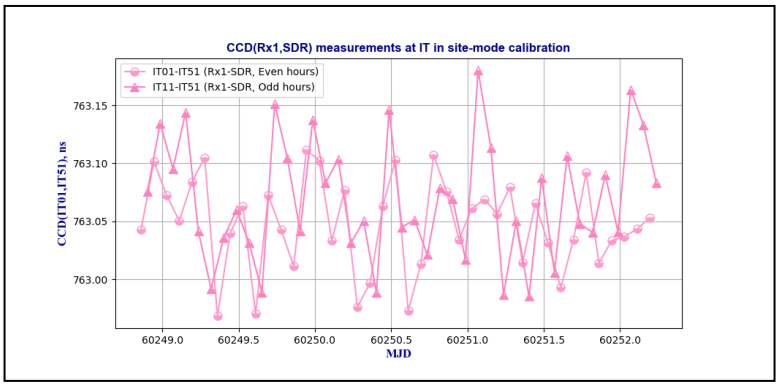

Figure 7-97 CCD(Rx1,SDR) measurements on IT01

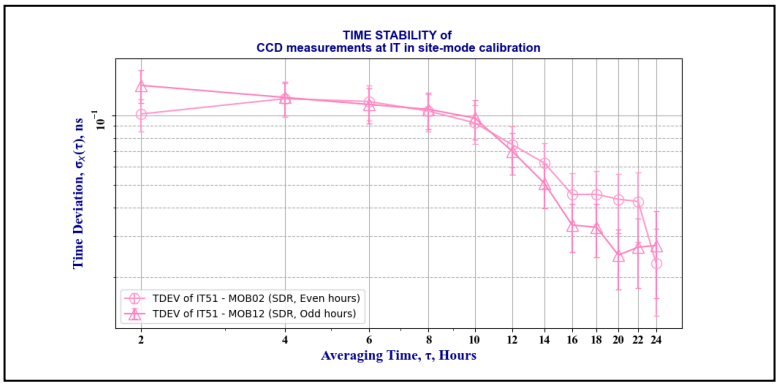

Figure 7-98 Time deviation of CCD(Rx1,SDR) measurements on IT01

Table 7-41 and Table 7-42 summarize the statistics and final calculation results of CCD(Rx1,Rx2) and CCD(Rx1,SDR), respectively.

Table 7-41 Statistics of [IT01-IT21] and [IT01-IT51] CCD measurements at IT

CCD Data Denotation	CCD Data Statistics	TDEV[CCD]		

	mean Unit: ns	stdev Unit: ns	TDEV Unit: ns	@ τ Unit: hr	No. of Samples	No. of Gaps
CCD_{even}(IT01,IT21)	-2.614	0.030	0.014	12	41	0
CCD_{odd}(IT11,IT21)	-2.617	0.034	0.020	12	41	0
CCD_{even}(IT01,IT51)	763.048	0.040	0.018	12	41	0
CCD_{odd}(IT11,IT51)	763.069	0.053	0.023	12	41	0

Table 7-42 [IT01-IT21] and [IT01-IT51] CCD measurement results at IT

Rx Differ. Rx1-<i_{Rx}>	CCD_{avg}(IT01,<i_{Rx}>) Unit: ns	μCCD(IT01,<i_{Rx}>) Unit: ns	CCD_{diff}(IT01,<i_{Rx}>) Unit: ns	Total No. of Samples
Rx1-Rx2	-2.616	0.020	0.003	82
Rx1-SDR	763.059	0.023	-0.021	82

7.3.11 CCD measurements at CH

Figure 7-99 and Figure 7-100 show the site top view of CH and the view of MOB during the on-site measurements at CH.

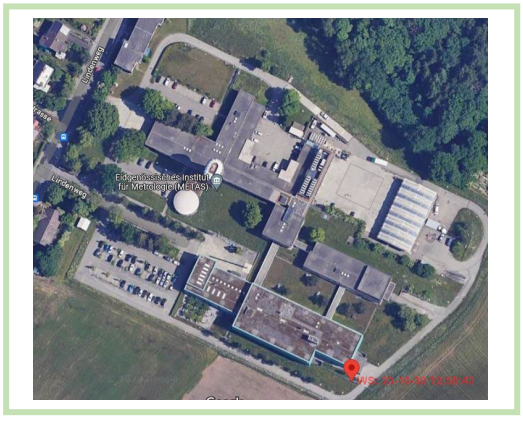

Figure 7-99 Site top view of CH

Figure 7-100 View of MOB at CH

Figure 7-101 and Figure 7-102 show the CCD measurement data plot and TDEV of the data plot on the Rx1 channel of ES CH01.

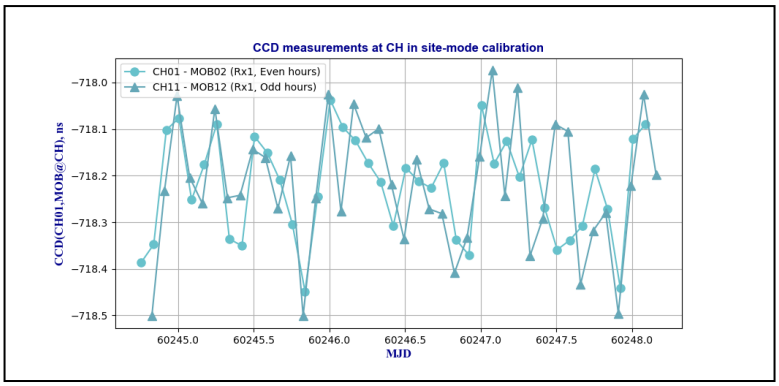

Figure 7-101 CCD measurements at CH in site-mode calibration (<ki>=CH01)

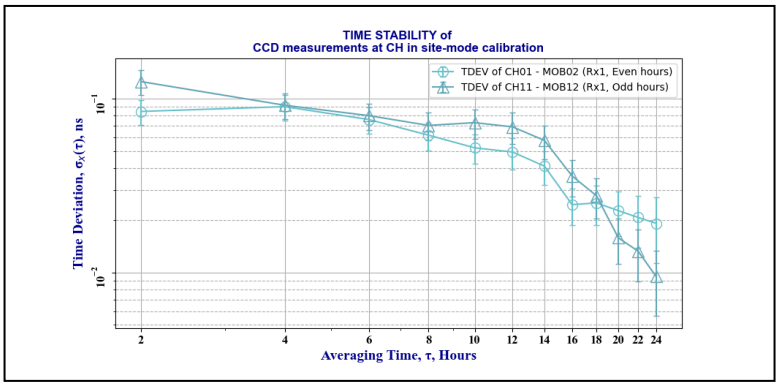

Figure 7-102 Time deviation of CCD measurements at CH in site-mode calibration (<ki>=CH01)

Figure 7-103 and Figure 7-104 show the CCD measurement data plot and TDEV of the data plot on the Rx2 channel of ES CH01.

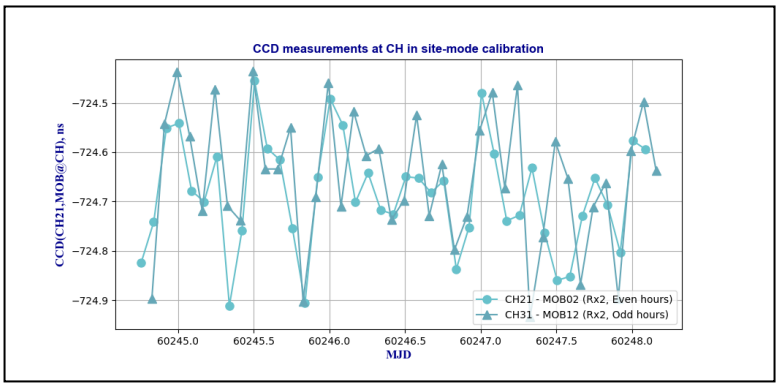

Figure 7-103 CCD measurements at CH in site-mode calibration (<ki>=CH21)

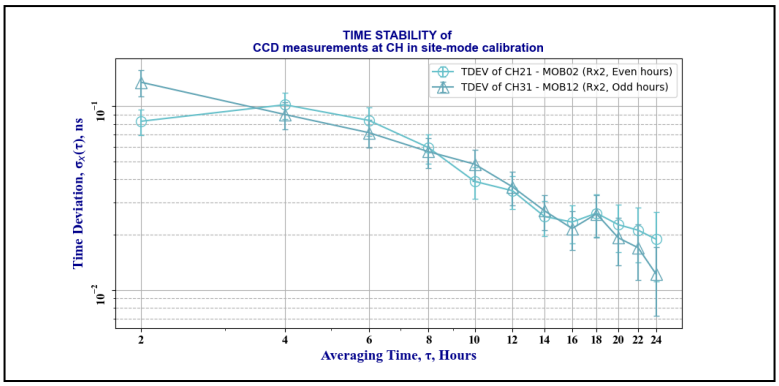

Figure 7-104 Time deviation of CCD measurements at CH in site-mode calibration (<ki>=CH21)

Figure 7-105 and Figure 7-106 show the CCD measurement data plot and TDEV of the data plot on the SDR channel of ES CH01.

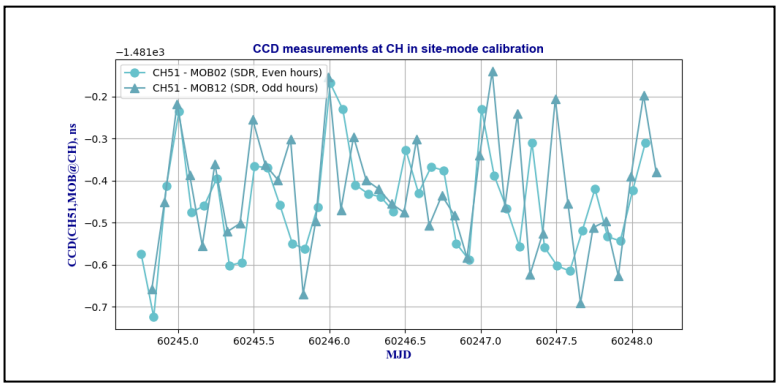

Figure 7-105 CCD measurements at CH in site-mode calibration (<ki>=CH51)

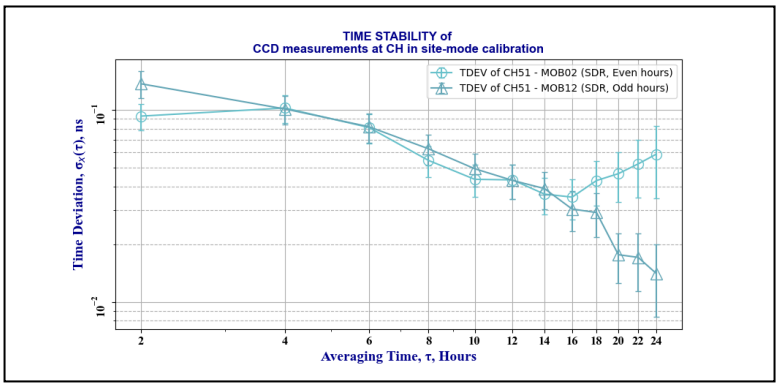

Figure 7-106 Time deviation of CCD measurements at CH in site-mode calibration (<ki>=CH51)

Table 7-43 lists the statistics of the CCD measurements on ES CH01, including Rx1, Rx2 and SDR channels. Table 7-44 gives the results of the CCD measurements calculation on ES CH01.

Table 7-43 Statistics of [CH01-MOB02] CCD measurements at CH

CCD Data Denotation	CCD Data Statistics		TDEV[CCD]		No. of Samples	No. of Gaps
	mean Unit: ns	stdev Unit: ns	TDEV Unit: ns	@ τ Unit: hr		
CCD_{even}(CH01,MOB@CH)	-718.222	0.110	0.049	12	41	0
CCD_{odd}(CH11,MOB@CH)	-718.221	0.137	0.069	12	41	0
CCD_{even}(CH21,MOB@CH)	-724.684	0.111	0.035	12	41	0
CCD_{odd}(CH31,MOB@CH)	-724.650	0.135	0.036	12	41	0
CCD_{even}(CH51,MOB@CH)	-1481.451	0.122	0.043	12	41	0
CCD_{odd}(CH51,MOB@CH)	-1481.424	0.141	0.043	12	41	0

Table 7-44 [CH01-MOB02] CCD measurement results at CH

Rx Channel	CCD_{avg}(CH01,MOB@CH) Unit: ns	uCCD(CH01,MOB@CH) Unit: ns	CCD_{diff}(CH01,MOB@CH) Unit: ns	Total No. of Samples
Rx1	-718.221	0.069	-0.001	82
Rx2	-724.667	0.036	-0.035	82
SDR	-1481.438	0.043	-0.027	82

To investigate the relative CCD measurements between three local Rx channels within the same ES, Figure 7-107 and Figure 7-108 show the data plot and TDEV of the CCD between Rx1 and Rx2 of ES CH01, respectively. And Figure 7-109 and Figure 7-110 show the data plot and TDEV of the CCD between Rx1 and SDR of ES CH01, respectively.

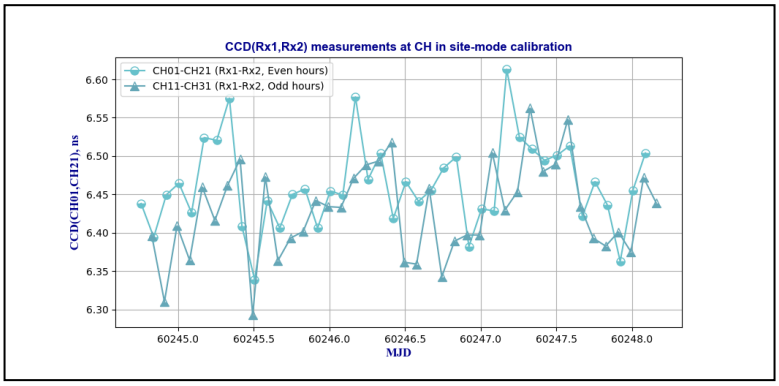

Figure 7-107 CCD(Rx1,Rx2) measurements on CH01

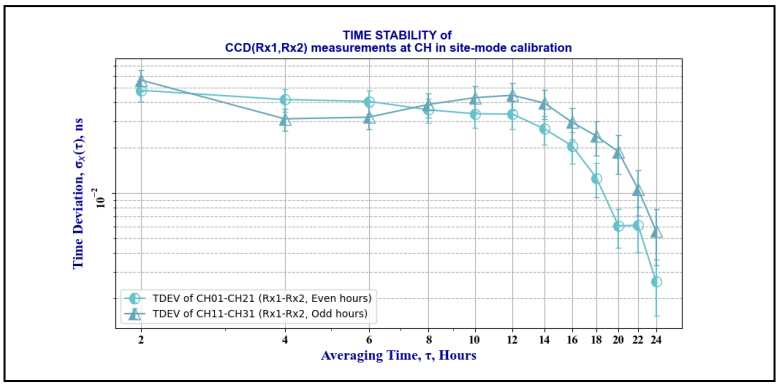

Figure 7-108 Time deviation of CCD(Rx1,Rx2) measurements on CH01

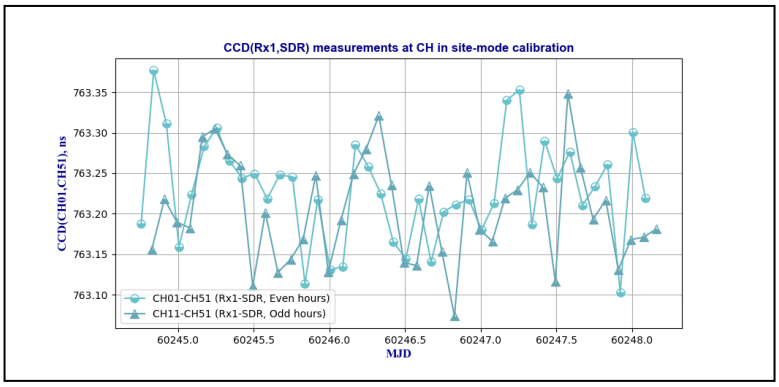

Figure 7-109 CCD(Rx1,SDR) measurements on CH01

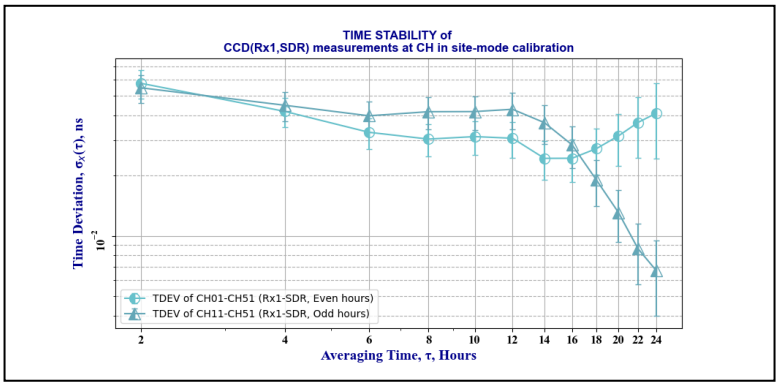

Figure 7-110 Time deviation of CCD(Rx1,SDR) measurements on CH01

Table 7-45 and Table 7-46 summarize the statistics and final calculation results of CCD(Rx1,Rx2) and CCD(Rx1,SDR), respectively.

Table 7-45 Statistics of [Rx1-Rx2] and [Rx1-SDR] CCD measurements on CH01

CCD Data Denotation	CCD Data Statistics	TDEV[CCD]		

	mean Unit: ns	stdev Unit: ns	TDEV Unit: ns	@ τ Unit: hr	No. of Samples	No. of Gaps
CCD_{even}(CH01,CH21)	6.462	0.057	0.033	12	41	0
CCD_{odd}(CH11,CH31)	6.429	0.060	0.045	12	41	0
CCD_{even}(CH01,CH51)	763.229	0.064	0.031	12	41	0
CCD_{odd}(CH11,CH51)	763.203	0.063	0.043	12	41	0

Table 7-46 [Rx1-Rx2] and [Rx1-SDR] CCD measurement results on CH01

Rx Differ Rx1-<i_{Rx}>	CCD_{avg}(CH01,<i_{Rx}>) Unit: ns	uCCD(CH01,<i_{Rx}>) Unit: ns	CCD_{diff}(CH01,<i_{Rx}>) Unit: ns	Total No. of Samples
Rx1-Rx2	6.446	0.045	0.034	82
Rx1-SDR	763.216	0.043	0.026	82

7.3.12 Summary on CCD measurement results at the sites

Table 7-47 summarizes the CCD measurement results of Rx channels of SATRE modems at all the sites. And Table 7-48 summarizes the CCD measurement results of SDR channels at all the sites.

Table 7-47 List of CCD measurement results on Rx1/Rx2 channels at the sites

ES Site ID <k>	Designated ES Code <ki>	Rx Channel	CCD_{avg}(ki,MOB@k) Unit: ns	uCCD(ki,MOB@k) Unit: ns	CCD_{diff}(ki,MOB@k) Unit: ns	Total No. of Samples
TIM	TIM01	Rx1	-742.509	0.107	-0.057	70
		Rx2	-746.240	0.054	-0.057	70
PL	PL01	Rx1	-716.164	0.040	0.088	46
PTB	PTB05	Rx1	-712.503	0.070	0.007	86
		Rx2	-717.355	0.069	0.016	86
	PTB04	Rx1	-729.108	0.067	-0.008	92
VSL	VSL01	Rx1	-721.166	0.077	-0.003	85
	VSL21	Rx2	-721.239	0.080	-0.007	85
LTFB	LTFB01	Rx1	-715.242	0.135	-0.063	71
		Rx2	-715.352	0.128	-0.042	56
ROA	ROA01	Rx1	-703.592	0.175	0.048	105

		Rx2	-703.674	0.178	0.055	105
OP	OP01	Rx1	-7862.162	0.077	-0.013	81
NPL	NPL02	Rx1	-10.483	0.187	-0.029	75
SP	SP01	Rx1	-728.648	0.046	-0.005	72
		Rx2	-731.313	0.073	0.002	69
IT	IT01	Rx1	-718.801	0.074	-0.032	82
		Rx2	-716.185	0.074	-0.035	82
CH	CH01	Rx1	-718.221	0.069	-0.001	82
		Rx2	-724.667	0.036	-0.035	82

Table 7-48 List of CCD measurement results on SDR channels at the sites

ES Site ID	Designated ES Code	Rx Channel	CCD_{avg}(ki,MOB@k)	uCCD(ki,MOB@k)	CCD_{diff}(ki,MOB@k)	Total No. of Samples
<k>	<ki>		Unit: ns	Unit: ns	Unit: ns	
PL	PL51	SDR	-1625.422	0.150	0.046	55
PTB	PTB55	SDR	-1593.083	0.063	-0.014	86
VSL	VSL51	SDR	-1566.259	0.047	-0.015	81
ROA	ROA51	SDR	-1571.383	0.162	0.084	105
OP	OP51	SDR	-3623.507	0.056	--	40
SP	SP51	SDR	-1599.086	0.188	0.031	70
IT	IT51	SDR	-1481.859	0.075	-0.011	82
CH	CH51	SDR	-1481.438	0.043	-0.027	82

Accordingly, the standard deviation of the even and odd hour CCD measurement difference of all the participating Rx channels can be calculated as:

$$\begin{aligned} \mathrm{stdev}\{\mathrm{CCD_{diff}(ki, MOB@k)}\} &= 0.039 \text{ ns}, \quad && for\ Rx1\&Rx2\ channels\ of\ SATRE\ modems \\ &= 0.041 \text{ ns}, && for\ SDR\ channels \end{aligned}$$

The relative CCD between two local Rx channels within the same ES are summarized in Table 7-49 and Table 7-50, where Rx1 channel is taken as the reference channel of an ES and the internal delay difference between Rx1 channel and Rx2/SDR channel is calculated.

Table 7-49 List of CCD measurement results on [Rx1-Rx2] channels at the sites

ES Site ID	Designated ES Rx Differ Code	$CCD_{avg}(ki_{Rx1},ki_{Rx2})$	uCCD(ki_{Rx1},ki_{Rx2})	$CCD_{diff}(ki_{Rx1},ki_{Rx2})$	Total No. of Samples
<k>	<ki_{Rx1}-ki_{Rx2}>	Unit: ns	Unit: ns	Unit: ns	
TIM	TIM01-TIM21	3.731	0.058	0.000	70
PTB	PTB05-PTB25	4.852	0.020	-0.009	86
VSL	VSL01-VSL21	0.072	0.018	0.004	85
LTFB	LTFB01-LTFB21	0.145	0.013	-0.018	54
ROA	ROA01-ROA21	0.083	0.019	-0.006	105
SP	SP01-SP21	2.669	0.078	-0.003	69
IT	IT01-IT21	-2.616	0.020	0.003	82
CH	CH01-CH21	6.446	0.045	0.034	82

Table 7-50 List of CCD measurement results on [Rx1-SDR] channels at the sites

ES Site ID	Designated ES Rx Differ Code	$CCD_{avg}(ki_{Rx1},ki_{SDR})$	uCCD(ki_{Rx1},ki_{SDR})	$CCD_{diff}(ki_{Rx1},ki_{SDR})$	Total No. of Samples
<k>	<ki_{Rx1}-ki_{SDR}>	Unit: ns	Unit: ns	Unit: ns	
PL	PL01-PL51	909.235	0.135	0.002	46
PTB	PTB05-PTB55	880.580	0.014	0.021	86
VSL	VSL01-VSL51	845.089	0.070	0.020	81
ROA	ROA01-ROA51	867.791	0.026	-0.036	105
OP	OP01-OP51	-4238.648	0.027	--	40
SP	SP01-SP51	870.438	0.198	-0.038	70
IT	IT01-IT51	763.059	0.023	-0.021	82
CH	CH01-CH51	763.216	0.043	0.026	82

7.4 CCD closure measurements

Since the MOB was taken as the common reference for all the participating ESs during the whole calibration campaign, the condition of its internal DLD constancy is related to the uncertainty of the calibration results on TW links under calibration. Therefore, closure measurements were performed at the start and end of the calibration campaign, respectively to verify the consistency of the internal delay asymmetry of the MOB. ES PTB05 with two Rx channels of SATRE modems was involved in closure measurements.

In this section, the label with '_start' or 'Start of Campaign' indicates the CCD measurements that were taken at the start of the calibration campaign, while the label with '_end' or 'End of Campaign' indicates the CCD measurements performed at the end of the calibration campaign for closure measurements.

7.4.1 Closure measurements on PTB05

The on-site CCD measurements on PTB05 were repeated twice for closure measurements. The first CCD measurement data are recorded in Section 7.3.3.1, and the second CCD measurement was performed at the end of the calibration campaign, of which the effective measurement duration is listed in Table 3-7.

Figure 7-111 shows the CCD measurements that were performed at the start and end of the calibration campaign on Rx1 of ES PTB05 for comparison. Figure 7-112 displays the TDEV of the two CCD measurements involving Rx1 of ES PTB05.

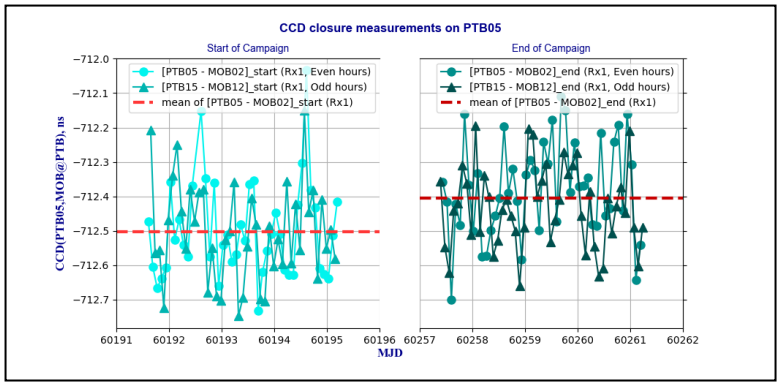

Figure 7-111 CCD closure measurements on PTB05 (Rx1 of ES PTB05)

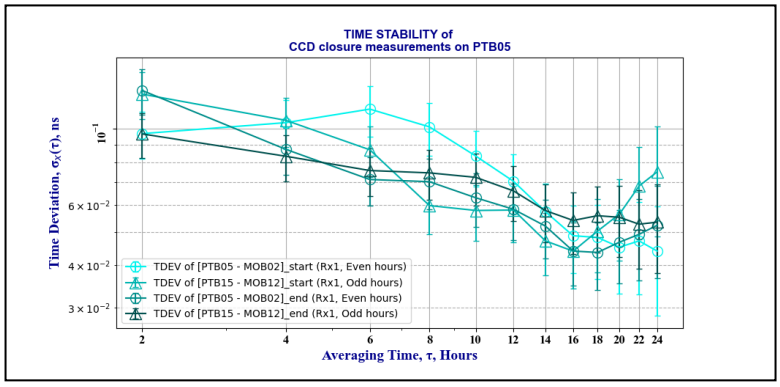

Figure 7-112 Time deviation of CCD closure measurements on PTB05 (Rx1 of ES PTB05)

Figure 7-113 shows the CCD measurements that were performed at the start and end of the calibration campaign on Rx2 of ES PTB05 for comparison. Figure 7-114 displays the TDEV of the twice CCD measurements on Rx2 of ES PTB05.

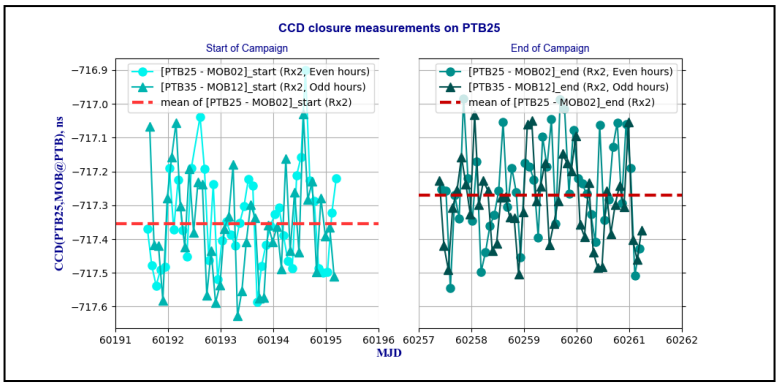

Figure 7-113 CCD closure measurements on PTB25 (Rx2 of ES PTB05)

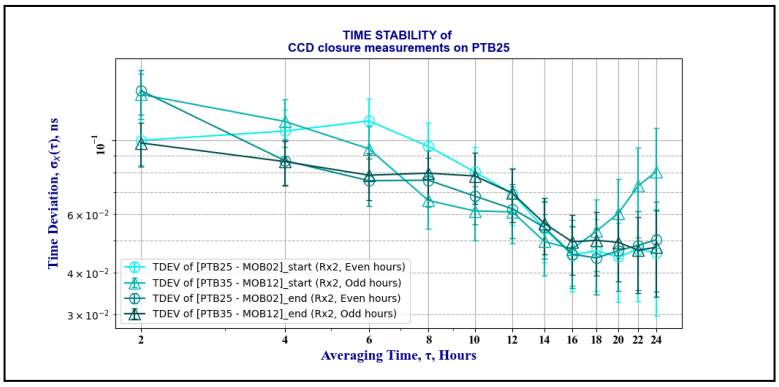

Figure 7-114 Time deviation of CCD closure measurements on PTB25 (Rx2 of ES PTB05)

Table 7-51 compares the statistics and the results of CCD closure measurements on ES PTB05, where the first CCD measurements data taken at the start of the campaign are taken from Table 7-11 and Table 7-12.

Table 7-51 Statistics of [PTB05-MOB02] CCD closure measurements on PTB05

Date	CCD Data Denotation	CCD Data Statistics		TDEV[CCD]		No. of Samples	No. of Gaps
		mean	stdev	TDEV	@ τ		
		Unit: ns	Unit: ns	Unit: ns	Unit: hr		
Start of Campaign	CCD_{even}(PTB05,MOB@PTB)	-712.500	0.140	0.070	12	43	1
	CCD_{odd}(PTB15,MOB@PTB)	-712.507	0.141	0.058	12	43	0
	CCD_{even}(PTB25,MOB@PTB)	-717.347	0.142	0.069	12	43	1
	CCD_{odd}(PTB35,MOB@PTB)	-717.363	0.153	0.061	12	43	0
End of Campaign	CCD_{even}(PTB05,MOB@PTB)	-712.378	0.139	0.058	12	46	0
	CCD_{odd}(PTB15,MOB@PTB)	-712.432	0.119	0.066	12	47	0
	CCD_{even}(PTB25,MOB@PTB)	-717.247	0.143	0.062	12	46	0

	CCD_{odd}(PTB35,MOB@PTB)	-717.293	0.123	0.069	12	47	0

7.4.2 Summary on closure measurements

The delay asymmetry inconsistency of the MOB is evaluated by the maximum of CSD and ΔCCD obtained from the closure measurements, as explained in equation (52). Table 7-52 lists the CSD and ΔCCD values for all the Rx channels involved in closure measurements.

Table 7-52 Verification of the instability of the MOB

ES Site ID <k>	**Designated ES Channel Code <$ki_{closure}$>**	**CSD($ki_{closure}$,MOB@k) Unit: ns**	**ΔCCD($ki_{closure}$,MOB@k) Unit: ns**
PTB	PTB05	0.091	0.122
	PTB15	0.088	0.075
	PTB25	0.093	0.100
	PTB35	0.092	0.070

From the summary of Table 7-52, ub,3 applied to this calibration campaign is obtained as:

$$ub,3 = \max\{\mathrm{CSD}(\mathrm{ki}_{\mathrm{closure}}, \mathrm{MOB@k}), \Delta\mathrm{CCD}(\mathrm{ki}_{\mathrm{closure}}, \mathrm{MOB@k})\} = 0.122 \text{ ns}$$

where $\mathrm{ki}_{\mathrm{closure}} = \{\mathrm{PTB05}, \mathrm{PTB15}, \mathrm{PTB25}, \mathrm{PTB35}\}$.

8 Site-mode calibration results

Based on the pre-setting parameters and on-site measurement data processed in Chapter 7, the site-mode calibration results for the participating TW links are calculated. The principle of the site-mode calibration approach refers to Section 4.2.1: “Site-mode calibration scheme”, and the computation of the CALR values refers to Section 6.2.2: “CALR data processing in site-mode calibration”. The 1-σ uncertainty of the CALR, which is denoted as uCALR, is analyzed and calculated, referring to Section 6.3: “Uncertainty budget of CALR”.

In this chapter, the site-mode calibrated TW links with new CALR and uCALR values are classified into three categories:

- TW calibration pairs between SATRE Rx1 channels of two remote ESs;
- TW calibration pairs between two local Rx channels;
- TW calibration pairs between the SDR channels of two remote ESs.

Note that all the new CALR values in this chapter are applied to the criteria that:

1) *REFDELAY(ki) values are set as Table 7-2;*
2) *ESDVAR values are set to zero.*

8.1 Site-mode calibration results of remote SATRE links

Table 8-1 lists the new CALR and uCALR values corresponding to remote TW links between Rx1 channels of the SATRE modem. The calculation of CALR values is done according to equation (43), where the SCD values are taken from Table 7-1, and the CCD values are taken from Table 7-47. Table 8-2 lists the components of Type A and Type B uncertainties in uCALR calculations. Table 8-3 lists the new CALR and uCALR values corresponding to remote TW links between [Rx1-Rx2] channels and [Rx2-Rx2] channels of the SATRE modem.

Table 8-1 List of new CALR and uCALR values of [Rx1-Rx1] remote links using site-mode calibration

TW Link		CALR (k_1i,k_2j)	uCALR (k_1i,k_2j)	Type A & Type B Uncertainties	
				ua	ub
<k_1i>	<k_2j>	Unit: ns	Unit: ns	Unit: ns	Unit: ns
TIM01	PL01	-16.575	0.442	0.114	0.427
TIM01	PTB05	-35.476	0.398	0.128	0.376
TIM01	PTB04	-18.871	0.399	0.126	0.379
TIM01	VSL01	-36.213	0.411	0.132	0.390
TIM01	LTFB01	-29.917	0.461	0.172	0.428
TIM01	ROA01	-52.397	0.483	0.205	0.437
TIM01	OP01	7107.053	0.399	0.132	0.377
TIM01	NPL02	-754.456	0.555	0.215	0.511
TIM01	SP01	-28.661	0.413	0.116	0.396
TIM01	IT01	-18.958	0.639	0.130	0.626
TIM01	CH01	-23.558	0.413	0.127	0.393
PL01	PTB05	-18.901	0.401	0.081	0.392

PL01	PTB04	-2.296	0.402	0.078	0.395
PL01	VSL01	-19.638	0.414	0.087	0.405
PL01	LTFB01	-13.342	0.452	0.141	0.430
PL01	ROA01	-35.822	0.475	0.180	0.439
PL01	OP01	7123.628	0.402	0.087	0.392
PL01	NPL02	-737.881	0.547	0.191	0.513
PL01	SP01	-12.086	0.416	0.061	0.411
PL01	IT01	-2.383	0.641	0.084	0.635
PL01	CH01	-6.983	0.416	0.080	0.408
PTB05	PTB04	16.605	0.353	0.097	0.339
PTB05	VSL01	-0.737	0.366	0.104	0.351
PTB05	LTFB01	5.559	0.409	0.152	0.379
PTB05	ROA01	-16.921	0.433	0.188	0.390
PTB05	OP01	7142.529	0.352	0.104	0.337
PTB05	NPL02	-718.980	0.512	0.200	0.471
PTB05	SP01	6.815	0.368	0.084	0.358
PTB05	IT01	16.518	0.611	0.102	0.602
PTB05	CH01	11.918	0.368	0.098	0.354
PTB04	VSL01	-17.342	0.368	0.102	0.354
PTB04	LTFB01	-11.046	0.410	0.151	0.382
PTB04	ROA01	-33.526	0.435	0.187	0.392
PTB04	OP01	7125.924	0.354	0.102	0.339
PTB04	NPL02	-735.585	0.513	0.199	0.473
PTB04	SP01	-9.790	0.369	0.081	0.360
PTB04	IT01	-0.087	0.612	0.100	0.604
PTB04	CH01	-4.687	0.369	0.096	0.357
VSL01	LTFB01	6.296	0.422	0.155	0.393
VSL01	ROA01	-16.184	0.446	0.191	0.403
VSL01	OP01	7143.266	0.368	0.109	0.351
VSL01	NPL02	-718.243	0.523	0.202	0.482
VSL01	SP01	7.552	0.383	0.090	0.372
VSL01	IT01	17.255	0.620	0.107	0.611
VSL01	CH01	12.655	0.383	0.103	0.368
LTFB01	ROA01	-22.480	0.492	0.221	0.440
LTFB01	OP01	7136.970	0.410	0.155	0.379
LTFB01	NPL02	-724.539	0.563	0.231	0.513
LTFB01	SP01	1.256	0.423	0.143	0.399
LTFB01	IT01	10.959	0.646	0.154	0.627
LTFB01	CH01	6.359	0.423	0.152	0.395
ROA01	OP01	7159.450	0.434	0.191	0.390

ROA01	NPL02	-702.059	0.581	0.256	0.521
ROA01	SP01	23.736	0.447	0.181	0.409
ROA01	IT01	33.439	0.662	0.190	0.634
ROA01	CH01	28.839	0.447	0.188	0.406
OP01	NPL02	-7861.509	0.513	0.202	0.471
OP01	SP01	-7135.714	0.369	0.090	0.358
OP01	IT01	-7126.011	0.612	0.107	0.602
OP01	CH01	-7130.611	0.369	0.103	0.354
NPL02	SP01	725.795	0.524	0.193	0.487
NPL02	IT01	735.498	0.716	0.201	0.687
NPL02	CH01	730.898	0.524	0.199	0.484
SP01	IT01	9.703	0.621	0.087	0.615
SP01	CH01	5.103	0.384	0.083	0.375
IT01	CH01	-4.600	0.621	0.101	0.612

Table 8-2 List of uCALR uncertainty categories of [Rx1-Rx1] remote links using site-mode calibration

TW Link		Type A uncertainties		Type B uncertainties				
		$u_{a,1}$	$u_{a,2}$	$u_{b,I}$	$u_{b,II}$	$u_{b,III}$	$u_{b,6}$ (k_1i,k_2j)	$u_{b,IV}$
<k_1i>	<k_2j>	Unit: ns	Unit: ns	Unit: ns	Unit: ns	Unit: ns	Unit: ns	Unit: ns
TIM01	PL01	0.107	0.040	0.192	0.040	0.306	0.210	0.224
TIM01	PTB05	0.107	0.070	0.192	0.040	0.230	0.059	0.224
TIM01	PTB04	0.107	0.067	0.192	0.040	0.234	0.072	0.224
TIM01	VSL01	0.107	0.077	0.192	0.040	0.251	0.117	0.224
TIM01	LTFB01	0.107	0.135	0.192	0.040	0.240	0.091	0.294
TIM01	ROA01	0.107	0.175	0.192	0.040	0.257	0.128	0.294
TIM01	OP01	0.107	0.077	0.192	0.040	0.230	0.059	0.224
TIM01	NPL02	0.107	0.187	0.192	0.040	0.369	0.294	0.294
TIM01	SP01	0.107	0.046	0.192	0.040	0.261	0.136	0.224
TIM01	IT01	0.107	0.074	0.192	0.040	0.550	0.503	0.224
TIM01	CH01	0.107	0.069	0.192	0.040	0.256	0.126	0.224
PL01	PTB05	0.040	0.070	0.192	0.040	0.302	0.204	0.156
PL01	PTB04	0.040	0.067	0.192	0.040	0.305	0.208	0.156
PL01	VSL01	0.040	0.077	0.192	0.040	0.318	0.228	0.156
PL01	LTFB01	0.040	0.135	0.192	0.040	0.310	0.215	0.224
PL01	ROA01	0.040	0.175	0.192	0.040	0.323	0.234	0.224
PL01	OP01	0.040	0.077	0.192	0.040	0.302	0.204	0.156
PL01	NPL02	0.040	0.187	0.192	0.040	0.418	0.353	0.224
PL01	SP01	0.040	0.046	0.192	0.040	0.326	0.238	0.156

PL01	IT01	0.040	0.074	0.192	0.040	0.584	0.540	0.156
PL01	CH01	0.040	0.069	0.192	0.040	0.322	0.232	0.156
PTB05	PTB04	0.070	0.067	0.192	0.040	0.228	0.050	0.156
PTB05	VSL01	0.070	0.077	0.192	0.040	0.246	0.105	0.156
PTB05	LTFB01	0.070	0.135	0.192	0.040	0.235	0.075	0.224
PTB05	ROA01	0.070	0.175	0.192	0.040	0.252	0.118	0.224
PTB05	OP01	0.070	0.077	0.192	0.040	0.225	0.030	0.156
PTB05	NPL02	0.070	0.187	0.192	0.040	0.365	0.290	0.224
PTB05	SP01	0.070	0.046	0.192	0.040	0.256	0.126	0.156
PTB05	IT01	0.070	0.074	0.192	0.040	0.548	0.500	0.156
PTB05	CH01	0.070	0.069	0.192	0.040	0.251	0.115	0.156
PTB04	VSL01	0.067	0.077	0.192	0.040	0.250	0.113	0.156
PTB04	LTFB01	0.067	0.135	0.192	0.040	0.239	0.085	0.224
PTB04	ROA01	0.067	0.175	0.192	0.040	0.255	0.125	0.224
PTB04	OP01	0.067	0.077	0.192	0.040	0.228	0.051	0.156
PTB04	NPL02	0.067	0.187	0.192	0.040	0.368	0.293	0.224
PTB04	SP01	0.067	0.046	0.192	0.040	0.259	0.132	0.156
PTB04	IT01	0.067	0.074	0.192	0.040	0.549	0.502	0.156
PTB04	CH01	0.067	0.069	0.192	0.040	0.254	0.122	0.156
VSL01	LTFB01	0.077	0.135	0.192	0.040	0.256	0.126	0.224
VSL01	ROA01	0.077	0.175	0.192	0.040	0.271	0.155	0.224
VSL01	OP01	0.077	0.077	0.192	0.040	0.246	0.105	0.156
VSL01	NPL02	0.077	0.187	0.192	0.040	0.379	0.307	0.224
VSL01	SP01	0.077	0.046	0.192	0.040	0.275	0.161	0.156
VSL01	IT01	0.077	0.074	0.192	0.040	0.557	0.510	0.156
VSL01	CH01	0.077	0.069	0.192	0.040	0.270	0.153	0.156
LTFB01	ROA01	0.135	0.175	0.192	0.040	0.261	0.137	0.294
LTFB01	OP01	0.135	0.077	0.192	0.040	0.235	0.075	0.224
LTFB01	NPL02	0.135	0.187	0.192	0.040	0.372	0.298	0.294
LTFB01	SP01	0.135	0.046	0.192	0.040	0.265	0.143	0.224
LTFB01	IT01	0.135	0.074	0.192	0.040	0.552	0.505	0.224
LTFB01	CH01	0.135	0.069	0.192	0.040	0.260	0.134	0.224
ROA01	OP01	0.175	0.077	0.192	0.040	0.252	0.118	0.224
ROA01	NPL02	0.175	0.187	0.192	0.040	0.383	0.311	0.294
ROA01	SP01	0.175	0.046	0.192	0.040	0.280	0.170	0.224
ROA01	IT01	0.175	0.074	0.192	0.040	0.560	0.513	0.224
ROA01	CH01	0.175	0.069	0.192	0.040	0.275	0.162	0.224
OP01	NPL02	0.077	0.187	0.192	0.040	0.366	0.290	0.224
OP01	SP01	0.077	0.046	0.192	0.040	0.256	0.126	0.156
OP01	IT01	0.077	0.074	0.192	0.040	0.548	0.500	0.156

OP01	CH01	0.077	0.069	0.192	0.040	0.251	0.115	0.156
NPL02	SP01	0.187	0.046	0.192	0.040	0.385	0.314	0.224
NPL02	IT01	0.187	0.074	0.192	0.040	0.619	0.578	0.224
NPL02	CH01	0.187	0.069	0.192	0.040	0.382	0.310	0.224
SP01	IT01	0.046	0.074	0.192	0.040	0.561	0.515	0.156
SP01	CH01	0.046	0.069	0.192	0.040	0.279	0.168	0.156
IT01	CH01	0.074	0.069	0.192	0.040	0.559	0.513	0.156

Table 8-3 List of new CALR and uCALR values of [Rx1-Rx2] & [Rx2-Rx2] remote links using site-mode calibration

TW Link		**CALR (k_1i,k_2j)**	**uCALR (k_1i,k_2j)**	**Type A & Type B Uncertainties**	
				ua	**ub**
<k_1i>	**<k_2j>**	**Unit: ns**	**Unit: ns**	**Unit: ns**	**Unit: ns**
TIM01	PTB25	-30.624	0.397	0.127	0.376
TIM01	VSL21	-36.140	0.412	0.134	0.390
TIM01	ROA21	-52.315	0.484	0.208	0.437
TIM01	SP21	-25.996	0.416	0.130	0.396
TIM01	IT21	-21.574	0.639	0.130	0.626
TIM01	CH21	-17.112	0.408	0.113	0.393
TIM21	PL01	-20.306	0.401	0.067	0.396
TIM21	PTB05	-39.207	0.352	0.088	0.340
TIM21	PTB25	-34.355	0.351	0.088	0.340
TIM21	PTB04	-22.602	0.353	0.086	0.343
TIM21	VSL01	-39.944	0.367	0.094	0.355
TIM21	VSL21	-39.871	0.368	0.097	0.355
TIM21	LTFB01	-33.648	0.409	0.145	0.383
TIM21	ROA01	-56.128	0.434	0.183	0.393
TIM21	ROA21	-56.046	0.435	0.186	0.393
TIM21	OP01	7103.322	0.353	0.094	0.340
TIM21	NPL02	-758.187	0.513	0.195	0.474
TIM21	SP01	-32.392	0.368	0.071	0.362
TIM21	SP21	-29.727	0.373	0.091	0.362
TIM21	IT01	-22.689	0.611	0.092	0.604
TIM21	IT21	-25.305	0.611	0.092	0.604
TIM21	CH01	-27.289	0.369	0.088	0.358
TIM21	CH21	-20.843	0.364	0.065	0.358
PL01	PTB25	-14.049	0.400	0.080	0.392
PL01	VSL21	-19.565	0.415	0.089	0.405
PL01	ROA21	-35.740	0.476	0.182	0.439

PL01	SP21	-9.421	0.419	0.083	0.411
PL01	IT21	-4.999	0.641	0.084	0.635
PL01	CH21	-0.537	0.411	0.054	0.408
PTB05	VSL21	-0.664	0.367	0.106	0.351
PTB05	ROA21	-16.839	0.434	0.191	0.390
PTB05	SP21	9.480	0.372	0.101	0.358
PTB05	IT21	13.902	0.611	0.102	0.602
PTB05	CH21	18.364	0.363	0.079	0.354
PTB25	PTB04	11.753	0.352	0.096	0.339
PTB25	VSL01	-5.589	0.366	0.103	0.351
PTB25	VSL21	-5.516	0.367	0.106	0.351
PTB25	LTFB01	0.707	0.408	0.152	0.379
PTB25	ROA01	-21.773	0.433	0.188	0.390
PTB25	ROA21	-21.691	0.434	0.191	0.390
PTB25	OP01	7137.677	0.352	0.103	0.337
PTB25	NPL02	-723.832	0.512	0.199	0.471
PTB25	SP01	1.963	0.367	0.083	0.358
PTB25	SP21	4.628	0.372	0.100	0.358
PTB25	IT01	11.666	0.611	0.101	0.602
PTB25	IT21	9.050	0.611	0.101	0.602
PTB25	CH01	7.066	0.367	0.098	0.354
PTB25	CH21	13.512	0.363	0.078	0.354
PTB04	VSL21	-17.269	0.369	0.104	0.354
PTB04	ROA21	-33.444	0.436	0.190	0.392
PTB04	SP21	-7.125	0.374	0.099	0.360
PTB04	IT21	-2.703	0.612	0.100	0.604
PTB04	CH21	1.759	0.365	0.076	0.357
VSL01	ROA21	-16.102	0.447	0.194	0.403
VSL01	SP21	10.217	0.387	0.106	0.372
VSL01	IT21	14.639	0.620	0.107	0.611
VSL01	CH21	19.101	0.378	0.085	0.368
VSL21	LTFB01	6.223	0.423	0.157	0.393
VSL21	ROA01	-16.257	0.447	0.192	0.403
VSL21	ROA21	-16.175	0.448	0.195	0.403
VSL21	OP01	7143.193	0.368	0.111	0.351
VSL21	NPL02	-718.316	0.523	0.203	0.482
VSL21	SP01	7.479	0.383	0.092	0.372
VSL21	SP21	10.144	0.387	0.108	0.372
VSL21	IT01	17.182	0.620	0.109	0.611
VSL21	IT21	14.566	0.620	0.109	0.611

VSL21	CH01	12.582	0.383	0.106	0.368
VSL21	CH21	19.028	0.379	0.088	0.368
LTFB01	ROA21	-22.398	0.493	0.223	0.440
LTFB01	SP21	3.921	0.427	0.153	0.399
LTFB01	IT21	8.343	0.646	0.154	0.627
LTFB01	CH21	12.805	0.419	0.140	0.395
ROA01	SP21	26.401	0.451	0.190	0.409
ROA01	IT21	30.823	0.662	0.190	0.634
ROA01	CH21	35.285	0.443	0.179	0.406
ROA21	OP01	7159.368	0.436	0.194	0.390
ROA21	NPL02	-702.141	0.582	0.258	0.521
ROA21	SP01	23.654	0.448	0.184	0.409
ROA21	SP21	26.319	0.452	0.192	0.409
ROA21	IT01	33.357	0.662	0.193	0.634
ROA21	IT21	30.741	0.662	0.193	0.634
ROA21	CH01	28.757	0.448	0.191	0.406
ROA21	CH21	35.203	0.444	0.182	0.406
OP01	SP21	-7133.049	0.373	0.106	0.358
OP01	IT21	-7128.627	0.612	0.107	0.602
OP01	CH21	-7124.165	0.364	0.085	0.354
NPL02	SP21	728.460	0.527	0.201	0.487
NPL02	IT21	732.882	0.716	0.201	0.687
NPL02	CH21	737.344	0.520	0.190	0.484
SP01	IT21	7.087	0.621	0.087	0.615
SP01	CH21	11.549	0.379	0.058	0.375
SP21	IT01	7.038	0.623	0.104	0.615
SP21	IT21	4.422	0.623	0.104	0.615
SP21	CH01	2.438	0.388	0.100	0.375
SP21	CH21	8.884	0.384	0.081	0.375
IT01	CH21	1.846	0.618	0.082	0.612
IT21	CH01	-1.984	0.621	0.101	0.612
IT21	CH21	4.462	0.618	0.082	0.612

8.2 Site-mode calibration results of local Rx channels

Table 8-4 lists the new CALR and uCALR values corresponding to local TW links between Rx channels of the local ES. The calculation of CALR values is done according to equation (44), where the SCD values are taken from Table 7-1, the CCD values are taken from Table 7-49 and Table 7-50. In addition, the CALR value of a TW link between the Rx2/SDR channel of a local ES and a remote ES are calculated by equation (45).

Table 8-4 List of new CALR and uCALR values of local Rx channels

TW Link		CALR (ki_{Rx1},ki_{Rx2})	uCALR (ki_{Rx1},ki_{Rx2})	ua	ub
<ki_{Rx1}>	<ki_{Rx2}>	Unit: ns	Unit: ns	Unit: ns	Unit: ns
TIM01	TIM21	3.731	0.058	0.058	0.000
PL01	PL51	909.235	0.135	0.135	0.000
PTB05	PTB25	4.852	0.020	0.020	0.000
PTB05	PTB55	880.580	0.014	0.014	0.000
VSL01	VSL21	0.072	0.018	0.018	0.000
VSL01	VSL51	845.089	0.070	0.070	0.000
LTFB01	LTFB21	0.145	0.013	0.013	0.000
ROA01	ROA21	0.083	0.019	0.019	0.000
ROA01	ROA51	867.791	0.026	0.026	0.000
OP01	OP51	-4238.648	0.027	0.027	0.000
SP01	SP21	2.669	0.078	0.078	0.000
SP01	SP51	870.438	0.198	0.198	0.000
IT01	IT21	-2.616	0.020	0.020	0.000
IT01	IT51	763.059	0.023	0.023	0.000
CH01	CH21	6.446	0.045	0.045	0.000
CH01	CH51	763.216	0.043	0.043	0.000

8.3 Site-mode calibration results of SDR TW links

Table 8-5 lists the new CALR and uCALR values corresponding to remote TW links between SDR channels of two ESs by means of site-mode calibration. The calculation of CALR values is done according to equation (43), where the SCD values are taken from Table 7-1, the CCD values are taken from Table 7-48. Table 8-6 lists the components of Type A and Type B uncertainties in uCALR calculations.

Table 8-5 List of new CALR and uCALR values of SDR TW links using site-mode calibration

TW Link		CALR (k_1i,k_2j)	uCALR (k_1i,k_2j)	Type A & Type B Uncertainties	
				ua	ub
<k_1i>	<k_2j>	Unit: ns	Unit: ns	Unit: ns	Unit: ns
PL51	PTB55	-47.579	0.454	0.163	0.424
PL51	VSL51	-83.803	0.463	0.157	0.436
PL51	ROA51	-77.289	0.527	0.221	0.479
PL51	OP51	1975.715	0.453	0.160	0.424
PL51	SP51	-50.906	0.538	0.241	0.481
PL51	IT51	-148.583	0.676	0.168	0.655

PL51	CH51	-153.024	0.465	0.156	0.438
PTB55	VSL51	-36.224	0.360	0.079	0.351
PTB55	ROA51	-29.710	0.427	0.174	0.390
PTB55	OP51	2023.294	0.347	0.084	0.337
PTB55	SP51	-3.327	0.440	0.198	0.392
PTB55	IT51	-101.004	0.610	0.098	0.602
PTB55	CH51	-105.445	0.362	0.076	0.354
VSL51	ROA51	6.514	0.437	0.169	0.403
VSL51	OP51	2059.518	0.359	0.073	0.351
VSL51	SP51	32.897	0.449	0.194	0.405
VSL51	IT51	-64.780	0.617	0.089	0.611
VSL51	CH51	-69.221	0.374	0.064	0.368
ROA51	OP51	2053.004	0.426	0.171	0.390
ROA51	SP51	26.383	0.515	0.248	0.451
ROA51	IT51	-71.294	0.658	0.179	0.634
ROA51	CH51	-75.735	0.439	0.168	0.406
OP51	SP51	-2026.621	0.439	0.196	0.393
OP51	IT51	-2124.298	0.610	0.094	0.602
OP51	CH51	-2128.739	0.361	0.071	0.354
SP51	IT51	-97.677	0.667	0.202	0.635
SP51	CH51	-102.118	0.451	0.193	0.408
IT51	CH51	-4.441	0.619	0.086	0.612

Table 8-6 List of uCALR uncertainty categories of SDR TW links

TW Link		Type A uncertainties		Type B uncertainties				
		$u_{a,1}$	$u_{a,2}$	$u_{b,I}$	$u_{b,II}$	$u_{b,III}$	$u_{b,6}(k_1i,k_2j)$	$u_{b,IV}$
$<k_1i>$	$<k_2j>$	Unit: ns	Unit: ns	Unit: ns	Unit: ns	Unit: ns	Unit: ns	Unit: ns
PL51	PTB55	0.150	0.063	0.192	0.040	0.302	0.204	0.224
PL51	VSL51	0.150	0.047	0.192	0.040	0.318	0.228	0.224
PL51	ROA51	0.150	0.162	0.192	0.040	0.323	0.234	0.294
PL51	OP51	0.150	0.056	0.192	0.040	0.302	0.204	0.224
PL51	SP51	0.150	0.188	0.192	0.040	0.326	0.238	0.294
PL51	IT51	0.150	0.075	0.192	0.040	0.584	0.540	0.224
PL51	CH51	0.150	0.043	0.192	0.040	0.322	0.232	0.224
PTB55	VSL51	0.063	0.047	0.192	0.040	0.246	0.105	0.156
PTB55	ROA51	0.063	0.162	0.192	0.040	0.252	0.118	0.224
PTB55	OP51	0.063	0.056	0.192	0.040	0.225	0.030	0.156
PTB55	SP51	0.063	0.188	0.192	0.040	0.256	0.126	0.224

PTB55	IT51	0.063	0.075	0.192	0.040	0.548	0.500	0.156
PTB55	CH51	0.063	0.043	0.192	0.040	0.251	0.115	0.156
VSL51	ROA51	0.047	0.162	0.192	0.040	0.271	0.155	0.224
VSL51	OP51	0.047	0.056	0.192	0.040	0.246	0.105	0.156
VSL51	SP51	0.047	0.188	0.192	0.040	0.275	0.161	0.224
VSL51	IT51	0.047	0.075	0.192	0.040	0.557	0.510	0.156
VSL51	CH51	0.047	0.043	0.192	0.040	0.270	0.153	0.156
ROA51	OP51	0.162	0.056	0.192	0.040	0.252	0.118	0.224
ROA51	SP51	0.162	0.188	0.192	0.040	0.280	0.170	0.294
ROA51	IT51	0.162	0.075	0.192	0.040	0.560	0.513	0.224
ROA51	CH51	0.162	0.043	0.192	0.040	0.275	0.162	0.224
OP51	SP51	0.056	0.188	0.192	0.040	0.256	0.126	0.224
OP51	IT51	0.056	0.075	0.192	0.040	0.548	0.500	0.156
OP51	CH51	0.056	0.043	0.192	0.040	0.251	0.115	0.156
SP51	IT51	0.188	0.075	0.192	0.040	0.561	0.515	0.224
SP51	CH51	0.188	0.043	0.192	0.040	0.279	0.168	0.224
IT51	CH51	0.075	0.043	0.192	0.040	0.559	0.513	0.156

9 ES baseline-mode measurement data

Different from the direct CCD measurements performed in site-mode calibration, the CCD measurements between an ES and the MOB located at the same site are conducted via a remote 'bridging ES'. This indirect CCD measurement method is called 'bridged CCD measurement'. The operation principle of the bridged CCD measurements and the baseline-mode calibration method are explained in Section 4.2.2: "Baseline-mode calibration scheme".

This chapter processes all on-site bridged CCD measurement data prepared for CALR and its uncertainty calculation with the baseline-mode calibration method. The denotations and data processing methods displayed in this chapter follow the description in Chapter 6.

The bridged CCD measurements correspond to Measurement B2 and/or Measurement B4 as described in Figure 4-4. In the following tables and figures, the 'Bridging ES channel' indicates the remote ES channel used for the calculation of the bridged CCD. Take Measurement B2 for instance, the 'Bridging ES channel' represents the remote station ES1 when measuring the bridged CCD data between ES2 and the MOB at Site 2. The bridged TW link, which contains more than 20 samples of the bridged CCD measurement data, is considered to be an effective bridged link. And only the effective bridged link is taken into account in the calculation. When there is no effective bridged link between the ES and the MOB, the bridged CCD measurement result is omitted in the following tables and figures. The outliers in the bridged CCD measurement data are removed by applying a 3-σ filter.

In the following tables of the bridged CCD measurement results on each ES channel, the samples at the sites are taken within the effective measurement duration as listed in Table 3-7. The bridged CCD measurement results are calculated using equation (37) / equation (38), equation (39), equation (40) and equation (42). In Section 9.1, all the bridged CCD measurements are calculated on the Rx channels of SATRE modem in each ES. In Section 9.2, all the bridged CCD measurements are calculated on the SDR channel of each ES.

In the following figures of the CCD/bridged CCD measurement results on each ES, the direct CCD measurement results of the same ES, taken from Table 7-47, are included for comparison. The circular markers of the data points indicate the Bridged CCD_{avg}(ki,MOB@k) values, and the lengths of the error bars above and below the data points indicate the uBridged CCD(ki,MOB@k) values accordingly.

9.1 Bridged CCD measurement results on SATRE channels at the sites

9.1.1 Bridged CCD measurements at TIM

9.1.1.1 Bridged CCD measurement on TIM01

Table 9-1 summarizes the results of the bridged CCD measurements on TIM01, where all the effective bridging ES channels are taken into account in the calculation.

Table 9-1 Bridged CCD measurement results on TIM01

Bridging ES channel	Bridged CCD_{avg}(TIM01,MOB@TIM)	uBridged CCD(TIM01,MOB@TIM)	Bridged CCD_{diff}(TIM01,MOB@TIM)	Total No. of Samples
	Unit: ns	Unit: ns	Unit: ns	
PTB05	-742.282	0.060	0.009	69
PTB25	-742.028	0.044	0.016	53
PTB04	-742.689	0.068	-0.119	59
VSL01	-742.552	0.076	0.000	67
ROA01	-742.406	0.106	0.015	68

ROA21	-742.297	0.105	0.002	47
OP01	-742.458	0.068	-0.057	56
NPL02	-742.298	0.095	-0.125	45
SP01	-742.208	0.082	-0.028	67
SP21	-742.667	0.087	-0.070	50
IT01	-742.538	0.151	0.049	69
IT21	-742.264	0.084	0.020	51
CH01	-742.723	0.052	-0.105	68
CH21	-742.387	0.060	-0.173	51

Figure 9-1 shows the value and the 1-σ measurement uncertainty of the bridged CCD measurement results on TIM01, which were obtained via diverse participating bridging ESs, respectively. As a comparison, the direct CCD measurement result of TIM01 is also included in the figure.

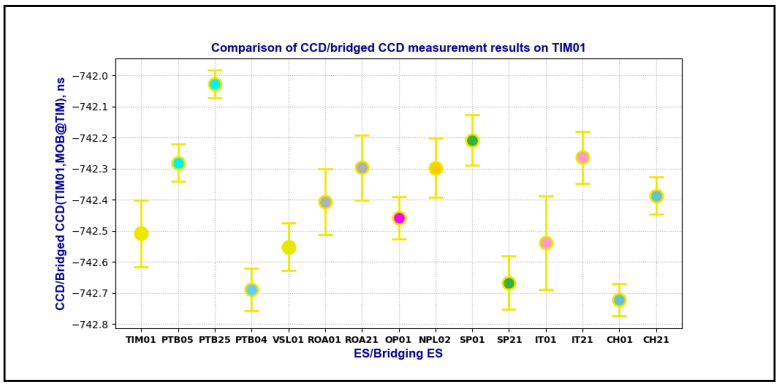

Figure 9-1 Comparison of CCD/bridged CCD measurement results on TIM01

9.1.1.2 Bridged CCD measurement on TIM21

Table 9-2 summarizes the results of the bridged CCD measurements on TIM21, where all the effective bridging ES channels are taken into account in the calculation.

Table 9-2 Bridged CCD measurement results on TIM21

Bridging ES channel	Bridged CCD_{avg}(TIM21,MOB@TIM)	uBridged CCD(TIM21,MOB@TIM)	Bridged CCD_{diff}(TIM21,MOB@TIM)	Total No. of Samples
	Unit: ns	Unit: ns	Unit: ns	
PTB05	-746.189	0.049	0.013	68
PTB25	-745.930	0.036	0.024	53
PTB04	-746.478	0.044	-0.142	60
VSL01	-746.368	0.063	0.000	67
ROA01	-746.136	0.105	0.005	68
ROA21	-746.009	0.129	0.002	47
OP01	-746.335	0.067	-0.069	56

NPL02	-746.137	0.098	-0.117	45
SP01	-746.094	0.078	-0.032	67
SP21	-746.552	0.085	-0.079	50
IT01	-746.398	0.148	0.048	69
IT21	-746.113	0.077	0.024	51
CH01	-746.513	0.040	-0.106	68
CH21	-746.173	0.044	-0.181	51

Figure 9-2 shows the value and the 1-σ measurement uncertainty of the bridged CCD measurement results on TIM21, which were obtained via diverse participating bridging ESs, respectively. As a comparison, the direct CCD measurement result of TIM21 is also included in the figure.

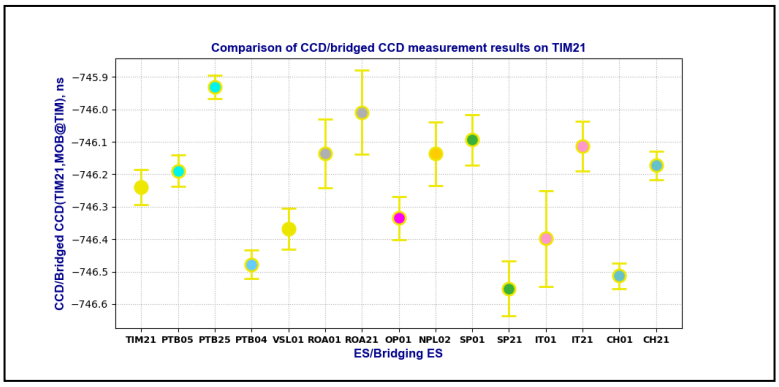

Figure 9-2 Comparison of CCD/bridged CCD measurement results on TIM21

9.1.2 Bridged CCD measurements at PL

Table 9-3 summarizes the results of the bridged CCD measurements on PL01, where all the effective bridging ES channels are taken into account in the calculation.

Table 9-3 Bridged CCD measurement results on PL01

Bridging ES channel	Bridged CCD_{avg}(PL01,MOB@TIM) Unit: ns	uBridged CCD(PL01,MOB@PL) Unit: ns	Bridged CCD_{diff}(PL01,MOB@PL) Unit: ns	Total No. of Samples
TIM01	-716.215	0.053	-0.007	44
PTB05	-716.125	0.027	--	21
PTB04	-716.592	0.061	0.051	45
ROA01	-716.134	0.075	--	25
ROA21	-716.016	0.066	--	21
CH01	-716.563	0.167	0.025	50
CH21	-716.108	0.178	-0.057	44

Figure 9-3 shows the value and the 1-σ measurement uncertainty of the bridged CCD measurement results on PL01, which are obtained via diverse participating bridging ESs, respectively. As a comparison, the direct CCD measurement result of PL01 is also included in the figure.

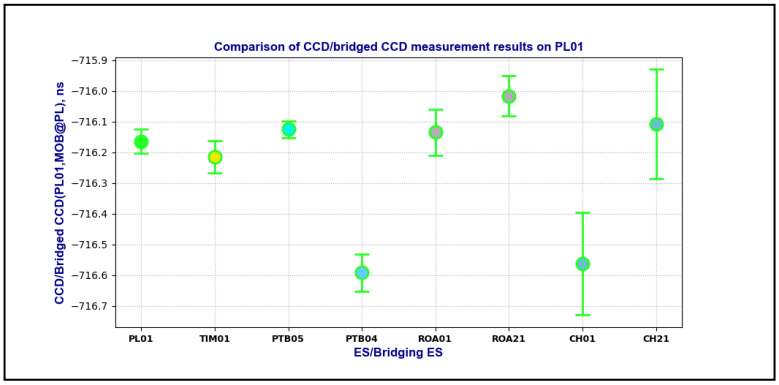

Figure 9-3 Comparison of CCD/bridged CCD measurement results on PL01

9.1.3 Bridged CCD measurements at PTB

9.1.3.1 Bridged CCD measurements on PTB05

Table 9-4 summarizes the results of the bridged CCD measurements on PTB05, where all the effective bridging ES channels are taken into account in the calculation.

Table 9-4 Bridged CCD measurement results on PTB05

Bridging ES channel	Bridged CCD_{avg}(PTB05,MOB@PTB)	uBridged CCD(PTB05,MOB@PTB)	Bridged CCD_{diff}(PTB05,MOB@PTB)	Total No. of Samples
	Unit: ns	Unit: ns	Unit: ns	
TIM01	-712.637	0.065	-0.003	81
TIM21	-712.451	0.059	-0.017	74
PL01	-712.507	0.048	--	21
PTB04	-713.404	0.103	-0.008	85
VSL01	-712.727	0.083	0.079	85
ROA01	-712.518	0.163	-0.020	85
ROA21	-712.445	0.220	-0.012	80
OP01	-712.940	0.060	0.030	72
NPL02	-712.334	0.141	-0.018	81
SP01	-712.078	0.096	-0.053	81
SP21	-713.606	0.115	-0.041	64
IT01	-712.771	0.038	0.055	86
IT21	-712.410	0.033	0.049	79
CH01	-713.339	0.075	0.007	86
CH21	-712.558	0.065	0.013	79

Figure 9-4 shows the value and the 1-σ measurement uncertainty of the bridged CCD measurement results of PTB05, which are obtained via diverse participating bridging ESs, respectively. As a comparison, the direct CCD measurement result of PTB05 is also included in the figure.

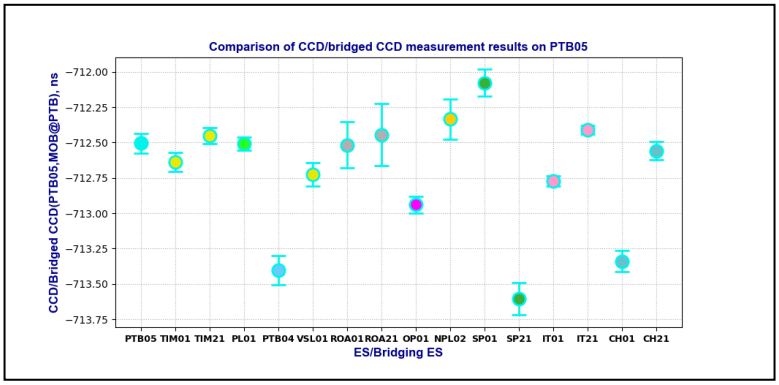

Figure 9-4 Comparison of CCD/bridged CCD measurement results on PTB05

9.1.3.2 Bridged CCD measurements on PTB25

Table 9-5 summarizes the results of the bridged CCD measurements on PTB25, where all the effective bridging ES channels are taken into account in the calculation.

Table 9-5 Bridged CCD measurement results on PTB25

Bridging ES channel	Bridged CCD_{avg}(PTB25,MOB@PTB) Unit: ns	uBridged CCD(PTB25,MOB@PTB) Unit: ns	Bridged CCD_{diff}(PTB25,MOB@PTB) Unit: ns	Total No. of Samples
TIM01	-717.659	0.081	-0.007	81
TIM21	-717.469	0.076	-0.024	74
PL01	-717.662	0.049	--	21
PTB04	-718.760	0.123	-0.022	85
VSL01	-717.878	0.091	0.088	85
ROA01	-717.512	0.279	-0.034	85
ROA21	-717.437	0.343	-0.016	80
OP01	-718.231	0.074	0.013	71
NPL02	-717.544	0.146	-0.026	81
SP01	-717.224	0.106	-0.045	81
SP21	-718.755	0.131	-0.037	64
IT01	-717.826	0.046	0.057	86
IT21	-717.464	0.038	0.052	79
CH01	-718.502	0.073	-0.012	86
CH21	-717.720	0.062	-0.006	79

Figure 9-5 shows the value and the 1-σ measurement uncertainty of the bridged CCD measurement results of PTB25, which are obtained via diverse participating bridging ESs, respectively. As a comparison, the direct CCD measurement result of PTB25 is also included in the figure.

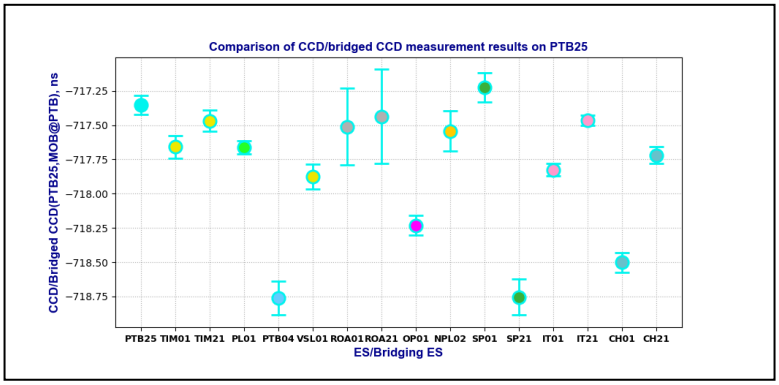

Figure 9-5 Comparison of CCD/bridged CCD measurement results on PTB25

9.1.3.3 Bridged CCD measurements of PTB04

Table 9-6 summarizes the results of the bridged CCD measurements on PTB04, where all the effective bridging ES channels are taken into account in the calculation.

Table 9-6 Bridged CCD measurement results on PTB04

Bridging ES channel	Bridged CCD_{avg}(PTB04,MOB@PTB) Unit: ns	uBridged CCD(PTB04,MOB@PTB) Unit: ns	Bridged CCD_{diff}(PTB04,MOB@PTB) Unit: ns	Total No. of Samples
TIM01	-729.060	0.048	0.051	83
TIM21	-728.943	0.050	0.018	80
PL01	-728.742	0.075	0.084	70
PTB05	-728.269	0.065	0.084	92
PTB25	-727.762	0.051	0.089	90
VSL01	-728.865	0.109	0.023	91
ROA01	-728.863	0.131	0.091	91
ROA21	-728.856	0.113	0.102	89
OP01	-728.830	0.048	0.033	88
NPL02	-728.728	0.094	-0.039	81
SP01	-728.523	0.100	-0.006	88
SP21	-730.059	0.161	-0.052	56
IT01	-729.118	0.075	0.003	92
IT21	-728.799	0.056	0.009	88
CH01	-729.296	0.099	0.039	92
CH21	-728.738	0.065	0.055	90

Figure 9-6 shows the value and the 1-σ measurement uncertainty of the bridged CCD measurement results on PTB04, which are obtained via diverse participating bridging ESs, respectively. As a comparison, the direct CCD measurement result of PTB04 is also included in the figure.

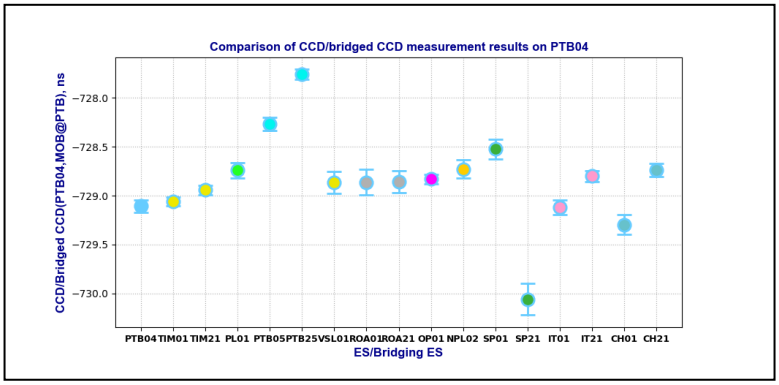

Figure 9-6 Comparison of CCD/bridged CCD measurement results on PTB04

9.1.4 Bridged CCD measurements at VSL

9.1.4.1 Bridged CCD measurements on VSL01

Table 9-7 summarizes the results of the bridged CCD measurements on VSL01, where all the effective bridging ES channels are taken into account in the calculation.

Table 9-7 Bridged CCD measurement results on VSL01

Bridging ES channel	Bridged CCD_{avg}(VSL01,MOB@VSL) Unit: ns	uBridged CCD(VSL01,MOB@VSL) Unit: ns	Bridged CCD_{diff}(VSL01,MOB@VSL) Unit: ns	Total No. of Samples
TIM01	-721.038	0.134	-0.009	81
TIM21	-720.926	0.132	0.002	79
PTB05	-720.939	0.089	0.060	85
PTB25	-720.595	0.076	0.043	82
PTB04	-721.429	0.107	-0.044	85
ROA01	-721.075	0.181	-0.156	87
ROA21	-720.982	0.223	-0.171	82
OP01	-721.218	0.123	-0.027	86
NPL02	-721.020	0.120	0.048	79
SP01	-720.814	0.133	-0.014	53
IT01	-721.276	0.121	-0.018	86
IT21	-720.951	0.129	-0.003	83
CH01	-721.454	0.118	0.085	84
CH21	-721.036	0.123	0.060	80

Figure 9-7 shows the value and the 1-σ measurement uncertainty of the bridged CCD measurement results on VSL01, which are obtained via diverse participating bridging ESs, respectively. As a comparison, the direct CCD measurement result of VSL01 is also included in the figure.

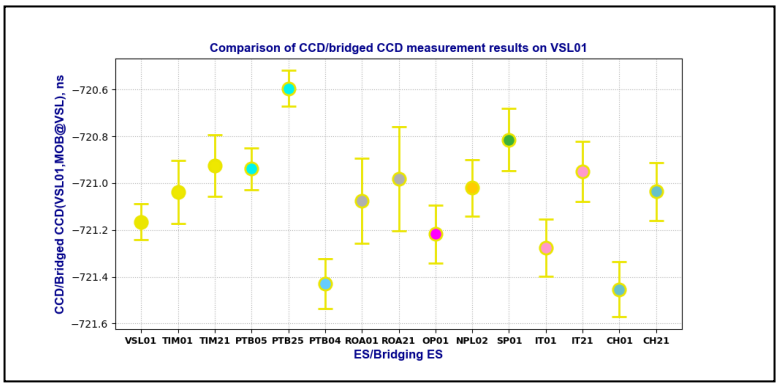

Figure 9-7 Comparison of CCD/bridged CCD measurement results on VSL01

9.1.4.2 Bridged CCD measurements on VSL21

Table 9-8 summarizes the results of the bridged CCD measurements on VSL21, where all the effective bridging ES channels are taken into account in the calculation.

Table 9-8 Bridged CCD measurement results on VSL21

Bridging ES channel	Bridged CCD_{avg}(VSL21,MOB@VSL) Unit: ns	uBridged CCD(VSL21,MOB@VSL) Unit: ns	Bridged CCD_{diff}(VSL21,MOB@VSL) Unit: ns	Total No. of Samples
TIM01	-721.113	0.139	0.000	81
TIM21	-721.002	0.136	0.012	79
PTB05	-721.023	0.083	0.060	85
PTB25	-720.680	0.081	0.044	82
PTB04	-721.501	0.108	-0.042	85
ROA01	-721.177	0.189	-0.119	87
ROA21	-721.083	0.233	-0.134	82
OP01	-721.290	0.120	-0.037	86
NPL02	-721.116	0.127	0.017	80
SP01	-720.933	0.132	-0.001	53
IT01	-721.356	0.111	-0.020	86
IT21	-721.032	0.124	-0.005	83
CH01	-721.517	0.167	0.100	86
CH21	-721.104	0.174	0.083	82

Figure 9-8 shows the value and the 1-σ measurement uncertainty of the bridged CCD measurement results on VSL21, which are obtained via diverse participating bridging ESs, respectively. As a comparison, the direct CCD measurement result of VSL21 is also included in the figure.

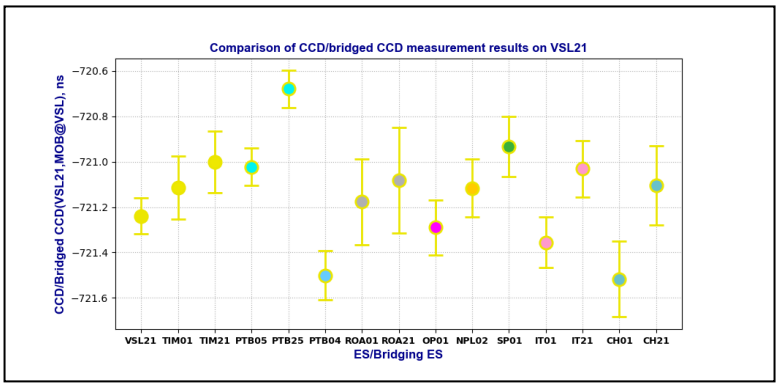

Figure 9-8 Comparison of CCD/bridged CCD measurement results on VSL21

9.1.5 Bridged CCD measurements at LTFB

Table 9-9 summarizes the results of the bridged CCD measurements on LTFB01, where all the effective bridging ES channels are taken into account in the calculation.

Table 9-9 Bridged CCD measurement results on LTFB01

Bridging ES channel	Bridged CCD_{avg}(LTFB01,MOB@LTFB)	uBridged CCD(LTFB01,MOB@LTFB)	Bridged CCD_{diff}(LTFB01,MOB@LTFB)	Total No. of Samples
	Unit: ns	Unit: ns	Unit: ns	
TIM01	-715.257	0.109	-0.026	78
TIM21	-715.088	0.115	-0.007	78
PTB05	-715.094	0.091	--	28
PTB25	-714.716	0.111	--	28
PTB04	-715.512	0.098	--	27
ROA01	-715.151	0.105	--	29
ROA21	-715.080	0.076	--	29
OP01	-715.390	0.110	-0.035	79
IT01	-715.347	0.082	--	29
IT21	-715.068	0.078	--	29
CH01	-715.538	0.091	--	25
CH21	-715.070	0.111	--	27

Figure 9-9 shows the value and the 1-σ measurement uncertainty of the bridged CCD measurement results on LTFB01, which are obtained via diverse participating bridging ESs, respectively. As a comparison, the direct CCD measurement result of LTFB01 is also included in the figure.

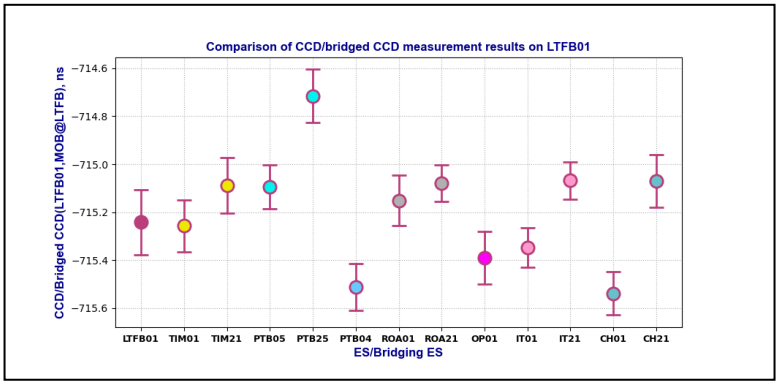

Figure 9-9 Comparison of CCD/bridged CCD measurement results on LTFB01

9.1.6 Bridged CCD measurements at ROA

9.1.6.1 Bridged CCD measurements on ROA01

Table 9-10 summarizes the results of the bridged CCD measurements on ROA01, where all the effective bridging ES channels are taken into account in the calculation.

Table 9-10 Bridged CCD measurement results on ROA01

Bridging ES channel	Bridged CCD_{avg}(ROA01,MOB@ROA)	uBridged CCD(ROA01,MOB@ROA)	Bridged CCD_{diff}(ROA01,MOB@ROA)	Total No. of Samples
	Unit: ns	Unit: ns	Unit: ns	
TIM01	-703.622	0.187	0.045	102
TIM21	-703.508	0.151	0.046	100
PL01	-703.716	0.084	--	29
PTB05	-703.650	0.110	0.040	102
PTB25	-703.42	0.083	0.024	100
PTB04	-703.863	0.396	-0.040	105
VSL01	-703.748	0.209	0.022	105
LTFB01	-703.728	0.155	--	51
OP01	-703.781	0.222	-0.019	74
NPL02	-703.612	0.181	0.048	98
SP01	-703.468	0.096	0.099	100
SP21	-704.093	0.167	-0.027	53
IT01	-703.743	0.231	-0.023	105
IT21	-703.499	0.164	-0.029	99
CH01	-703.889	0.371	0.003	105
CH21	-703.627	0.200	-0.003	105

Figure 9-10 shows the value and the 1-σ measurement uncertainty of the bridged CCD measurement results on ROA01, which are obtained via diverse participating bridging ESs, respectively. As a comparison, the direct CCD measurement result of ROA01 is also included in the figure.

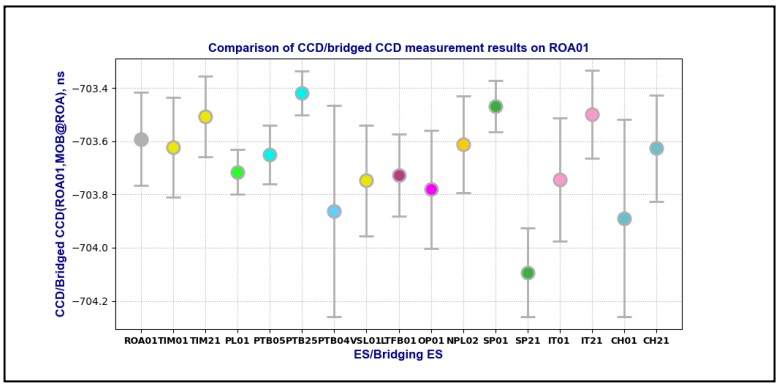

Figure 9-10 Comparison of CCD/bridged CCD measurement results on ROA01

9.1.6.2 Bridged CCD measurements on ROA21

Table 9-11 summarizes the results of the bridged CCD measurements on ROA21, where all the effective bridging ES channels are taken into account in the calculation.

Table 9-11 Bridged CCD measurement results on ROA21

Bridging ES channel	Bridged CCD_{avg}(ROA21,MOB@ROA)	uBridged CCD(ROA21,MOB@ROA)	Bridged CCD_{diff}(ROA21,MOB@ROA)	Total No. of Samples
	Unit: ns	Unit: ns	Unit: ns	
TIM01	-703.636	0.175	0.051	102
TIM21	-703.523	0.135	0.051	100
PL01	-703.646	0.091	--	29
PTB05	-703.488	0.102	0.037	102
PTB25	-703.258	0.093	0.021	100
PTB04	-703.729	0.377	-0.024	105
VSL01	-703.689	0.205	0.040	105
LTFB01	-703.684	0.145	--	51
OP01	-703.682	0.222	-0.004	74
NPL02	-703.553	0.191	0.058	97
SP01	-703.427	0.094	0.107	100
SP21	-704.010	0.247	-0.021	55
IT01	-703.736	0.220	-0.016	105
IT21	-703.492	0.155	-0.021	99
CH01	-703.815	0.368	0.014	105
CH21	-703.553	0.198	0.008	105

Figure 9-11 shows the value and the 1-σ measurement uncertainty of the bridged CCD measurement results on ROA21, which are obtained via diverse participating bridging ESs, respectively. As a comparison, the direct CCD measurement result of ROA21 is also included in the figure.

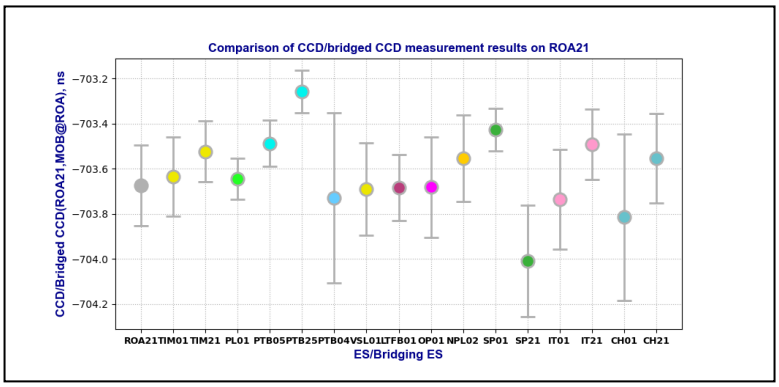

Figure 9-11 Comparison of CCD/bridged CCD measurement results on ROA21

9.1.7 Bridged CCD measurements at OP

Table 9-12 summarizes the results of the bridged CCD measurements on OP01, where all the effective bridging ES channels are taken into account in the calculation.

Table 9-12 Bridged CCD measurement results on OP01

Bridging ES channel	Bridged CCD_{avg}(OP01,MOB@OP)	uBridged CCD(OP01,MOB@OP)	Bridged CCD_{diff}(OP01,MOB@OP)	Total No. of Samples
	Unit: ns	Unit: ns	Unit: ns	
TIM01	-7862.161	0.085	-0.005	81
TIM21	-7861.910	0.095	0.014	80
PL01	-7861.999	0.081	--	26
PTB05	-7861.711	0.083	-0.008	79
PTB25	-7861.274	0.093	-0.039	76
PTB04	-7862.432	0.093	-0.105	79
VSL01	-7862.110	0.112	-0.051	80
LTFB01	-7862.061	0.184	0.035	76
ROA01	-7861.889	0.139	--	41
ROA21	-7861.863	0.097	--	41
NPL02	-7861.817	0.139	-0.052	73
SP01	-7861.572	0.077	0.000	81
SP21	-7862.800	0.068	0.054	79
IT01	-7862.228	0.100	0.071	81
IT21	-7861.937	0.092	0.068	80
CH01	-7862.592	0.095	--	41
CH21	-7861.973	0.084	--	41

Figure 9-12 shows the value and the 1-σ measurement uncertainty of the bridged CCD measurement results on OP01, which are obtained via diverse participating bridging ESs, respectively. As a comparison, the direct CCD measurement result of OP01 is also included in the figure.

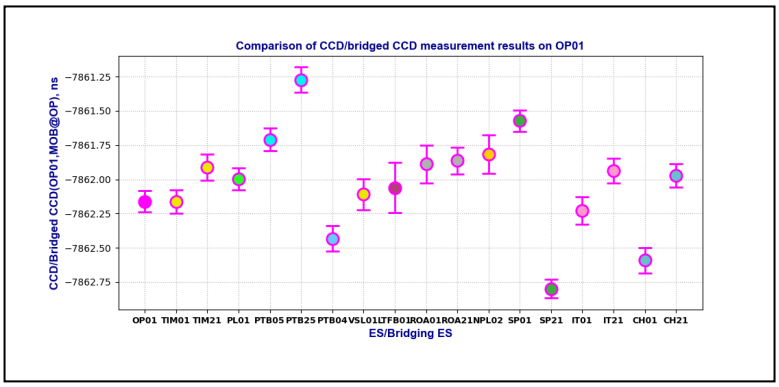

Figure 9-12 Comparison of CCD/bridged CCD measurement results on OP01

9.1.8 Bridged CCD measurements at NPL

Table 9-13 summarizes the results of the bridged CCD measurements on NPL02, where all the effective bridging ES channels are taken into account in the calculation.

Table 9-13 Bridged CCD measurement results on NPL02

Bridging ES channel	Bridged CCD_{avg}(NPL02,MOB@NPL)	uBridged CCD(NPL02,MOB@NPL)	Bridged CCD_{diff}(NPL02,MOB@NPL)	Total No. of Samples
	Unit: ns	Unit: ns	Unit: ns	
TIM01	-10.560	0.165	0.060	77
TIM21	-10.415	0.129	0.074	76
PTB05	-10.726	0.209	-0.034	71
PTB25	-10.450	0.178	-0.033	69
PTB04	-11.055	0.156	-0.141	75
VSL01	-10.641	0.257	-0.061	77
ROA01	-10.443	0.196	0.001	76
ROA21	-10.335	0.217	-0.010	75
OP01	-10.824	0.173	0.040	72
SP01	-10.270	0.154	0.032	69
SP21	-11.022	0.169	0.014	55
IT01	-10.695	0.195	0.044	77
IT21	-10.476	0.176	0.039	76
CH01	-10.998	0.198	-0.031	72
CH21	-10.631	0.210	-0.007	76

Figure 9-13 shows the value and the 1-σ measurement uncertainty of the bridged CCD measurement results on NPL02, which were obtained via diverse participating bridging ESs, respectively. As a comparison, the direct CCD measurement result of NPL02 is also included in the figure.

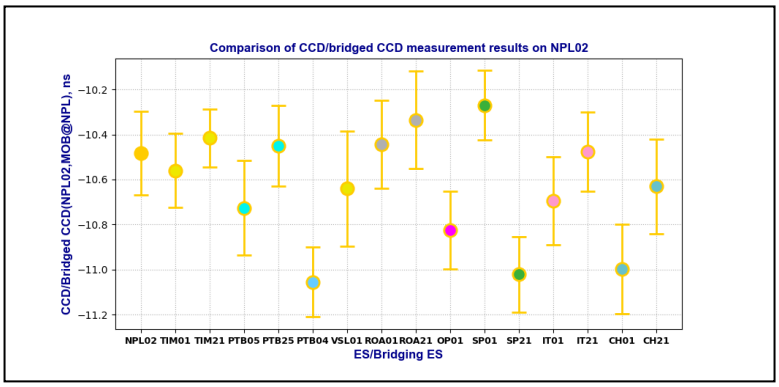

Figure 9-13 Comparison of CCD/bridged CCD measurement results on NPL02

9.1.9 Bridged CCD measurements at SP

9.1.9.1 Bridged CCD measurements on SP01

Table 9-14 summarizes the results of the bridged CCD measurements on SP01, where all the effective bridging ES channels are taken into account in the calculation.

Table 9-14 Bridged CCD measurement results on SP01

Bridging ES channel	Bridged CCD_{avg}(SP01,MOB@SP)	uBridged CCD(SP01,MOB@TIM)	Bridged CCD_{diff}(SP01,MOB@SP)	Total No. of Samples
	Unit: ns	Unit: ns	Unit: ns	
TIM01	-728.879	0.051	-0.043	69
TIM21	-728.608	0.045	-0.058	68
PTB05	-729.078	0.060	-0.011	63
PTB25	-728.824	0.074	-0.039	60
VSL01	-729.046	0.106	0.053	69
ROA01	-728.880	0.093	-0.053	59
ROA21	-728.761	0.118	-0.051	55
OP01	-729.206	0.048	-0.045	68
NPL02	-728.885	0.093	-0.050	62
IT01	-729.000	0.097	-0.062	70
IT21	-728.779	0.100	-0.072	66
CH01	-729.202	0.140	-0.013	68
CH21	-728.847	0.094	-0.008	67

Figure 9-14 shows the value and the 1-σ measurement uncertainty of the bridged CCD measurement results on SP01, which were obtained via diverse participating bridging ESs, respectively. As a comparison, the direct CCD measurement result of SP01 is also included in the figure.

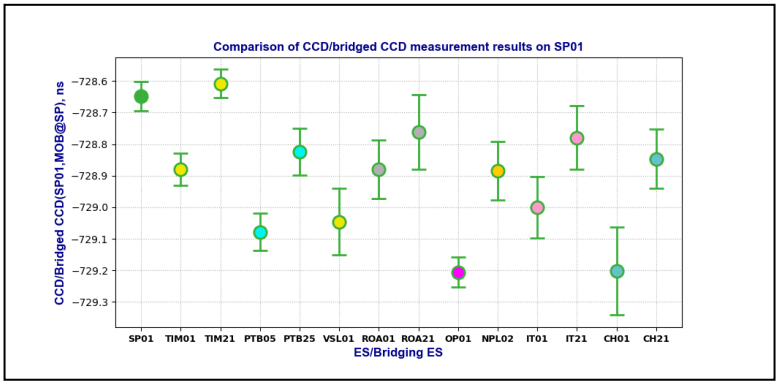

Figure 9-14 Comparison of CCD/bridged CCD measurement results on SP01

9.1.9.2 Bridged CCD measurements on SP21

Table 9-15 summarizes the results of the bridged CCD measurements on SP21, where all the effective bridging ES channels are taken into account in the calculation.

Table 9-15 Bridged CCD measurement results on SP21

Bridging ES channel	Bridged CCD_{avg}(SP21,MOB@SP) Unit: ns	uBridged CCD(SP21,MOB@TIM) Unit: ns	Bridged CCD_{diff}(SP21,MOB@SP) Unit: ns	Total No. of Samples
TIM01	-731.223	0.080	0.007	58
TIM21	-730.950	0.070	-0.011	57
PTB05	-730.062	0.062	0.048	44
PTB25	-729.823	0.092	0.019	43
VSL01	-730.741	0.105	0.053	65
OP01	-730.645	0.048	0.005	68
NPL02	-731.008	0.104	-0.011	61
IT01	-730.948	0.071	0.052	69
IT21	-730.730	0.070	0.035	65
CH01	-730.792	0.051	--	21
CH21	-730.437	0.058	--	21

Figure 9-15 shows the value and the 1-σ measurement uncertainty of the bridged CCD measurement results on SP21, which were obtained via diverse participating bridging ESs, respectively. As a comparison, the direct CCD measurement result of SP21 is also included in the figure.

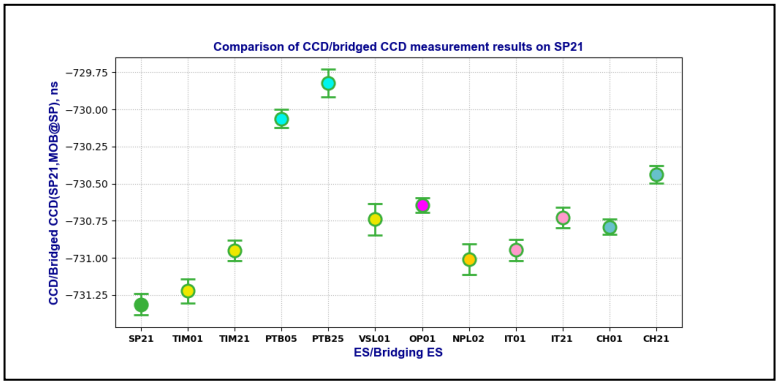

Figure 9-15 Comparison of CCD/bridged CCD measurement results on SP21

9.1.10 Bridged CCD measurements at IT

9.1.10.1 Bridged CCD measurements on IT01

Table 9-16 summarizes the results of the bridged CCD measurements on IT01, where all the effective bridging ES channels are taken into account in the calculation.

Table 9-16 Bridged CCD measurement results on IT01

Bridging ES channel	Bridged CCD_{avg}(IT01,MOB@IT) Unit: ns	uBridged CCD(IT01,MOB@IT) Unit: ns	Bridged CCD_{diff}(IT01,MOB@IT) Unit: ns	Total No. of Samples
TIM01	-718.699	0.074	0.001	81
TIM21	-718.590	0.068	-0.001	80
PTB05	-718.453	0.056	0.000	82
PTB25	-718.182	0.060	-0.015	79
PTB04	-718.830	0.082	-0.034	82
VSL01	-718.710	0.199	-0.013	81
LTFB01	-718.588	0.089	--	34
ROA01	-718.575	0.089	0.055	82
ROA21	-718.528	0.072	0.027	81
OP01	-718.736	0.057	0.015	78
NPL02	-718.568	0.080	0.032	70
SP01	-718.457	0.078	0.031	82
SP21	-719.180	0.058	-0.007	77
CH01	-718.869	0.136	-0.022	75
CH21	-718.547	0.142	-0.015	82

Figure 9-16 shows the value and the 1-σ measurement uncertainty of the bridged CCD measurement results on SP01, which are obtained via diverse participating bridging ESs, respectively. As a comparison, the direct CCD measurement result of IT01 is also included in the figure.

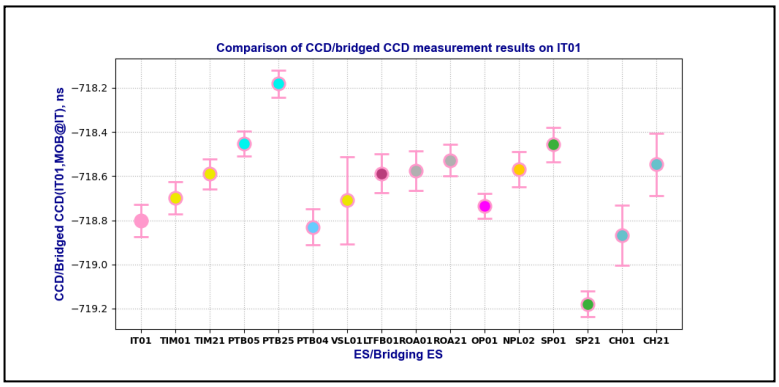

Figure 9-16 Comparison of CCD/bridged CCD measurement results on IT01

9.1.10.2 Bridged CCD measurements on IT21

Table 9-17 summarizes the results of the bridged CCD measurements on IT21, where all the effective bridging ES channels are taken into account in the calculation.

Table 9-17 Bridged CCD measurement results on IT21

Bridging ES channel	Bridged CCD_{avg}(IT21,MOB@IT)	uBridged CCD(IT21,MOB@IT)	Bridged CCD_{diff}(IT21,MOB@IT)	Total No. of Samples
	Unit: ns	Unit: ns	Unit: ns	
TIM01	-716.171	0.072	-0.009	81
TIM21	-716.064	0.059	-0.012	80
PTB05	-716.043	0.067	-0.003	82
PTB25	-715.772	0.070	-0.018	79
PTB04	-716.401	0.076	-0.027	82
VSL01	-716.250	0.191	-0.018	81
LTFB01	-716.075	0.065	--	34
ROA01	-716.069	0.082	0.037	82
ROA21	-716.022	0.075	0.008	81
OP01	-716.280	0.066	-0.006	78
NPL02	-715.993	0.087	0.034	70
SP01	-715.945	0.063	0.021	82
SP21	-716.671	0.070	-0.018	77
CH01	-716.409	0.128	-0.027	75
CH21	-716.088	0.127	-0.020	82

Figure 9-17 shows the value and the 1-σ measurement uncertainty of the bridged CCD measurement results on SP21, which are obtained via diverse participating bridging ESs, respectively. As a comparison, the direct CCD measurement result of IT21 is also included in the figure.

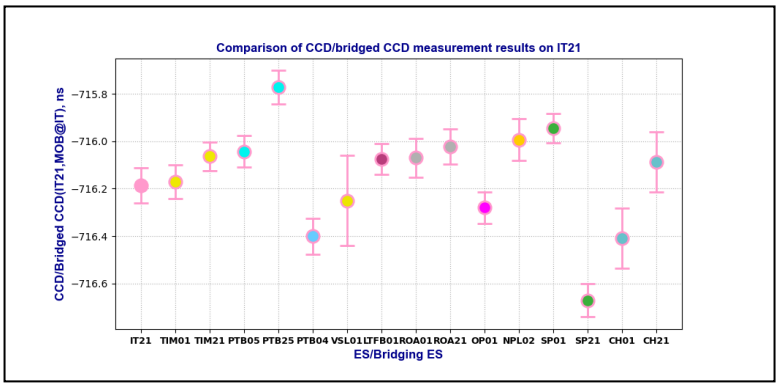

Figure 9-17 Comparison of CCD/bridged CCD measurement results on IT21

9.1.11 Bridged CCD measurements at CH

9.1.11.1 Bridged CCD measurements on CH01

Table 9-18 summarizes the results of the bridged CCD measurements on CH01, where all the effective bridging ES channels are taken into account in the calculation.

Table 9-18 Bridged CCD measurement results on CH01

Bridging ES channel	Bridged CCD_{avg}(CH01,MOB@CH)	uBridged CCD(CH01,MOB@CH)	Bridged CCD_{diff}(CH01,MOB@CH)	Total No. of Samples
	Unit: ns	Unit: ns	Unit: ns	
TIM01	-718.107	0.057	0.000	80
TIM21	-718.007	0.048	-0.012	76
PL01	-717.845	0.020	--	24
PTB05	-717.391	0.059	0.061	82
PTB25	-717.029	0.060	0.035	77
PTB04	-718.013	0.117	0.009	82
VSL01	-717.925	0.137	-0.055	80
LTFB01	-717.981	0.091	--	33
ROA01	-717.857	0.161	0.051	82
ROA21	-717.854	0.151	0.055	80
OP01	-717.975	0.026	--	41
NPL02	-717.868	0.113	-0.009	68
SP01	-717.610	0.065	0.065	75
SP21	-718.670	0.061	--	21
IT01	-718.146	0.065	0.003	75
IT21	-717.858	0.044	0.014	73

Figure 9-18 shows the value and the 1-σ measurement uncertainty of the bridged CCD measurement results on CH01, which are obtained via diverse participating bridging ESs, respectively. As a comparison, the direct CCD measurement result of CH01 is also included in the figure.

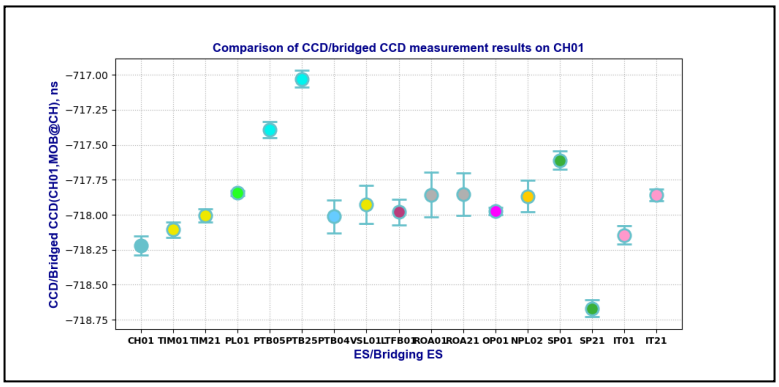

Figure 9-18 Comparison of CCD/bridged CCD measurement results on CH01

9.1.11.2 Bridged CCD measurements on CH21

Table 9-19 summarizes the results of the bridged CCD measurements on CH21, where all the effective bridging ES channels are taken into account in the calculation.

Table 9-19 Bridged CCD measurement results on CH21

Bridging ES channel	Bridged CCD_{avg}(CH21,MOB@CH)	uBridged CCD(CH21,MOB@CH)	Bridged CCD_{diff}(CH21,MOB@CH)	Total No. of Samples
	Unit: ns	Unit: ns	Unit: ns	
TIM01	-724.616	0.040	-0.007	80
TIM21	-724.519	0.047	-0.019	76
PL01	-724.531	0.041	--	25
PTB05	-724.376	0.044	0.039	82
PTB25	-724.012	0.052	0.011	77
PTB04	-724.932	0.069	-0.013	82
VSL01	-724.675	0.144	-0.081	80
LTFB01	-724.653	0.063	--	27
ROA01	-724.482	0.069	0.026	75
ROA21	-724.489	0.072	0.032	73
OP01	-724.878	0.035	--	41
NPL02	-724.453	0.083	-0.016	68
SP01	-724.255	0.139	0.037	78
IT01	-724.791	0.060	-0.007	80
IT21	-724.502	0.039	-0.008	78

Figure 9-19 shows the value and the 1-σ measurement uncertainty of the bridged CCD measurement results on CH21, which are obtained via diverse participating bridging ESs, respectively. As a comparison, the direct CCD measurement result of CH21 is also included in the figure.

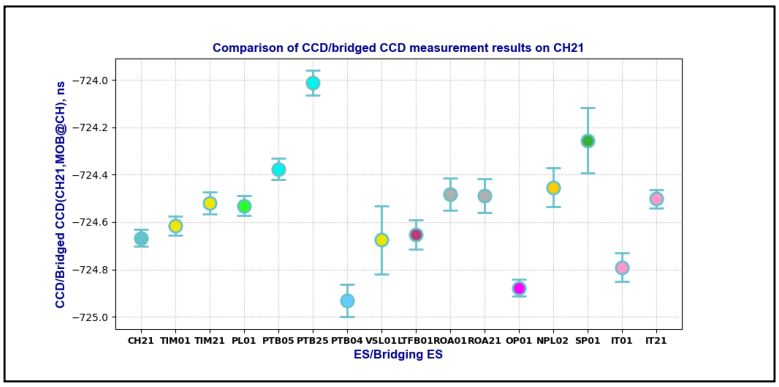

Figure 9-19 Comparison of CCD/bridged CCD measurement results on CH21

9.2 Bridged CCD measurement results on SDR channels at the sites

9.2.1 Bridged CCD measurements on VSL51

Table 9-20 summarizes the results of the bridged CCD measurements on VSL51, where all the effective bridging ES channels are taken into account in the calculation.

Table 9-20 Bridged CCD measurement results on VSL51

Bridging ES channel	Bridged CCD_{avg}(VSL51,MOB@VSL)	uBridged CCD(VSL51,MOB@VSL)	Bridged CCD_{diff}(VSL51,MOB@VSL)	Total No. of Samples
	Unit: ns	Unit: ns	Unit: ns	
OP51	-1566.361	0.120	--	42

Figure 9-20 shows the value and the 1-σ measurement uncertainty of the bridged CCD measurement results on VSL51, which are obtained via diverse participating bridging ESs, respectively. As a comparison, the direct CCD measurement result of VSL51 is also included in the figure.

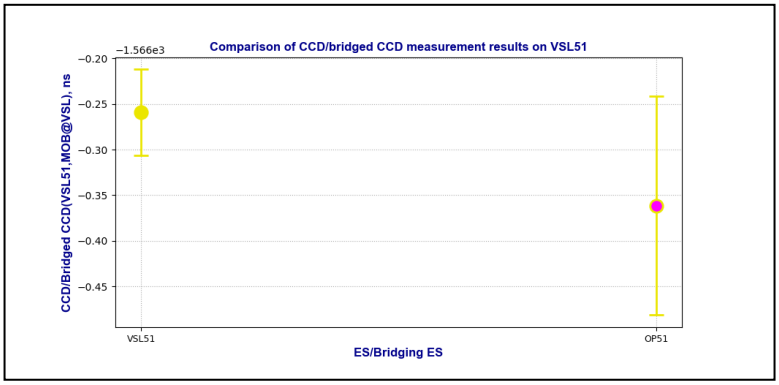

Figure 9-20 Comparison of CCD/bridged CCD measurement results on VSL51

9.2.2 Bridged CCD measurements on OP51

Table 9-21 summarizes the results of the bridged CCD measurements on OP51, where all the effective bridging ES channels are taken into account in the calculation.

Table 9-21 Bridged CCD measurement results on OP51

Bridging ES channel	Bridged CCD_{avg}(OP51,MOB@OP)	uBridged CCD(OP51,MOB@OP)	Bridged CCD_{diff}(OP51,MOB@OP)	Total No. of Samples
	Unit: ns	Unit: ns	Unit: ns	
VSL51	-3623.510	0.118	-0.072	80
ROA51	-3623.230	0.086	--	41
IT51	-3623.379	0.098	0.097	81

Figure 9-21 shows the value and the 1-σ measurement uncertainty of the bridged CCD measurement results on OP51 which are obtained via diverse participating bridging ESs, respectively. As a comparison, the direct CCD measurement result of OP51 is also included in the figure.

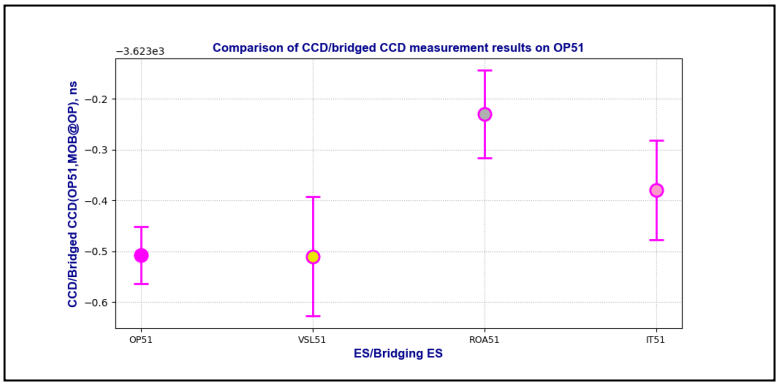

Figure 9-21 Comparison of CCD/bridged CCD measurement results on OP51

9.2.3 Bridged CCD measurements on SP51

Table 9-22 summarizes the results of the bridged CCD measurements on SP51, where all the effective bridging ES channels are taken into calculation.

Table 9-22 Bridged CCD measurement results on SP51

Bridging ES channel	Bridged CCD_{avg}(SP51,MOB@SP) Unit: ns	uBridged CCD(SP51,MOB@SP) Unit: ns	Bridged CCD_{diff}(SP51,MOB@SP) Unit: ns	Total No. of Samples
ROA51	-1598.841	0.371	--	33
OP51	-1599.221	0.088	--	35
IT51	-1598.663	0.244	0.342	67

Figure 9-22 shows the value and the 1-σ measurement uncertainty of the bridged CCD measurement results on SP51 which are obtained via diverse participating bridging ESs, respectively. As a comparison, the direct CCD measurement result of SP51 is also included in the figure.

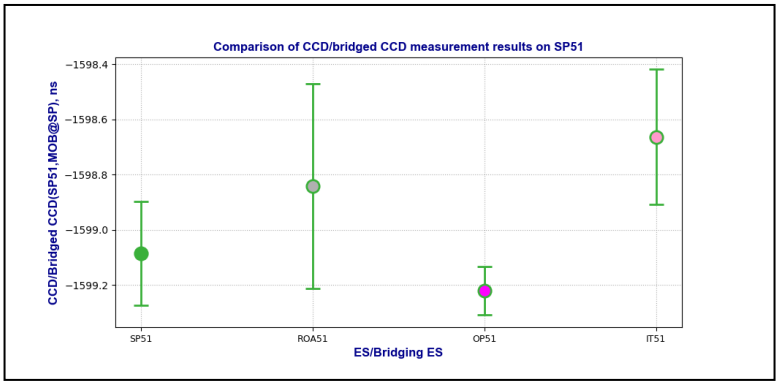

Figure 9-22 Comparison of CCD/bridged CCD measurement results on SP51

9.2.4 Bridged CCD measurements on IT51

Table 9-23 summarizes the results of the bridged CCD measurements on IT51, where all the effective bridging ES channels are taken into account in the calculation.

Table 9-23 Bridged CCD measurement results on IT51

Bridging ES channel	Bridged CCD_{avg}(IT51,MOB@IT) Unit: ns	uBridged CCD(IT51,MOB@IT) Unit: ns	Bridged CCD_{diff}(IT51,MOB@IT) Unit: ns	Total No. of Samples
ROA51	-1481.709	0.088	0.017	82
OP51	-1482.079	0.075	--	41

Figure 9-23 shows the value and the 1-σ measurement uncertainty of the bridged CCD measurement results on IT51 which are obtained via diverse participating bridging ESs, respectively. As a comparison, the direct CCD measurement result of IT51 is also included in the figure.

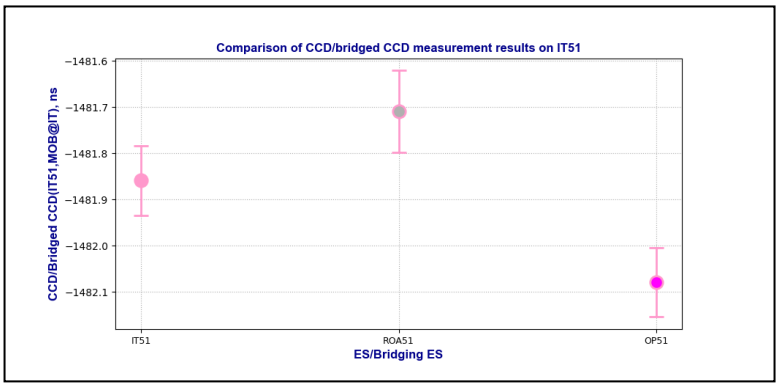

Figure 9-23 Comparison of CCD/bridged CCD measurement results on IT51

10 Baseline-mode calibration results

Based on the pre-setting parameters and CCD measurement data computed in Chapter 7 as well as the bridged CCD measurement data processed in Chapter 9, the baseline-mode calibration results on the participating TW links are calculated. The principle of the baseline-mode calibration method refers to Section 4.2.2: "Baseline-mode calibration scheme", and the computation of the CALR values refers to Section 6.2.3: "CALR data processing in baseline-mode calibration". The 1-σ uncertainty of the CALR, which is denoted as uCALR, is analyzed and calculated, referring to Section 6.3: "Uncertainty budget of CALR".

For a pair of ESs in a TW link, the baseline-mode calibration is performed by two separate on-site measurements: Measurement B1 and Measurement B2, as mentioned in Section 4.2.2. If applicable, Measurement B3 and Measurement B4 will be added by swapping the CCD and bridged CCD measurement approaches of the two ESs. In this chapter, the denotation "$CALR_{MeasB}(k_1i,k_2j)$" represents the baseline-mode calibration results obtained for a pair of ESs based on Measurement B1 plus Measurement B2 or based on Measurement B3 plus Measurement B4 according to equation (46)/equation(47). The denotation "$CALR(k_1i,k_2j)$" represents the final CALR results of a TW link according to equation (48).

In this chapter, the TW links between the Rx1 channel of two remote ESs are calibrated using baseline-mode calibration, and the calibration results are classified into two categories:

- TW calibration pairs and final TW link calibration results between the SATRE Rx1 channels of two remote ESs;
- TW calibration pairs and final TW link calibration results between the SDR channels of two remote ESs.

Note that all the new CALR values in this chapter are applied to the criteria that:

1) *REFDELAY(ki) values are set according to Table 7-2;*
2) *ESDVAR values are set to zero.*

10.1 Baseline-mode CALR calibration results on SATRE channels

10.1.1 Baseline-mode CALR calibration pairs of SATRE channels

Table 10-1 lists the CCD/bridged CCD results taken into CALR calculation and the new CALR and uCALR results for a pair of channels of ESs which include [Rx1-Rx1] link. In Table 10-1, values in column $CCD_{avg}(k_1i,MOB@k_1)$ and $u CCD_{avg}(k_1i,MOB@k_1)$ are obtained from Table 7-47, and values in column Bridged $CCD_{avg}(k_2i,MOB@k_2)$ and uBridged $CCD_{avg}(k_2i,MOB@k_2)$ are taken from Table 9-1 to Table 9-19 accordingly. $CALR_{MeasB}(k_1i,k_2j)$ is the new CALR value for a pair of ESs calculated by equation (46) / equation (47), and $u CALR_{MeasB}(k_1i,k_2j)$ is the 1-σ uncertainty of $CALR_{MeasB}(k_1i,k_2j)$.

Table 10-1 List of ES pairs of [Rx1-Rx1] SATRE channels in baseline-mode measurements

TW Pair		CCD_{avg} $(k_1i,MOB@k_1)$	uCCD $(k_1i,MOB@k_1)$	Bridged CCD_{avg} $(k_2j,MOB@k_2)$	uBridged CCD $(k_2j,MOB@k_2)$	$CALR_{MeasB}$ (k_1i,k_2j)	$u CALR_{MeasB}$ (k_1i,k_2j)
<k_1i>	<k_2j>	Unit: ns	Unit: ns	Unit: ns	Unit: ns	Unit: ns	Unit: ns
TIM01	PL01	-742.509	0.107	-716.215	0.053	-16.524	0.444
TIM01	PTB05	-742.509	0.107	-712.637	0.065	-35.342	0.397
PTB05	TIM01	-712.503	0.070	-742.282	0.060	35.249	0.353
TIM01	PTB04	-742.509	0.107	-729.060	0.048	-18.919	0.396

PTB04	TIM01	-729.108	0.067	-742.689	0.068	19.051	0.356
TIM01	VSL01	-742.509	0.107	-721.038	0.134	-36.341	0.466
VSL01	TIM01	-721.166	0.077	-742.552	0.076	36.256	0.371
TIM01	LTFB01	-742.509	0.107	-715.257	0.109	-29.902	0.454
TIM01	ROA01	-742.509	0.107	-703.622	0.187	-52.367	0.487
ROA01	TIM01	-703.592	0.175	-742.406	0.106	52.294	0.483
TIM01	OP01	-742.509	0.107	-7862.161	0.085	7107.052	0.401
OP01	TIM01	-7862.162	0.077	-742.458	0.068	-7107.104	0.356
TIM01	NPL02	-742.509	0.107	-10.560	0.165	-754.379	0.548
NPL02	TIM01	-10.483	0.187	-742.298	0.095	754.245	0.518
TIM01	SP01	-742.509	0.107	-728.879	0.051	-28.430	0.413
SP01	TIM01	-728.648	0.046	-742.208	0.082	28.360	0.374
TIM01	IT01	-742.509	0.107	-718.699	0.074	-19.060	0.639
IT01	TIM01	-718.801	0.074	-742.538	0.151	18.987	0.648
TIM01	CH01	-742.509	0.107	-718.107	0.057	-23.672	0.411
CH01	TIM01	-718.221	0.069	-742.723	0.052	23.772	0.368
PL01	PTB05	-716.164	0.040	-712.507	0.048	-18.897	0.397
PTB05	PL01	-712.503	0.070	-716.125	0.027	18.862	0.399
PL01	PTB04	-716.164	0.040	-728.742	0.075	-2.662	0.404
PTB04	PL01	-729.108	0.067	-716.592	0.061	2.724	0.405
PL01	ROA01	-716.164	0.040	-703.716	0.084	-35.698	0.419
ROA01	PL01	-703.592	0.175	-716.134	0.075	35.792	0.479
PL01	OP01	-716.164	0.040	-7861.999	0.081	7123.465	0.403
PL01	CH01	-716.164	0.040	-717.845	0.020	-7.359	0.410
CH01	PL01	-718.221	0.069	-716.563	0.167	7.382	0.474
PTB05	PTB04	-712.503	0.070	-728.269	0.065	15.766	0.352
PTB04	PTB05	-729.108	0.067	-713.404	0.103	-15.704	0.395
PTB05	VSL01	-712.503	0.070	-720.939	0.089	-0.964	0.369
VSL01	PTB05	-721.166	0.077	-712.727	0.083	0.961	0.369
PTB05	LTFB01	-712.503	0.070	-715.094	0.091	5.411	0.362
PTB05	ROA01	-712.503	0.070	-703.650	0.110	-16.863	0.411
ROA01	PTB05	-703.592	0.175	-712.518	0.163	16.936	0.496
PTB05	OP01	-712.503	0.070	-7861.711	0.083	7142.078	0.354
OP01	PTB05	-7862.162	0.077	-712.940	0.060	-7142.092	0.350
PTB05	NPL02	-712.503	0.070	-10.726	0.209	-718.737	0.520
NPL02	PTB05	-10.483	0.187	-712.334	0.141	718.811	0.560
PTB05	SP01	-712.503	0.070	-729.078	0.060	7.245	0.370
SP01	PTB05	-728.648	0.046	-712.078	0.096	-7.240	0.373
PTB05	IT01	-712.503	0.070	-718.453	0.056	16.170	0.609
IT01	PTB05	-718.801	0.074	-712.771	0.038	-16.250	0.608

PTB05	CH01	-712.503	0.070	-717.391	0.059	11.088	0.366
CH01	PTB05	-718.221	0.069	-713.339	0.075	-11.082	0.369
PTB04	VSL01	-729.108	0.067	-721.429	0.107	-17.079	0.409
VSL01	PTB04	-721.166	0.077	-728.865	0.109	17.099	0.411
PTB04	LTFB01	-729.108	0.067	-715.512	0.098	-10.776	0.366
PTB04	ROA01	-729.108	0.067	-703.863	0.396	-33.255	0.561
ROA01	PTB04	-703.592	0.175	-728.863	0.131	33.281	0.488
PTB04	OP01	-729.108	0.067	-7862.432	0.093	7126.194	0.358
OP01	PTB04	-7862.162	0.077	-728.830	0.048	-7126.202	0.351
PTB04	NPL02	-729.108	0.067	-11.055	0.156	-735.013	0.503
NPL02	PTB04	-10.483	0.187	-728.728	0.094	735.205	0.517
SP01	PTB04	-728.648	0.046	-728.523	0.100	9.205	0.410
PTB04	IT01	-729.108	0.067	-718.830	0.082	-0.058	0.613
IT01	PTB04	-718.801	0.074	-729.118	0.075	0.097	0.613
PTB04	CH01	-729.108	0.067	-718.013	0.117	-4.895	0.414
CH01	PTB04	-718.221	0.069	-729.296	0.099	4.875	0.377
VSL01	ROA01	-721.166	0.077	-703.748	0.209	-16.028	0.460
ROA01	VSL01	-703.592	0.175	-721.075	0.181	16.093	0.512
VSL01	OP01	-721.166	0.077	-7862.110	0.112	7143.214	0.410
OP01	VSL01	-7862.162	0.077	-721.218	0.123	-7143.214	0.413
VSL01	NPL02	-721.166	0.077	-10.641	0.257	-718.085	0.552
NPL02	VSL01	-10.483	0.187	-721.020	0.120	718.097	0.564
VSL01	SP01	-721.166	0.077	-729.046	0.106	7.950	0.426
SP01	VSL01	-728.648	0.046	-720.814	0.133	-7.904	0.429
VSL01	IT01	-721.166	0.077	-718.710	0.199	17.164	0.667
IT01	VSL01	-718.801	0.074	-721.276	0.121	-17.145	0.647
VSL01	CH01	-721.166	0.077	-717.925	0.137	12.359	0.432
CH01	VSL01	-718.221	0.069	-721.454	0.118	-12.367	0.425
LTFB01	ROA01	-715.242	0.135	-703.728	0.155	-22.344	0.485
ROA01	LTFB01	-703.592	0.175	-715.151	0.105	22.389	0.485
LTFB01	OP01	-715.242	0.135	-7862.061	0.184	7136.869	0.482
OP01	LTFB01	-7862.162	0.077	-715.390	0.110	-7136.822	0.402
LTFB01	IT01	-715.242	0.135	-718.588	0.089	10.746	0.648
IT01	LTFB01	-718.801	0.074	-715.347	0.082	-10.854	0.616
LTFB01	CH01	-715.242	0.135	-717.981	0.091	6.119	0.427
CH01	LTFB01	-718.221	0.069	-715.538	0.091	-6.063	0.379
ROA01	OP01	-703.592	0.175	-7861.889	0.139	7159.177	0.488
OP01	ROA01	-7862.162	0.077	-703.781	0.222	-7159.261	0.455
ROA01	NPL02	-703.592	0.175	-10.443	0.196	-702.099	0.584
NPL02	ROA01	-10.483	0.187	-703.612	0.181	702.079	0.582

ROA01	SP01	-703.592	0.175	-728.880	0.093	23.968	0.454
SP01	ROA01	-728.648	0.046	-703.468	0.096	-23.860	0.391
ROA01	IT01	-703.592	0.175	-718.575	0.089	33.213	0.664
IT01	ROA01	-718.801	0.074	-703.743	0.231	-33.288	0.679
ROA01	CH01	-703.592	0.175	-717.857	0.161	28.475	0.507
CH01	ROA01	-718.221	0.069	-703.889	0.371	-28.542	0.554
OP01	NPL02	-7862.162	0.077	-10.824	0.173	-7861.168	0.508
NPL02	OP01	-10.483	0.187	-7861.817	0.139	7861.164	0.559
OP01	SP01	-7862.162	0.077	-729.206	0.048	-7135.156	0.369
SP01	OP01	-728.648	0.046	-7861.572	0.077	7135.124	0.369
OP01	IT01	-7862.162	0.077	-718.736	0.057	-7126.076	0.610
IT01	OP01	-718.801	0.074	-7862.228	0.100	7126.077	0.636
OP01	CH01	-7862.162	0.077	-717.975	0.026	-7130.857	0.364
CH01	OP01	-718.221	0.069	-7862.592	0.095	7131.041	0.373
NPL02	SP01	-10.483	0.187	-728.885	0.093	726.032	0.530
SP01	NPL02	-728.648	0.046	-10.270	0.154	-726.008	0.513
NPL02	IT01	-10.483	0.187	-718.568	0.080	735.265	0.716
IT01	NPL02	-718.801	0.074	-10.695	0.195	-735.286	0.718
NPL02	CH01	-10.483	0.187	-717.868	0.113	730.545	0.564
CH01	NPL02	-718.221	0.069	-10.998	0.198	-730.383	0.528
SP01	IT01	-728.648	0.046	-718.457	0.078	9.359	0.621
IT01	SP01	-718.801	0.074	-729.000	0.097	-9.351	0.627
SP01	CH01	-728.648	0.046	-717.610	0.065	4.492	0.383
CH01	SP01	-718.221	0.069	-729.202	0.140	-4.549	0.437
IT01	CH01	-718.801	0.074	-718.146	0.065	-4.675	0.620
CH01	IT01	-718.221	0.069	-718.869	0.136	4.668	0.651

Table 10-2 lists the uncertainty categories of Rx1 channel pairs in baseline-mode measurements, which lead to the results of uCALR$_{MeasB}$ (k_1i,k_2j) in Table 10-1. The uncertainty categories are defined in Section 6.3.

Table 10-2 List of uCALR$_{MeasB}$ uncertainty categories of SATRE Rx1 channel pairs in baseline-mode measurements

TW Pair		Type A Uncertainties		Type B Uncertainties					
		ua,1	ua,2	ub	ub,I	ub,II	ub, III	ub,6 (k_1i,k_2j)	ub, IV
<k_1i>	<k_2j>	Unit: ns	Unit: ns	Unit: ns	Unit: ns	Unit: ns	Unit: ns	Unit: ns	Unit: ns
TIM01	PL01	0.107	0.053	0.427	0.192	0.040	0.306	0.210	0.224
TIM01	PTB05	0.107	0.065	0.376	0.192	0.040	0.230	0.059	0.224
PTB05	TIM01	0.070	0.060	0.340	0.192	0.040	0.230	0.059	0.156
TIM01	PTB04	0.107	0.048	0.379	0.192	0.040	0.234	0.072	0.224
PTB04	TIM01	0.067	0.068	0.343	0.192	0.040	0.234	0.072	0.156

TIM01	VSL01	0.107	0.134	0.434	0.192	0.040	0.251	0.117	0.294
VSL01	TIM01	0.077	0.076	0.355	0.192	0.040	0.251	0.117	0.156
TIM01	LTFB01	0.107	0.109	0.428	0.192	0.040	0.240	0.091	0.294
TIM01	ROA01	0.107	0.187	0.437	0.192	0.040	0.257	0.128	0.294
ROA01	TIM01	0.175	0.106	0.437	0.192	0.040	0.257	0.128	0.294
TIM01	OP01	0.107	0.085	0.377	0.192	0.040	0.230	0.059	0.224
OP01	TIM01	0.077	0.068	0.340	0.192	0.040	0.230	0.059	0.156
TIM01	NPL02	0.107	0.165	0.511	0.192	0.040	0.369	0.294	0.294
NPL02	TIM01	0.187	0.095	0.474	0.192	0.040	0.369	0.294	0.224
TIM01	SP01	0.107	0.051	0.396	0.192	0.040	0.261	0.136	0.224
SP01	TIM01	0.046	0.082	0.362	0.192	0.040	0.261	0.136	0.156
TIM01	IT01	0.107	0.074	0.626	0.192	0.040	0.550	0.503	0.224
IT01	TIM01	0.074	0.151	0.626	0.192	0.040	0.550	0.503	0.224
TIM01	CH01	0.107	0.057	0.393	0.192	0.040	0.256	0.126	0.224
CH01	TIM01	0.069	0.052	0.358	0.192	0.040	0.256	0.126	0.156
PL01	PTB05	0.040	0.048	0.392	0.192	0.040	0.302	0.204	0.156
PTB05	PL01	0.070	0.027	0.392	0.192	0.040	0.302	0.204	0.156
PL01	PTB04	0.040	0.075	0.395	0.192	0.040	0.305	0.208	0.156
PTB04	PL01	0.067	0.061	0.395	0.192	0.040	0.305	0.208	0.156
PL01	ROA01	0.040	0.084	0.409	0.192	0.040	0.323	0.234	0.156
ROA01	PL01	0.175	0.075	0.439	0.192	0.040	0.323	0.234	0.224
PL01	OP01	0.040	0.081	0.392	0.192	0.040	0.302	0.204	0.156
PL01	CH01	0.040	0.020	0.408	0.192	0.040	0.322	0.232	0.156
CH01	PL01	0.069	0.167	0.438	0.192	0.040	0.322	0.232	0.224
PTB05	PTB04	0.070	0.065	0.339	0.192	0.040	0.228	0.050	0.156
PTB04	PTB05	0.067	0.103	0.375	0.192	0.040	0.228	0.050	0.224
PTB05	VSL01	0.070	0.089	0.351	0.192	0.040	0.246	0.105	0.156
VSL01	PTB05	0.077	0.083	0.351	0.192	0.040	0.246	0.105	0.156
PTB05	LTFB01	0.070	0.091	0.343	0.192	0.040	0.235	0.075	0.156
PTB05	ROA01	0.070	0.110	0.390	0.192	0.040	0.252	0.118	0.224
ROA01	PTB05	0.175	0.163	0.434	0.192	0.040	0.252	0.118	0.294
PTB05	OP01	0.070	0.083	0.337	0.192	0.040	0.225	0.030	0.156
OP01	PTB05	0.077	0.060	0.337	0.192	0.040	0.225	0.030	0.156
PTB05	NPL02	0.070	0.209	0.471	0.192	0.040	0.365	0.290	0.224
NPL02	PTB05	0.187	0.141	0.508	0.192	0.040	0.365	0.290	0.294
PTB05	SP01	0.070	0.060	0.358	0.192	0.040	0.256	0.126	0.156
SP01	PTB05	0.046	0.096	0.358	0.192	0.040	0.256	0.126	0.156
PTB05	IT01	0.070	0.056	0.602	0.192	0.040	0.548	0.500	0.156
IT01	PTB05	0.074	0.038	0.602	0.192	0.040	0.548	0.500	0.156
PTB05	CH01	0.070	0.059	0.354	0.192	0.040	0.251	0.115	0.156

CH01	PTB05	0.069	0.075	0.354	0.192	0.040	0.251	0.115	0.156
PTB04	VSL01	0.067	0.107	0.389	0.192	0.040	0.250	0.113	0.224
VSL01	PTB04	0.077	0.109	0.389	0.192	0.040	0.250	0.113	0.224
PTB04	LTFB01	0.067	0.098	0.346	0.192	0.040	0.239	0.085	0.156
PTB04	ROA01	0.067	0.396	0.392	0.192	0.040	0.255	0.125	0.224
ROA01	PTB04	0.175	0.131	0.436	0.192	0.040	0.255	0.125	0.294
PTB04	OP01	0.067	0.093	0.339	0.192	0.040	0.228	0.051	0.156
OP01	PTB04	0.077	0.048	0.339	0.192	0.040	0.228	0.051	0.156
PTB04	NPL02	0.067	0.156	0.473	0.192	0.040	0.368	0.293	0.224
NPL02	PTB04	0.187	0.094	0.473	0.192	0.040	0.368	0.293	0.224
SP01	PTB04	0.046	0.100	0.395	0.192	0.040	0.259	0.132	0.224
PTB04	IT01	0.067	0.082	0.604	0.192	0.040	0.549	0.502	0.156
IT01	PTB04	0.074	0.075	0.604	0.192	0.040	0.549	0.502	0.156
PTB04	CH01	0.067	0.117	0.391	0.192	0.040	0.254	0.122	0.224
CH01	PTB04	0.069	0.099	0.357	0.192	0.040	0.254	0.122	0.156
VSL01	ROA01	0.077	0.209	0.403	0.192	0.040	0.271	0.155	0.224
ROA01	VSL01	0.175	0.181	0.446	0.192	0.040	0.271	0.155	0.294
VSL01	OP01	0.077	0.112	0.386	0.192	0.040	0.246	0.105	0.224
OP01	VSL01	0.077	0.123	0.386	0.192	0.040	0.246	0.105	0.224
VSL01	NPL02	0.077	0.257	0.482	0.192	0.040	0.379	0.307	0.224
NPL02	VSL01	0.187	0.120	0.518	0.192	0.040	0.379	0.307	0.294
VSL01	SP01	0.077	0.106	0.405	0.192	0.040	0.275	0.161	0.224
SP01	VSL01	0.046	0.133	0.405	0.192	0.040	0.275	0.161	0.224
VSL01	IT01	0.077	0.199	0.632	0.192	0.040	0.557	0.510	0.224
IT01	VSL01	0.074	0.121	0.632	0.192	0.040	0.557	0.510	0.224
VSL01	CH01	0.077	0.137	0.402	0.192	0.040	0.270	0.153	0.224
CH01	VSL01	0.069	0.118	0.402	0.192	0.040	0.270	0.153	0.224
LTFB01	ROA01	0.135	0.155	0.440	0.192	0.040	0.261	0.137	0.294
ROA01	LTFB01	0.175	0.105	0.440	0.192	0.040	0.261	0.137	0.294
LTFB01	OP01	0.135	0.184	0.425	0.192	0.040	0.235	0.075	0.294
OP01	LTFB01	0.077	0.110	0.379	0.192	0.040	0.235	0.075	0.224
LTFB01	IT01	0.135	0.089	0.627	0.192	0.040	0.552	0.505	0.224
IT01	LTFB01	0.074	0.082	0.606	0.192	0.040	0.552	0.505	0.156
LTFB01	CH01	0.135	0.091	0.395	0.192	0.040	0.260	0.134	0.224
CH01	LTFB01	0.069	0.091	0.361	0.192	0.040	0.260	0.134	0.156
ROA01	OP01	0.175	0.139	0.434	0.192	0.040	0.252	0.118	0.294
OP01	ROA01	0.077	0.222	0.390	0.192	0.040	0.252	0.118	0.224
ROA01	NPL02	0.175	0.196	0.521	0.192	0.040	0.383	0.311	0.294
NPL02	ROA01	0.187	0.181	0.521	0.192	0.040	0.383	0.311	0.294
ROA01	SP01	0.175	0.093	0.409	0.192	0.040	0.280	0.170	0.224

SP01	ROA01	0.046	0.096	0.376	0.192	0.040	0.280	0.170	0.156
ROA01	IT01	0.175	0.089	0.634	0.192	0.040	0.560	0.513	0.224
IT01	ROA01	0.074	0.231	0.634	0.192	0.040	0.560	0.513	0.224
ROA01	CH01	0.175	0.161	0.448	0.192	0.040	0.275	0.162	0.294
CH01	ROA01	0.069	0.371	0.406	0.192	0.040	0.275	0.162	0.224
OP01	NPL02	0.077	0.173	0.471	0.192	0.040	0.366	0.290	0.224
NPL02	OP01	0.187	0.139	0.508	0.192	0.040	0.366	0.290	0.294
OP01	SP01	0.077	0.048	0.358	0.192	0.040	0.256	0.126	0.156
SP01	OP01	0.046	0.077	0.358	0.192	0.040	0.256	0.126	0.156
OP01	IT01	0.077	0.057	0.602	0.192	0.040	0.548	0.500	0.156
IT01	OP01	0.074	0.100	0.624	0.192	0.040	0.548	0.500	0.224
OP01	CH01	0.077	0.026	0.354	0.192	0.040	0.251	0.115	0.156
CH01	OP01	0.069	0.095	0.354	0.192	0.040	0.251	0.115	0.156
NPL02	SP01	0.187	0.093	0.487	0.192	0.040	0.385	0.314	0.224
SP01	NPL02	0.046	0.154	0.487	0.192	0.040	0.385	0.314	0.224
NPL02	IT01	0.187	0.080	0.687	0.192	0.040	0.619	0.578	0.224
IT01	NPL02	0.074	0.195	0.687	0.192	0.040	0.619	0.578	0.224
NPL02	CH01	0.187	0.113	0.520	0.192	0.040	0.382	0.310	0.294
CH01	NPL02	0.069	0.198	0.484	0.192	0.040	0.382	0.310	0.224
SP01	IT01	0.046	0.078	0.615	0.192	0.040	0.561	0.515	0.156
IT01	SP01	0.074	0.097	0.615	0.192	0.040	0.561	0.515	0.156
SP01	CH01	0.046	0.065	0.375	0.192	0.040	0.279	0.168	0.156
CH01	SP01	0.069	0.140	0.408	0.192	0.040	0.279	0.168	0.224
IT01	CH01	0.074	0.065	0.612	0.192	0.040	0.559	0.513	0.156
CH01	IT01	0.069	0.136	0.633	0.192	0.040	0.559	0.513	0.224

Table 10-3 lists the CCD/bridged CCD results taken into CALR calculation and the new CALR and uCALR results for a pair of channels of ESs which include [Rx1-Rx2] & [Rx2-Rx2] links. In Table 10-3, values in column $CCD_{avg}(k_1i,MOB@k_1)$ and $u CCD_{avg}(k_1i,MOB@k_1)$ are obtained from Table 7-47, and values in column Bridged $CCD_{avg}(k_2i,MOB@k_2)$ and uBridged $CCD_{avg}(k_2i,MOB@k_2)$ are taken from Table 9-1 to Table 9-19 accordingly. $CALR_{MeasB}(k_1i,k_2j)$ is the new CALR value for a pair of ESs calculated by equation (46) / equation (47), and $u CALR_{MeasB}(k_1i,k_2j)$ is the 1-σ uncertainty of $CALR_{MeasB}(k_1i,k_2j)$.

Table 10-3 List of ES pairs of [Rx1-Rx2] & [Rx2-Rx2] SATRE channels in baseline-mode measurements

TW Pair		CCD_{avg} $(k_1i,MOB@k_1)$	uCCD $(k_1i,MOB@k_1)$	Bridged CCD_{avg} $(k_2j,MOB@k_2)$	uBridged CCD $(k_2j,MOB@k_2)$	$CALR_{MeasB}$ (k_1i,k_2j)	$u CALR_{MeasB}$ (k_1i,k_2j)
$<k_1i>$	$<k_2j>$	Unit: ns	Unit: ns	Unit: ns	Unit: ns	Unit: ns	Unit: ns
TIM01	PTB25	-742.509	0.107	-717.659	0.081	-30.320	0.400
PTB25	TIM01	-717.355	0.069	-742.028	0.044	30.143	0.350
TIM01	VSL21	-742.509	0.107	-721.113	0.139	-36.266	0.468
TIM01	ROA21	-742.509	0.107	-703.636	0.175	-52.353	0.483

ROA21	TIM01	-703.674	0.178	-742.297	0.105	52.103	0.483
TIM01	SP21	-742.509	0.107	-731.223	0.080	-26.086	0.418
SP21	TIM01	-731.313	0.073	-742.667	0.087	26.154	0.379
TIM01	IT21	-742.509	0.107	-716.171	0.072	-21.588	0.639
IT21	TIM01	-716.185	0.074	-742.264	0.084	21.329	0.615
TIM01	CH21	-742.509	0.107	-724.616	0.040	-17.163	0.409
CH21	TIM01	-724.667	0.036	-742.387	0.060	16.990	0.365
TIM21	PTB05	-746.240	0.054	-712.451	0.059	-39.259	0.350
PTB05	TIM21	-712.503	0.070	-746.189	0.049	39.156	0.351
TIM21	PTB25	-746.240	0.054	-717.469	0.076	-34.241	0.353
PTB25	TIM21	-717.355	0.069	-745.930	0.036	34.045	0.349
TIM21	PTB04	-746.240	0.054	-728.943	0.050	-22.767	0.351
PTB04	TIM21	-729.108	0.067	-746.478	0.044	22.840	0.352
TIM21	VSL01	-746.240	0.054	-720.926	0.132	-40.184	0.415
VSL01	TIM21	-721.166	0.077	-746.368	0.063	40.072	0.369
TIM21	VSL21	-746.240	0.054	-721.002	0.136	-40.108	0.416
TIM21	LTFB01	-746.240	0.054	-715.088	0.115	-33.802	0.403
TIM21	ROA01	-746.240	0.054	-703.508	0.151	-56.212	0.425
ROA01	TIM21	-703.592	0.175	-746.136	0.105	56.024	0.482
TIM21	ROA21	-746.240	0.054	-703.523	0.135	-56.197	0.419
ROA21	TIM21	-703.674	0.178	-746.009	0.129	55.815	0.489
TIM21	OP01	-746.240	0.054	-7861.910	0.095	7103.070	0.357
OP01	TIM21	-7862.162	0.077	-746.335	0.067	-7103.227	0.355
TIM21	NPL02	-746.240	0.054	-10.415	0.129	-758.255	0.494
NPL02	TIM21	-10.483	0.187	-746.137	0.098	758.084	0.519
TIM21	SP01	-746.240	0.054	-728.608	0.045	-32.432	0.368
SP01	TIM21	-728.648	0.046	-746.094	0.078	32.246	0.373
TIM21	SP21	-746.240	0.054	-730.950	0.070	-30.090	0.372
SP21	TIM21	-731.313	0.073	-746.552	0.085	30.039	0.379
TIM21	IT01	-746.240	0.054	-718.590	0.068	-22.900	0.611
IT01	TIM21	-718.801	0.074	-746.398	0.148	22.847	0.647
TIM21	IT21	-746.240	0.054	-716.064	0.059	-25.426	0.610
IT21	TIM21	-716.185	0.074	-746.113	0.077	25.178	0.614
TIM21	CH01	-746.240	0.054	-718.007	0.048	-27.503	0.365
CH01	TIM21	-718.221	0.069	-746.513	0.040	27.562	0.367
TIM21	CH21	-746.240	0.054	-724.519	0.047	-20.991	0.365
CH21	TIM21	-724.667	0.036	-746.173	0.044	20.776	0.362
PL01	PTB25	-716.164	0.040	-717.662	0.049	-13.742	0.397
PL01	ROA21	-716.164	0.040	-703.646	0.091	-35.768	0.421
ROA21	PL01	-703.674	0.178	-716.016	0.066	35.592	0.479

PL01	CH21	-716.164	0.040	-724.531	0.041	-0.673	0.412
CH21	PL01	-724.667	0.036	-716.108	0.178	0.481	0.475
PTB05	VSL21	-712.503	0.070	-721.023	0.083	-0.880	0.368
PTB05	ROA21	-712.503	0.070	-703.488	0.102	-17.025	0.409
ROA21	PTB05	-703.674	0.178	-712.445	0.220	16.781	0.518
PTB05	SP21	-712.503	0.070	-730.062	0.062	8.229	0.370
SP21	PTB05	-731.313	0.073	-713.606	0.115	-8.377	0.415
PTB05	IT21	-712.503	0.070	-716.043	0.067	13.760	0.610
IT21	PTB05	-716.185	0.074	-712.410	0.033	-13.995	0.608
PTB05	CH21	-712.503	0.070	-724.376	0.044	18.073	0.364
CH21	PTB05	-724.667	0.036	-712.558	0.065	-18.309	0.362
PTB25	PTB04	-717.355	0.069	-727.762	0.051	10.407	0.350
PTB04	PTB25	-729.108	0.067	-718.760	0.123	-10.348	0.401
PTB25	VSL01	-717.355	0.069	-720.595	0.076	-6.160	0.366
VSL01	PTB25	-721.166	0.077	-717.878	0.091	6.112	0.371
PTB25	VSL21	-717.355	0.069	-720.680	0.081	-6.075	0.367
PTB25	LTFB01	-717.355	0.069	-714.716	0.111	0.181	0.401
PTB25	ROA01	-717.355	0.069	-703.420	0.083	-21.945	0.371
ROA01	PTB25	-703.592	0.175	-717.512	0.279	21.930	0.545
PTB25	ROA21	-717.355	0.069	-703.258	0.093	-22.107	0.374
ROA21	PTB25	-703.674	0.178	-717.437	0.343	21.773	0.581
PTB25	OP01	-717.355	0.069	-7861.274	0.093	7136.789	0.356
OP01	PTB25	-7862.162	0.077	-718.231	0.074	-7136.801	0.353
PTB25	NPL02	-717.355	0.069	-10.450	0.178	-723.865	0.509
NPL02	PTB25	-10.483	0.187	-717.544	0.146	724.021	0.561
PTB25	SP01	-717.355	0.069	-728.824	0.074	2.139	0.372
SP01	PTB25	-728.648	0.046	-717.224	0.106	-2.094	0.409
PTB25	SP21	-717.355	0.069	-729.823	0.092	3.138	0.376
SP21	PTB25	-731.313	0.073	-718.755	0.131	-3.228	0.420
PTB25	IT01	-717.355	0.069	-718.182	0.060	11.047	0.609
IT01	PTB25	-718.801	0.074	-717.826	0.046	-11.195	0.609
PTB25	IT21	-717.355	0.069	-715.772	0.070	8.637	0.610
IT21	PTB25	-716.185	0.074	-717.464	0.038	-8.941	0.608
PTB25	CH01	-717.355	0.069	-717.029	0.060	5.874	0.366
CH01	PTB25	-718.221	0.069	-718.502	0.073	-5.919	0.368
PTB25	CH21	-717.355	0.069	-724.012	0.052	12.857	0.365
CH21	PTB25	-724.667	0.036	-717.720	0.062	-13.147	0.361
PTB04	VSL21	-729.108	0.067	-721.501	0.108	-17.007	0.409
PTB04	ROA21	-729.108	0.067	-703.729	0.377	-33.389	0.548
ROA21	PTB04	-703.674	0.178	-728.856	0.113	33.192	0.484

SP21	PTB04	-731.313	0.073	-730.059	0.161	8.076	0.432
PTB04	IT21	-729.108	0.067	-716.401	0.076	-2.487	0.612
IT21	PTB04	-716.185	0.074	-728.799	0.056	2.394	0.611
PTB04	CH21	-729.108	0.067	-724.932	0.069	2.024	0.369
CH21	PTB04	-724.667	0.036	-728.738	0.065	-2.129	0.364
VSL01	ROA21	-721.166	0.077	-703.689	0.205	-16.087	0.459
ROA21	VSL01	-703.674	0.178	-720.982	0.223	15.918	0.529
VSL01	SP21	-721.166	0.077	-730.741	0.105	9.645	0.426
VSL01	IT21	-721.166	0.077	-716.250	0.191	14.704	0.664
IT21	VSL01	-716.185	0.074	-720.951	0.129	-14.854	0.649
VSL01	CH21	-721.166	0.077	-724.675	0.144	19.109	0.434
CH21	VSL01	-724.667	0.036	-721.036	0.123	-19.231	0.422
ROA01	VSL21	-703.592	0.175	-721.177	0.189	16.195	0.515
ROA21	VSL21	-703.674	0.178	-721.083	0.233	16.019	0.533
OP01	VSL21	-7862.162	0.077	-721.290	0.120	-7143.142	0.412
NPL02	VSL21	-10.483	0.187	-721.116	0.127	718.193	0.565
SP01	VSL21	-728.648	0.046	-720.933	0.132	-7.785	0.429
IT01	VSL21	-718.801	0.074	-721.356	0.111	-17.065	0.646
IT21	VSL21	-716.185	0.074	-721.032	0.124	-14.773	0.648
CH01	VSL21	-718.221	0.069	-721.517	0.167	-12.304	0.441
CH21	VSL21	-724.667	0.036	-721.104	0.174	-19.163	0.440
LTFB01	ROA21	-715.242	0.135	-703.684	0.145	-22.388	0.482
ROA21	LTFB01	-703.674	0.178	-715.080	0.076	22.236	0.441
LTFB01	IT21	-715.242	0.135	-716.075	0.065	8.233	0.645
IT21	LTFB01	-716.185	0.074	-715.068	0.078	-8.517	0.616
LTFB01	CH21	-715.242	0.135	-724.653	0.063	12.791	0.422
CH21	LTFB01	-724.667	0.036	-715.070	0.111	-12.977	0.412
SP21	ROA01	-731.313	0.073	-704.093	0.167	-25.900	0.448
ROA01	IT21	-703.592	0.175	-716.069	0.082	30.707	0.663
IT21	ROA01	-716.185	0.074	-703.499	0.164	-30.916	0.659
ROA01	CH21	-703.592	0.175	-724.482	0.069	35.100	0.447
CH21	ROA01	-724.667	0.036	-703.627	0.200	-35.250	0.454
ROA21	OP01	-703.674	0.178	-7861.863	0.097	7159.069	0.440
OP01	ROA21	-7862.162	0.077	-703.682	0.222	-7159.360	0.455
ROA21	NPL02	-703.674	0.178	-10.335	0.217	-702.289	0.592
NPL02	ROA21	-10.483	0.187	-703.553	0.191	702.020	0.586
ROA21	SP01	-703.674	0.178	-728.761	0.118	23.767	0.499
SP01	ROA21	-728.648	0.046	-703.427	0.094	-23.901	0.390
SP21	ROA21	-731.313	0.073	-704.010	0.247	-25.983	0.483
ROA21	IT01	-703.674	0.178	-718.528	0.072	33.084	0.662

IT01	ROA21	-718.801	0.074	-703.736	0.220	-33.295	0.675
ROA21	IT21	-703.674	0.178	-716.022	0.075	30.578	0.663
IT21	ROA21	-716.185	0.074	-703.492	0.155	-30.923	0.657
ROA21	CH01	-703.674	0.178	-717.854	0.151	28.390	0.505
CH01	ROA21	-718.221	0.069	-703.815	0.368	-28.616	0.552
ROA21	CH21	-703.674	0.178	-724.489	0.072	35.025	0.449
CH21	ROA21	-724.667	0.036	-703.553	0.198	-35.324	0.453
OP01	SP21	-7862.162	0.077	-730.645	0.048	-7133.717	0.369
SP21	OP01	-731.313	0.073	-7862.800	0.068	7133.687	0.372
OP01	IT21	-7862.162	0.077	-716.280	0.066	-7128.532	0.611
IT21	OP01	-716.185	0.074	-7861.937	0.092	7128.402	0.614
OP01	CH21	-7862.162	0.077	-724.878	0.035	-7123.954	0.364
CH21	OP01	-724.667	0.036	-7861.973	0.084	7123.976	0.366
NPL02	SP21	-10.483	0.187	-731.008	0.104	728.155	0.565
SP21	NPL02	-731.313	0.073	-11.022	0.169	-727.921	0.521
NPL02	IT21	-10.483	0.187	-715.993	0.087	732.690	0.717
IT21	NPL02	-716.185	0.074	-10.476	0.176	-732.889	0.713
NPL02	CH21	-10.483	0.187	-724.453	0.083	737.130	0.526
CH21	NPL02	-724.667	0.036	-10.631	0.210	-737.196	0.529
SP01	IT21	-728.648	0.046	-715.945	0.063	6.847	0.620
IT21	SP01	-716.185	0.074	-728.779	0.100	-6.956	0.647
SP01	CH21	-728.648	0.046	-724.255	0.139	11.137	0.433
CH21	SP01	-724.667	0.036	-728.847	0.094	-11.350	0.388
SP21	IT01	-731.313	0.073	-719.180	0.058	7.417	0.622
IT01	SP21	-718.801	0.074	-730.948	0.071	-7.403	0.623
SP21	IT21	-731.313	0.073	-716.671	0.070	4.908	0.623
IT21	SP21	-716.185	0.074	-730.730	0.070	-5.005	0.623
SP21	CH01	-731.313	0.073	-718.670	0.061	2.887	0.387
CH01	SP21	-718.221	0.069	-730.792	0.051	-2.959	0.385
CH21	SP21	-724.667	0.036	-730.437	0.058	-9.760	0.381
IT01	CH21	-718.801	0.074	-724.791	0.060	1.970	0.620
CH21	IT01	-724.667	0.036	-718.547	0.142	-2.100	0.650
IT21	CH01	-716.185	0.074	-717.858	0.044	-2.347	0.618
CH01	IT21	-718.221	0.069	-716.409	0.128	2.208	0.650
IT21	CH21	-716.185	0.074	-724.502	0.039	4.297	0.618
CH21	IT21	-724.667	0.036	-716.088	0.127	-4.559	0.647

10.1.2 Baseline-mode final calibration results of SATRE TW links

Based on the calibration results in Table 10-1 and Table 10-3, the final CALR values of TW links are listed in Table 10-4 and Table 10-5, respectively. For a pair of SATRE channels in remote, the calibration result of $CALR_{MeasB}(k_1i,k_2j)$

is taken as the final CALR value when only Measurement B1 plus Measurement B2 or Measurement B3 plus Measurement B4 existed. When all the Measurement B1-Measurement B4 are available, the final CALR value is computed via equation (48). In this case, the maximum Type B uncertainty of both calibration results is taken as the final Type B uncertainty ub of the TW link.

Table 10-4 List of new CALR and uCALR values of [Rx1-Rx1] SATRE channels using baseline-mode calibration

TW Link		CALR (k_1i,k_2j)	uCALR (k_1i,k_2j)	Type A & Type B Uncertainties	
				ua	ub
<k_1i>	<k_2j>	Unit: ns	Unit: ns	Unit: ns	Unit: ns
TIM01	PL01	-16.524	0.444	0.119	0.427
TIM01	PTB05	-35.296	0.384	0.078	0.376
TIM01	PTB04	-18.985	0.386	0.076	0.379
TIM01	VSL01	-36.298	0.446	0.101	0.434
TIM01	LTFB01	-29.902	0.454	0.153	0.428
TIM01	ROA01	-52.331	0.462	0.149	0.437
TIM01	OP01	7107.078	0.386	0.085	0.377
TIM01	NPL02	-754.312	0.531	0.144	0.511
TIM01	SP01	-28.395	0.403	0.076	0.396
TIM01	IT01	-19.024	0.635	0.106	0.626
TIM01	CH01	-23.722	0.400	0.074	0.393
PL01	PTB05	-18.879	0.395	0.049	0.392
PL01	PTB04	-2.693	0.399	0.062	0.395
PL01	ROA01	-35.745	0.452	0.106	0.439
PL01	OP01	7123.465	0.403	0.090	0.392
PL01	CH01	-7.370	0.448	0.093	0.438
PTB05	PTB04	15.735	0.383	0.078	0.375
PTB05	VSL01	-0.963	0.360	0.080	0.351
PTB05	LTFB01	5.411	0.362	0.115	0.343
PTB05	ROA01	-16.900	0.455	0.136	0.434
PTB05	OP01	7142.085	0.344	0.073	0.337
PTB05	NPL02	-718.774	0.533	0.161	0.508
PTB05	SP01	7.242	0.365	0.070	0.358
PTB05	IT01	16.210	0.605	0.061	0.602
PTB05	CH01	11.085	0.361	0.068	0.354
PTB04	VSL01	-17.089	0.399	0.092	0.389
PTB04	LTFB01	-10.776	0.366	0.119	0.346
PTB04	ROA01	-33.268	0.492	0.229	0.436
PTB04	OP01	7126.198	0.347	0.073	0.339
PTB04	NPL02	-735.109	0.492	0.135	0.473
PTB04	SP01	-9.205	0.410	0.110	0.395
PTB04	IT01	-0.077	0.608	0.075	0.604

PTB04	CH01	-4.885	0.402	0.090	0.391
VSL01	ROA01	-16.061	0.476	0.168	0.446
VSL01	OP01	7143.214	0.399	0.099	0.386
VSL01	NPL02	-718.091	0.547	0.174	0.518
VSL01	SP01	7.927	0.417	0.096	0.405
VSL01	IT01	17.155	0.644	0.128	0.632
VSL01	CH01	12.363	0.415	0.104	0.402
LTFB01	ROA01	-22.366	0.463	0.145	0.440
LTFB01	OP01	7136.845	0.445	0.132	0.425
LTFB01	IT01	10.800	0.635	0.098	0.627
LTFB01	CH01	6.091	0.408	0.099	0.395
ROA01	OP01	7159.219	0.463	0.162	0.434
ROA01	NPL02	-702.089	0.553	0.185	0.521
ROA01	SP01	23.914	0.424	0.112	0.409
ROA01	IT01	33.251	0.653	0.156	0.634
ROA01	CH01	28.508	0.501	0.223	0.448
OP01	NPL02	-7861.166	0.530	0.150	0.508
OP01	SP01	-7135.140	0.364	0.064	0.358
OP01	IT01	-7126.076	0.628	0.079	0.624
OP01	CH01	-7130.949	0.362	0.071	0.354
NPL02	SP01	726.020	0.505	0.132	0.487
NPL02	IT01	735.276	0.702	0.146	0.687
NPL02	CH01	730.464	0.542	0.151	0.520
SP01	IT01	9.355	0.619	0.076	0.615
SP01	CH01	4.520	0.417	0.088	0.408
IT01	CH01	-4.672	0.640	0.091	0.633

Table 10-5 List of new CALR and uCALR values of [Rx1-Rx2] & [Rx2-Rx2] SATRE channels using baseline-mode calibration

TW Link		CALR (k_1i,k_2j)	uCALR (k_1i,k_2j)	Type A & Type B Uncertainties	
				ua	ub
<k_1i>	<k_2j>	Unit: ns	Unit: ns	Unit: ns	Unit: ns
TIM01	PTB25	-30.232	0.385	0.079	0.376
TIM01	VSL21	-36.266	0.468	0.175	0.434
TIM01	ROA21	-52.228	0.461	0.146	0.437
TIM01	SP21	-26.120	0.405	0.088	0.396
TIM01	IT21	-21.459	0.631	0.085	0.626
TIM01	CH21	-17.076	0.398	0.067	0.393
TIM21	PTB05	-39.207	0.345	0.059	0.340

TIM21	PTB25	-34.143	0.346	0.061	0.340
TIM21	PTB04	-22.804	0.347	0.054	0.343
TIM21	VSL01	-40.128	0.399	0.087	0.390
TIM21	VSL21	-40.108	0.416	0.146	0.390
TIM21	LTFB01	-33.802	0.403	0.127	0.383
TIM21	ROA01	-56.118	0.456	0.130	0.437
TIM21	ROA21	-56.006	0.457	0.132	0.437
TIM21	OP01	7103.148	0.348	0.075	0.340
TIM21	NPL02	-758.170	0.491	0.127	0.474
TIM21	SP01	-32.339	0.366	0.057	0.362
TIM21	SP21	-30.065	0.369	0.071	0.362
TIM21	IT01	-22.873	0.632	0.093	0.626
TIM21	IT21	-25.302	0.608	0.067	0.604
TIM21	CH01	-27.533	0.362	0.054	0.358
TIM21	CH21	-20.883	0.361	0.046	0.358
PL01	PTB25	-13.742	0.397	0.063	0.392
PL01	ROA21	-35.680	0.452	0.107	0.439
PL01	CH21	-0.577	0.449	0.095	0.438
PTB05	VSL21	-0.880	0.368	0.109	0.351
PTB05	ROA21	-16.903	0.461	0.154	0.434
PTB05	SP21	8.303	0.401	0.083	0.392
PTB05	IT21	13.877	0.606	0.063	0.602
PTB05	CH21	18.191	0.359	0.056	0.354
PTB25	PTB04	10.377	0.384	0.082	0.375
PTB25	VSL01	-6.136	0.360	0.079	0.351
PTB25	VSL21	-6.075	0.367	0.106	0.351
PTB25	LTFB01	0.181	0.401	0.131	0.379
PTB25	ROA01	-21.938	0.467	0.173	0.434
PTB25	ROA21	-21.940	0.479	0.202	0.434
PTB25	OP01	7136.795	0.346	0.079	0.337
PTB25	NPL02	-723.943	0.531	0.152	0.508
PTB25	SP01	2.116	0.400	0.077	0.392
PTB25	SP21	3.183	0.404	0.094	0.392
PTB25	IT01	11.121	0.606	0.063	0.602
PTB25	IT21	8.789	0.606	0.064	0.602
PTB25	CH01	5.897	0.361	0.068	0.354
PTB25	CH21	13.002	0.359	0.056	0.354
PTB04	VSL21	-17.007	0.409	0.127	0.389
PTB04	ROA21	-33.290	0.488	0.219	0.436
PTB04	SP21	-8.076	0.432	0.177	0.395

PTB04	IT21	-2.441	0.608	0.069	0.604
PTB04	CH21	2.077	0.362	0.061	0.357
VSL01	ROA21	-16.003	0.481	0.180	0.446
VSL01	SP21	9.645	0.426	0.130	0.405
VSL01	IT21	14.779	0.644	0.127	0.632
VSL01	CH21	19.170	0.415	0.104	0.402
VSL21	ROA01	-16.195	0.515	0.258	0.446
VSL21	ROA21	-16.019	0.533	0.293	0.446
VSL21	OP01	7143.142	0.412	0.143	0.386
VSL21	NPL02	-718.193	0.565	0.226	0.518
VSL21	SP01	7.785	0.429	0.140	0.405
VSL21	IT01	17.065	0.646	0.133	0.632
VSL21	IT21	14.773	0.648	0.144	0.632
VSL21	CH01	12.304	0.441	0.181	0.402
VSL21	CH21	19.163	0.440	0.178	0.402
LTFB01	ROA21	-22.312	0.461	0.138	0.440
LTFB01	IT21	8.375	0.634	0.092	0.627
LTFB01	CH21	12.884	0.406	0.095	0.395
ROA01	SP21	25.900	0.448	0.182	0.409
ROA01	IT21	30.811	0.647	0.132	0.634
ROA01	CH21	35.175	0.429	0.138	0.406
ROA21	OP01	7159.215	0.420	0.155	0.390
ROA21	NPL02	-702.155	0.556	0.194	0.521
ROA21	SP01	23.834	0.466	0.119	0.451
ROA21	SP21	25.983	0.483	0.258	0.409
ROA21	IT01	33.190	0.651	0.151	0.634
ROA21	IT21	30.751	0.647	0.129	0.634
ROA21	CH01	28.503	0.499	0.221	0.448
ROA21	CH21	35.175	0.429	0.139	0.406
OP01	SP21	-7133.702	0.364	0.067	0.358
OP01	IT21	-7128.467	0.607	0.078	0.602
OP01	CH21	-7123.965	0.360	0.062	0.354
NPL02	SP21	728.038	0.542	0.141	0.523
NPL02	IT21	732.789	0.701	0.141	0.687
NPL02	CH21	737.163	0.506	0.148	0.484
SP01	IT21	6.901	0.640	0.073	0.635
SP01	CH21	11.244	0.418	0.089	0.408
SP21	IT01	7.410	0.618	0.069	0.615
SP21	IT21	4.957	0.619	0.072	0.615
SP21	CH01	2.923	0.380	0.064	0.375

SP21	CH21	9.760	0.381	0.068	0.375
IT01	CH21	2.035	0.639	0.087	0.633
IT21	CH01	-2.278	0.639	0.084	0.633
IT21	CH21	4.428	0.638	0.078	0.633

10.2 Baseline-mode CALR calibration results on SDR channels

10.2.1 Baseline-mode CALR calibration pairs of SDR channels

Table 10-6 lists the CCD/bridged CCD results taken into CALR calculation and the new CALR and uCALR results for a pair of ESs. In Table 10-6, values in column $CCD_{avg}(k_1i,MOB@k_1)$ and $u CCD_{avg}(k_1i,MOB@k_1)$ are obtained from Table 7-48, and values in column Bridged $CCD_{avg}(k_2i,MOB@k_2)$ and uBridged $CCD_{avg}(k_2i,MOB@k_2)$ are taken from Table 9-20 to Table 9-23 accordingly. $CALR_{MeasB}(k_1i,k_2j)$ is the new CALR value for a pair of ESs calculated by equation (46) / equation (47), and $u CALR_{MeasB}(k_1i,k_2j)$ is the 1-σ uncertainty of $CALR_{MeasB}(k_1i,k_2j)$.

Table 10-6 List of ES pairs of SDR channels in baseline-mode measurements

TW Pair		CCD_{avg} $(k_1i,MOB@k_1)$	uCCD $(k_1i,MOB@k_1)$	Bridged CCD_{avg} $(k_2j,MOB@k_2)$	uBridged CCD $(k_2j,MOB@k_2)$	$CALR_{MeasB}$ (k_1i,k_2j)	$u CALR_{MeasB}$ (k_1i,k_2j)
$<k_1i>$	$<k_2j>$	Unit: ns	Unit: ns	Unit: ns	Unit: ns	Unit: ns	Unit: ns
VSL51	OP51	-1566.259	0.047	-3623.510	0.118	2059.521	0.407
OP51	VSL51	-3623.507	0.056	-1566.361	0.120	-2059.416	0.409
ROA51	OP51	-1571.383	0.162	-3623.230	0.086	2052.727	0.431
ROA51	SP51	-1571.383	0.162	-1598.841	0.371	26.138	0.606
ROA51	IT51	-1571.383	0.162	-1481.709	0.088	-71.444	0.660
OP51	SP51	-3623.507	0.056	-1599.221	0.088	-2026.486	0.373
OP51	IT51	-3623.507	0.056	-1482.079	0.075	-2124.078	0.610
IT51	OP51	-1481.859	0.075	-3623.379	0.098	2124.170	0.615
IT51	SP51	-1481.859	0.075	-1598.663	0.244	97.254	0.685

Table 10-7 lists the uncertainty categories of SDR channel pairs in baseline-mode measurements, which lead to the results of $u CALR_{MeasB}$ (k_1i,k_2j) in Table 10-6. The uncertainty categories are defined in Section 6.3.

Table 10-7 List of $u CALR_{MeasB}$ uncertainty categories of SDR channel pairs in baseline-mode measurements

TW Pair		Type A Uncertainties		Type B Uncertainties					
		ua,1	ua,2	ub	ub,I	ub,II	ub, III	ub,6 (k_1i,k_2j)	ub, IV
$<k_1i>$	$<k_2j>$	Unit: ns	Unit: ns	Unit: ns	Unit: ns	Unit: ns	Unit: ns	Unit: ns	Unit: ns
VSL51	OP51	0.047	0.118	0.386	0.192	0.040	0.246	0.105	0.224
OP51	VSL51	0.056	0.120	0.386	0.192	0.040	0.246	0.105	0.224
ROA51	OP51	0.162	0.086	0.390	0.192	0.040	0.252	0.118	0.224

ROA51	SP51	0.162	0.371	0.451	0.192	0.040	0.280	0.170	0.294
ROA51	IT51	0.162	0.088	0.634	0.192	0.040	0.560	0.513	0.224
OP51	SP51	0.056	0.088	0.358	0.192	0.040	0.256	0.126	0.156
OP51	IT51	0.056	0.075	0.602	0.192	0.040	0.548	0.500	0.156
IT51	OP51	0.075	0.098	0.602	0.192	0.040	0.548	0.500	0.156
IT51	SP51	0.075	0.244	0.635	0.192	0.040	0.561	0.515	0.224

10.2.2 Baseline-mode final calibration results of SDR TW links

Based on the calibration results in Table 10-6, the final CALR values of TW links are listed in Table 10-8. For a pair of SDR channels in remote, the calibration result of $CALR_{MeasB}(k_1i,k_2j)$ is taken as the final CALR value when only Measurement B1 plus Measurement B2 or Measurement B3 plus Measurement B4 exist. When all the Measurement B1-Measurement B4 are available, the final CALR values are computed via equation (48). In this case, the maximum Type B uncertainty of both calibration results is taken as the final Type B uncertainty ub of the TW link.

Table 10-8 List of new CALR and uCALR values of SDR TW links using baseline-mode calibration

TW Link		**CALR** (k_1i,k_2j)	**uCALR** (k_1i,k_2j)	**Type A & Type B Uncertainties**	
				ua	**ub**
$<k_1i>$	**$<k_2j>$**	**Unit: ns**	**Unit: ns**	**Unit: ns**	**Unit: ns**
VSL51	OP51	2059.468	0.397	0.092	0.386
ROA51	OP51	2052.727	0.431	0.183	0.390
ROA51	SP51	26.138	0.606	0.405	0.451
ROA51	IT51	-71.444	0.660	0.184	0.634
OP51	SP51	-2026.486	0.373	0.104	0.358
OP51	IT51	-2124.124	0.607	0.077	0.602
SP51	IT51	-97.254	0.685	0.255	0.635

11 Comparison with previous calibration data

In this chapter, the old and new CALR values are compared to evaluate the maintainability of the ES internal latency asymmetry as well as verify the consistency of the new CALR values.

11.1 Denotations of CALR values in comparison of old and new

In order to distinguish between the new CALR values from this calibration campaign and the existing CALR values in use that were obtained from the previous calibrations, the various CALR values in comparison are denoted as follows:

$\mathrm{CALR_{old}}$ is the old CALR value obtained from the previous calibration, to which a specific CAL ID has been assigned. According to equation (8), it can be expressed as:

$$\mathrm{CALR_{old}}(\mathrm{k_1i},\ \mathrm{k_2j}) \triangleq -[\mathrm{SCD}(\mathrm{k_1}) - \mathrm{SCD}(\mathrm{k_2})] + 0.5[\mathrm{DLD}(\mathrm{k_1i}) - \mathrm{DLD}(\mathrm{k_2j})] \quad (61)$$

where both SCD and DLD values are taken from the previous calibration. $\mathrm{CALR_{old}}(\mathrm{k_1i},\ \mathrm{k_2j})$ values are listed in the CALR column of ITU files, and $u\mathrm{CALR_{old}}(\mathrm{k_1i},\ \mathrm{k_2j})$ values are listed in the header of the ITU files.

$\mathrm{CALR_{interim}}$ is the equivalent $\mathrm{CALR_{old}}$ value in use at present, which takes into consideration the ESDVAR value after a CAL ID was assigned to the old CALR value. The relation between $\mathrm{CALR_{old}}$ and $\mathrm{CALR_{interim}}$ and the corresponding 1-σ uncertainty of $\mathrm{CALR_{interim}}$ is as follows:

$$\mathrm{CALR_{interim}}(\mathrm{k_1i},\ \mathrm{k_2j}) \stackrel{\mathrm{def}}{=} \mathrm{CALR_{old}}(\mathrm{k_1i},\ \mathrm{k_2j}) + 0.5[\mathrm{ESDVAR}(\mathrm{k_1i}) - \mathrm{ESDVAR}(\mathrm{k_2j})] \quad (62)$$

$$\mu\mathrm{CALR_{interim}}(\mathrm{k_1i},\ \mathrm{k_2j}) = \sqrt{\mu\mathrm{CALR_{old}}(\mathrm{k_1i},\ \mathrm{k_2j})^2 + [0.5\mathrm{ESIG}(\mathrm{k_1i})]^2 + [0.5\mathrm{ESIG}(\mathrm{k_2j})]^2} \quad (63)$$

$\mathrm{CALR_{new}}$ is the new CALR value calculated from measurement data from this calibration campaign by resetting the ESDVAR value back to zero. $\mathrm{CALR_{new}}(\mathrm{k_1i},\ \mathrm{k_2j})$ is obtained by equation (43) in site-mode calibration and is obtained by equation (48) in baseline-mode calibration.

$\mathrm{CALR_{deviation}}$ is the deviation between the equivalent old CALR and the new CALR values, and it is defined as:

$$\mathrm{CALR_{deviation}}(\mathrm{k_1i},\ \mathrm{k_2j}) \stackrel{\mathrm{def}}{=} \mathrm{CALR_{new}}(\mathrm{k_1i},\ \mathrm{k_2j}) - \mathrm{CALR_{interim}}(\mathrm{k_1i},\ \mathrm{k_2j}) \quad (64)$$

with its 1-σ uncertainty of

$$u\mathrm{CALR_{deviation}}(\mathrm{k_1i},\ \mathrm{k_2j}) = \sqrt{\mu\mathrm{CALR_{new}}(\mathrm{k_1i},\ \mathrm{k_2j})^2 + \mu\mathrm{CALR_{interim}}(\mathrm{k_1i},\ \mathrm{k_2j})^2} \quad (65)$$

11.2 Summary on previous calibration data

Table 11-1 and Table 11-2 summarize all the previous CALR values currently in use for all the participating TW links. In Table 11-1 and Table 11-2, CAL ID, MJD of CAL ID, $\mathrm{CALR_{old}}$, $u\mathrm{CALR_{old}}$, ESDVAR, and ESIG data are subtracted from the first-day on-site measurement ITU file of the LOC station during this calibration campaign. $\mathrm{CALR_{interim}}$ and $u\mathrm{CALR_{interim}}$ are calculated according to equation (62) and equation (63), respectively.

Among all the TWSTFT EU-to-EU links, links to the pivot ES PTB05 are used as main links for UTC calculation, while links that are not directed to PTB05 are categorized as non-UTC links.

11.2.1 Previous CALR and uCALR values of UTC TW links

Table 11-1 List of previous CALR and uCALR values of UTC links

TW Link		CAL ID	$CALR_{old}$	$uCALR_{old}$	ESDVAR	ESIG	$CALR_{interim}$	$uCALR_{interim}$	MJD of CAL ID
LOC	REM								
<k_1i>	<k_2j>		Unit: ns	Unit: ns	Unit: ns	Unit: ns	Unit: ns	Unit: ns	
PTB05	VSL01	549①	1.570	1.100	12.320	0.200	-0.745	1.128	59397
VSL01	PTB05	549①	-1.570	1.100	16.950	0.460	0.745	1.128	59397
PTB05	ROA01	547①	-22.530	1.100	12.320	0.200	-16.370	1.105	59397
ROA01	PTB05	547①	22.530	1.100	0.000	0.000	16.370	1.105	59397
PTB55	OP51	546①	2027.320	0.700	12.320	0.200	2024.397	0.711	59397
OP51	PTB55	546①	-2027.320	0.700	18.166	0.156	-2024.397	0.711	59397
PTB05	NPL02	550①	-724.690	1.200	12.320	0.200	-718.750	1.213	59397
NPL02	PTB05	550①	724.690	1.200	0.440	0.300	718.750	1.213	59397
PTB05	SP01	548①	1.950	1.300	12.320	0.200	7.410	1.308	59397
SP01	PTB05	548①	-1.950	1.300	1.400	0.200	-7.410	1.308	59397
PTB05	IT01	584②	13.700	1.400	12.320	0.200	19.860	1.404	59630
IT01	PTB05	584②	-13.700	1.400	0.000	0.000	-19.860	1.404	59630
PTB05	CH01	543①	5.940	1.200	12.320	0.200	12.100	1.204	59397
CH01	PTB05	543①	-5.940	1.200	0.000	0.000	-12.100	1.204	59397

① CAL IDs ranging from 533 to 583 are reported in [RD05].

② CAL ID 584 is reported in [RD12].

11.2.2 Previous CALR and uCALR values of non-UTC TW links

Table 11-2 List of previous CALR and uCALR values of non-UTC links

TW Link		CAL ID	$CALR_{old}$	$uCALR_{old}$	ESDVAR	ESIG	$CALR_{interim}$	$uCALR_{interim}$	MJD of CAL ID
LOC	REM								
<k_1i>	<k_2j>		Unit: ns	Unit: ns	Unit: ns	Unit: ns	Unit: ns	Unit: ns	
PTB05	OP01	545①	7137.460	1.100	12.320	0.200	7143.620	1.105	59397
OP01	PTB05	545①	-7137.460	1.100	0.000	0.000	-7143.620	1.105	59397
VSL01	ROA01	580①	-23.880	1.600	16.950	0.460	-15.405	1.616	59397
ROA01	VSL01	580①	23.880	1.600	0.000	0.000	15.405	1.616	59397
VSL01	OP01	577①	7136.010	1.600	16.950	0.460	7144.485	1.616	59397
OP01	VSL01	577①	-7136.010	1.600	0.000	0.000	-7144.485	1.616	59397
VSL01	NPL02	569①	-726.170	6.800	16.950	0.460	-717.915	6.806	59397

NPL02	VSL01	569[①]	726.170	6.800	0.440	0.300	717.915	6.806	59397
VSL01	SP01	582[①]	0.750	1.800	16.950	0.460	8.525	1.817	59397
SP01	VSL01	582[①]	-0.750	1.800	1.400	0.200	-8.525	1.817	59397
VSL01	IT01	588[③]	12.300	1.700	16.950	0.460	20.775	1.715	59639
IT01	VSL01	588[③]	-12.300	1.700	0.000	0.000	-20.775	1.715	59639
VSL01	CH01	558[①]	4.500	1.700	16.950	0.460	12.975	1.715	59397
CH01	VSL01	558[①]	-4.500	1.700	0.000	0.000	-12.975	1.715	59397
ROA01	OP01	574[①]	7160.190	1.600	0.000	0.000	7160.190	1.600	59397
OP01	ROA01	574[①]	-7160.190	1.600	0.000	0.000	-7160.190	1.600	59397
ROA01	NPL02	567[①]	-702.340	1.700	0.000	0.000	-702.560	1.707	59397
NPL02	ROA01	567[①]	702.340	1.700	0.440	0.300	702.560	1.707	59397
ROA01	SP01	578[①]	24.440	1.800	0.000	0.000	23.740	1.803	59397
SP01	ROA01	578[①]	-24.440	1.800	1.400	0.200	-23.740	1.803	59397
ROA01	IT01	586[③]	36.300	1.700	0.000	0.000	36.300	1.700	59639
IT01	ROA01	586[③]	-36.300	1.700	0.000	0.000	-36.300	1.700	59639
ROA01	CH01	555[①]	28.510	1.700	0.000	0.000	28.510	1.700	59397
CH01	ROA01	555[①]	-28.510	1.700	0.000	0.000	-28.510	1.700	59397
OP01	NPL02	566[①]	-7862.420	1.700	0.000	0.000	-7862.640	1.707	59397
NPL02	OP01	566[①]	7862.420	1.700	0.440	0.300	7862.640	1.707	59397
OP01	SP01	575[①]	-7135.760	1.800	0.000	0.000	-7136.460	1.803	59397
SP01	OP01	575[①]	7135.760	1.800	1.400	0.200	7136.460	1.803	59397
OP01	IT01	585[③]	-7123.900	1.800	0.000	0.000	-7123.900	1.800	59639
IT01	OP01	585[③]	7123.900	1.800	0.000	0.000	7123.900	1.800	59639
OP01	CH01	554[①]	-7131.620	1.700	0.000	0.000	-7131.620	1.700	59397
CH01	OP01	554[①]	7131.620	1.700	0.000	0.000	7131.620	1.700	59397
NPL02	SP01	568[①]	726.880	4.300	0.440	0.300	726.400	4.304	59397
SP01	NPL02	568[①]	-726.880	4.300	1.400	0.200	-726.400	4.304	59397
NPL02	IT01	589[③]	738.700	1.900	0.440	0.300	737.620	1.909	59639
IT01	NPL02	589[③]	-738.700	1.900	0.000	0.000	-737.620	1.909	59639
NPL02	CH01	552[①]	730.830	1.800	0.440	0.300	731.050	1.806	59397
CH01	NPL02	552[①]	-730.830	1.800	0.000	0.000	-731.050	1.806	59397
SP01	IT01	587[③]	11.900	1.900	1.400	0.200	12.600	1.903	59639
IT01	SP01	587[③]	-11.900	1.900	0.000	0.000	-12.600	1.903	59639
SP01	CH01	556[①]	4.090	1.800	1.400	0.200	4.790	1.803	59397

CH01	SP01	556[①]	-4.090	1.800	0.000	0.000	-4.790	1.803	59397
IT01	CH01	592[③]	-7.400	1.900	0.000	0.000	-7.400	1.900	59639
CH01	IT01	592[③]	7.400	1.900	0.000	0.000	7.400	1.900	59639

① CAL IDs ranging from 533 to 583 are reported in [RD05].

② CAL ID 584 is reported in [RD12].

③ CAL IDs ranging from 585 to 592 are reported in [RD13].

11.3 Comparisons between previous and new CALR values

Table 11-3 and Table 11-4 give the new and old CALR comparison results based on two calibration methods, where $CALR_{new}$ and $uCALR_{new}$ under site-mode and baseline-mode calibration methods are taken from the calibration results in Table 8-1 and Table 10-4, $CALR_{deviation}$ and $uCALR_{deviation}$ are calculated according to equation (64) and equation (65).

In Figure 11-1 and Figure 11-2, the data points with the cross and square markers indicate the $CALR_{deviation}$ values calculated via site-mode and baseline-mode methods, respectively, and the lengths of the error bars above and below the data points indicate the 1-σ uncertainty of $uCALR_{deviation}$ values accordingly. Error bars in green indicate the absolute value of $CALR_{deviation}$ is within 1 ns, while error bars in orange indicate the absolute value of $CALR_{deviation}$ is between 1 ns and 3 ns.

11.3.1 CALR deviation value comparison on UTC TW links

Table 11-3 Comparisons of new and old CALR and $uCALR$ values of UTC links

CALR(k_1i,k_2j)		Site-mode Calibration				Baseline-mode Calibration			
		$CALR_{new}$	$uCALR_{new}$	$CALR_{deviatio}$	$uCALR_{deviatio}$	$CALR_{new}$	$uCALR_{new}$	$CALR_{deviatio}$	$uCALR_{deviatio}$
<k_1i>	<k_2j>	Unit: ns	Unit: ns	Unit: ns	Unit: ns	Unit: ns	Unit: ns	Unit: ns	Unit: ns
PTB05	VSL01	-0.737	0.366	0.008	1.186	-0.963	0.360	-0.218	1.184
PTB05	ROA01	-16.921	0.433	-0.551	1.187	-16.900	0.455	-0.530	1.195
PTB55	OP51	2023.294	0.347	-1.103	0.791	--	--	--	--
PTB05	NPL02	-718.980	0.512	-0.230	1.317	-718.774	0.533	-0.024	1.325
PTB05	SP01	6.815	0.368	-0.595	1.359	7.242	0.365	-0.168	1.358
PTB05	IT01	16.518	0.611	-2.042	1.534	16.210	0.605	-2.350	1.532
PTB05	CH01	11.918	0.368	-0.182	1.259	11.085	0.361	-1.015	1.257

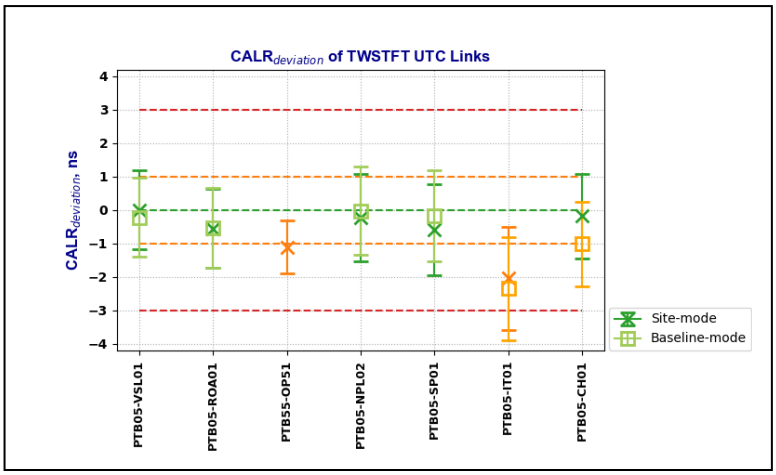

Figure 11-1 CALR deviation values of UTC links

11.3.2 CALR deviation value comparison on non-UTC TW links

Table 11-4 Comparisons of new and old CALR and uCALR values of non-UTC links

CALR(k_1i,k_2j)		Site-mode Calibration				Baseline-mode Calibration			
		$CALR_{new}$	$uCALR_{new}$	$CALR_{deviatio}$	$uCALR_{deviatio}$	$CALR_{new}$	$uCALR_{new}$	$CALR_{deviatio}$	$uCALR_{deviatio}$
<k_1i>	<k_2j>	Unit: ns	Unit: ns	Unit: ns	Unit: ns	Unit: ns	Unit: ns	Unit: ns	Unit: ns
PTB05	OP01	7142.529	0.352	-1.091	1.160	7142.085	0.344	-1.535	1.157
VSL01	ROA01	-16.184	0.446	-0.779	1.676	-16.061	0.476	-0.656	1.685
VSL01	OP01	7143.266	0.368	-1.219	1.657	7143.214	0.399	-1.271	1.665
VSL01	NPL02	-718.243	0.523	-0.328	6.826	-718.091	0.547	-0.176	6.828
VSL01	SP01	7.552	0.383	-0.973	1.857	7.927	0.417	-0.598	1.864
VSL01	IT01	17.255	0.620	-2.220	1.826	17.155	0.644	-2.320	1.835
VSL01	CH01	12.655	0.383	-0.320	1.757	12.363	0.415	-0.612	1.764
ROA01	OP01	7159.450	0.434	-0.740	1.658	7159.219	0.463	-0.971	1.666
ROA01	NPL02	-702.059	0.581	0.501	1.803	-702.089	0.553	0.471	1.794
ROA01	SP01	23.736	0.447	-0.004	1.858	23.914	0.424	0.174	1.852
ROA01	IT01	33.439	0.662	-1.561	1.827	33.251	0.653	-1.749	1.824
ROA01	CH01	28.839	0.447	0.329	1.758	28.508	0.501	-0.002	1.772
OP01	NPL02	-7861.509	0.513	1.131	1.782	-7861.166	0.530	1.474	1.787
OP01	SP01	-7135.714	0.369	0.746	1.840	-7135.140	0.364	1.320	1.839
OP01	IT01	-7126.011	0.612	-0.811	1.904	-7126.076	0.628	-0.876	1.909
OP01	CH01	-7130.611	0.369	1.009	1.740	-7130.949	0.362	0.671	1.738
NPL02	SP01	725.795	0.524	-0.605	4.336	726.020	0.505	-0.380	4.334
NPL02	IT01	735.498	0.716	-2.122	2.039	735.276	0.702	-2.344	2.034
NPL02	CH01	730.898	0.524	-0.152	1.880	730.464	0.542	-0.586	1.886
SP01	IT01	9.703	0.621	-1.597	2.004	9.355	0.619	-1.945	2.003
SP01	CH01	5.103	0.384	0.313	1.843	4.520	0.417	-0.270	1.851

IT01	CH01	-4.600	0.621	1.500	2.002	-4.672	0.640	1.428	2.008

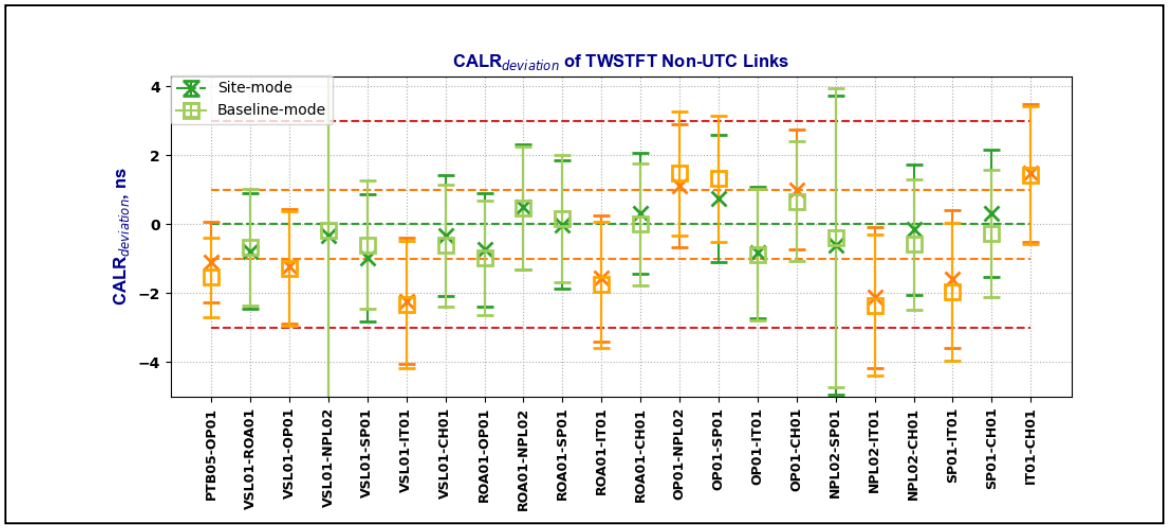

Figure 11-2 CALR deviation values of TWSTFT non-UTC links

12 Comparisons between site-mode and baseline-mode CALR results

In this chapter, the comparisons between the two calibration methods are done in the following two aspects: evaluate the conformity between the CALR results obtained by the two methods, and validate the time transfer accuracy of the TW link under the new CALRs.

12.1 Denotations of CALR values in comparison of site-mode and baseline-mode

Denote the new CALR value and its 1-σ uncertainty obtained via site-mode calibration as $\mathrm{CALR}_{\mathrm{site}}$ and $u\mathrm{CALR}_{\mathrm{site}}$, and the new CALR value and its 1-σ uncertainty calculated from baseline-mode calibration as $\mathrm{CALR}_{\mathrm{baseline}}$ and $u\mathrm{CALR}_{\mathrm{baseline}}$, the following relations are obtained:

$$\mathrm{CALR}_{\mathrm{site}}(\mathrm{k_1i},\ \mathrm{k_2j}) = \mathrm{CALR}_{\mathrm{norminal}}(\mathrm{k_1i},\ \mathrm{k_2j}) \pm u\mathrm{CALR}_{\mathrm{site}}(\mathrm{k_1i},\ \mathrm{k_2j}) \quad (66)$$

$$\mathrm{CALR}_{\mathrm{baseline}}(\mathrm{k_1i},\ \mathrm{k_2j}) = \mathrm{CALR}_{\mathrm{norminal}}(\mathrm{k_1i},\ \mathrm{k_2j}) \pm u\mathrm{CALR}_{\mathrm{baseline}}(\mathrm{k_1i},\ \mathrm{k_2j}) \quad (67)$$

where $\mathrm{CALR}_{\mathrm{norminal}}(\mathrm{k_1i},\ \mathrm{k_2j})$ is assumed to be the norminal CALR value for the TW link [k_1i-k_2j].

Then the difference between $\mathrm{CALR}_{\mathrm{site}}$ and $\mathrm{CALR}_{\mathrm{baseline}}$ is expected to be zero-mean with a corresponding confidence interval, which is expressed as:

$$\begin{aligned}\mathrm{CALR}_{\mathrm{delta}}(\mathrm{k_1i},\ \mathrm{k_2j}) &\stackrel{\mathrm{def}}{=} [\mathrm{CALR}_{\mathrm{site}}(\mathrm{k_1i},\ \mathrm{k_2j}) - \mathrm{CALR}_{\mathrm{baseline}}(\mathrm{k_1i},\ \mathrm{k_2j})] \\ &= \ 0 \pm \sqrt{u\mathrm{CALR}_{\mathrm{site}}(\mathrm{k_1i},\ \mathrm{k_2j})^2 + u\mathrm{CALR}_{\mathrm{baseline}}(\mathrm{k_1i},\ \mathrm{k_2j})^2}\end{aligned} \quad (68)$$

2-σ uncertainty is chosen as the uncertainty of $\mathrm{CALR}_{\mathrm{delta}}$ to guarantee 95% confidence intervals, as below:

$$u\mathrm{CALR}_{\mathrm{delta}}(\mathrm{k_1i},\ \mathrm{k_2j}) = 2 \times \sqrt{u\mathrm{CALR}_{\mathrm{site}}(\mathrm{k_1i},\ \mathrm{k_2j})^2 + u\mathrm{CALR}_{\mathrm{baseline}}(\mathrm{k_1i},\ \mathrm{k_2j})^2} \quad (69)$$

When the $\mathrm{CALR}_{\mathrm{delta}}$ value of a TW link falls into the uncertainty range of $u\mathrm{CALR}_{\mathrm{delta}}$, it shows the accepted conformity between the calibration results obtained from the two methods under the corresponding confidence interval.

The Triangle Closure is used to verify the calibration accuracy of the TW links with new CALRs. The principle of the triangle closure measurements refers to [RD08]. The triangle closure computation is summarized as follows, where the deduction process refers to equation (9).

$$\begin{aligned}\mathrm{TriClosure}(\mathrm{k_1i},\mathrm{k_2j},\mathrm{k_3m}) &\stackrel{\mathrm{def}}{=} [\mathrm{UTC}(\mathrm{k_1}) - \mathrm{UTC}(\mathrm{k_2})] + [\mathrm{UTC}(\mathrm{k_2}) - \mathrm{UTC}(\mathrm{k_3})] + [\mathrm{UTC}(\mathrm{k_3}) - \mathrm{UTC}(\mathrm{k_1})] \\ &= \underbrace{0.5[\mathrm{TW}(\mathrm{k_1i}) - \mathrm{TW}(\mathrm{k_2j})] + 0.5[\mathrm{TW}(\mathrm{k_2j}) - \mathrm{TW}(\mathrm{k_3m})] + 0.5[\mathrm{TW}(\mathrm{k_3m}) - \mathrm{TW}(\mathrm{k_1i})]}_{\mathrm{TW}_{\mathrm{sum}}(\mathrm{k_1i},\mathrm{k_2j},\mathrm{k_3m})} \\ &+ \underbrace{\mathrm{CALR}_{\mathrm{new}}(\mathrm{k_1i},\mathrm{k_2j}) + \mathrm{CALR}_{\mathrm{new}}(\mathrm{k_2j},\mathrm{k_3m}) + \mathrm{CALR}_{\mathrm{new}}(\mathrm{k_3m},\mathrm{k_1i})}_{\mathrm{CALR}_{\mathrm{sum}}(\mathrm{k_1i},\mathrm{k_2j},\mathrm{k_3m})} \\ &\triangleq \mathrm{TW}_{\mathrm{sum}}(\mathrm{k_1i},\mathrm{k_2j},\mathrm{k_3m}) + \mathrm{CALR}_{\mathrm{sum}}(\mathrm{k_1i},\mathrm{k_2j},\mathrm{k_3m})\end{aligned} \quad (70)$$

In site-mode calibration, $\mathrm{CALR}_{\mathrm{sum}}(\mathrm{k_1i},\mathrm{k_2j},\mathrm{k_3m}) = 0$. Therefore, $\mathrm{TW}_{\mathrm{sum}}(\mathrm{k_1i},\mathrm{k_2j},\mathrm{k_3m})$ indicates the triangle closure results obtained from the site-mode calibration method. Triangle closures in baseline-mode are obtained by adding the $\mathrm{CALR}_{\mathrm{sum}}(\mathrm{k_1i},\mathrm{k_2j},\mathrm{k_3m})$ of the baseline-mode calibration values to $\mathrm{TW}_{\mathrm{sum}}(\mathrm{k_1i},\mathrm{k_2j},\mathrm{k_3m})$. In the ideal scenario, there is $\mathrm{TriClosure}(\mathrm{k_1i},\mathrm{k_2j},\mathrm{k_3m}) = 0$; hence, the offset of the actual $\mathrm{TriClosure}$ value from zero can reflect the vector sum of the involved three TW links time transfer accuracy with the new CALRs.

12.2 Site-mode and baseline-mode CALR results comparison

Table 12-1, Table 12-2, and Table 12-3 give the CALR comparison results between the two calibration methods, site-mode and baseline-mode, where $CALR_{site}$ and $u CALR_{site}$ are taken from the calibration results in Table 8-1, $CALR_{baseline}$ and $u CALR_{baseline}$ are taken from Table 10-4, and $CALR_{delta}$ and $u CALR_{delta}$ are calculated according to equation (68) and equation (69).

In Figure 12-1, Figure 12-2, and Figure 12-3, the solid square markers represent the $CALR_{delta}$ values, which show the difference between site-mode and baseline-mode calibration results, and the lengths of the error bars above and below the markers indicate the 2-σ uncertainty of $u CALR_{delta}$ values, respectively. Error bars in green indicate the absolute value of $CALR_{delta}$ is within 0.5 ns, while error bars in orange indicate the absolute value of $CALR_{delta}$ is between 0.5 ns and 1 ns.

12.2.1 Site-mode and baseline-mode CALR results comparison on UTC TW links

Table 12-1 Comparisons on site-mode and baseline-mode CALR values of UTC links

$CALR(k_1 i, k_2 j)$		Site-mode CALR Results		Baseline-mode CALR Results		CALR differ.	
		$CALR_{site}$	$u CALR_{site}$	$CALR_{baseline}$	$u CALR_{baseline}$	$CALR_{delta}$	(2-σ) $u CALR_{delta}$
$<k_1 i>$	$<k_2 j>$	Unit: ns	Unit: ns	Unit: ns	Unit: ns	Unit: ns	Unit: ns
PL01	PTB05	-18.901	0.401	-18.879	0.395	-0.022	1.126
PTB05	PTB04	16.605	0.353	15.735	0.383	0.870	1.042
PTB05	VSL01	-0.737	0.366	-0.963	0.360	0.226	1.027
PTB05	LTFB01	5.559	0.409	5.411	0.362	0.148	1.092
PTB05	ROA01	-16.921	0.433	-16.900	0.455	-0.021	1.256
PTB05	NPL02	-718.980	0.512	-718.774	0.533	-0.206	1.478
PTB05	SP01	6.815	0.368	7.242	0.365	-0.427	1.037
PTB05	IT01	16.518	0.611	16.210	0.605	0.308	1.720
PTB05	CH01	11.918	0.368	11.085	0.361	0.833	1.031

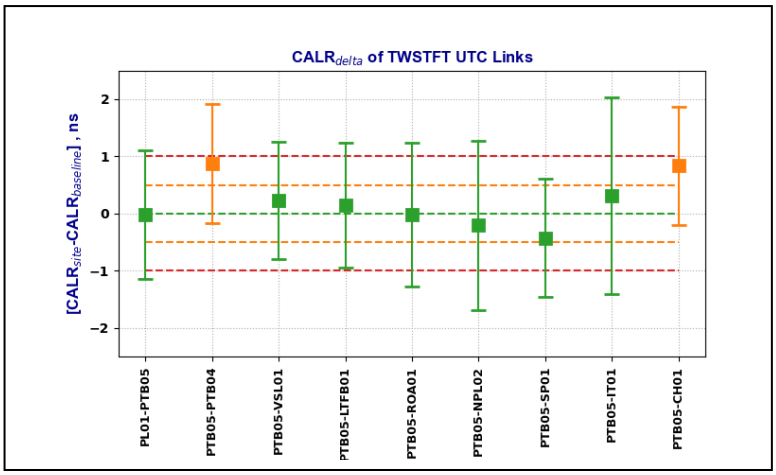

Figure 12-1 New CALR value comparisons between site-mode and baseline-mode calibration for UTC links

12.2.2 Site-mode and baseline-mode CALR results comparison on non-UTC TW links

Table 12-2 Comparisons on site-mode and baseline-mode CALR values of non-UTC links

CALR(k_1i,k_2j)		Site-mode CALR Results		Baseline-mode CALR Results		CALR differ.	
		$CALR_{site}$	$uCALR_{site}$	$CALR_{baseline}$	$uCALR_{baseline}$	$CALR_{delta}$	(2-σ) $uCALR_{delta}$
<k_1i>	<k_2j>	Unit: ns	Unit: ns	Unit: ns	Unit: ns	Unit: ns	Unit: ns
TIM01	PL01	-16.575	0.442	-16.524	0.444	-0.051	1.253
TIM01	PTB05	-35.476	0.398	-35.296	0.384	-0.180	1.106
TIM01	PTB04	-18.871	0.399	-18.985	0.386	0.114	1.110
TIM01	VSL01	-36.213	0.411	-36.298	0.446	0.085	1.213
TIM01	LTFB01	-29.917	0.461	-29.902	0.454	-0.015	1.294
TIM01	ROA01	-52.397	0.483	-52.331	0.462	-0.066	1.337
TIM01	OP01	7107.053	0.399	7107.078	0.386	-0.025	1.110
TIM01	NPL02	-754.456	0.555	-754.312	0.531	-0.144	1.536
TIM01	SP01	-28.661	0.413	-28.395	0.403	-0.266	1.154
TIM01	IT01	-18.958	0.639	-19.024	0.635	0.066	1.802
TIM01	CH01	-23.558	0.413	-23.722	0.400	0.164	1.150
PL01	PTB04	-2.296	0.402	-2.693	0.399	0.397	1.133
PL01	ROA01	-35.822	0.475	-35.745	0.452	-0.077	1.311
PL01	OP01	7123.628	0.402	7123.465	0.403	0.163	1.138
PL01	CH01	-6.983	0.416	-7.370	0.448	0.387	1.223
PTB05	OP01	7142.529	0.352	7142.085	0.344	0.444	0.984
PTB04	VSL01	-17.342	0.368	-17.089	0.399	-0.253	1.086
PTB04	LTFB01	-11.046	0.410	-10.776	0.366	-0.270	1.099
PTB04	ROA01	-33.526	0.435	-33.268	0.492	-0.258	1.313
PTB04	OP01	7125.924	0.354	7126.198	0.347	-0.274	0.991
PTB04	NPL02	-735.585	0.513	-735.109	0.492	-0.476	1.422

PTB04	SP01	-9.790	0.369	-9.205	0.410	-0.585	1.103
PTB04	IT01	-0.087	0.612	-0.077	0.608	-0.010	1.725
PTB04	CH01	-4.687	0.369	-4.885	0.402	0.198	1.091
VSL01	ROA01	-16.184	0.446	-16.061	0.476	-0.123	1.305
VSL01	OP01	7143.266	0.368	7143.214	0.399	0.052	1.086
VSL01	NPL02	-718.243	0.523	-718.091	0.547	-0.152	1.514
VSL01	SP01	7.552	0.383	7.927	0.417	-0.375	1.132
VSL01	IT01	17.255	0.620	17.155	0.644	0.100	1.788
VSL01	CH01	12.655	0.383	12.363	0.415	0.292	1.129
LTFB01	ROA01	-22.480	0.492	-22.366	0.463	-0.114	1.351
LTFB01	OP01	7136.970	0.410	7136.845	0.445	0.125	1.210
LTFB01	IT01	10.959	0.646	10.800	0.635	0.159	1.812
LTFB01	CH01	6.359	0.423	6.091	0.408	0.268	1.175
ROA01	OP01	7159.450	0.434	7159.219	0.463	0.231	1.269
ROA01	NPL02	-702.059	0.581	-702.089	0.553	0.030	1.604
ROA01	SP01	23.736	0.447	23.914	0.424	-0.178	1.232
ROA01	IT01	33.439	0.662	33.251	0.653	0.188	1.860
ROA01	CH01	28.839	0.447	28.508	0.501	0.331	1.343
OP01	NPL02	-7861.509	0.513	-7861.166	0.530	-0.343	1.475
OP01	SP01	-7135.714	0.369	-7135.140	0.364	-0.574	1.037
OP01	IT01	-7126.011	0.612	-7126.076	0.628	0.065	1.754
OP01	CH01	-7130.611	0.369	-7130.949	0.362	0.338	1.034
NPL02	SP01	725.795	0.524	726.020	0.505	-0.225	1.455
NPL02	IT01	735.498	0.716	735.276	0.702	0.222	2.005
NPL02	CH01	730.898	0.524	730.464	0.542	0.434	1.508
SP01	IT01	9.703	0.621	9.355	0.619	0.348	1.754
SP01	CH01	5.103	0.384	4.520	0.417	0.583	1.134
IT01	CH01	-4.600	0.621	-4.672	0.640	0.072	1.784

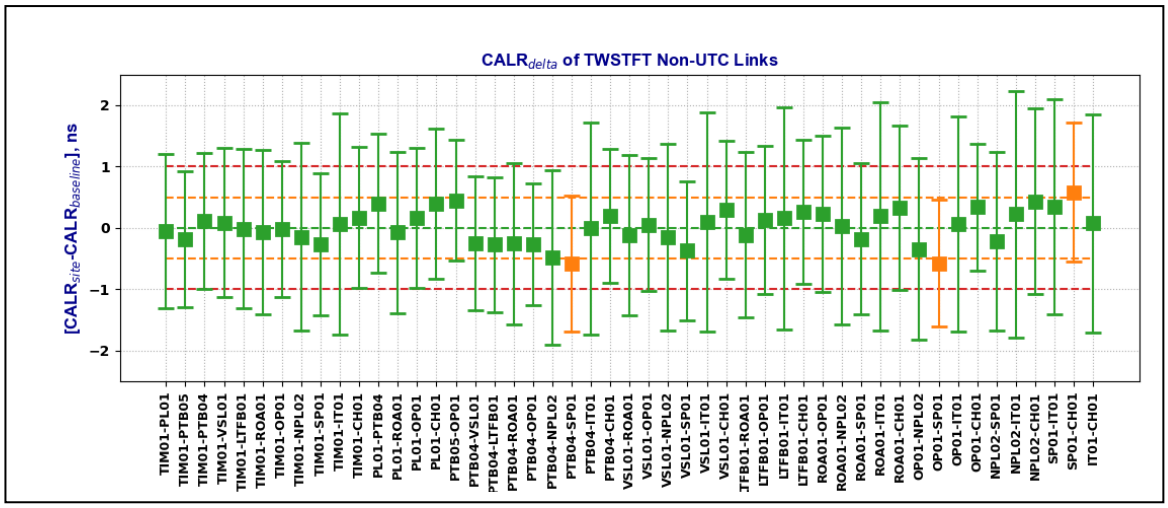

Figure 12-2 New CALR value comparisons between site-mode and baseline-mode calibration for non-UTC links

12.2.3 Site-mode and baseline-mode CALR results comparison on SDR TW links

Table 12-3 Comparisons on site-mode and baseline-mode CALR values of SDR links

CALR(k_1i,k_2j)		Site-mode CALR Results		Baseline-mode CALR Results		CALR differ.	
		$\mathrm{CALR}_{\mathrm{site}}$	$u\mathrm{CALR}_{\mathrm{site}}$	$\mathrm{CALR}_{\mathrm{baseline}}$	$u\mathrm{CALR}_{\mathrm{baseline}}$	$\mathrm{CALR}_{\mathrm{delta}}$	(2-σ) $u\mathrm{CALR}_{\mathrm{delta}}$
<k_1i>	<k_2j>	Unit: ns	Unit: ns	Unit: ns	Unit: ns	Unit: ns	Unit: ns
VSL51	OP51	2059.518	0.359	2059.468	0.397	0.050	1.070
ROA51	OP51	2053.004	0.426	2052.727	0.431	0.277	1.212
ROA51	SP51	26.383	0.515	26.138	0.606	0.245	1.591
ROA51	IT51	-71.294	0.658	-71.444	0.660	0.150	1.864
OP51	SP51	-2026.621	0.439	-2026.486	0.373	-0.135	1.152
OP51	IT51	-2124.298	0.610	-2124.124	0.607	-0.174	1.721
SP51	IT51	-97.677	0.667	-97.254	0.685	-0.423	1.912

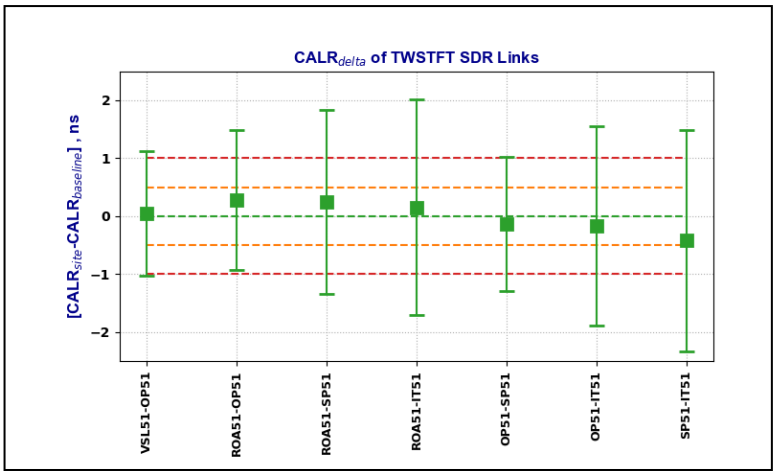

Figure 12-3 New CALR value comparisons between site-mode and baseline-mode calibration for SDR TW links

12.3 Triangle closure verification on site-mode and baseline-mode calibration results

Table 12-4 lists the triangle closure results with the new site-mode CALRs and baseline-mode CALRs, respectively. In Table 12-4, the TW measurement data are taken from MJD 60171 to MJD 60249, which spans the whole period of on-site measurements for all the ESs. The mean and stdev of the daily average data of the TW_{sum} are listed as the site-mode triangle closure results. $CALR_{sum}$ values are computed from baseline-mode CALR values listed in Table 10-4 and Table 10-8. And TriClosure values are calculated according to equation (70).

Table 12-4 Triangle closures verification on site-mode and baseline-mode CALR results

Triangle closure link	Site-mode triangle closure results $TW_{sum}(k_1i,k_2j,k_3m)$			Baseline-mode triangle closure results				
<k_1i>-<k_2j>-<k_3m>	mean	stdev	No. of days	$CALR_{baseline}$ (k_1i,k_2j)	$CALR_{baseline}$ (k_2j,k_3m)	$CALR_{baseline}$ (k_3m,k_1i)	$CALR_{sum}$ (k_1i,k_2j,k_3m)	TriClosure (k_1i,k_2j,k_3m)
TIM01-PL01-PTB05	0.093	0.036	43	-16.524	-18.879	35.296	-0.107	-0.014
TIM01-PL01-PTB04	0.274	0.039	48	-16.524	-2.693	18.985	-0.232	0.042
TIM01-PL01-ROA01	-0.007	0.050	6	-16.524	-35.745	52.331	0.062	0.055
TIM01-PL01-OP01	0.223	0.041	26	-16.524	7123.465	-7107.078	-0.137	0.086
TIM01-PL01-CH01	0.201	0.036	54	-16.524	-7.370	23.722	-0.172	0.029
TIM01-PTB05-PTB04	0.634	0.045	78	-35.296	15.735	18.985	-0.576	0.058
TIM01-PTB05-VSL01	0.016	0.061	76	-35.296	-0.963	36.298	0.039	0.055
TIM01-PTB05-LTFB01	0.033	0.035	28	-35.296	5.411	29.902	0.017	0.050
TIM01-PTB05-ROA01	-0.163	0.059	78	-35.296	-16.900	52.331	0.135	-0.028
TIM01-PTB05-OP01	0.321	0.030	78	-35.296	7142.085	-7107.078	-0.289	0.032
TIM01-PTB05-NPL02	-0.227	0.047	75	-35.296	-718.774	754.312	0.242	0.015
TIM01-PTB05-SP01	-0.333	0.050	78	-35.296	7.242	28.395	0.341	0.008
TIM01-PTB05-IT01	0.114	0.047	78	-35.296	16.210	19.024	-0.062	0.052
TIM01-PTB05-CH01	0.551	0.050	78	-35.296	11.085	23.722	-0.489	0.062
TIM01-PTB04-VSL01	-0.250	0.065	74	-18.985	-17.089	36.298	0.224	-0.026

TIM01-PTB04-LTFB01	-0.177	0.030	27	-18.985	-10.776	29.902	0.141	-0.036
TIM01-PTB04-ROA01	-0.094	0.087	78	-18.985	-33.268	52.331	0.078	-0.016
TIM01-PTB04-OP01	-0.174	0.037	75	-18.985	7126.198	-7107.078	0.135	-0.039
TIM01-PTB04-NPL02	-0.369	0.065	73	-18.985	-735.109	754.312	0.218	-0.151
TIM01-PTB04-SP01	-0.378	0.068	71	-18.985	-9.205	28.395	0.205	-0.173
TIM01-PTB04-IT01	0.041	0.044	78	-18.985	-0.077	19.024	-0.038	0.003
TIM01-PTB04-CH01	0.184	0.034	78	-18.985	-4.885	23.722	-0.148	0.036
TIM01-VSL01-ROA01	-0.046	0.062	75	-36.298	-16.061	52.331	-0.028	-0.074
TIM01-VSL01-OP01	0.130	0.073	72	-36.298	7143.214	-7107.078	-0.162	-0.032
TIM01-VSL01-NPL02	0.020	0.069	73	-36.298	-718.091	754.312	-0.077	-0.057
TIM01-VSL01-SP01	-0.109	0.070	71	-36.298	7.927	28.395	0.024	-0.085
TIM01-VSL01-IT01	0.091	0.059	75	-36.298	17.155	19.024	-0.119	-0.028
TIM01-VSL01-CH01	0.245	0.058	76	-36.298	12.363	23.722	-0.213	0.032
TIM01-LTFB01-ROA01	-0.077	0.044	27	-29.902	-22.366	52.331	0.063	-0.014
TIM01-LTFB01-OP01	0.124	0.034	42	-29.902	7136.845	-7107.078	-0.135	-0.011
TIM01-LTFB01-IT01	0.120	0.050	27	-29.902	10.800	19.024	-0.078	0.042
TIM01-LTFB01-CH01	0.124	0.044	30	-29.902	6.091	23.722	-0.089	0.035
TIM01-ROA01-OP01	0.172	0.051	69	-52.331	7159.219	-7107.078	-0.190	-0.018
TIM01-ROA01-NPL02	0.106	0.077	76	-52.331	-702.089	754.312	-0.108	-0.002
TIM01-ROA01-SP01	0.100	0.086	78	-52.331	23.914	28.395	-0.022	0.078
TIM01-ROA01-IT01	0.049	0.045	78	-52.331	33.251	19.024	-0.056	-0.007
TIM01-ROA01-CH01	0.045	0.094	78	-52.331	28.508	23.722	-0.101	-0.056
TIM01-OP01-NPL02	-0.247	0.049	74	7107.078	-7861.166	754.312	0.224	-0.023
TIM01-OP01-SP01	-0.338	0.059	78	7107.078	-7135.140	28.395	0.333	-0.005
TIM01-OP01-IT01	-0.004	0.041	78	7107.078	-7126.076	19.024	0.026	0.022
TIM01-OP01-CH01	0.187	0.049	75	7107.078	-7130.949	23.722	-0.149	0.038
TIM01-NPL02-SP01	-0.113	0.080	75	-754.312	726.020	28.395	0.103	-0.010
TIM01-NPL02-IT01	0.084	0.041	76	-754.312	735.276	19.024	-0.012	0.072
TIM01-NPL02-CH01	0.225	0.072	75	-754.312	730.464	23.722	-0.126	0.099
TIM01-SP01-IT01	0.039	0.056	78	-28.395	9.355	19.024	-0.016	0.023
TIM01-SP01-CH01	0.281	0.047	78	-28.395	4.520	23.722	-0.153	0.128
TIM01-IT01-CH01	-0.040	0.049	78	-19.024	-4.672	23.722	0.026	-0.014
PL01-PTB05-PTB04	0.461	0.051	43	-18.879	15.735	2.693	-0.451	0.010
PL01-PTB05-OP01	0.197	0.046	21	-18.879	7142.085	-7123.465	-0.259	-0.062
PL01-PTB05-CH01	0.446	0.056	43	-18.879	11.085	7.370	-0.424	0.022
PL01-PTB04-ROA01	0.143	0.124	10	-2.693	-33.268	35.745	-0.216	-0.073
PL01-PTB04-OP01	-0.114	0.062	28	-2.693	7126.198	-7123.465	0.040	-0.074
PL01-PTB04-CH01	0.256	0.044	58	-2.693	-4.885	7.370	-0.208	0.048
PL01-ROA01-CH01	-0.119	0.086	9	-35.745	28.508	7.370	0.133	0.014
PL01-OP01-CH01	0.214	0.045	10	7123.465	-7130.949	7.370	-0.114	0.100

PTB05-PTB04-VSL01	0.364	0.084	74	15.735	-17.089	0.963	-0.391	-0.027
PTB05-PTB04-LTFB01	0.466	0.051	36	15.735	-10.776	-5.411	-0.452	0.014
PTB05-PTB04-ROA01	0.705	0.101	78	15.735	-33.268	16.900	-0.633	0.072
PTB05-PTB04-OP01	0.143	0.028	75	15.735	7126.198	-7142.085	-0.152	-0.009
PTB05-PTB04-NPL02	0.493	0.114	75	15.735	-735.109	718.774	-0.600	-0.107
PTB05-PTB04-SP01	0.589	0.095	72	15.735	-9.205	-7.242	-0.712	-0.123
PTB05-PTB04-IT01	0.562	0.049	78	15.735	-0.077	-16.210	-0.552	0.010
PTB05-PTB04-CH01	0.269	0.035	78	15.735	-4.885	-11.085	-0.235	0.034
PTB05-VSL01-ROA01	0.146	0.065	75	-0.963	-16.061	16.900	-0.124	0.022
PTB05-VSL01-OP01	-0.175	0.052	75	-0.963	7143.214	-7142.085	0.166	-0.009
PTB05-VSL01-NPL02	0.255	0.067	74	-0.963	-718.091	718.774	-0.280	-0.025
PTB05-VSL01-SP01	0.244	0.064	72	-0.963	7.927	-7.242	-0.278	-0.034
PTB05-VSL01-IT01	-0.003	0.047	77	-0.963	17.155	-16.210	-0.018	-0.021
PTB05-VSL01-CH01	-0.287	0.070	76	-0.963	12.363	-11.085	0.315	0.028
PTB05-LTFB01-ROA01	0.105	0.059	33	5.411	-22.366	16.900	-0.055	0.050
PTB05-LTFB01-OP01	-0.190	0.041	32	5.411	7136.845	-7142.085	0.171	-0.019
PTB05-LTFB01-IT01	-0.023	0.054	35	5.411	10.800	-16.210	0.001	-0.022
PTB05-LTFB01-CH01	-0.407	0.052	33	5.411	6.091	-11.085	0.417	0.010
PTB05-ROA01-OP01	-0.310	0.065	77	-16.900	7159.219	-7142.085	0.234	-0.076
PTB05-ROA01-NPL02	0.169	0.048	76	-16.900	-702.089	718.774	-0.215	-0.046
PTB05-ROA01-SP01	0.274	0.040	78	-16.900	23.914	-7.242	-0.228	0.046
PTB05-ROA01-IT01	-0.230	0.056	78	-16.900	33.251	-16.210	0.141	-0.089
PTB05-ROA01-CH01	-0.672	0.111	78	-16.900	28.508	-11.085	0.523	-0.149
PTB05-OP01-NPL02	0.296	0.081	77	7142.085	-7861.166	718.774	-0.307	-0.011
PTB05-OP01-SP01	0.316	0.075	77	7142.085	-7135.140	-7.242	-0.297	0.019
PTB05-OP01-IT01	0.202	0.032	78	7142.085	-7126.076	-16.210	-0.201	0.001
PTB05-OP01-CH01	-0.050	0.037	78	7142.085	-7130.949	-11.085	0.051	0.001
PTB05-NPL02-SP01	0.000	0.075	77	-718.774	726.020	-7.242	0.004	0.004
PTB05-NPL02-IT01	-0.260	0.069	76	-718.774	735.276	-16.210	0.292	0.032
PTB05-NPL02-CH01	-0.556	0.117	76	-718.774	730.464	-11.085	0.605	0.049
PTB05-SP01-IT01	-0.409	0.045	78	7.242	9.355	-16.210	0.387	-0.022
PTB05-SP01-CH01	-0.605	0.080	78	7.242	4.520	-11.085	0.677	0.072
PTB05-IT01-CH01	-0.476	0.056	78	16.210	-4.672	-11.085	0.453	-0.023
PTB04-VSL01-ROA01	-0.217	0.087	74	-17.089	-16.061	33.268	0.118	-0.099
PTB04-VSL01-OP01	0.052	0.073	70	-17.089	7143.214	-7126.198	-0.073	-0.021
PTB04-VSL01-NPL02	0.147	0.113	71	-17.089	-718.091	735.109	-0.071	0.076
PTB04-VSL01-SP01	0.016	0.082	62	-17.089	7.927	9.205	0.043	0.059
PTB04-VSL01-IT01	-0.203	0.064	74	-17.089	17.155	0.077	0.143	-0.060
PTB04-VSL01-CH01	-0.198	0.079	73	-17.089	12.363	4.885	0.159	-0.039
PTB04-LTFB01-ROA01	-0.137	0.084	33	-10.776	-22.366	33.268	0.126	-0.011

PTB04-LTFB01-OP01	0.117	0.049	30	-10.776	7136.845	-7126.198	-0.129	-0.012
PTB04-LTFB01-IT01	-0.094	0.059	32	-10.776	10.800	0.077	0.101	0.007
PTB04-LTFB01-CH01	-0.234	0.051	33	-10.776	6.091	4.885	0.200	-0.034
PTB04-ROA01-OP01	0.240	0.068	74	-33.268	7159.219	-7126.198	-0.247	-0.007
PTB04-ROA01-NPL02	0.385	0.176	75	-33.268	-702.089	735.109	-0.248	0.137
PTB04-ROA01-SP01	0.387	0.185	70	-33.268	23.914	9.205	-0.149	0.238
PTB04-ROA01-IT01	-0.087	0.058	78	-33.268	33.251	0.077	0.060	-0.027
PTB04-ROA01-CH01	-0.236	0.053	78	-33.268	28.508	4.885	0.125	-0.111
PTB04-OP01-NPL02	-0.057	0.064	74	7126.198	-7861.166	735.109	0.141	0.084
PTB04-OP01-SP01	-0.135	0.034	69	7126.198	-7135.140	9.205	0.263	0.128
PTB04-OP01-IT01	-0.218	0.039	75	7126.198	-7126.076	0.077	0.199	-0.019
PTB04-OP01-CH01	-0.175	0.040	75	7126.198	-7130.949	4.885	0.134	-0.041
PTB04-NPL02-SP01	-0.109	0.099	69	-735.109	726.020	9.205	0.116	0.007
PTB04-NPL02-IT01	-0.330	0.095	75	-735.109	735.276	0.077	0.244	-0.086
PTB04-NPL02-CH01	-0.332	0.053	75	-735.109	730.464	4.885	0.240	-0.092
PTB04-SP01-IT01	-0.380	0.093	72	-9.205	9.355	0.077	0.227	-0.153
PTB04-SP01-CH01	-0.278	0.074	72	-9.205	4.520	4.885	0.200	-0.078
PTB04-IT01-CH01	-0.186	0.037	78	-0.077	-4.672	4.885	0.136	-0.050
VSL01-ROA01-OP01	-0.006	0.063	60	-16.061	7159.219	-7143.214	-0.056	-0.062
VSL01-ROA01-NPL02	0.048	0.088	71	-16.061	-702.089	718.091	-0.059	-0.011
VSL01-ROA01-SP01	0.169	0.095	71	-16.061	23.914	-7.927	-0.074	0.095
VSL01-ROA01-IT01	-0.095	0.037	75	-16.061	33.251	-17.155	0.035	-0.060
VSL01-ROA01-CH01	-0.260	0.087	75	-16.061	28.508	-12.363	0.084	-0.176
VSL01-OP01-NPL02	-0.141	0.053	72	7143.214	-7861.166	718.091	0.139	-0.002
VSL01-OP01-SP01	-0.099	0.055	72	7143.214	-7135.140	-7.927	0.147	0.048
VSL01-OP01-IT01	0.030	0.047	76	7143.214	-7126.076	-17.155	-0.017	0.013
VSL01-OP01-CH01	0.064	0.094	70	7143.214	-7130.949	-12.363	-0.098	-0.034
VSL01-NPL02-SP01	0.014	0.068	68	-718.091	726.020	-7.927	0.002	0.016
VSL01-NPL02-IT01	0.004	0.052	73	-718.091	735.276	-17.155	0.030	0.034
VSL01-NPL02-CH01	0.000	0.113	72	-718.091	730.464	-12.363	0.010	0.010
VSL01-SP01-IT01	-0.165	0.053	71	7.927	9.355	-17.155	0.127	-0.038
VSL01-SP01-CH01	-0.077	0.082	69	7.927	4.520	-12.363	0.084	0.007
VSL01-IT01-CH01	-0.190	0.058	74	17.155	-4.672	-12.363	0.120	-0.070
LTFB01-ROA01-IT01	-0.118	0.047	31	-22.366	33.251	-10.800	0.085	-0.033
LTFB01-ROA01-CH01	-0.131	0.075	32	-22.366	28.508	-6.091	0.051	-0.080
LTFB01-OP01-IT01	-0.004	0.050	29	7136.845	-7126.076	-10.800	-0.031	-0.035
LTFB01-IT01-CH01	-0.041	0.052	26	10.800	-4.672	-6.091	0.037	-0.004
ROA01-OP01-NPL02	-0.175	0.111	68	7159.219	-7861.166	702.089	0.142	-0.033
ROA01-OP01-SP01	-0.258	0.125	71	7159.219	-7135.140	-23.914	0.165	-0.093
ROA01-OP01-IT01	0.125	0.047	77	7159.219	-7126.076	-33.251	-0.108	0.017

ROA01-OP01-CH01	0.305	0.087	76	7159.219	-7130.949	-28.508	-0.238	0.067
ROA01-NPL02-SP01	-0.107	0.081	75	-702.089	726.020	-23.914	0.017	-0.090
ROA01-NPL02-IT01	0.142	0.093	76	-702.089	735.276	-33.251	-0.064	0.078
ROA01-NPL02-CH01	0.295	0.198	76	-702.089	730.464	-28.508	-0.133	0.162
ROA01-SP01-IT01	0.093	0.080	78	23.914	9.355	-33.251	0.018	0.111
ROA01-SP01-CH01	0.331	0.162	78	23.914	4.520	-28.508	-0.074	0.257
ROA01-IT01-CH01	-0.036	0.056	78	33.251	-4.672	-28.508	0.071	0.035
OP01-NPL02-SP01	-0.019	0.076	77	-7861.166	726.020	7135.140	-0.006	-0.025
OP01-NPL02-IT01	-0.166	0.048	75	-7861.166	735.276	7126.076	0.186	0.020
OP01-NPL02-CH01	-0.216	0.075	69	-7861.166	730.464	7130.949	0.247	0.031
OP01-SP01-IT01	-0.296	0.056	78	-7135.140	9.355	7126.076	0.291	-0.005
OP01-SP01-CH01	-0.246	0.070	75	-7135.140	4.520	7130.949	0.329	0.083
OP01-IT01-CH01	-0.231	0.064	78	-7126.076	-4.672	7130.949	0.201	-0.030
NPL02-SP01-IT01	-0.152	0.089	76	726.020	9.355	-735.276	0.099	-0.053
NPL02-SP01-CH01	-0.054	0.129	76	726.020	4.520	-730.464	0.076	0.022
NPL02-IT01-CH01	-0.183	0.107	76	735.276	-4.672	-730.464	0.140	-0.043
SP01-IT01-CH01	-0.279	0.087	78	9.355	-4.672	-4.520	0.163	-0.116
ROA51-SP51-IT51	0.179	0.043	8	26.138	-97.254	71.444	0.328	0.507
OP51-SP51-IT51	-0.341	0.040	7	-2026.486	-97.254	2124.124	0.384	0.043

13 Conclusions

Good preparation and professional operation from mobile station provider Timetech and all the participating stations leaded to a successful calibration campaign in 2023. Highlights from this calibration campaign can be concluded as follows:

- Wide range and number of TW stations in participation;
- The Rx2 channel of SATRE modems and SDR Rx channels were taken into calibration with the same NTP setting;
- Both site-mode and baseline-mode calibration are applied in CALR calculations for method comparison.

Meanwhile, new findings have been discovered compared to the previous calibration campaigns, which include the following aspects:

- The phenomenon of diurnals is not dominant.

  During the previous calibration campaign, diurnals in the CCD measurements were the dominant factor which influenced the fluctuations of the CCD data. As a result, the peak value of the TDEV plots normally existed at a 10 hours' time interval for most of the TW stations. However, the TDEV plots of the CCD measurement data followed a -1/2 slope, which was mainly due to white phase noise, for most of the stations in this calibration campaign. This might be caused by the increase in the transmission bandwidth, where the chip rate of 1 Mchip/s was replaced by the chip rate of 2.5 Mchip/s after the previous calibration campaign in 2019.

- PN interference is not significant.

  From the statistics of the on-site measurement data, we can find that both the mean and the deviation of the CCD (and bridged CCD) measurements during even-hour and odd-hour sessions were equivalent. This effect is different from the previous calibration campaigns, where possible interference between the transmitted PN codes was observed. This might be due to the fact that, larger number of participating TW stations made the transmitted PN codes during even and odd hour sessions equivalent. Therefore, no significant PN interference was observed in this calibration campaign.

- Comparisons of site-mode and baseline-mode calibration results

  Testing the quality of the new calibration values using triangle closures revealed that, the baseline results are much closure to zero than the results obtained with the site-mode for most triangle closures. Thus, the baseline-mode calibration values are preferred to be used as the final CALRs applied to the ITU files.

Note that all the CALibration Results (CALRs) obtained by this calibration campaign are only valid under the same operating conditions as the calibration campaign duration. It is each TW station's responsibility to conserve the same operating conditions in the long term in order to maintain the validity of the CALRs.

14 Acknowledgement

The authors would like to express special thanks to Dr. Thorsten Feldmann from Timetech and Dr. Dirk Piester from PTB for their great contribution to uncertainty evaluations for this document.

Throughout the whole calibration campaign, technical support with high professionalism was received from the TimeTech team. The authors deeply appreciate their engagement and dedication.

The accomplishment of this successful calibration campaign relied on all the support, collaboration, and efforts from all the participating stations and colleagues. And all the gratitude to all the partners.

Part II

GSOP TWSTFT CALIBRATION REPORT

This part includes the calibration results of TWSTFT links between SP, PTB, IT, OP, and ROA.

TWSTFT CALIBRATION REPORT

GSOP

UNCLASSIFIED

Prepared by: P. Ortega (ROA)

Approved by: H. Esteban (ROA)

Authorized by: I. Sesia (INRIM)

Customer Approval Approval level: R

Code: GAL-TN-ROA-GSOP-2024001

Version: 2

Date: 16/07/2024

TABLE OF CONTENTS

List of tables and figures

1. INTRODUCTION

1.1. SCOPE OF THE DOCUMENT

This document presents the results of the 2023 campaign intended for the calibration of the time transfer links established via TWSTFT between five UTC(k) laboratories associated to the Galileo Time Service Provider. It was produced in the frame of WP 10.1.4.3 of the GSOP contract between INRiM and ROA.

This is the fourth calibration campaign involving a mobile TWSTFT station since the full Deployment and Operations phase of the Galileo Program. The latest calibrations took place in summer 2014, spring 2016 and the third in spring 2019 the PHASE I and finally the PHASE II in March 2020.

The calibration was carried out from August to November 2023 and involved UTC(k) laboratories previously mentioned.

1.2. CHANGE FORECAST

This document reports on the work done during the TWSTFT calibration campaign in 2023, in the frame of the Galileo TSP contract. No further issues are planned.

1.3. DOCUMENT STRUCTURE

Section 1 of this document gives the introduction, comprising the scope of the document, document structure and a document baseline (in terms of applicable and reference documents and acronyms used).

Section 2 presents an overview of the contractual baseline regarding time transfer between the partners associated with the TSP. It describes the current contractual relation between UTC(k) laboratories and the provider of the satellite transponder capacity used in the time transfer via TWSTFT.

Section 3 describes the calibration campaign undertaken between August and November of 2023 and lists the involved institutes and relevant parameters.

Section 4 presents the theoretical framework for a calibration of TWSTFT links involving a mobile station.

Section 5 illustrates the installation of the mobile station used and contains the measurement schedule adhered to.

Section 6 states the main problems encountered during the campaign and shows the collection of raw results obtained from the calibration campaign.

Section 7 explains how the determined CALR value shall be introduced in TWSTFT results reports.

Appendix I presents the calibration results for stations employing Software-Defined Radio (SDR) in reception.

Appendix II illustrates the TWSTFT calibration results for stations utilizing SATRE modem channel 2 (Rx2) in reception.

This Report concludes with a summary of the lessons learnt throughout this calibration campaign (Section 8).

1.4. DOCUMENTS

1.4.1. APPLICABLE DOCUMENTS

The following documents are applicable and have been used as the basis for this work.

Table 1-1: Applicable documents.

Ref.	Title	Code	Version	Date
AD01	Time and geodetic Validation Facility Requirements Document	ESA-DTEN-NG-REQ-03766	1.1	

1.4.2. REFERENCE DOCUMENTS

The following documents are used as reference in this document.

Table 1-2: Reference documents.

Ref.	Title	Code	Version	Date
RD01	Directive for operational use and data handling in two-way satellite time and frequency transfer (TWSTFT)	Rapport BIPM-2011/01, Bureau International des Poids et Mesures, Sèvres, 25 pp., 2011		2011
RD02	The operational use of two-way satellite time and frequency transfer employing PN codes	ITU Radiocommunication Sector, Recommendation ITU-R TF.1153-4, Geneva, Switzerland, 2015.		08/2015
RD03	Time transfer with nanosecond accuracy for the realization of International Atomic Time	Metrologia, 45, (2008), pp. 185 – 198		2008
RD04	TWSTFT Calibration Guidelines for UTC Time Links		3.0	2016
RD05	Galileo TVF TWSTFT Relative Calibration Report	TGVF-PTB-1F000-RP0001	4.1	June 2012
RD06	Galileo TVF TWSTFT Relative Calibration Report	TGVF-PTB-1F000-RP0002	1.0	March 2013
RD07	Galileo IOV TVF TWSTFT PTF1 Calibration Report	TGVF-PTB-1F000-RP0003	3.0	March 2014
RD08	Galileo TGVF-FOC TWSTFT Calibration Report	GAL-TN-ROA-TGVFFOC-20036	2.0	2015-02-16
RD09	Galileo GAL-TN-ROA-TGVFFOC Calibration Report	GAL-TN-ROA-TGVFFOC-20056	1.0	06/09/2016
RD10	TVFFOC TWSTFT Calibration: Site Preparation document checklist	GAL-TN-ROA-GSOP-001	2.4	2016-05-24
RD11	MODEL SR620 Universal Time Interval Counter, Stanford Research Systems, Revision 2.7 (2006).		2.7	2006
RD12	J. Achkar; D. Rovera; I. Sesia; P. Tavella, "Determination of differential delays of earth stations in Paris and Torino from the calibrated OP-IT TWSTFT link", in Proceedings of 2016 European Frequency and Time Forum (EFTF).	DOI:10.1109/EFTF.2016.7477800	2.7	2016
RD13	TWSTFT Calibration	GAL-TN-ROA-GSOP-2019001	4	2019

1.5. ACRONYMS AND ABBREVIATIONS

Table 1-3: List of Acronyms and Abbreviations

Acronym	Definition
AGS	Americom Government Services
AOS	Astrogeodynamical Observatory of the Polish Academy of Sciences
BIPM	Bureau International des Poids et Mesures
CCTF	Consultative Committee for Time and Frequency
CSD	Combined Standard Deviation
C/N0	Carrier-to-noise ratio
EPS	European Participating Stations (in TWSTFT)
ESA	European Space Agency
ESXi	Is an enterprise-class, type-1 hypervisor developed for deploying and serving virtual computers. The name ESXi originated as an abbreviation of Elastic Sky X "integrated"
FDIS	Frequency Distribution Amplifier
FOC	Full Operational Capacity
GCC	Galileo Control Centre
GEO	Geo-stationary satellite
GMS	(Galileo) Ground Mission Segment
GPS	Global Positioning System
GST	Galileo System Time
GST(MC)	GST physical realization point within PTF
IERS	International Earth Rotation and Reference Systems Service
IIOTIC	Intelligent In/Out and Time Interval Counter

Acronym	Definition
IOV	In-Orbit Validation
INRIM	Istituto Nazionale di Ricerca Metrologica
ITU	International Telecommunication Union
LTFB	Laboratoire Temps Fréquence de Besançon
METAS	Federal Institute of Metrology
MJD	Modified Julian Date
NMI	National Metrology Institute
NPL	National Physical Laboratory
OP	LNE-SYRTE, Observatoire de Paris
PDIS	Pulse distribution amplifier
PL	Warsaw, Poland
PTB	Physikalisch-Technische Bundesanstalt
RISE	Research Institutes of Sweden
ROA	Real Instituto y Observatorio de la Armada
SOW	Statement of Work
TAI	International Atomic Time
TAS (- F)	Thales Alenia Space (- France)
TDEV	Time Deviation. Is a measure of time stability based on the modified Allan variance
TIC	Time Interval Counter
TIM	TimeTech GmbH, Stuttgart, Germany. Also the fixed station at TimeTech, used in calibration experiments
TVF	Timing Validation Facility
TSP	Time Service Provider
TWSTFT	Two-Way Satellite Time and Frequency Transfer
UTC	Coordinated Universal Time
UTC(k)	Version of UTC realized at each of the contributing NMI(k)s
VSL	Dutch Metrology Institute
WG	Working Group
WP	Work Package
	TWSTFT specific acronyms
ADUO	Additional diurnal of unknown origin
CALR(i, k)/CALR	Calibration value, which has to be added to the raw TWSTFT measurement result between stations (i, k) to yield the true time difference between the time scale maintained at stations i and k.
CC	Common clock.
CCD(i, k)	Common-clock difference, TWSTFT measurement result between two TWSTFT setups (i, k) at one site, connected to the same clock.
CI	Calibration Identification
DLD(i)	Difference of signal propagation delay through the transmit and receive path of station i, Tx(i) – Rx(i).
ESDVAR(k)	Earth station delay variation, with respect to the Earth station delay at the time of calibration (if available).
MOB	Mobile station, short form for a transportable TWSTFT ground station used in calibration experiments.
REFDELAY	Reference delay, time difference between the local time scale and the modem 1PPS output synchronous with the Tx signal.
Rx(i)	Signal delay in the receive path of TWSTFT station i.
SCD(i)	Sagnac delay for a signal propagating from the GEO satellite to station i.
SCU(i)	Sagnac delay for a signal propagating from the station i to the GEO satellite.
SP(i)	Complete signal path delay from station i to station k, SPU(k) + SPT(k) + SPD(i)
SPD(i)	Signal path downlink delay
SPT(i)	Signal path delay through the transponder from station i to station k.

Acronym	Definition
SPU(i)	Signal path uplink delay
TS(i)	Local time scale, physically represented by the 1PPSTX signal generated by the modem, i being 1 for station 1 and 2 for station 2.
TW(i)	Counter reading in TWSTFT station i.
TX(i)	Signal delay in the transmit path of the TWSTFT station i.

2. TIME TRANSFER IN THE GALILEO TSP CONTEXT

2.1. OVERVIEW

The operation of a Global Navigation Satellite System requires accurate synchronization among the various elements in the ground and space segment. The core navigation function of Galileo is based on Galileo System Time (GST) as realized in the Precise Timing Facilities (PTF). They are located in the Galileo Control Centres (GCC) which are part of the Ground Mission Segment (GMS). The additional use of Galileo as a time dissemination system requires that the relation between GST and international time references such as Coordinated Universal Time (UTC) and International Atomic Time (TAI), maintained by the Bureau International des Poids et Mesures (BIPM) with input from the International Earth Rotation and Reference Systems Service (IERS), is well defined and broadcast in the Galileo Signal in Space. The required support for such "metrological time-keeping" is provided by the Time Validation Facility which is a part of the Time and Geodetic Validation Facility.

During the GalileoSat Development and Validation ("IOV") phase, only PTF1, located in the GCC-2 at Fucino Space Centre, Ortucchio (L'Aquila), Italy, was operational. PTF2 (Oberpfaffenhofen, DE) accomplished the readiness in 2014, during the Deployment and Operations ("FOC") phase of the Galileo Program. This Report deals with the calibration of the time links between PTF1 and PTF2, and associated UTC(k) laboratories, INRIM, OP, PTB, ROA, and SP based on TWSTFT [RD01, RD02]. In the case of INRIM and ROA, the time links were calibrated involving two TW stations: the main station (ROA01, IT02) and spare one (ROA02, IT01). This exercise is the sixth of its kind. The first and second ones (March 2012 [RD05], and March 2013 [RD06]) were done with reference to preceding GPS-based calibrations. The third, fourth and fifth ones (October-November 2013 [RD07], June-August 2014 [RD08], and April-June 2016 [RD09]), involved the same traveling TWSTFT station and followed the method described in [RD03], similarly to the current one.

In this context the present campaign followed the TWSTFT calibration guidelines [RD04.

2.2. TWSTFT OPERATION STATUS

Satellite transponder capacity with the required connectivity between Europe (extending to Poland and Sweden) and the US (extending to Boulder, Colorado, in the West), is very scarce. From summer 2009 onwards, the Telesat owned satellite T-11N at the location 37.5 degrees West longitude has been used. The access to the satellite was initially managed by Americom Government Services (AGS). 13 institutes - 2 in the US, and 11 in Europe, including TimeTech GmbH, Stuttgart, Germany (in short TimeTech) as industrial partner - agreed on the contract with AGS. The two Galileo PTFs were integrated into the network at a later stage. The European participating stations (EPS), among them the TVF partners mentioned above, signed an Agreement with PTB dealing with the cost sharing, the practice of invoicing, and other administrative issues. Since July 2011 the lease agent for the satellite transponder capacity was changed to RiteNet, MD. The current contract runs from January 1, 2021 to December 31, 2025.

The technical parameters of the satellite were:

Beacon frequency: 11699.5 MHz

<u>For the Europe to Europe link:</u>

Carrier ID, 112677
Uplink, 14253.950 MHz, horizontal polarization
Downlink, 10953.950 MHz, vertical polarization

<u>For the transatlantic link:</u>

In Europe:

Carrier ID, 112673
Uplink, 14047.740 MHz, horizontal polarization
Downlink, 11497.060 MHz, vertical polarization

2.3. CONTRACTUAL ARRANGEMENTS FOR GALILEO TSP TWSTFT CALIBRATIONS

According to the GSOp Statement of Work and TSP contract, a calibration exercise involving a traveling TWSTFT station and comprising PTF1, PTF2, INRIM, OP, PTB, ROA, and SP, should be organized and evaluated by ROA every three years. The last one took place from February 26th to May 26th of 2019 (Phase I), and from the 10th to the 27th of March of 2020 (Phase II).

The provision of the mobile TWSTFT station (designated as MOB in this Report) and its operation was directly subcontracted to TimeTech by INRiM.

3. ORGANIZATION OF THE CAMPAIGN

3.1. DIRECTLY INVOLVED INSTITUTES AND ORGANISATIONS

INRIM:
Dr Ilaria Sesia
Istituto Nazionale di Ricerca Metrologica, Optics Division
Strada delle Cacce, 91
10135 TORINO, Italy

LNE-SYRTE:
Dr Joseph Achkar
LNE-SYRTE,Observatoire de Paris, Université PSL, CNRS, Sorbonne Université
61 avenue de l'Observatoire
75014 PARIS, France

PTB:
Dr Dirk Piester
Physikalisch-Technische Bundesanstalt, WG 4.42 Time Dissemination
Bundesallee 100
D-38116 Braunschweig, Germany

RISE:
Dr Kenneth Jaldehag
Research Institutes of Sweden
Measurement Technology - Time and Frequency
Brinellgatan 4, 504 62 Borås, Sweden

ROA:
Dr Héctor Esteban
Real Instituto y Observatorio de la Armada
Sección de Hora
Plaza de las Tres Marinas s/n
11100 San Fernando (Cádiz), Spain

TIM:
Dr Thorsten Feldmann
TimeTech GmbH
Curiestrasse 2
D-70563 Stuttgart, Germany

3.2. TRAVEL SCHEDULE AND MEASUREMENT PERIODS

3.2.1. TRAVEL SCHEDULE

Table 3-1: Travel Schedule adhered to by the mobile TWSTFT station (MOB).

From	To	Distance	Time to travel
Stuttgart	Warsaw	1135 km	12 hr
Warsaw	Poznan	314 km	4 hr
Poznan	Braunschweig	487 km	6 hr
Braunschweig	Delft	483 km	6 hr
Delft	Besançon	693 km	9hr
Besançon	San Fernando	1997 km	20 hr
San Fernando	Paris	1853 km	19 hr
Paris	London	482 km	7 hr
London	Boras	1610 km	20 hr
Boras	Stuttgart	1312 km	16 hr
Stuttgart	Bern-Wabern	333 km	4 hr
Bern-Wabern	Turin	423 km	5 hr
Turin	Braunschweig	1096 km	12 hr
Braunschweig	Stuttgart	516 km	6 hr

Due to air conditioning issues, the mobile TWSTFT station (MOB) returned to TIM (Stuttgart), after operation at Rise (Boras) to carry out repairs. This event changed the initial schedule and delayed the calibration campaign until the 29th of November, instead of the 10th of November, as originally planned.

3.2.2. EFFECTIVE MEASUREMENT SCHEDULE

Table 3-2: Periods of data taking of MOB while installed at the various sites.

MOB at	Week#	From Date and Time (UTC)	To Date and Time (UTC)	MJD
TIM CCD1	34	Tue, 15 Aug 2023 14:00	Fri, 18 Aug 2023 15:00	60170 – 60174
PL	35	Wed, 23 Aug 2023 20:00	Mon, 28 Aug 2023 05:00	60179 – 60184
AOS	36	Mon, 28 Aug 2023 15:00	Fri, 01 Sep 2023 16:00	60184 – 60188
PTB CCD1	37	Mon, 04 Sep 2023 11:00	Fri, 08 Sep 2023 05:00	60191 – 60195
VSL	38	Tue, 12 Sep 2023 13:00	Fri, 15 Sep 2023 06:00	60199 – 60202
LTFB	39	Mon, 18 Sep 2023 15:00	Fri, 22 Sep 2023 06:00	60205 – 60209
ROA	40	Sat, 23 Sep 2023 18:00	Thu, 28 Sep 2023 06:00	60210 – 60215
OP	41	Mon, 02 Oct 2023 17:00	Sat, 07 Oct 2023 05:00	60219– 60224
NPL	42	Mon, 09 Oct 2023 16:00	Fri, 13 Oct 2023 07:00	60226 - 60230
RISE	43	Mon, 16 Oct 2023 11:00	Thu, 19 Oct 2023 14:00	60233 – 60236
TIM repair	44	Mon, 23 Oct 2023 21:30	Tue, 24 Oct 2023 10:30	60240 – 60241
METAS	44	Fri, 27 Oct 2023 13:30	Tue, 31 Oct 2023 04:00	60244 – 60248
INRIM	45	Tue, 31 Oct 2023 18:00	Sat, 04 Nov 2023 06:00	60248 – 60252
PTB CCD2	46	Tue, 07 Nov 2023 13:00	Mon, 13 Nov 2023 06:00	60255 – 60261
TIM CCD2	47, 48	Tue, 14 Nov 2023 15:00	Mon, 27 Nov 2023 06:00	60262 – 60275

The mobile TWSTFT station was unavailable during the operational stay in LTFB the 18th of August in the period from 10:50 to 15:15 and also at TimeTech dependencies from 10:00 on the 19th of November to 16:00 on the 20th of November.

3.3. TWSTFT STATION INFORMATION

Table 3-3: Designation and location of TWSTFT stations involved

T&F Lab. Code	Location	TWSTFT St code even hours	TWSTFT St code odd hours	Position deg: min: sec
INRIM	Torino IT	IT21	IT31	LA: N 45:00:53.987 LO: E 007:38:20.686 HT: 306.6 m
INRIM	Torino IT	IT01	IT11	LA: N 45:00:53.987 LO: E 007:38:20.686 HT: 306.6 m
ROA	San Fernando ES	ROA01	ROA11	LA: N 36:27:47.784 LO: W 006:12:22.682 HT: 80.8 m
ROA	San Fernando ES	ROA21	ROA31	LA: N 36:27:47.784 LO: W 006:12:22.847 HT: 80.8 m
LNE-SYRTE (OP)	Paris FR	OP01	OP11	LA: N 48:50:09.236 LO: E 002:20:05.873 HT: 78.0 m
RISE	Boras SE	SP01	SP11	LA: N 57:42:55.000 LO: E 012:53:27.000 HT: 225.0 m
RISE	Boras SE	SP21	SP31	LA: N 57:42:55.000 LO: E 012:53:27.000 HT: 225.0 m
PTB	Braunschweig DE	PTB05	PTB15	LA: N 52:17:49.787 LO: E 010:27:37.966 HT: 143.4 m
PTB	Braunschweig DE	PTB04	PTB14	LA: N 52:17:49.787 LO: E 010:27:37.966 HT: 143.4 m
TIM	Stuttgart DE	TIM01	TIM11	LA: N 48:44.16.272 LO: E 09:06:45.106 HT: 529.0 m
MOB	Stuttgart DE	MOB02	MOB12	Mobile

Table 3-3 summarizes the TWSTFT stations involved, including MOB which was shipped in sequence between TimeTech (TIM), INRIM, ROA, OP, SP and PTB. The station code (columns 3 and 4 in Table 3-33) is part of the designation of data lines [RD01, RD02] in which measurement results are reported.

4. BACKGROUND INFORMATION ON TWSTFT

4.1. BACKGROUND INFORMATION ON TWSTFT

In this section, we recall the theoretical background and derive the equations necessary for the determination of calibration constants. We follow, if possible and expedient, the description and naming of the ITU-R Recommendation TF.1153-4 [RD02] and extend or deviate thereof only if necessary. In particular, we use some of the common abbreviating acronyms in the text and in the equations, which are listed in Table 1-3.

TWSTFT between two remote stations 1 and 2 is based on two combined coincident measurements at both stations. Each measurement represents the determination of the time of arrival of a radio signal that is phase coherent to the remote atomic time scale and transmitted from the remote station with respect to the local time scale. The measurement result obtained at one site, e.g. TW(1), is the time difference reading from a time-interval counter (TIC). It comprises the difference between the two time scales involved and also the complete delay along the signal path from station 2 to station 1. For the ground station, we distinguish only between the transmission (TX) and receiving (RX) parts. We use Figure 4-1 to describe the individual signal delay components, e. g., for the signal received at site 1.

Figure 4-1: Schematics of a TWSTFT set-up, including the designation of the various signal delays [RD03]

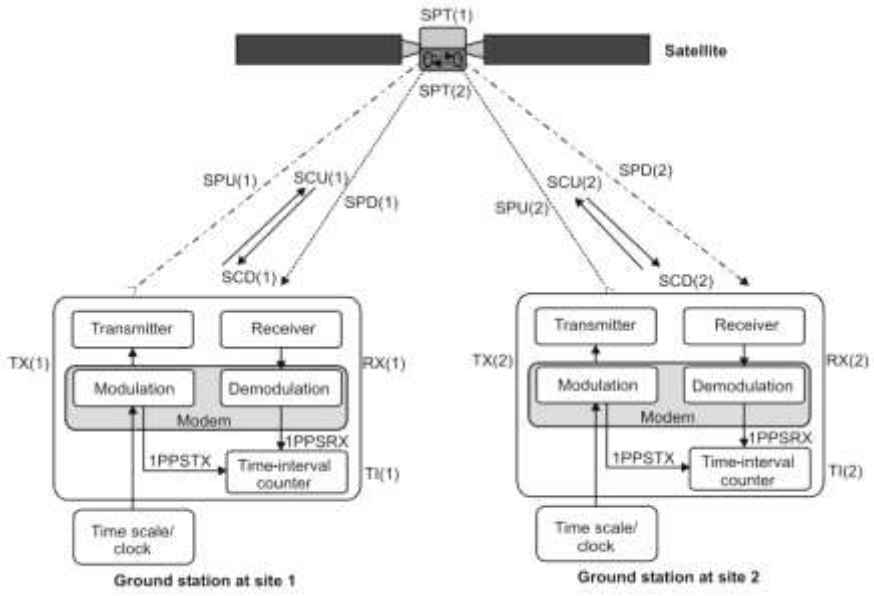

The signal delay consists of the remote site transmitter delay TX(2), the overall signal path delay to the satellite and back to site 1 on Earth, SP(2) (sum of the signal path uplink delay SPU(2), the satellite path delay through the transponder SPT(2), and the signal path downlink delay SPD(1)), the local receiver delay RX(1), and the delay due to the Sagnac effect, which is computed from the positions of the ground stations and the geostationary satellite. We account for the Sagnac effect according to [RD02] by introducing Sagnac corrections for both the uplink and downlink to and from the satellite, SCU(2) = -SCD(2) and SCD(1) = -SCU(1), respectively, which have to be determined separately from the positions of the stations and the satellite. The new version of [RD02], in force since august 2015, considers that the earth is not perfectly spherical. Instead, it is considered as an ellipsoid at first approximation, and takes into account the transformation from geodetic to geocentric coordinates.

At site 2, the equivalent measurement is carried out simultaneously, and we obtain two measurement results, TW(1) and TW(2):

$$(1) \qquad \mathrm{TW}(1) = \mathrm{TS}(1)\text{-}\mathrm{TS}(2) + \underbrace{\mathrm{TX}(2) + \mathrm{SP}(2) + \mathrm{RX}(1) + \mathrm{SCD}(1)\text{-}\mathrm{SCD}(2)}_{\text{signal delay on site 1}}.$$

(2) $$\mathrm{TW(2)} = \mathrm{TS(2)\text{-}TS(1)} + \underbrace{\mathrm{TX(1)} + \mathrm{SP(1)} + \mathrm{RX(2)} + \mathrm{SCD(2)\text{-}SCD(1)}}_{\text{signal delay on site 2}}.$$

We assume at this stage a complete reciprocity of the signal path: SP(1) = SP(2). As mentioned above, the signal path consists of three components, SPU, SPT, and SPD. The satellite transponder delay cancels only if both ground stations transmit via a single transponder on the satellite, which requires that both stations are within the same antenna footprint of the satellite. This is the situation prevailing for all links within Europe and thus valid in this campaign.

The timescale difference can be computed by subtraction of (2) from (1):

(3) $$\mathrm{TS(1)} - \mathrm{TS(2)} = 0.5 * [\mathrm{TW(1)} - \mathrm{TW(2)}] + \\ + \{0.5 * [\mathrm{DLD(1)} - \mathrm{DLD(2)}] - [\mathrm{SCD(1)} - \mathrm{SCD(2)}]\}.$$

Here, $\mathrm{DLD(i)}$ is the signal-delay difference between the transmitter and the receiver part of station i, $\mathrm{DLD(i)} = \mathrm{TX(i)} - \mathrm{RX(i)}$. The calibration value for the link between sites 1 and 2, is defined as the terms in curly brackets in eq. 3:

(4) $$\mathrm{CALR(1,2)} = + 0.5 * [\mathrm{DLD(1)} - \mathrm{DLD(2)}] - [\mathrm{SCD(1)} - \mathrm{SCD(2)}].$$

For its determination, two different approaches are in principle possible, the so-called site mode which requires common clock measurements taken at each site and the baseline mode which avoids that. Both methods include the use of a mobile TWSTFT station (MOB), in addition to the permanent ground stations. According to (3) and (4), a calibration constant can then be calculated from:

(5) $$\mathrm{CALR(1,2)} = [\mathrm{TS(1)} - \mathrm{TS(2)}]_{\mathrm{LINK}} - 0.5 * [\mathrm{TW(1)} - \mathrm{TW(2)}].$$

The baseline mode is subsequently described in more detail. First, the MOB is operated in parallel to station 1, both connected to a single clock. Eq. 3 is, thus, simplified to:

(6) $$0 = 0.5 * [\mathrm{TW(1)} - \mathrm{TW(MOB@1)}] + \{0.5 * [\mathrm{DLD(1)} - \mathrm{DLD(MOB)}]\}.$$

We define the common-clock difference, CCD(MOB@1,1), as the last addend in (6), and determine it consequently from a TWSTFT measurement between 1 and MOB as

(7) $$\mathrm{CCD(MOB@1,1)} = 0.5 * [\mathrm{TW(MOB@1)} - \mathrm{TW(1)}] = \\ = 0.5 * [\mathrm{DLD(1)} - \mathrm{DLD(MOB)}].$$

Note that $\mathrm{DLD(MOB)}$ is a term that is assumed to be constant during the whole campaign and thus independent of the location where MOB is operated. This assumption cannot be proven during the campaign. Only at its end a second common-clock measurement at the station where the campaign started may give evidence.

From site 1 the MOB is transported to site 2 and connected to the corresponding time scale TS(2). The time-scale difference $\mathrm{TS(1)} - \mathrm{TS(2)}$ can be measured by performing a TWSTFT measurement between the MOB located at site 2 and site 1; combining (3) with (7), this last particularized for site 2, and considering (6), we get:

(8) $$[\mathrm{TS(1)} - \mathrm{TS(2)}]_{\mathrm{LINK}} = 0.5 * [\mathrm{TW(1)} - \mathrm{TW(MOB@2)}] - \mathrm{CCD(1,MOB@1)} + \\ - [\mathrm{SCD(1)} - - \mathrm{SCD(2)}]$$

and therefore, according to (5):

(9) $$\mathrm{CALR(1,2)} = \mathrm{CCD(MOB@1,1)} +$$

$$-0.5 * \left[\left(\mathrm{TW(MOB@2)} - \mathrm{TW(1)}\right) - \left(\mathrm{TW(2)} - \mathrm{TW(1)}\right)\right] + \\ - \mathrm{SCD(1)} + \mathrm{SCD(2)}.$$

Where, the second term is known as Bridged $\mathrm{CCD(MOB@2,2)}$.

The site mode was the approach used between pairs of UTC(k) laboratories. This approach of performing a calibration includes the repetition of the CCD measurement described by (7) at a second site. This gives a second common-clock difference value at site 2:

(10) $$\mathrm{CCD(MOB@2,2)} = 0.5 * [\mathrm{TW(MOB@2)} - \mathrm{TW(2)}]$$

Forming (7) – (10) gives:

(11) $$\mathrm{CCD(MOB@1,1)} - \mathrm{CCD(MOB@2,2)} = 0.5 * [\mathrm{DLD(1)} - \mathrm{DLD(MOB)}] - 0.5 * [\mathrm{DLD(2)} - \mathrm{DLD(MOB)}] = \\ = 0.5 * [\mathrm{DLD(1)} - \mathrm{DLD(2)}].$$

And thus from (4):

(12) $$\mathrm{CALR(1,2)} = [\mathrm{CCD(MOB@1,1)} - \mathrm{CCD(MOB@2,2)}] - [\mathrm{SCD(1)} - \mathrm{SCD(2)}].$$

4.2. THE REFDELAY ISSUE

At this point it is necessary to introduce the quantity REFDELAY. According to [RD01, RD02] it represents the time difference between the local reference point for time scale TS(k) and the physical signal involved in the measurement process, 1PPSTX(k). It is reported in a separate column in the standard ITU file according to [RD02]. Software adhering to the standard includes it in the calculation, e.g. when CCD shall be calculated. The physical connections between the local time scale reference points and the two TWSTFT ground stations involved differ in general. As an example, Figure 5-2 depicts the situation where the 10 MHz and the two 1 PPS signals connected to the TWSTFT ground station, here in particular the MOB, are from the same physical source. In this case, REFDELAY is just a constant that would change only if cable connections are changed.

More specific than (7), one has to consider

(13) $$\mathrm{CCD(MOB@k,k)_{true}} = 0.5*\left(\mathrm{TW(MOB@k)} - \mathrm{TW(k)}\right) + \\ + \mathrm{REFDELAY(MOB@k)} - \mathrm{REFDELAY(k)} = \\ = 0.5 * \left(\mathrm{TW(MOB@k)} - \mathrm{TW(k)}\right) + \mathrm{REFDLYdiff(MOB@k,k)}.$$

We note that the calculation involves only differences of REFDELAY values, mobile station minus fixed station. At each site, these differences were constant. This facilitated the evaluation since the ITU files for the station MOB do not automatically contain the correct REFDELAY values. The use of (13) is appropriate for all links involved. The delay between the fast-rising pulses that define the local reference point for time scale TS(k) and the physical signal connected to MOB, was determined using the same time interval counter at all stations, such that this counter's systematic time-interval measurement uncertainty involved in the measurement process was negligible [RD13]. The values REFDLYdiff and the Sagnac Corrections are reported in Table 4-1.

Table 4-1: Correction of ITU files provided by MOB and Sagnac Corrections

Location of MOB installation, ID station	REFDLY(MOB@k) [ns]	REFDLY(UTC(k)) [ns]	REFDLYdiff(MOB@k,k) [ns]	SCD(Loc) [ns]
TIM CCD1	101.066	705.791	-604.725	104.78
TIM CCD2	101.048	706.072	-605.024	104.78
INRIM	168.818	834.009	-665.191	109.52
ROA	295.009	964.858	-669.849	91.26
OP	79.454	828.280	-748.826	92.18
SP	38.564	784.720	-746.156	90.01
PTB (PTB05) CCD1	20.228	736.134	-715.906	99.32
PTB (PTB05) CCD2	53.035	736.134	-683.009	99.32
PTB (PTB04) CCD1	20.228	777.949	-757.721	99.32
PTB (PTB04) CCD2	53.035	777.949	-724.914	99.32

Combining equations 9 and 13, we get:

$$\begin{aligned}(14)\quad \mathrm{CALR}(1,2) = {} & \mathrm{CCD}(\mathrm{MOB@1},1) + \mathrm{REFDLYdiff}(\mathrm{MOB@1},1) + \\ & -0.5 * \left[\left(\mathrm{TW}(\mathrm{MOB@2}) - \mathrm{TW}(1)\right) - \left(\mathrm{TW}(2) - \mathrm{TW}(1)\right)\right] + \\ & -\mathrm{REFDLYdiff}(\mathrm{MOB@2},2) - \mathrm{SCD}(1) + \mathrm{SCD}(2).\end{aligned}$$

Likewise, combining equations 12 and 13 for the site-mode, we get:

$$\begin{aligned}(15)\quad \mathrm{CALR}(1,2) = {} & \mathrm{CCD}(\mathrm{MOB@1},1) + \mathrm{REFDLYdiff}(\mathrm{MOB@1},1) + \\ & -\mathrm{CCD}(\mathrm{MOB@2},2) - \mathrm{REFDLYdiff}(\mathrm{MOB@2},2) + \\ & -\mathrm{SCD}(1) + \mathrm{SCD}(2).\end{aligned}$$

Finally, eq. 18 shows how the calibration value enters in the calculation of time scale differences (simplified from [RD01]):

$$\begin{aligned}(16)\quad \mathrm{TS}(1) - \mathrm{TS}(2) = {} & \\ & + 0.5 * \left[\mathrm{TW}(1) - \mathrm{TW}(2)\right] + \mathrm{REFDELAY}(1) - \mathrm{REFDELAY}(2) + \mathrm{CALR}(1,2).\end{aligned}$$

4.3. CALIBRATION METHOD

In order not to perturb the operations of PTF1 and PTF2 and to follow the same procedure than in previous calibration, the baseline mode (eq. 14) was used during the current campaign for the calibration of all the links.

In the baseline mode, the net result of previous equation entails cancellation or at least mitigation of MOB code effect, so avoiding REFDLYdiff and Sagnac effect, eq. 14 for A and B stations, it becomes:

$$\begin{aligned}\mathrm{CCD}(\mathrm{MOB@A},\mathrm{A}) - 0.5 * \left[\left(\mathrm{TW}(\mathrm{MOB@B}) - \mathrm{TW}(\mathrm{A})\right) - \left(\mathrm{TW}(\mathrm{B}) - \mathrm{TW}(\mathrm{A})\right)\right] = \\ = 0.5 * \left(\mathrm{MOB}_{\mathrm{M}}^{\mathrm{A}} - \mathrm{A}_{\mathrm{A}}^{\mathrm{M}}\right) - 0.5 * \left[\left(\mathrm{MOB}_{\mathrm{M}}^{\mathrm{A}} - \mathrm{A}_{\mathrm{A}}^{\mathrm{M}}\right) - \left(\mathrm{B}_{\mathrm{B}}^{\mathrm{A}} - \mathrm{A}_{\mathrm{A}}^{\mathrm{B}}\right)\right] \\ = 0.5 * \left(\mathrm{B}_{\mathrm{B}}^{\mathrm{A}} - \mathrm{A}_{\mathrm{A}}^{\mathrm{B}}\right)\end{aligned}$$

where the subscripts and superscripts indicate the code transmitted and received respectively, finally resulting in the expected combination for the TW link between A and B stations.

5. OPERATION OF MOB

For completeness of this document we repeat part of the documentation provided as [RD10].

5.1. SIGNAL SCHEME

Figure 5-1 shows a simplified block diagram of the mobile TSTFT calibration station and the interfaces between the institute or laboratory and the mobile station. UTC(k) designates the reference time scale of the institute. If the UTC(k) interface is not directly accessible, the laboratory provides a signal UTC CAL along with the offset and the uncertainty with respect to UTC(k).

Figure 5-1: Interfaces to the MOB station – Cable Identification

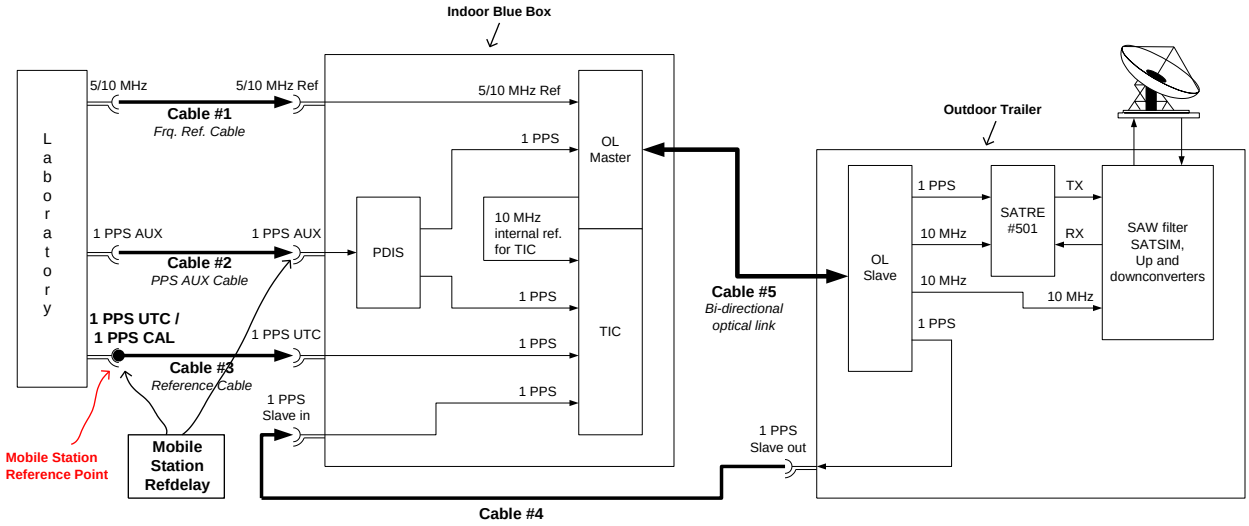

Table 5-1: Description of cables used

Cable #	Signal name	Cable length	Cable type	Cable diameter	Connectors	Connector diameter
Cable #1	5/10 MHz Ref	7.5 m	RG223	5.40 mm	N(M) - N(M)	19 mm
Cable #2	1 PPS AUX	7.5 m	RG223	5.40 mm	N(M) - N(M)	19 mm
Cable #3	1 PPS UTC	7.5 m	Sucotest 18	4.60 mm	N(M) - N(M)	19 mm
Cable #4	Test cable	200 m	Ecoflex 10	6.40 mm	N(M) - N(M)	19 mm
Cable #5	Optical cable	200 m	LWL-4HMC	6.00 mm	HMC - HMC	23 mm

All 5 cables are provided with the traveling equipment. The cable #4 is a test cable used to verify the 1 PPS of the optical link slave with the TIC inside the Blue Box: It is used to check that there is no error of outdoor synchronization with respect to 1 PPS AUX. The use of the Reference cable #3 is mandatory, since the Reference Point of the mobile station is defined at the endpoint of this cable.

5.2. OPLINK PRINCIPLE OF OPERATION

The optical link (OPLINK) connecting the indoor "Master" with the outdoor "Slave" in the mobile station refers to all time interval measurements to the 1 PPS AUX input, independent of the phase of the reference frequency. The TIC that is an integral part of the Master replaces the external counter that was used to be shipped around in previous years. It measures the 1 PPS signal from PDIS inside Blue Box to Master Oplink, 1 PPS from Oplink Slave (via cable #4) and 1 PPS UTC signal with respect to 1 PPS AUX. In case that 1 PPS UTC cannot be provided continuously to the input of cable #3, it should be connected at start-up of the blue box, and some 1 PPS signal, potentially offset from UTC(k), should if available, be connected to #3 at all times. The 1 PPS Auxiliary signal from the laboratory to the Blue Box is regenerated in the trailer. This signal is verified by connecting it to the TIC in the Blue Box using cable #4. The installation of this cable is mandatory and is needed for assessment of the proper function of OPLINK. The measurement results are recorded and should give the same value at each site.

The operation of the optical link has the additional effect that it provides coherent and phase stable 10 MHz & 1 PPS signals to the SATRE modem in the mobile station, hence the frequency input to that SATRE modem follows the phase of the local 1 PPS AUX signal. The IIOTIC in the SATRE modem that is part of the mobile station measures a constant value and this value need not be applied as a correction. This is in contrast to normal SATRE modem operation, where the difference between the TX 1 PPS and the local 1 PPS connected to the SATRE modem is measured with the built-in IIOTIC, and the measurement result has to be applied in the data evaluation (known as REFDELAY).

5.3. TWSTFT MEASUREMENT SCHEDULE DURING THE CAMPAIGN

The operation schedule shown as Table 5-2 was implemented for the calibration, irrespective of the actual installation of the mobile station. This allowed long-term monitoring of all links involved. In this report, measurements involving the fixed station at TimeTech (TIM01, TIM11) are discussed only in the context with the repeated common-clock measurement made that demonstrated the stability of the MOB during the exercise. The schedule below does not show the other TWSTFT links established during even hours by the TWSTFT stations participating in this campaign.

Table 5-2: TWSTFT schedule implemented during the campaign, even hour sessions

First	Last	Action	Length	OP01		SP01		PTB05		TI01		ROA01		MOB02		TIM01		PTB04		Lab
				TX	RX	TX	RX	TX	RX	TX	RX	TX	RX	TX	RX	TX	RX	TX	RX	
				a		d		e		i		k		v		t		m		file Char
hhmmss	hhmmss		s	-20		-40		40		-60		-100		-70		-30		100		offset kH
UTC	UTC			0		3		4		6		7		31		14		24		TX code
		U/D link		EUR	EUR	EUR	EUR	EUR	EUR	EUR	EUR	EUR	EUR	EUR	EUR	EUR	EUR	EUR	EUR	
0:00:00	0:00:59	Prep.time	60	0	14	3	19	4		6	20	7	10	31		14	0	24	9	
0:01:00	0:02:59	Measure	120	0	14	3	19	4		6	20	7	10	31		14	0	24	9	
0:03:00	0:03:59	Prep.time	60	0	0	3	24	4	14	6	19	7	7	31	1	14	4	24	3	
0:04:00	0:05:59	Measure	120	0	0	3	24	4	14	6	19	7	7	31	1	14	4	24	3	
		U/D link		EUR	EUR	EUR	EUR	EUR	EUR	EUR	EUR	EUR	EUR	EUR	EUR	EUR	TRA	TRA	EUR	EUR
0:06:00	0:06:59	Prep.time	60	0	19	3	3	4	4	6	6	7	17	31	9	14	7	24	2	
0:07:00	0:08:59	Measure	120	0	19	3	3	4	4	6	6	7	17	31	9	14	7	24	2	
		U/D link		EUR	EUR	EUR	EUR	EUR	EUR	EUR	EUR	EUR	EUR	EUR	EUR	EUR	EUR	EUR	EUR	
0:09:00	0:09:59	Prep.time	60	0	1	3	2	4	5	6	7	7	6	31	11	14	17	24	10	
0:10:00	0:11:59	Measure	120	0	1	3	2	4	5	6	7	7	6	31	11	14	17	24	10	
		U/D link		EUR	EUR	EUR	EUR	EUR	EUR	EUR	EUR	EUR	EUR	EUR	EUR	TRA	TRA	EUR	EUR	
0:12:00	0:12:59	Prep.time	60	0	2	3	1	4	6	6	4	7	5	31	24	14	6	24	31	
0:13:00	0:14:59	Measure	120	0	2	3	1	4	6	6	4	7	5	31	24	14	6	24	31	
		U/D link		EUR	EUR	EUR	EUR	EUR	EUR	EUR	EUR	EUR	EUR	EUR	EUR	EUR	EUR	EUR	EUR	
0:15:00	0:15:59	Prep.time	60	0	3	3	0	4	7	6	5	7	4	31	17	14	24	24	14	
0:16:00	0:17:59	Measure	120	0	3	3	0	4	7	6	5	7	4	31	17	14	24	24	14	
		U/D link		EUR	EUR	EUR	EUR	EUR	EUR	EUR	EUR	EUR	EUR	EUR	EUR	EUR	EUR	EUR	EUR	
0:18:00	0:18:59	Prep.time	60	0	4	3	7	-4	0	6	2	7	3	31	14	14	31	24	24	
0:19:00	0:20:59	Measure	120	0	4	3	7	4	0	6	2	7	3	31	14	14	31	24	24	
0:21:00	0:21:59	Prep.time	60	0	5	3	6	4	1	6	3	7	2	31	20	14	9	24		
0:22:00	0:23:59	Measure	120	0	5	3	6	4	1	6	3	7	2	31	20	14	9	24		
		U/D link		EUR	EUR	EUR	EUR	EUR	EUR	EUR	EUR	EUR	EUR	EUR	EUR	EUR	EUR	EUR	EUR	
0:24:00	0:24:59	Prep.time	60	0	6	3	5	4	2	6	0	7	1	31	31	14	10	24	11	
0:25:00	0:26:59	Measure	120	0	6	3	5	4	2	6	0	7	1	31	31	14	10	24	11	
0:27:00	0:27:59	Prep.time	60	0	7	3	4	4	3	6	1	7	0	31	10	14	11	24		
0:28:00	0:29:59	Measure	120	0	7	3	4	4	3	6	1	7	0	31	10	14	11	24		
		U/D link		EUR	EUR	EUR	EUR	EUR	EUR	EUR	EUR	EUR	EUR	EUR	EUR	EUR	EUR	EUR	EUR	
0:30:00	0:30:59	Prep.time	60	0	31	3	20	4	19	6	11	7	14	31	0	14	7	24	1	
0:31:00	0:32:59	Measure	120	0	31	3	20	4	19	6	11	7	14	31	0	14	7	24	1	
		U/D link		TRA	TRA	TRA	TRA	EUR	EUR	EUR	EUR	EUR	EUR	EUR	EUR	EUR	EUR	EUR	EUR	
0:33:00	0:33:59	Prep.time	60	0	7	3	6	4	31	6	10	7	9	31	4	14	2	24		
0:34:00	0:35:59	Measure	120	0	7	3	6	4	31	6	10	7	9	31	4	14	2	24		
		U/D link		TRA	TRA	EUR	EUR	EUR	EUR	EUR	EUR	EUR	EUR	EUR	EUR	EUR	EUR	EUR	EUR	
0:36:00	0:36:59	Prep.time	60	0	6	3	14	4	9	6		7		31	2	14	3	24		
0:37:00	0:38:59	Measure	120	0	6	3	14	4	9	6		7		31	2	14	3	24		
		U/D link		EUR	EUR	EUR	EUR	EUR	EUR	EUR	EUR	EUR	EUR	EUR	EUR	EUR	EUR	EUR	EUR	
0:39:00	0:39:59	Prep.time	60	0	24	3	17	4	10	6	31	7	11	31	6	14	19	24	0	
0:40:00	0:41:59	Measure	120	0	24	3	17	4	10	6	31	7	11	31	6	14	19	24	0	
		U/D link		EUR	EUR	TRA	TRA	EUR	EUR	EUR	EUR	EUR	EUR	EUR	EUR	EUR	EUR	EUR	EUR	
0:42:00	0:42:59	Prep.time	60	0	17	3	7	4	11	6	9	7	31	31	7	14	1	24		
0:43:00	0:44:59	Measure	120	0	17	3	7	4	11	6	9	7	31	31	7	14	1	24		
		U/D link		EUR	EUR	EUR	EUR	TRA	TRA	EUR	EUR	EUR	EUR	EUR	EUR	EUR	EUR	EUR	EUR	
0:45:00	0:45:59	Prep.time	60	0	15	3	9	4	7	6	17	7	24	31		14	20	24	7	
0:46:00	0:47:59	Measure	120	0	15	3	9	4	7	6	17	7	24	31		14	20	24	7	
0:48:00	0:48:59	Prep.time	60	0	9	3	10	4	6	6	24	7	20	31	15	14	14	24	6	
0:49:00	0:50:59	Measure	120	0	9	3	10	4	6	6	24	7	20	31	15	14	14	24	6	
		U/D link		EUR	EUR	EUR	EUR	EUR	EUR	TRA	TRA	TRA	TRA	EUR	EUR	EUR	EUR	EUR	EUR	
0:51:00	0:51:59	Prep.time	60	0	10	3	11	4	17	6	6	7	7	31		14	5	24		
0:52:00	0:53:59	Measure	120	0	10	3	11	4	17	6	6	7	7	31		14	5	24		
0:54:00	0:54:59	Prep.time	60	0	11	3	31	4	20	6	7	7	6	31	3	14	15	24		
0:55:00	0:56:59	Measure	120	0	11	3	31	4	20	6	7	7	6	31	3	14	15	24		
		U/D link		EUR	EUR	EUR	EUR	EUR	EUR	EUR	EUR	EUR	EUR	EUR	EUR	EUR	EUR	EUR	EUR	
0:57:00	0:57:59	Prep.time	60	0	20	3	3	4	24	6	14	7	19	31		14	6	24	4	
0:58:00	0:59:59	Measure	120	0	20	3	3	4	24	6	14	7	19	31		14	6	24	4	

Table 5-3: TWSTFT schedule implemented during the campaign, odd hour sessions

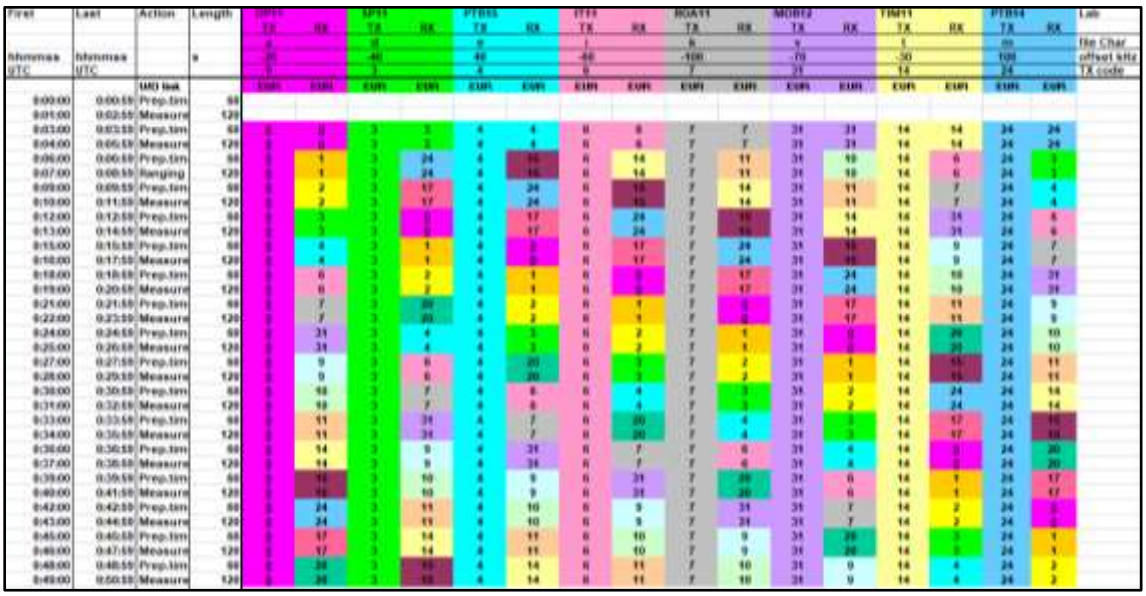

6. DOCUMENTATION OF DATA COLLECTION AND RESULTS

CC measurements were made at each visited UTC(k) laboratory. Here, as in all cases we distinguish first between data collected in even and odd hours, respectively. The average was calculated separately for each data set. The uncertainty values were found in some cases significantly smaller than the ordinate difference between even and odd hour data. This actually suggests some systematic effects in the modems involved, namely that the measurement obtained for one link between two stations depends on the other signals present that are transmitted by other stations at the same time. We thus estimate the statistical uncertainty of each CC value based on the worst TDEV value obtained for the range of useful averaging time (range from 12 to 24 hours), and was included a contribution to the uncertainty budget based on the findings.

In total, at least 100 pairs of link data for each time link in even and odd hours were taken. The only exception to this was the smaller number of data involving SP01, IT01 and ROA02, about 60, as a result of a problem related to MOB's schedule with SP01, and the operation in the last two stations, restricted to odd hours.

Usually, diurnal variations in the TWSTFT data were observed. The cause of the diurnals is not well understood, and they might prevent from reaching a 1 ns-uncertainty for the CALR values in some cases.

6.1. DATA COLLECTION AND INDIVIDUAL RESULTS RELATIVES TO MOB STATION

6.1.1. MOB AT TIM – CLOSURE MEASUREMENT IN PHASE I

The fixed TWSTFT installation operated by TimeTech served as reference for the assessment of the performance of the mobile station during the trip. To this end, CC measurements were made before and after the trip. The following results, illustrated in Figure 6-1 and Figure 6-2 were obtained:

$[\mathrm{CCD} + \mathrm{REFDLYdiff}](\mathrm{MOB@TIM, TIM})\_1$: mean_even = -753.53 ns, TDEV = 0.13 ns, N: 45 values
mean_odd = -753.52 ns, TDEV = 0.13 ns, N: 43 values

$[\mathrm{CCD} + \mathrm{REFDLYdiff}](\mathrm{MOB@TIM, TIM})\_2$: mean_even = -753.20ns, TDEV = 0.18 ns, N: 90 values
mean_odd = -753.19ns, TDEV = 0.19 ns, N: 88 values

The statistical measurement uncertainty is estimated by the worst TDEV value observed rather than by $\mathrm{sigma}/\sqrt{\mathrm{N}}$. The latter statement applies for all subsequent data sets.

For the closure measurement estimation, the TDEV values are combined with the corresponding statistical uncertainty associated to the estimation of each REFDLYdiff value, providing the uncertainty u_{CCDi} ; i = 1, 2.

Since the combined standard deviation $\mathrm{CSD} = \sqrt{(u_{CCD1})^2 + (u_{CCD2})^2} = 0.22$ ns (0.23 ns in odd hours) was lower than the change in the CCD value along the trip, $\mathrm{CCD}_1 - \mathrm{CCD}_2 = 0.33$ ns (0.33 ns too in odd hours), the implication of these results is that one can be confident that the observed change in the common clock difference (CCD) is a real effect and not an anomaly caused by measurement uncertainty.

Figure 6-1: Result of common clock measurements MOB at TimeTech during MJD 60170-60174

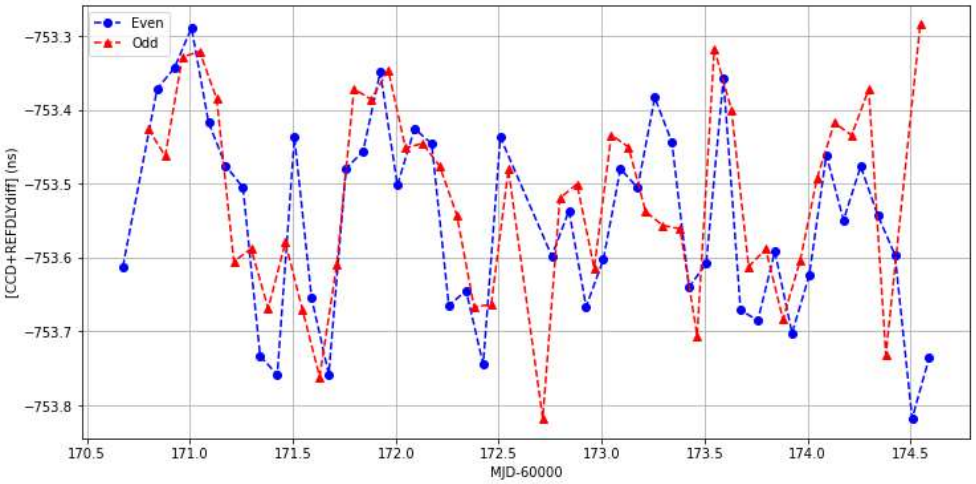

Figure 6-2: Result of common-clock measurements MOB at TimeTech during MJD 60268-60274

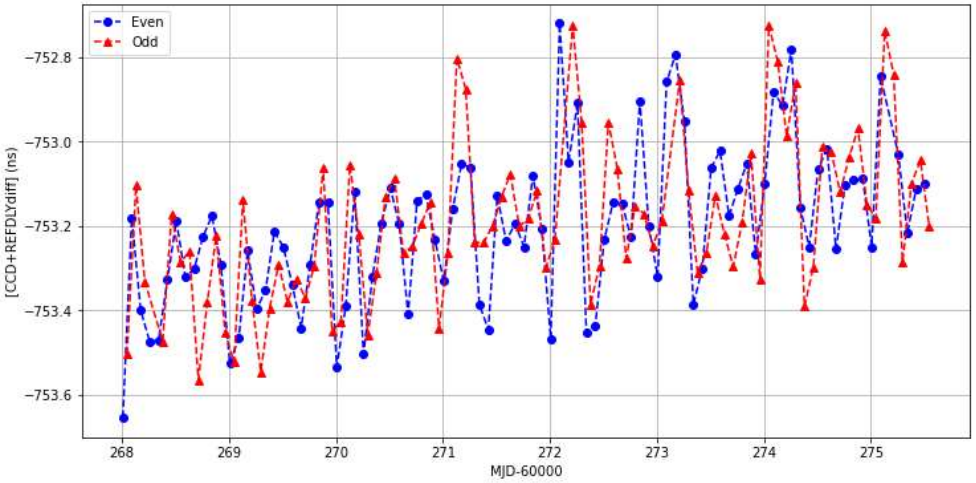

6.1.2. MOB AT PTB

While the mobile station was at PTB, time links were calibrated involving two TW stations, PTB5 and PTB4. They were also performed in two distinct phases, MJD 60191-60195 and MJD 60257-60261. The following picture shows the trailer during its stay at PTB.

Figure 6-3: View of the mobile station at PTB

The results obtained for both stations (PTB4 and PTB5) and for the two measurements phases, are illustrated from Figure 6-4 to Figure 6-7:

$[CCD + REFDLYdiff](MOB@PTB5, PTB5)\_1$: mean_even = -723.57 ns, TDEV=0.11 ns, N: 40 values
mean_odd = -723.56 ns, TDEV=0.12 ns, N: 39 values

Figure 6-4: Result of common-clock measurements MOB at PTB5 during MJD 60191-60195

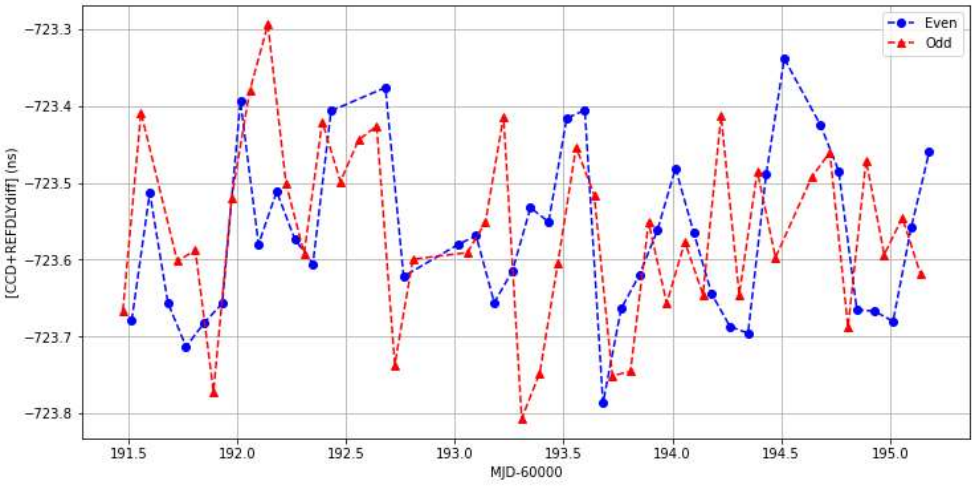

$[CCD + REFDLYdiff](MOB@PTB4, PTB4)\_1$: mean_even = -740.57 ns, TDEV=0.13 ns, N: 43 values
mean_odd = -740.57 ns, TDEV=0.14 ns, N: 43 values

Figure 6-5: Result of common-clock measurements MOB at PTB4 during MJD 60191-60195

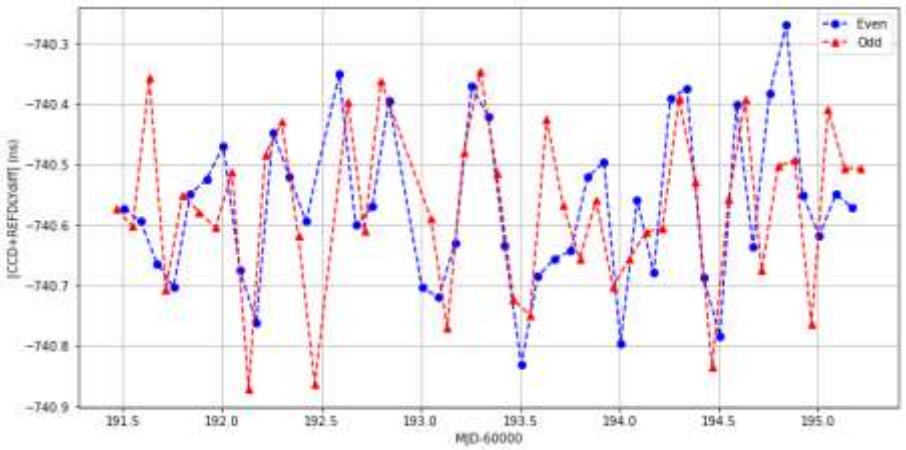

[CCD + REFDLYdiff](MOB@PTB5, PTB5)_2: mean_even = -723.45 ns, TDEV=0.13 ns, N: 51 values
mean_odd = -723.50 ns, TDEV=0.12 ns, N: 51 values

Figure 6-6: Result of common-clock measurements MOB at PTB5 during MJD 60257-60261

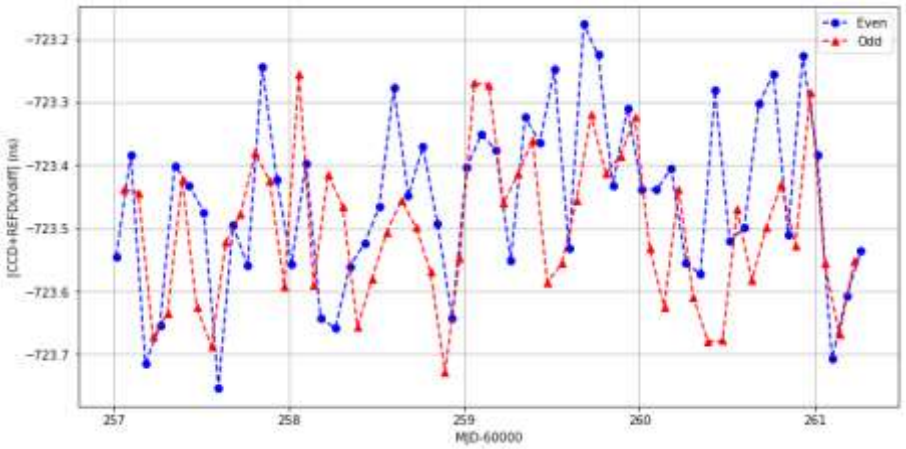

[CCD + REFDLYdiff](MOB@PTB4, PTB4)_2: mean_even = -740.18ns, TDEV=0.15 ns, N: 51 values
mean_odd = -740.17 ns, TDEV=0.14 ns, N: 47 values

Figure 6-7: Result of common-clock measurements MOB at PTB4 during MJD 60257-60261

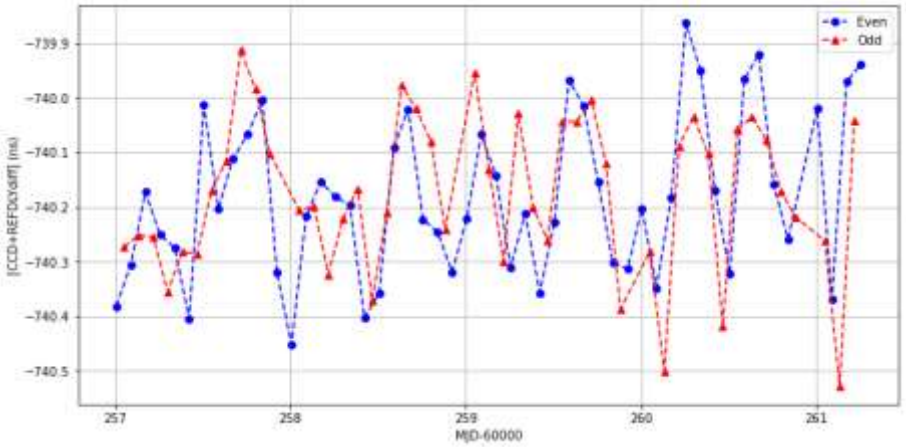

6.1.3. MOB AT ROA

The picture of the Figure 6-8 illustrates the trailer installed at ROA.

Figure 6-8: View of the mobile station at ROA

The following result, illustrated in Figure 6-9, was obtained:

$[CCD + REFDLYdiff](MOB@ROA, ROA)$: mean_even = -714.41ns, TDEV=0.26 ns, N: 51 values
mean_odd = -714.47 ns, TDEV=0.29 ns, N: 51 values

Figure 6-9: Result of common-clock measurements MOB at ROA during MJD 60210-60215

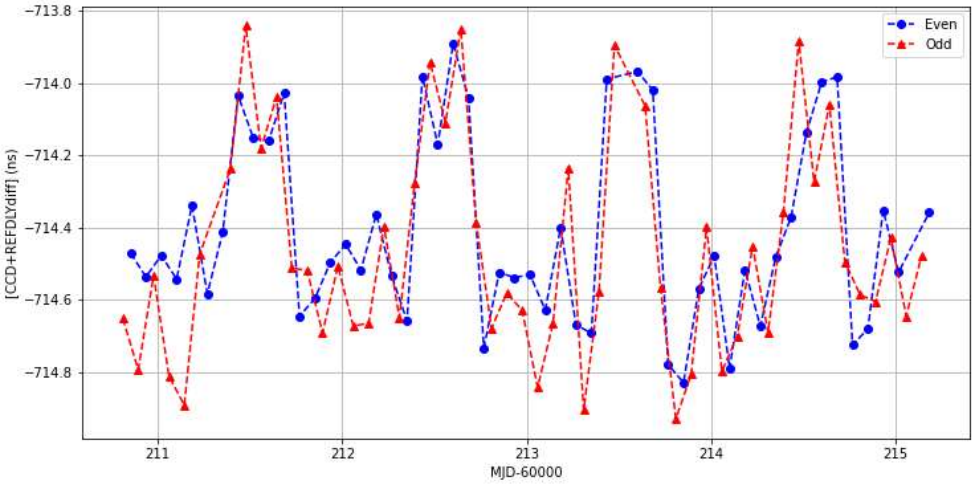

6.1.4. MOB AT OP

The picture of the Figure 6-10 shows the trailer while was installing at OP.

Figure 6-10: View of the mobile station at OP

The following result, illustrated in Figure 6-11, was obtained:

$[CCD + REFDLYdiff](MOB@OP, OP)$: mean_even = -7873.14 ns, TDEV=0.11 ns, N: 51 values
mean_odd = -7873.23 ns, TDEV=0.12 ns, N: 50 values

Figure 6-11: Result of common-clock measurements MOB at OP during MJD 60220-60224

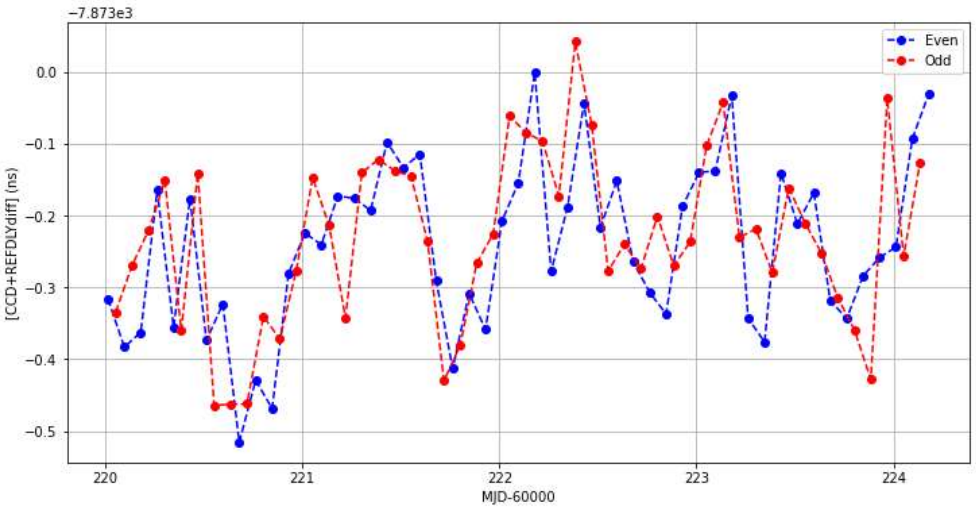

6.1.5. MOB AT SP

The photography of the Figure 6-12 shows the MOB and RISE fixed stations.

Figure 6-12: View of the mobile station at RISE

The result obtained, illustrated in Figure 6-13, was obtained:

$[CCD + REFDLYdiff](MOB@SP, SP)$: mean_even = -739.69 ns, TDEV=0.10 ns, N: 35 values
mean_odd = -739.70 ns, TDEV=0.09 ns, N:36 values

Figure 6-13: Result of common-clock measurements MOB at SP during MJD 60233-60236

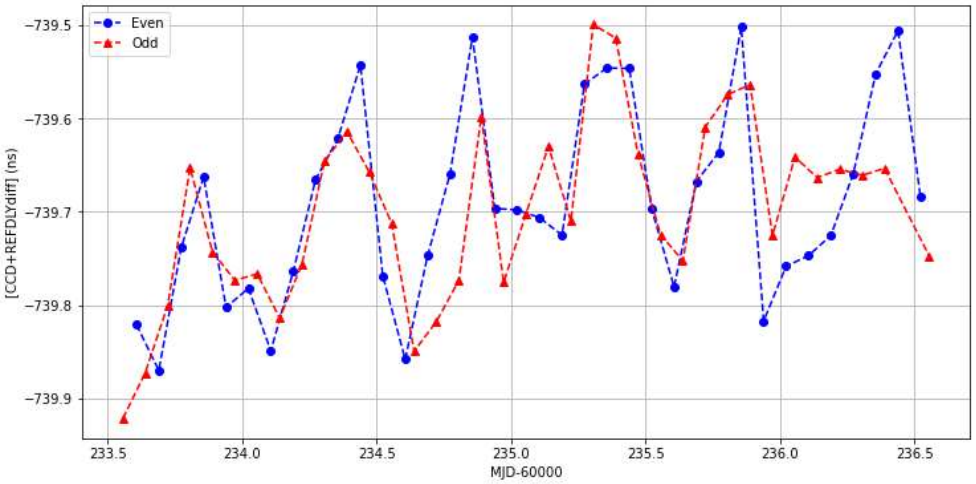

6.1.6. MOB AT INRIM

Figure 6-14 shows a photograph of the trailer while was installing at INRIM:

Figure 6-14: View of the mobile station at INRIM

The following result, depicted in Figure 6-15, was obtained:

$[\mathrm{CCD} + \mathrm{REFDLYdiff}](\mathrm{MOB@IT, IT})$: mean_even = -729.87 ns, TDEV=0.15 ns, N: 44 values
mean_odd = -729.84 ns, TDEV=0.14 ns, N: 43 values

Figure 6-15: Result of common-clock measurements MOB at IT during MJD 60248-60252

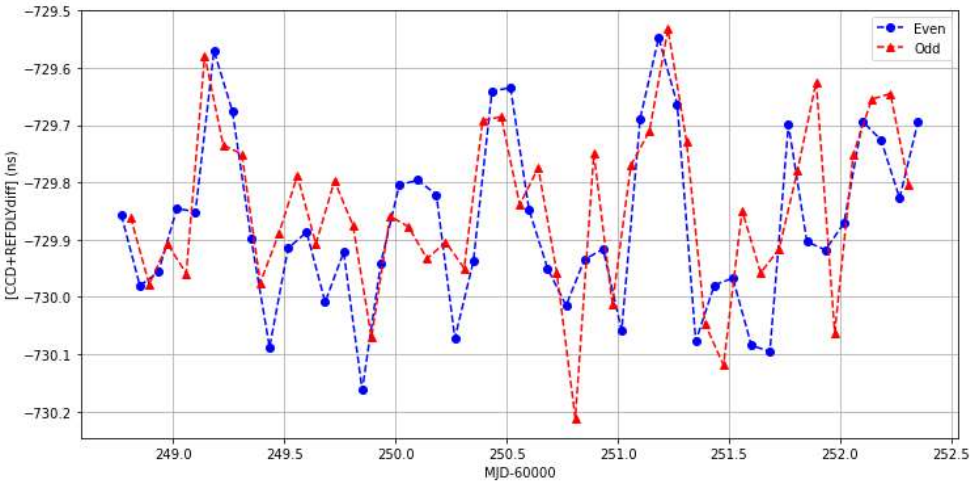

6.2. TWSTFT LINK CALIBRATION VALUES

From now on, all values reported in tables are stated in ns.

6.2.1. TWSTFT LINK CALIBRATION VALUES

As PTB had two measurements phases, the results are set as the average of both phases for PTB05, and for PTB04 was used the measurement data from the 2nd closure measurement duration, due to instabilities during the initialisation of the station during 1st measurement duration. Table 6-1 shows the results obtained for INRIM, OP, ROA, PTB and SP for all possible pair combinations of their channels 1, when eq. 14 is applied.

Table 6-1: CALR values (ns) for all possible combinations, ESDVAR reset to zero

New CALR for station "j" against "k", ESDVAR set to zero			
Station "j", Station "k"	SCD(j)	SCD(k)	CALR (eq.14)
CALR*(SP01,PTB05)	90.01	99.32	**-7.29**
CALR*(SP01,PTB04)	90.01	99.32	**9.14**
CALR*(SP01,IT01)	90.01	109.52	**9.32**
CALR*(SP01,OP01)	90.01	92.18	**7135.11**
CALR*(SP01,ROA01)	90.01	91.26	**-23.93**
CALR*(PTB05,PTB04)	99.32	99.32	**15.85**
CALR*(PTB05,IT01)	99.32	109.52	**16.20**
CALR*(PTB05,OP01)	99.32	92.18	**7142.10**
CALR*(PTB05,ROA01)	99.32	91.26	**-16.90**
CALR*(PTB04,IT01)	99.32	109.52	**-0.08**
CALR*(PTB04,OP01)	99.32	92.18	**7126.18**
CALR*(PTB04,ROA01)	99.32	91.26	**-33.33**
CALR*(IT01,OP01)	109.52	92.18	**7126.06**
CALR*(IT01,ROA01)	109.52	91.26	**-33.28**
CALR*(OP01,ROA01)	92.18	91.26	**-7159.33**

The calibration values in Table 6-1(CALR*) have been obtained from the one half of the sum of the average values collected separately in even and odd hours, and take into account that the earth stations delay variations (ESDVAR) will be re-set to zero after the calibration. [RD02] suggests that each TWSTFT network decides whether the ESDVAR is re-set or not when a delay calibration takes place. It is usual practice for TWSTFT calibrations in Europe to do so, therefore the "final" CALR values are given with ESDVAR set to zero (if applicable). It is, however, convenient to compare the new values against old ones corrected by the ESDVAR, as this gives a clue on the stability with time of the installations at the stations which are connected. We report thus such $CALR_{interim,}$ subsequently for old CALR modified by ESDVAR, as shown in the Table 6-2.

Table 6-2: CALRi$_{interim}$ for all possible combinations, except for PTB04 station

CALRinterim for station "j" against "k", ESDVAR unchanged				
	$CALR_{OLD}$(j, k)	ESDVAR(j)	ESDVAR(k)	$CALR_{OLD}$(j, k) + 0.5*[ESDVAR(j) - ESDVAR(k)]
CALR(SP01,PTB05)	-1.95	1.40	12.32	**-7.41**
CALR(SP01,IT01)	11.90	1.40	2.60	**11.32**
CALR(SP01,OP01)	7135.76	1.40	0.00	**7136.46**
CALR(SP01,ROA01)	-24.44	1.40	0.00	**-23.74**
CALR(PTB05,IT01)	13.70	12.32	2.60	**18.56**
CALR(PTB05,OP01)	7137.46	12.32	0.00	**7143.62**
CALR(PTB05,ROA01)	-22.53	12.32	0.00	**-16.37**
CALR(IT01,OP01)	7123.90	2.60	0.00	**7125.20**
CALR(IT01,ROA01)	-36.30	2.60	0.00	**-35.00**
CALR(OP01,ROA01)	-7160.19	0.00	0.00	**-7160.19**

The "*" in $CALR^*(j,k)$ means that $CALR^*(j,k)$ is not generally equal to $-CALR^*(k,j)$. $CALR(1,2)$ new calibration values of Table 6-3, with calibration switch S = 1, are computed by the weighted average of the corresponding values of the last column of Table 6-1: $CALR(1,2) = (W1 * CALR^*(1,2) - W2 * CALR^*(2,1))/(W1 + W2)$, where $W1$ and $W2$ weights are based on the TDEV results.

In Table 6-3 the results obtained hitherto are contrasted with the previously assumed CALR values [RD08], conveniently updated with the ESDVAR values.

Table 6-3: CALR$_{interim}$ and new CALR values (in ns) obtained during the campaign

Link	CALRinterim	CALR	CALR variation
SP01 - PTB05	-7.41	-7.29	**0.12**
SP01 - IT01	11.32	9.32	**-2.00**
SP01 - OP01	7136.46	7135.11	**-1.35**
SP01 - ROA01	-23.74	-23.93	**-0.19**
PTB05 - IT01	18.56	16.2	**-2.36**
PTB05 - OP01	7143.62	7142.1	**-1.52**
PTB05 - ROA01	-16.37	-16.9	**-0.53**
IT01 - OP01	7125.20	7126.06	**0.86**
IT01 - ROA01	-35.00	-33.28	**1.72**
OP01 - ROA01	-7160.19	-7159.33	**0.86**

It should be noted that the observed differences illustrated in Figure 6-16 not meaningful. The discrepancy can be considered not significant when a difference lies below the expanded uncertainty (red line), obtained for a coverage factor of 2 (which gives a level of confidence of approximately 95 %), taking as reference the traditionally stated uncertainty of 1 ns for this kind of links.

Figure 6-16: Differences between new CALR and CALR$_{interim}$ values

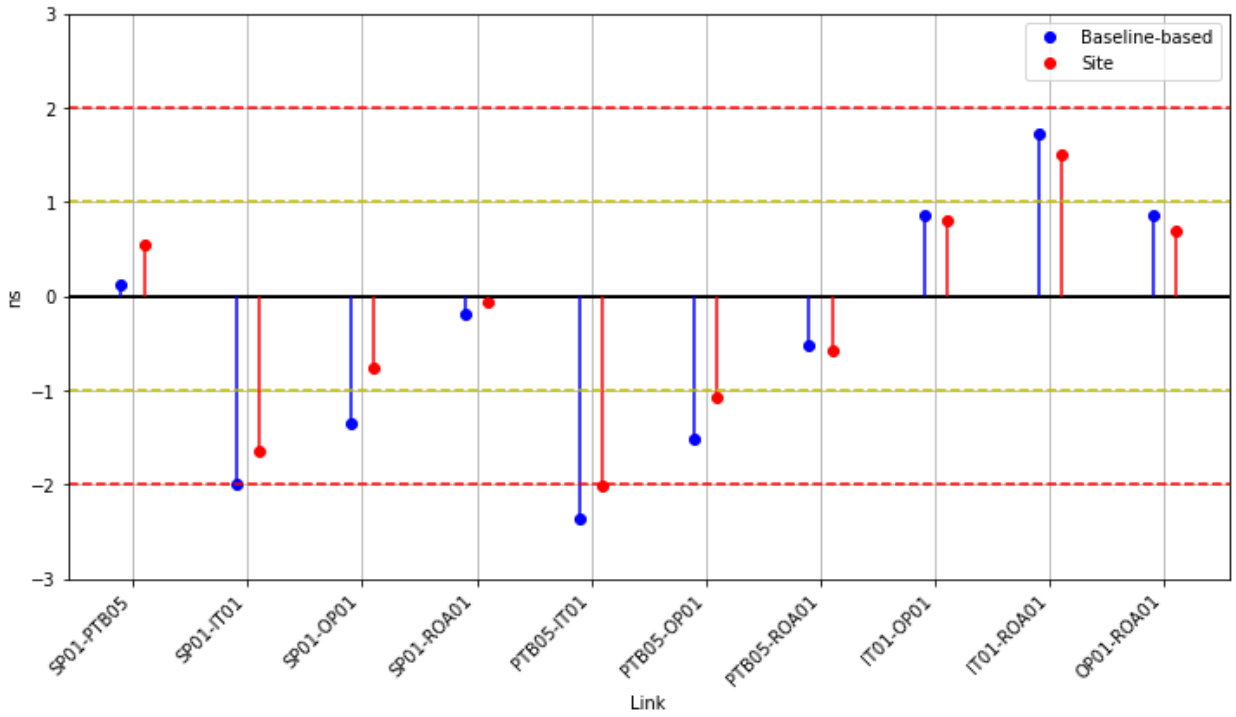

6.2.2. SUMMARY AND DISCUSSION OF UNCERTAINTY CONTRIBUTIONS

A large part of this section is based on the reasoning and conclusions of annex I in [RD04].

The total calibration uncertainty U is given by the square-root of the sum of squares of the components coming from statistical analysis, or type "a" (ua), and components type "b" or evaluated by means other than the statistical analysis of series of observations (ub):

Two statistical uncertainty components were identified:

ua(i) reflects the instability of CCD or indirect CCD (baseline mode) measurements at site i. These include the contributions of the fixed TWSTFT installation (remote installation in baseline mode), the traveling two-way equipment, and the uncertainty associated with the difference of REFDELAY values.

As explained in section 6.1.1, the statistical measurement uncertainty was stated by the worst TDEV value estimated for the range from 12 to 24 hours, rather than by $\mathrm{sigma}/\sqrt{\mathrm{N}}$ (with sigma the standard deviation of the CCD data, N = number of data points).

This approach takes into account some systematic effects observed occasionally in the modems involved, namely that the measurement results obtained for a link between two stations depends on the signals present that are transmitted by other stations at the same time. It also takes account diurnal variations noted in the TWSTFT data.

The various contributions to the uncertainty type "b" were classified into the following groups: Mobile TWSTFT station and related equipment (I), Laboratory station and related equipment (II), Interface between mobile TWSTFT station and local UTC(k) realization (III) and the satellite link and environment (IV).

I) Mobile TWSTFT station and related equipment

During the campaign the internal delays of the mobile station might differ due to different environmental conditions at the different sites and mechanical stress on components and cabling during traveling. This group of uncertainty components takes into account changes of environmental parameters during the period of installation at a given site and the differences encountered between different sites.

ub,1 – uncertainty due to the impact of temperature variations.

The impact of the environmental temperature is estimated assuming that the indoor equipment is located in a temperature controlled environment at standard 23°C +/- 2 K rms at all sites. The equipment in the trailer is controlled to be within 4 K rms at all sites.

To take into account the impact after visiting two labs, the uncertainty at one site is then multiplied by $\sqrt{2}$. In the table below the uncertainty due to temperature changes is listed.

Table 6-4: Uncertainty due to the impact of temperature variations

location	device	Temp coef.	unit	variation	unit	Contribution to ub,1 (ps)
indoor	PDIS	6	ps/K	2	K	12
	TIC	2	ps/K	2	K	4
	OPLINK master	25	ps/K	2	K	50
outdoor	OPLINK slave	10	ps/K	4	K	40
	modem	30	ps/K	4	K	120
				ub,1 (ps) =		**$136\times\sqrt{2}=192$**

ub,2 – uncertainty due to other contributions related to mobile TWSTFT station.

Other uncertainty contributions in these equipments are:

Table 6-5: Uncertainty due to other contributions related to mobile TWSTFT station

device	Contribution to ub,2 (ps)		comment
OPLINK master	PPS uncertainty	10	Specification
OPLINK slave	PPS uncertainty	20	Specification
modem	Meas. resolution	10	Specification
	ub,2 (ps) =	**$25\times\sqrt{2}=35$**	

ub,3 – instability of the portable station.

The third contribution is the difference between the initial CCD between the mobile station and a fixed reference station and measured closure after the campaign (see section 6.1.1).

The quadratic sum of these three contributions to the uncertainty provides the next value for the uncertainty encompassing contributions group I:

ub,I = 0.27 ns

ub,I and subsequent uncertainties defined by groups, represent the 1-σ uncertainty, rounded to 0.01 ns.

II) Laboratory station and related equipment

ub,4 – uncertainty due to the impact of temperature variations.

The stability due to temperature variations of the fixed stations can be estimated in a similar way as set out in Table 6-6.

Table 6-6: Uncertainty due to the impact of temperature variations

location	device	Temp coef.	unit	variation	unit	Contribution to ub,4 (ps)
Site 1	modem	30	ps/K	2	K	60

Site 2	modem	30	ps/K	2	K	60
				ub,4 (ps) =		85

ub,5 – uncertainty due to other contributions in laboratory stations.

This uncertainty contribution resulting from the instabilities of the fixed stations and signal distribution systems has been estimated considering the measurement resolution of modems.

For each link calibrated according to the link-mode approach, this contribution was estimated as:

ub,5 = 0.020 ns

The quadratic sum of both contributions to the uncertainty provides the uncertainty contribution group II:

ub,II = 0.09 ns

III) Interface between mobile TWSTFT station and UTC(k) realization

ub,6(i) – contribution derived from statistical uncertainty already calculated (statistical uncertainty associated to the estimation of the REFDLYdiff value).

ub,7 – uncertainty due to contributions in equipments related to laboratory stations.

This uncertainty contribution resulting from the instabilities signal distribution systems has been estimated considering the instability of PDIS/FDIS and rise time of 1PPS signals [RD11-12].

For each link calibrated according to the link-mode approach, this contribution was estimated in:

ub,7 = 0.200 ns

ub,8 – uncertainty due to TIC resolution.

According to the description in the manual of the widely used TIC SR620 [RD11], ub,8 is the measurement resolution, or the smallest statistically significant change which can be measured.

This uncertainty component is effectively reduced by averaging to be < 25 ps, or < 36 ps for both sites. Taking a sufficiently high number of samples averaged N, this contribution decreases becoming negligible.

ub,9 – uncertainty due to TIC systematic contributions.

Systematic contribution coming from the time base error (negligible value), the start and stop trigger level errors, and the internal delay asymmetry (predominant component, of about 0.5 ns).

Since the TIC was used in a relative mode [RD11], i.e. a single TIC was used at all labs to connect the mobile TWSTFT station to the local time reference UTC(k), the internal delay asymmetry ("systematic error") was substituted by the differential non-linearity (50 ps).

In such circumstances, ub,9 was estimated in 130 ps for each link.

Table 6-7 summarizes the group III uncertainty contribution values. All values are in ns.

Table 6-7: Uncertainty contributions and combined uncertainty - Group III

Case	ub,6(1)	ub,6(2)	ub,7	ub,8	ub,9	ub,III
CALR(UTC(j), UTC(k))	0.05	0.05	0.20	-	0.13	**0.25**

IV) Satellite link and environment

This group of uncertainties summarizes all effects attributed to the satellite link and outdoor environment. They comprise the instability of satellite communication parameters (signal power, C/N0, codes), atmospheric parameters (ionosphere, troposphere), and satellite motion (residual diurnals, residual Sagnac, path delay difference).

Previous studies have revealed that the causes of diurnal variations in the time transfer results are related to satellite motion, causing a residual Sagnac effect (A) and the path delay difference between the two ground stations to the satellite (B), respectively. In many cases, however, diurnal variations are observed that are substantially larger than could be explained with the two effects. In particular, it has been noted that the two mentioned effects are almost identical for all inner-European links (due to the very similar geometry of stations and satellite), but the amplitude of diurnal variations are quite different in magnitude and they seem to "come and go" in the course of time without a root cause would be known. In this case it is proposed to include a term "additional diurnal of unknown origin (ADUO)". This value has been estimated considering that: 1) the diurnal has a sinusoidal wave form, 2) the minimum measurement time interval was stated in three days, 3) CCD in this exercise showed a maximum amplitude (peak value) of about 1.2 ns, and 4) the worst-case scenario may occur, when the measurement time interval extends to 3 ¼ days and the six additional hours of data are close to a peak or trough. On these assumptions, this potential deviation can reach 0.2 ns. Consequently, 0.12 ns (0.2/√3, considering a uniform distribution) has been considered as the ADUO uncertainty contribution.

The table below gives the uncertainties budget that matches findings in this campaign quite well.

Table 6-8: Uncertainty contributions and combined uncertainty - Group IV

Sub group	Source	Contribution to ub,IV (ns)
Sat com	Tx power, C/N0	0.150
Atmosphere	Ionosphere	0.030
	Troposphere	0.001
	Temperature variations on ground station	0.100
	Humidity changes	0.010
Satellite motion	ADUO	0.120
	Residual Sagnac (A)	0.250
	Path delay difference (B)	0.002
Even and odd hours measures	Possible interferences between PRN codes	0.500
	ub,IV =	0.60

The combined uncertainty U is estimated as the square-root of the sum of squares of all contributions.

Table 6-9: Uncertainty contributions and combined uncertainty UTable 6-9 summarizes the uncertainty contribution case by case. All values are in ns, U represents the 1-σ uncertainty, rounded to 0.1 ns.

Table 6-9: Uncertainty contributions and combined uncertainty U

Case	ua(1)	ua,f(2)	ub,I	ub,II	ub,III	ub,IV	U
CALR(SP01,PTB05)	0.07	0.06	0.27	0.09	0.25	0.60	**0.72**
CALR(SP01,PTB04)	0.06	0.08	0.27	0.09	0.25	0.60	**0.72**
CALR(SP01,IT01)	0.08	0.10	0.27	0.09	0.25	0.60	**0.72**
CALR(SP01,OP01)	0.07	0.09	0.27	0.09	0.25	0.60	**0.72**

Case	ua(1)	ua,f(2)	ub,I	ub,II	ub,III	ub,IV	U
CALR(SP01,ROA01)	0.08	0.20	0.27	0.09	0.25	0.60	**0.74**
CALR(PTB05,PTB04)	0.09	0.10	0.27	0.09	0.25	0.60	**0.72**
CALR(PTB05,IT01)	0.09	0.09	0.27	0.09	0.25	0.60	**0.72**
CALR(PTB05,OP01)	0.11	0.10	0.27	0.09	0.25	0.60	**0.72**
CALR(PTB05,ROA01)	0.13	0.21	0.27	0.09	0.25	0.60	**0.75**
CALR(PTB04,IT01)	0.10	0.10	0.27	0.09	0.25	0.60	**0.72**
CALR(PTB04,OP01)	0.12	0.09	0.27	0.09	0.25	0.60	**0.73**
CALR(PTB04,ROA01)	0.40	0.25	0.27	0.09	0.25	0.60	**0.85**
CALR(IT01,OP01)	0.13	0.10	0.27	0.09	0.25	0.60	**0.73**
CALR(IT01,ROA01)	0.26	0.19	0.27	0.09	0.25	0.60	**0.78**
CALR(OP01,ROA01)	0.31	0.21	0.27	0.09	0.25	0.60	**0.80**

6.3. DISCUSSION OF RESULTS

During the campaign, new CALR values were determined with uncertainties of around 1 ns. These uncertainties are of similar order than those got in previous campaigns [RD03, RD07, RD08, RD09 and RD13]. Data collected at each site were of excellent quality, and only occasionally data were removed (by applying a 3-σ filter). The measurement noise was at the standard level.

The apparent changes in the CALR values for all the links show a non-significant discrepancy with respect to the old ones, with discrepancy values near 2 ns for all links, being most of them between the range of 0 and 1 ns.

It is thus proposed to apply the new values of CALR as is explained in the following section.

7. LESSONS LEARNT

The current campaign was the eighth one involving the mobile station provided by TimeTech. It is still possible to learn and improve some aspects looking towards future campaigns.

This calibration campaign took into account the lessons learned from the previous campaign [RD13] regarding to adverse weather conditions. The calendar was established to avoid the mobile station coinciding with the ice and snow season in the northernmost countries.

8. APPENDIX 1

The results obtained of calibration using *Software-Defined Radio* (SDR) in reception are shown in Table 8-2 for, taking into account:

1. The 'Baseline' mode has only been able to be applied to stations SP, OP and IT, since not all laboratories were observed by everyone during the entire campaign.
2. The results in 'Site' mode have been obtained for all stations.
3. PTB4 has no SDR.

Table 8-1: CALR values in 'Baseline' mode for SDR channels and all possible combinations

CALR for SDR channels [ns]	
Link	$CALR_{Baseline}$ [SDR]
SP51-IT51	**-97.24**
SP51-OP51	**2026.62**
IT51-OP51	**2124.09**

Table 8-2: CALR values in 'Site' mode for SDR channels and all possible combinations

CALR for SDR channels [ns]	
Link	$CALR_{site}$ [SDR]
SP51-PTB05	**3.28**
SP51-IT51	**-97.72**
SP51-OP51	**2026.60**
SP51-ROA51	**-26.50**
PTB55-IT51	**-101.00**
PTB55-OP51	**2023.30**
PTB55-ROA51	**-29.78**
IT51-OP51	**2124.35**
IT51-ROA51	**71.22**
OP51-ROA51	**-2053.06**

The results are quite consistent, since the differences among the 3 computed links shown in Table 8-1and Table 8-2 are less than 0.5 ns.

In order to verify the results of Table 8-2, an alignment of the uncalibrated SDR link to the TW calibrated (Site mode) have been carried out. Using ROA-IT link (Figure 8-1 for TW calibrated link and Figure 8-2 for SDR uncalibrated link) as an example, a double clock difference (DCD) between the data in the Figure 8-1 and those in Figure 8-2has been implemented, and the results are shown in Figure 8-3.

Figure 8-1: ROA–IT TW calibrated link (Site mode)

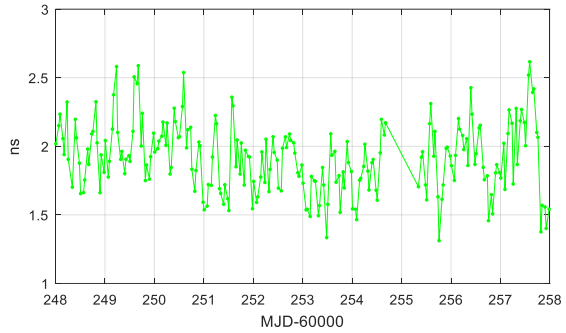

Figure 8-2: ROA-IT SDR uncalibrated link

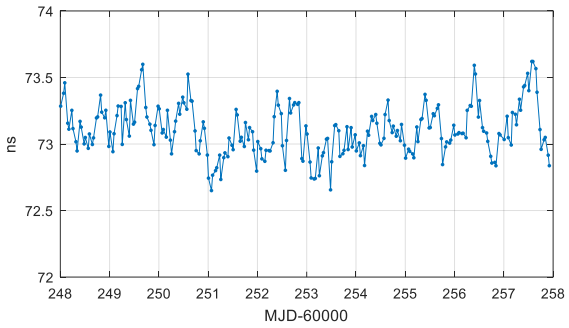

Figure 8-3: DCD: Difference between SDR link and calibrated TW link

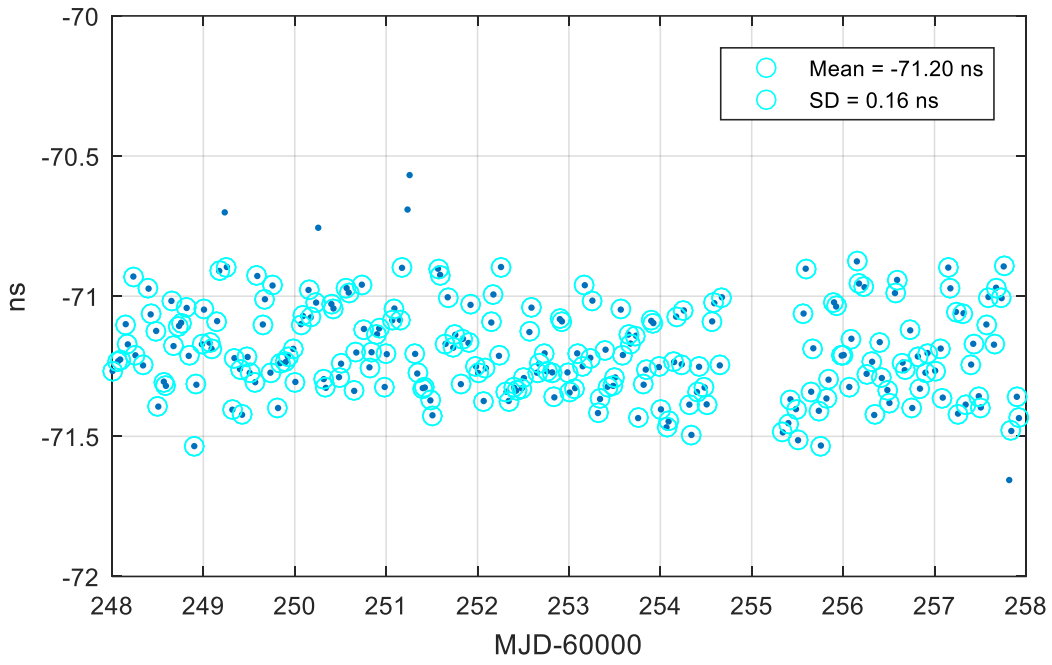

The Table 8-3 illustrates the differences between the two series of data. The DCD computation is based in the same ten days of data (form MJD 60248 to MJD 60257). Regarding the PTB5 station, 5-minute SDR files were employed with interpolation. The agreement was quite good, measuring below 0.5 ns, except for three links, where the maximum deviation reached 0.75 ns.

Table 8-3: Difference between aligned and calibrated SDR link

Aligned SDR vs. calibrated SDR [ns]			
Link	$CALR_{Aligned}$	$CALR_{site}$	Difference
SP51-PTB05	3.99	3.28	**0.71**
SP51-IT51	-96.97	-97.72	**0.75**
SP51-OP51	2026.98	2026.62	**0.36**
SP51-ROA51	-26.10	-26.50	**0.40**
PTB55-IT51	-100.35	-101.00	**0.65**
PTB55-OP51	2023.55	2023.30	**0.25**
PTB55-ROA51	-29.29	-29.78	**0.49**
IT51-OP51	2124.04	2124.35	**-0.31**
IT51-ROA51	71.20	71.22	**-0.02**
OP51-ROA51	-2052.98	-2053.06	**0.08**

9. APPENDIX 2

In this section, the results from utilizing the second channel (Rx2) of the SATRE Modem are presented. Due to the different link possibilities: Rx1-Rx2, Rx2-Rx1, Rx2-Rx2, multiple tables are presented for each of these configurations. OP station does not have or has not made use of its Rx2.

Table 9-1: TW CALR values for Rx1 (All) and Rx2 (ROA21) configuration.

Link ($Sta1_{Rx1}$ – $Sta2_{Rx2}$)	CALR Site [ns]	CALR Baseline [ns]
SP01 – ROA21	-23.73	**-23.98**
PTB05 – ROA21	-16.92	**-17.10**
IT01 – ROA21	-33.41	**-33.29**
OP01 – ROA21	-7159.42	**-7159.33**

Table 9-2: TW CALR values for Rx1 (All) and Rx2 (PTB25) configuration.

Link ($Sta1_{Rx1}$ – $Sta2_{Rx2}$)	CALR Site [ns]	CALR Baseline [ns]
SP01 – PTB25	-2.01	**-2.23**
ROA01 – PTB25	21.80	**21.93**
IT01 – PTB25	-11.70	**-11.17**
OP01 – PTB25	-7137.70	**-7136.83**

Table 9-3: TW CALR values for Rx1 (All) and Rx2 (IT21) configuration.

Link ($Sta1_{Rx1}$ – $Sta2_{Rx2}$)	CALR Site [ns]	CALR Baseline [ns]
SP01 – IT21	7.07	**6.80**
PTB05 – IT21	13.88	**13.77**
ROA01 – IT21	30.88	**30.78**
OP01 – IT21	-7128.62	**-7128.53**

Table 9-4: TW CALR values for Rx2 in both stations.

Link ($Sta1_{Rx2}$ – $Sta2_{Rx2}$)	CALR Site [ns]	CALR Baseline [ns]
SP21 – PTB25	-4.70	**-3.24**
SP21 – IT21	4.41	**4.93**
SP21 – ROA21	-26.39	**-25.96**
PTB25 – IT21	9.11	**8.75**
PTB25 – ROA21	-21.69	**-22.05**
IT21 – ROA21	-30.80	**-30.79**

In all the studied links the difference between the Site and Baseline results are clearly below 0.5 ns, except for the OP01–PTB25 link in Table 9-2 and SP21–PTB25 link in Table 9-4, with a difference of 0.87 ns and 1.46 ns respectively.

Acknowledgement

The commitment of TWFTFT colleagues during the writing of this report was essential for the successful closure of this activity.

It is gratefully acknowledged the professionalism and dedication of TimeTech staff over the whole duration of calibration campaign.

END OF DOCUMENT

Part III

Annex: Results Validation

This part demonstrates the comparison and validation of the calibration results obtained by VSL and ROA.

Annex: Results Validation

In this annex, CALibartion Results (CALRs) on TSP links are compared between VSL and ROA calcuation results. TSP links are defined as TW links between a pair of TSP stations, where TSP stations include PTB05, PTB04, ROA01, OP01, SP01, and IT01. CALRs in comparison include the [Rx1-Rx1], [Rx1-Rx2], and [Rx2-Rx2] channels of the SATRE modem, as well as the Rx channels of the SDR modem.

All the calibration results from this annex are cited from the following documents:

[RD1]. European TWSTFT Calibration Campaign 2023 Calibration Report, prepared by VSL.

[RD2]. GSOP TWSTFT calibration report, prepared by ROA.

A1. Comparison on CALR values of Rx1-Rx1 links between TSP stations

Table A1 and Figure A1 show the baseline-mode CALR value comparison between VSL and ROA calculation results on Rx1-Rx1 channels of the SATRE modem, where '$CALR_{baseline}$ from VSL' are obtained from [RD1] Table 10-4: List of new CALR and uCALR values of [Rx1-Rx1] SATRE channels using baseline-mode calibration and '$CALR_{baseline}$ from ROA' are obtained from [RD2] Table 6-1: CALR values (ns) for all possible combinations.

Table A1. Comparisons on baseline-mode CALR values from VSL and ROA towards Rx1-Rx1 links

$CALR_{baseline}(k_1i,k_2j)$		$CALR_{baseline}$ from VSL		$CALR_{baseline}$ from ROA		$CALR_{baseline}$ differ.	
		$\mathbf{CALR(VSL)}$	$\boldsymbol{u}\mathbf{CALR(VSL)}$	$\mathbf{CALR(ROA)}$	$\boldsymbol{u}\mathbf{CALR(ROA)}$	$\mathbf{CALR_{diff}}$	$\boldsymbol{u}\mathbf{CALR_{diff}}$
$<k_1i>$	$<k_2j>$	Unit: ns	Unit: ns	Unit: ns	Unit: ns	Unit: ns	Unit: ns
PTB05	PTB04	15.735	0.383	15.85	0.72	-0.12	0.82
PTB05	ROA01	-16.900	0.455	-16.90	0.75	0.00	0.88
PTB05	OP01	7142.085	0.344	7142.10	0.72	-0.02	0.80
PTB05	SP01	7.242	0.365	7.29	0.72	-0.05	0.81
PTB05	IT01	16.210	0.605	16.20	0.72	0.01	0.94
PTB04	ROA01	-33.268	0.492	-33.33	0.85	0.06	0.98
PTB04	OP01	7126.198	0.347	7126.18	0.73	0.02	0.81
PTB04	SP01	-9.205	0.410	-9.14	0.72	-0.06	0.83
PTB04	IT01	-0.077	0.608	-0.08	0.72	0.00	0.94
ROA01	OP01	7159.219	0.463	7159.33	0.80	-0.11	0.92
ROA01	SP01	23.914	0.424	23.93	0.74	-0.02	0.85
ROA01	IT01	33.251	0.653	33.28	0.78	-0.03	1.02
OP01	SP01	-7135.140	0.364	-7135.11	0.72	-0.03	0.81
OP01	IT01	-7126.076	0.628	-7126.06	0.73	-0.02	0.96
SP01	IT01	9.355	0.619	9.32	0.72	0.04	0.95

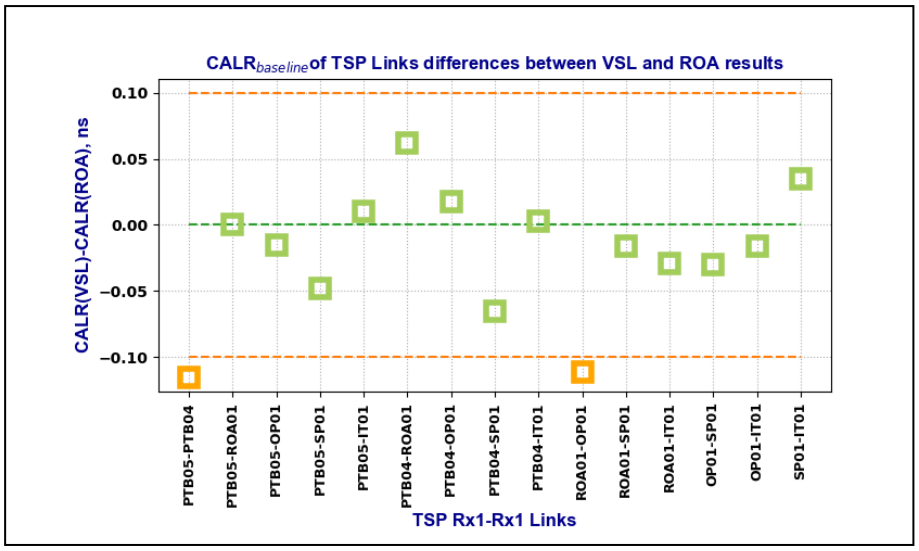

Figure A1. Baseline-mode CALR results comparison on TSP Rx1-Rx1 SATRE links

A2. Comparison on CALR values of Rx1-Rx2 and Rx2-Rx2 links between TSP stations

Table A2, Table A3, and Figure A2 present the CALRs comparison on the [Rx1-Rx2] and [Rx2-Rx2] channel links of the SATRE modem. The CALRs include calculation results from both site-mode and baseline-mode methods.

In Table A2, the data in column 'CALR$_{baseline}$ from VSL' are taken from [RD1] Table 10-5: List of new CALR and uCALR values of [Rx1-Rx2] and [Rx2-Rx2] SATRE channels using baseline-mode calibration. In Table A3, the data in column 'CALR$_{site}$ from VSL' are taken from [RD1] Table 8-3: List of new CALR and uCALR values of [Rx1-Rx2] and [Rx2-Rx2] remote links using site-mode calibration.

In Table A2 and Table A3, the columns 'CALR$_{baseline}$ from ROA' and 'CALR$_{site}$ from ROA' are obtained from [RD2] Table 9-1: TW CALR values for Rx1 (All) and Rx2 (ROA21) configuration, Table 9-2: TW CALR values for Rx1 (All) and Rx2 (PTB25) configuration,Table 9-3: TW CALR values for Rx1 (All) and Rx2 (IT21) configuration, and Table 9-4: TW CALR values for Rx2 in both stations.

Table A2. Comparisons on baseline-mode CALR values from VSL and ROA towards Rx1-Rx2/Rx2-Rx2 links

CALR$_{baseline}$(k_1i,k_2j)		CALR$_{baseline}$ from VSL		CALR$_{baseline}$ from ROA		CALR$_{baseline}$ differ.	
		$\mathrm{CALR(VSL)}$	$u\mathrm{CALR(VSL)}$	$\mathrm{CALR(ROA)}$	$u\mathrm{CALR(ROA)}$	$\mathrm{CALR_{diff}}$	$u\mathrm{CALR_{diff}}$
<k_1i>	<k_2j>	Unit: ns	Unit: ns	Unit: ns	Unit: ns	Unit: ns	Unit: ns
PTB05	ROA21	-16.903	0.461	-17.10	--	0.20	--
PTB05	SP21	8.303	0.401	--	--	--	--
PTB05	IT21	13.877	0.606	13.77	--	0.11	--
PTB04	PTB25	-10.377	0.384	--	--	--	--
PTB04	ROA21	-33.290	0.488	--	--	--	--
PTB04	SP21	-8.076	0.432	--	--	--	--
PTB04	IT21	-2.441	0.608	--	--	--	--
ROA01	PTB25	21.938	0.467	21.93	--	0.01	--
ROA01	SP21	25.900	0.448	--	--	--	--

ROA01	IT21	30.811	0.647	30.78	--	0.03	--
OP01	PTB25	-7136.795	0.346	-7136.83	--	0.03	--
OP01	ROA21	-7159.215	0.420	-7159.33	--	0.11	--
OP01	SP21	-7133.702	0.364	--	--	--	--
OP01	IT21	-7128.467	0.607	-7128.53	--	0.06	--
SP01	PTB25	-2.116	0.400	-2.23	--	0.11	--
SP01	ROA21	-23.834	0.466	-23.98	--	0.15	--
SP01	IT21	6.901	0.640	6.80	--	0.10	--
IT01	PTB25	-11.121	0.606	-11.17	--	0.05	--
IT01	ROA21	-33.190	0.651	-33.29	--	0.10	--
IT01	SP21	-7.410	0.618	--	--	--	--
PTB25	ROA21	-21.940	0.479	-22.05	--	0.11	--
PTB25	SP21	3.183	0.404	3.24	--	-0.06	--
PTB25	IT21	8.789	0.606	8.75	--	0.04	--
ROA21	SP21	25.983	0.483	25.96	--	0.02	--
ROA21	IT21	30.751	0.647	30.79	--	-0.04	--
SP21	IT21	4.957	0.619	4.93	--	0.03	--

Table A3. Comparisons on site-mode CALR values from VSL and ROA towards Rx1-Rx2/Rx2-Rx2 links

$CALR_{site}(k_1i,k_2j)$		$CALR_{site}$ from VSL		$CALR_{site}$ from ROA		$CALR_{site}$ differ.	
		$\mathbf{CALR(VSL)}$	$u\mathbf{CALR(VSL)}$	$\mathbf{CALR(ROA)}$	$u\mathbf{CALR(ROA)}$	$\mathbf{CALR_{diff}}$	$u\mathbf{CALR_{diff}}$
$<k_1i>$	$<k_2j>$	Unit: ns	Unit: ns	Unit: ns	Unit: ns	Unit: ns	Unit: ns
PTB05	ROA21	-16.839	0.434	-16.92	--	0.08	--
PTB05	SP21	9.480	0.372	--	--	--	--
PTB05	IT21	13.902	0.611	13.88	--	0.02	--
PTB04	PTB25	-11.753	0.352	--	--	--	--
PTB04	ROA21	-33.444	0.436	--	--	--	--
PTB04	SP21	-7.125	0.374	--	--	--	--
PTB04	IT21	-2.703	0.612	--	--	--	--
ROA01	PTB25	21.773	0.433	21.80	--	-0.03	--
ROA01	SP21	26.401	0.451	--	--	--	--
ROA01	IT21	30.823	0.662	30.88	--	-0.06	--
OP01	PTB25	-7137.677	0.352	-7137.70	--	0.02	--
OP01	ROA21	-7159.368	0.436	-7159.42	--	0.05	--
OP01	SP21	-7133.049	0.373	--	--	--	--
OP01	IT21	-7128.627	0.612	-7128.62	--	-0.01	--
SP01	PTB25	-1.963	0.367	-2.01	--	0.05	--
SP01	ROA21	-23.654	0.448	-23.73	--	0.08	--
SP01	IT21	7.087	0.621	7.07	--	0.02	--
IT01	PTB25	-11.666	0.611	-11.70	--	0.03	--
IT01	ROA21	-33.357	0.662	-33.41	--	0.05	--
IT01	SP21	-7.038	0.623	--	--	--	--
PTB25	ROA21	-21.691	0.434	-21.69	--	0.00	--
PTB25	SP21	4.628	0.372	4.70	--	-0.07	--

PTB25	IT21	9.050	0.611	9.11	--	-0.06	--
ROA21	SP21	26.319	0.452	26.39	--	-0.07	--
ROA21	IT21	30.741	0.662	30.80	--	-0.06	--
SP21	IT21	4.422	0.623	4.41	--	0.01	--

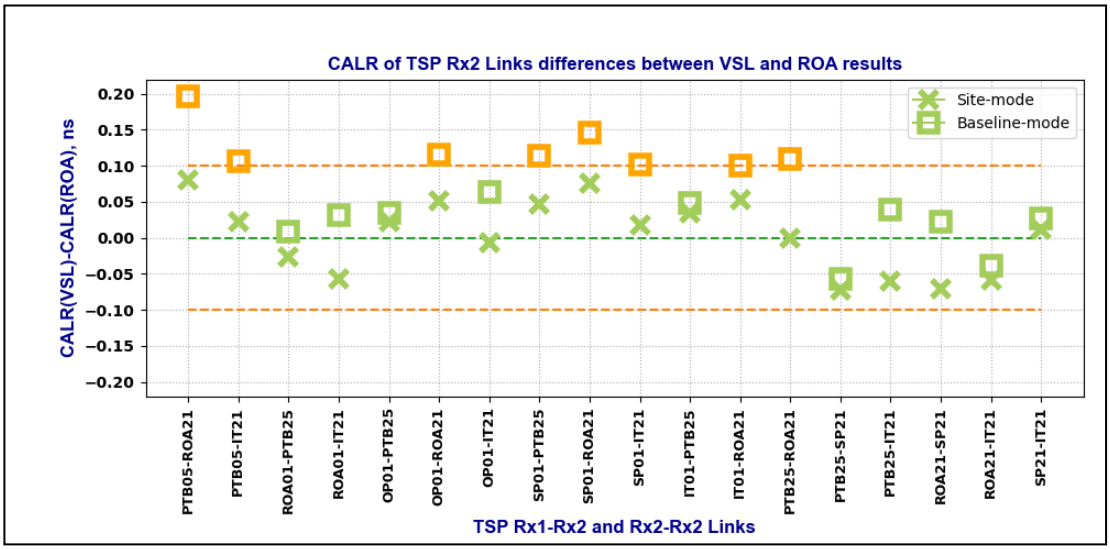

Figure A2. Site-mode/Baseline-mode CALR results comparison on TSP Rx1-Rx2 and Rx2-Rx2 links

A3. Comparison on CALR values of SDR links between TSP stations

Table A4, Table A5, and Figure A3 present the CALR comparison on the Rx channel links of the SDR modem. The CALRs include calculation results from both site-mode and baseline-mode methods.

In Table A4, data from the 'CALR$_{baseline}$ from VSL' column are taken from [RD1] Table 10-8 List of new CALR and uCALR values of SDR TW links using baseline-mode calibration, and data from 'CALR$_{baseline}$ from ROA' are taken from [RD2] Table 8-1: CALR values in 'Baseline' mode for SDR channels and all possible combinations. In Table A5, the column 'CALR$_{site}$ from VSL' are cited from [RD1] Table 8-5: List of new CALR and uCALR values of SDR TW links using site-mode calibration, and the column 'CALR$_{site}$ from ROA' are cited from [RD2] Table 8-2: CALR values in 'Site' mode for SDR channels and all possible combinations.

Table A4. Comparisons on baseline-mode CALR values from VSL and ROA towards SDR links

CALR$_{baseline}$(k_1i,k_2j)		CALR$_{baseline}$ from VSL		CALR$_{baseline}$ from ROA		CALR$_{baseline}$ differ.	
		$\mathrm{CALR(VSL)}$	$u\mathrm{CALR(VSL)}$	$\mathrm{CALR(ROA)}$	$u\mathrm{CALR(ROA)}$	$\mathrm{CALR_{diff}}$	$u\mathrm{CALR_{diff}}$
<k_1i>	<k_2j>	Unit: ns	Unit: ns	Unit: ns	Unit: ns	Unit: ns	Unit: ns
ROA51	OP51	2052.727	0.431	--	--	--	--
ROA51	SP51	26.138	0.606	--	--	--	--
ROA51	IT51	-71.444	0.660	--	--	--	--
OP51	SP51	-2026.486	0.373	-2026.62	--	0.13	--
OP51	IT51	-2124.124	0.607	-2124.09	--	-0.03	--

SP51	IT51	-97.254	0.685	-97.24	--	-0.01	--

Table A5. Comparisons on site-mode CALR values from VSL and ROA towards SDR links

$CALR_{site}(k_1i,k_2j)$		$CALR_{site}$ from VSL		$CALR_{site}$ from ROA		$CALR_{site}$ differ.	
		$CALR(VSL)$	$uCALR(VSL)$	$CALR(ROA)$	$uCALR(ROA)$	$CALR_{diff}$	$uCALR_{diff}$
$<k_1i>$	$<k_2j>$	Unit: ns	Unit: ns	Unit: ns	Unit: ns	Unit: ns	Unit: ns
PTB55	ROA51	-29.710	0.427	-29.78	--	0.07	--
PTB55	OP51	2023.294	0.347	2023.30	--	-0.01	--
PTB55	SP51	-3.327	0.440	-3.28	--	-0.05	--
PTB55	IT51	-101.004	0.610	-101.00	--	0.00	--
ROA51	OP51	2053.004	0.426	2053.06	--	-0.06	--
ROA51	SP51	26.383	0.515	26.50	--	-0.12	--
ROA51	IT51	-71.294	0.658	-71.22	--	-0.07	--
OP51	SP51	-2026.621	0.439	-2026.60	--	-0.02	--
OP51	IT51	-2124.298	0.610	-2124.35	--	0.05	--
SP51	IT51	-97.677	0.667	-97.72	--	0.04	--

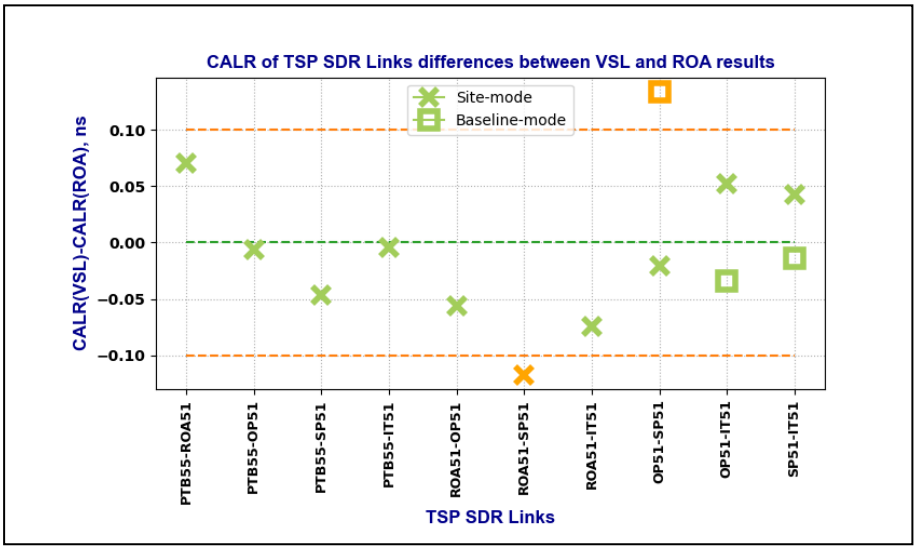

Figure A3. Site-mode/Baseline-mode CALR results comparison on TSP SDR links